INVESTIGATION OF THE STRUCTURE AND FUNCTION OF SECH, A NOVEL COMPONENT OF THE SEC MACHINERY IN *ESCHERICHIA COLI*

by

MAX ALEXANDER WYNNE

A thesis submitted to the University of Birmingham for the degree of

DOCTOR OF PHILOSOPHY

School of Biosciences
College of Life and Environmental Sciences
University of Birmingham
December 2022

Abstract

The Sec machinery translocates proteins across, or inserts proteins into, the cytoplasmic membrane and is responsible for translocation of approximately 20% of all proteins synthesised by the bacterium *Escherichia coli.* The aim of the work presented in this thesis was to investigate the function, mechanism and structure of a novel component of the Sec machinery, SecH (YecA). SecH contains two structural domains that were identified previously with the aid of bioinformatics: an N-terminal UPF0149 domain and a C-terminal metal binding domain (MBD). The MBD is nearly identical to the C-terminal MBD of the essential ATPase SecA, which mediates the interaction of SecA with the molecular chaperone SecB and with ribosomes. A phylogenetic analysis of the distribution of SecH in different bacterial species presented in this thesis suggested that SecH is strongly co-conserved with SecB. Biochemical and biophysical binding studies indicate that SecH binds to both SecB and ribosomes in a manner that is dependent on the MBD. Structural modelling, size exclusion chromatography and native mass spectrometry indicate that SecH dimerises in solution, and site-specific crosslinking suggests that it forms higher order oligomers *in vivo*. Copurification experiments indicate that SecH interacts with a broad range of client proteins when overexpressed and these include Sec substrates when expressed in strains with a Sec defect. These results are consistent with previous reports suggesting that SecH has molecular chaperone activity. SecH also copurifies strongly with SecA. Biochemical studies suggest SecH does not modulate the ATPase activity of SecA or increase the rate of ADP dissociation in the absence of SecYEG or substrate protein. However, structural modelling suggests that SecH may directly interact with SecA. Taken together, these results suggest that SecH is a novel component of the Sec machinery that interacts with the ribosome, SecB, SecA and also Sec substrate protein.

Acknowledgments

I owe a great deal of gratitude to my supervisor, Dr Damon Huber. From the moment I joined his lab, I received tremendous support and guidance that has helped me develop into a competent scientist. I will never cease to be amazed at the sheer depth of his knowledge and his love of science and I am truly thankful for the opportunity he gave me to work in his lab.

I'd like to thank some of the amazing people in T101 who made working in the lab each day even more fun, including Dr Mat, Dr Fatemah, Dr Kara, Sammi, Dana, Deema, Gabi, Manpreet and Chen. A special thank you is reserved for Dr Mat Milner. From the day I had my interview, you made me feel welcome and a part of T101. You are one of the most selfless people I've worked with and your calm nature and ability to solve any microbiological issue is a true wonder. I'd also like to thank my flatmate and resident mass spectrometry expert Kish. It's been a truly enjoyable 3 years living with you. The countless hours of watching football, cricket and endless other documentaries made living in Birmingham just that little bit more bearable.

Most importantly, I owe everything to my family. Without their support I would never have made it this far. Mum, your constant love and care for me has made me the person I am today. This PhD is as much yours as it is mine. Dad, I am extremely thankful for all the support you have given me for as long as I can remember. Josh, thank you for being an incredibly caring brother. Thank you for always checking up on me and protecting me throughout my life. You really are the best brother I could have asked for. I may have never shown it in the way I ought to, but I deeply love and appreciate you all.

A special thank you also is reserved for extended family members Tony and Sarah for all the support you have given me.

Finally, thank you to Hannah for all your love, kindness and support over the last few years. I have never met someone who understands me so well. You know exactly how to cheer me up in the sad times, comfort me in the hard times and on a daily basis you make me laugh until I can’t breathe. I hope you know how special you are. Here’s to many more years of happiness.

For Grandpa Heinz
(1932-2022)

“Don’t get nervous, you’ve done that all before. But just… slow. Don’t rush. You’ve got time. And think before you write! That’s all I can say. I’m sure you’ll be alright...”

Table of Contents

List of Figures

List of Tables

Chapter 1

Introduction

1.1. Bacterial secretion

Proteins are synthesised by the ribosome in the cytoplasm, however many proteins function outside of the cytoplasm. For example, close to 30% of the entire proteome in *Escherichia coli* is localised outside of the cytoplasm (Driessen and Nouwen, 2008). In gram-negative bacteria, proteins can be localised in the cytoplasm, periplasm, embedded in the inner or outer membrane, or secreted outside the cell. Specialised secretion systems are required to allow the passage of proteins across or into the cytoplasmic membrane. In bacteria, the two principal transport mechanisms across the cytoplasmic (i.e., inner) membrane are the Sec pathway and the twin arginine translocation (Tat) pathway. In *E. coli,* the Sec system is responsible for the translocation of 20% of all synthesised proteins (Cranford-Smith and Huber, 2018). The Sec system can translocate proteins either as they are being translated (coupled translocation), or after they have been translated (uncoupled translocation). Integral membrane proteins constitute 7.5% of synthesised proteins, and are principally translocated *via* the coupled translocated pathway (Cranford-Smith and Huber, 2018). 13.5% of synthesised proteins, however, are translocated through the uncoupled translocation pathway and consist largely of periplasmic and outer membrane proteins (Cranford-Smith and Huber, 2018).

1.2. Signal Sequences

Sec substrates are recognised by virtue of a signal encoded into the primary structure of the protein, called the signal sequence. Signal sequences vary in length from 18 – 30 amino acids (Fekkes and Driessen, 1999).

The signal sequence has three principal components: A N-terminus that is enriched in positively charged amino acids, a hydrophobic central region and a C-terminus that is enriched in polar amino acids (von Heijne, 1990). The positively charged amino-terminus has been suggested to make important electrostatic interactions with the membrane (von Heijne, 1990). Mutations in the N-terminal region to reduce the positive charge cause a reduction in the rate of translocation, but do not completely block translocation (Vlasuk et al., 1983).

The C-terminal polar region is known to be essential for recognition by the membrane-embedded signal peptidase which cleaves the signal sequence during or after translocation (Paetzel et al., 2002). Positions -1 and -3 relative to the polar region are critical for this recognition, where generally only small uncharged amino acids can be present and maintain recognition (Fikes et al., 1990). Many inner membrane proteins that are translocated by the Sec pathway do not contain signal sequences. In these cases, only the periplasmic loops are translocated through the inner membrane. These proteins contain α-helical stop-transfer signals which stops their translocation and ensures they remain in the membrane (von Heijne, 1994).

1.3. Components of the Bacterial Sec System

1.3.1. SecYEG

SecYEG is a multimeric complex that forms a translocation channel, which is responsible for the passage of proteins across the inner membrane. SecYEG is evolutionarily conserved throughout all kingdoms of life, with homologues found in eukaryotes and archaea (Veenendaal et al., 2004). In bacteria and archaea, SecYEG allows passage across the cytoplasmic membrane

whereas its eukaryotic homologues allow transit across the membrane of the endoplasmic reticulum (Greenfield and High, 1999).

SecY is a highly evolutionarily conserved membrane protein that forms the core channel of the translocon (Hartmann et al., 1994). It contains 10 membrane-spanning helices as well as regions that traverse both the cytoplasm and the periplasm (Van den Berg et al., 2004). The structure from *Methanococcus jannaschii* suggests that SecY forms an hourglass shape, with hydrophobic residues permeating at the site of constriction, forming a 'seal' to prevent diffusion of non-substrate molecules (Van den Berg et al., 2004). The second short transmembrane helix, TM2a, functions as a plug, which works by blocking the entrance to a cytoplasmic funnel which allows access to the channel. The signal sequence of secretory proteins is inserted into the channel as a loop and is recognised by transmembrane helices TM2 and TM7 (Van den Berg et al., 2004). SecY also contains a lateral gate involving transmembrane segments 2, 8, 7 and which opens to allow the insertion of membrane proteins into the membrane (du Plessis et al., 2009; Van den Berg et al., 2004).

While not directly involved in translocating substrates, SecE wraps around SecY forming a V-shape, and stabilises SecY (Lycklama a Nijeholt et al., 2013). SecG is not essential for viability but enhances the rate of translocation (Nishiyama et al., 1994). SecG contains a cytoplasmic loop that blocks the entrance to the SecY channel in the absence of SecA (Tanaka et al., 2015).

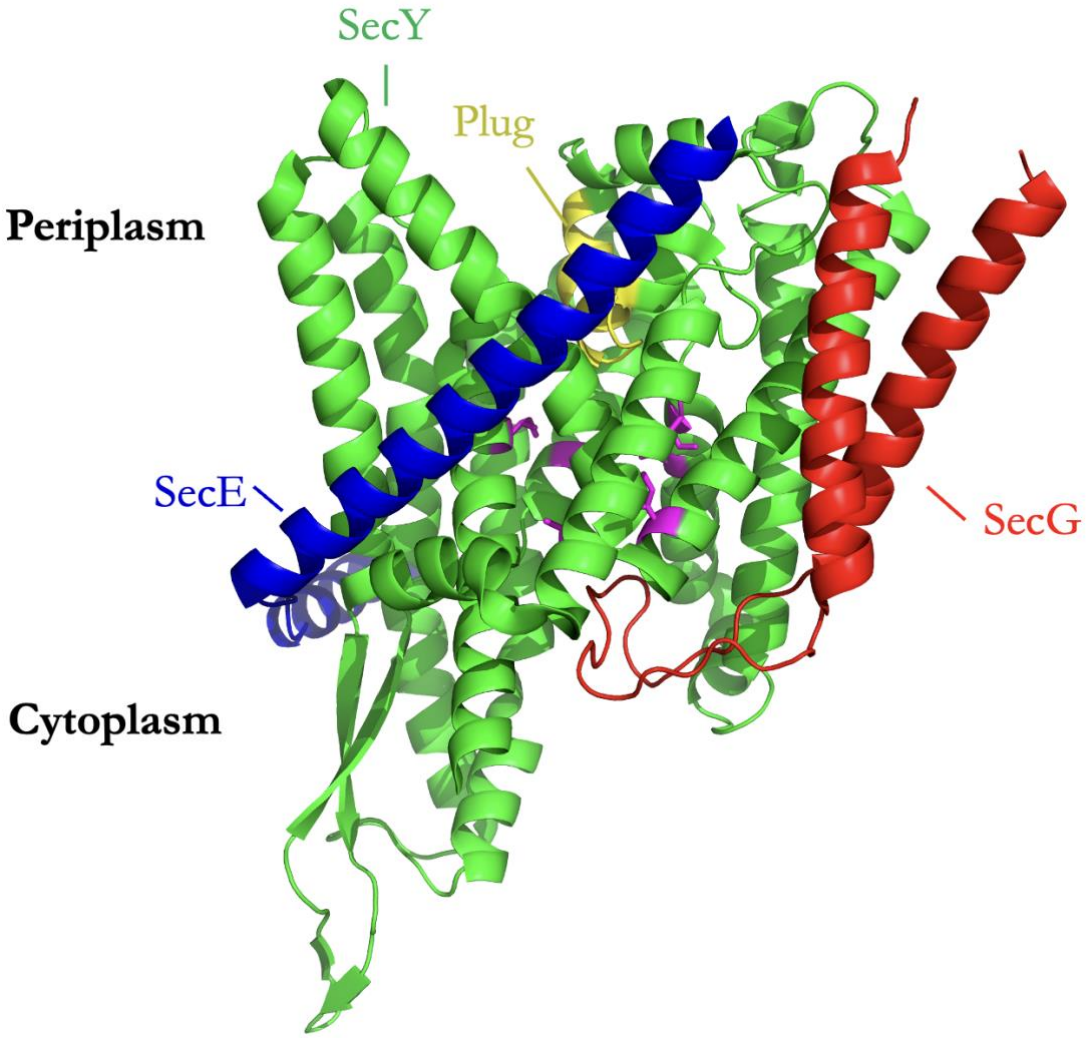

Figure 1 – Crystal structure of SecYEG in its resting state

Crystal structure of SecYEG from *Thermus thermophilus*. SecY, which forms the main protein-conducting channel, is coloured in green. The periplasmic plug is coloured in yellow and the hydrophobic amino acids which form a ring at the site of constriction are coloured in magenta. SecE is coloured in blue. SecG, and the cytoplasmic loop that blocks the entrance to the channel is coloured in red. PBD: 5AWW (Tanaka et al., 2015).

1.3.2. SecA

SecA, is an ATPase found in bacteria that, through the hydrolysis of ATP, functions to facilitate translocation of proteins though the SecYEG channel. In *E. coli,* the SecA monomer is a 102 kDa square-like protein and is comprised of six domains: (i) Nucleotide Binding Domain 1 (amino acids 1 -220 and 378-411) (ii) Pre-protein crosslinking domain (PPXD) (amino acids 221-377) (iii) Nucleotide Binding Domain 2 (amino acids 412-620) (iv) α-helical Scaffold Domain (amino acids 621-672 and 756 -832) (v) α- helical wing domain (amino acids 673-755) (vi) Carboxy-Terminal Linker (amino acids 833-901) (Jamshad et al., 2019).

Nucleotide Binding Domain 1 and 2 confer ATPase activity. NBD 1 and NBD 2 have an overall similar fold, and are proximal to each other, allowing for a nucleotide to bind in the interface between the two domains (Hunt et al., 2002). NBD 1 and 2 are structurally similar to DEAD-box proteins, a protein family which contains RNA helicases. DEAD refers to the consensus motif DExD/H in the Walker B motif (amino acids 205-227) that is responsible for nucleotide binding (Mitchell and Oliver, 1993). In *E. coli,* valine is present instead of alanine, giving the motif DEVD.

The PPXD was initially identified by crosslinking studies as an interacting site for preprotein and for signal peptide (Kimura et al., 1991) (Musial-Siwek et al., 2007). The PPXD is structurally very flexible, and this movement allows for opening and closing of a clamp that is formed with NBD 1 and NBD 2 that traps substrates (Zimmer and Rapoport, 2009). The PPXD is responsible for a large proportion of the interaction of SecA with SecY (Zimmer et al., 2008).

The HSD consists of an alpha helix that extends from the NBD1 to the HWD as well as a two-helix finger (2HF). The HSD is involved in protein-protein interactions, functioning as part of the interface of the SecA dimer, whilst also making contacts with SecY during translocation (Hunt et al., 2002; Zimmer et al., 2008). The helices of the 2HF, in the open conformation, protrude from SecA, and are inserted into the pore of SecYEG during translocation (Zimmer et al., 2008). The helical wing domain (HWD) is situated on one corner of the square-like SecA. It consists principally of α-helices and sits between the 2HF and the HSD.

At the extreme C-terminus is a highly flexible subdomain, the C-Terminal Tail (CTT). The CTT is comprised of a metal binding domain (MBD) and a disordered flexible linker domain (FLD). It has been suggested that the CTT plays a role in regulating SecA activity. Crosslinking studies propose that the FLD binds to the substrate-binding region, autoinhibiting SecA (Jamshad et al., 2019).

The MBD contains a $CXCXSX_3\Omega X_2C(H/C)$ motif which coordinates a metal ion *via* three cysteines, a serine and a histidine residue (Ω corresponds to aromatic amino acids) (Cranford-Smith et al., 2020; Dempsey et al., 2004). The MBD confers the ability to bind SecB and interact with the ribosome (Fekkes et al., 1997; Jamshad et al., 2019). The almost-invariant serine is important for determining the preference of the MBD for iron binding as well as for correct folding of the MBD (Cranford-Smith et al., 2020).

SecA is conformationally dynamic. In the open conformation, the PPXD (Figure 2, red) is distant from the HWD (Figure 2, yellow) and closer to NBD 2 (Figure 2, green). In the closed conformation, the PPXD is no longer in proximity to NBD 2, rotating away and bringing it

close to the HWD. The open conformation refers to the opening of the clamp, where substrates can bind in between the PPXD, NBDs and HSD (Zimmer et al., 2008). Upon binding to SecYEG, SecA undergoes a large conformational change. The PPXD makes a large rotation away from the HWD to the NBD 2, and the 2HF protrudes into SecYEG (Zimmer et al., 2008). The conformational changes result in an increase in SecA ATPase activity by reducing the affinity of SecA for ADP (Robson et al., 2009).

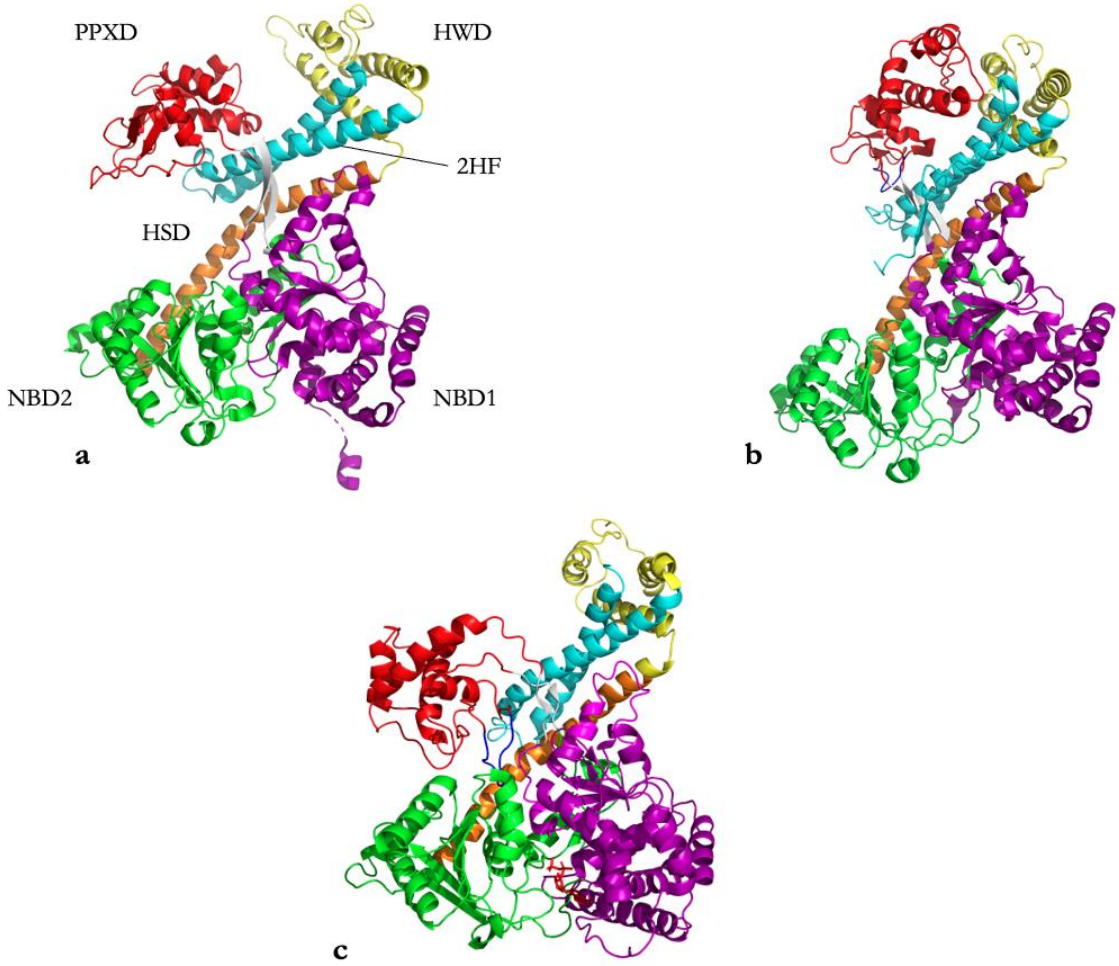

Figure 2 - Structures of SecA in different conformations.

The nucleotide binding domains I and II are in purple and green respectively. The helical scaffold domain is in orange, and the 2 helical finger is in cyan. The PPXD is in red, and the helical wing domain is in yellow. The loop of the PPXD that contacts the two nucleotide binding domains is highlighted in blue. The C-terminal tail is flexible and is therefore unresolved in crystal structures **a)** SecA from *Bacillus subtillis* in an open conformation, bound to ADP (PDB: 1TF2). **b)** SecA from *Bacillus subtilis* in a closed conformation, with the PPXD sitting up against the HWD (PBD: 1M6N). **c)** SecA from *Thermotoga maritima* when bound to SecY. The PPXD swings from the HWD to the NBDs and the PPXD loop (blue) contacts the NBDs (Zimmer et al., 2008) (PBD:3DIN).

1.3.2.1. MECHANISM OF SECA-DEPENDENT TRANSLOCATION THROUGH SECYEG

The mechanism by which SecA couples its ATPase activity to power preprotein translocation through SecYEG remains unclear, with several proposed mechanisms: The power stroke model, the Brownian ratchet model, and a unifying model. The ATPase activity of SecA is stimulated in several different ways. Binding to phospholipids, SecB, SecYEG and preproteins all stimulate SecA ATPase activity (Lill et al., 1990; Miller et al., 2002). In its cytoplasmic state, SecA is ADP bound, with a low ATPase activity (Sianidis et al., 2001). The ADP-bound state of SecA is very stable, and ADP release is the rate limiting step in its ATPase cycle (Fak et al., 2004).

The power stroke model was the first model to be proposed and has since been refined. It suggests a purely mechanical mechanism of conformational changes that physically push preprotein through SecYEG. When bound to ADP, SecA is in the open conformation, with the 2HF not inserted into SecYEG. Either ATP binding or hydrolysis causes clamp closure around the preprotein and insertion of the 2HF into SecYEG which actively pushes the nascent protein through the channel which occurs *via* a conserved tyrosine on the end of the 2HF which has been shown to crosslink to polypeptide chains (Catipovic et al., 2019; Erlandson et al., 2008).The 2HF retracts after ATP hydrolysis, and phosphate release causes the clamp to return to the open conformation. This model does not account for backsliding, as SecA is usually ADP-bound, where the clamp will be open therefore not interacting with the polypeptide and preventing reverse diffusion back through the channel. A ‘Push and Slide’ mechanism has further refined this model to account for backsliding of the preprotein (Bauer et al., 2014). In

this model, the 2HF interacts with only a subset of amino acids. Therefore, when faced with non-interacting amino acids, a power stroke may not lead to a pushing of the preprotein into SecYEG. Upon ATP hydrolysis, the 2HF retracts allowing the preprotein to diffuse in either direction. This diffusion would continue to occur until the 2HF contacts amino acids it is able to recognise, and a power stroke would occur.

In the Brownian ratchet model, the 2HF of SecA plays a key regulatory role in sensing and controlling diffusion of preprotein through SecYEG (Allen et al., 2016). SecA binding to SecYEG primes the channel, causing the channel to remain partially open. This allows restricted diffusion of less-bulky amino acids through the pore *via* Brownian motion. The presence of bulky amino acids, e.g., tryptophan, form blocks which cannot fit through the restricted aperture of SecYEG. The 2HF senses these blocks and through a conformational change, stimulates ADP release. ATP binding widens the aperture of the pore, allowing free diffusion of substrate again, before ATP hydrolysis narrows the channel. This prevents backsliding of already-translocated bulky amino acids in the periplasm back through the channel. Further, a proton-ratchet mechanism to aid Brownian motion has been suggested (Allen et al., 2022). The proton-motive force in *E. coli* causes a net negative electrochemical charge (and higher pH) on the cytoplasmic side of the membrane and is known to be important for Sec-mediated translocation (Schiebel et al., 1991). The electrochemical potential difference promotes diffusion of negatively charged amino acids through the channel. Given the relatively high pH at the cytosolic side of the membrane, lysine can be deprotonated before entering the channel, removing its positive charge, enhancing diffusion through the pore. When entering the lower pH environment of the periplasm, the lysine side chain can be re-protonated, restoring its

positive charge, biasing it against diffusing back towards the negative cytoplasmic side of the membrane (Allen et al., 2022).

The third proposed model is reciprocating piston mechanism (Kusters and Driessen, 2011). This model integrates both the ATP-powered mechanical pushing and passive diffusion. In this model, SecA binds to SecYEG as a dimer. One protomer actively interacts with the translocon whereas the second protomer interacts solely with the SecYEG-bound SecA. The dimerisation allows the PPXD of both protomers to contact the preprotein. ATP binding to SecA causes insertion of the signal sequence into the channel and release of SecB from SecA. Upon ATP hydrolysis, SecA then monomerises as one protomer dissociates. The conformational change caused by ATP hydrolysis allows for the first preprotein translocation step into the channel. It is then suggested that a soluble SecA protomer rebinds to SecYEG-bound SecA and captures part of the untranslocated preprotein. This capturing then allows for free diffusion by Brownian motion unidirectionally through the channel. ATP binding then causes a power stroke, further pushing the polypeptide through the pore. ATP hydrolysis causes SecA monomerization again and the processive cycle continues until completion.

1.3.2.2. NUCLEOTIDE EXCHANGE FACTORS

Nucleotide exchange factors (NEFs) are present across all domains of life, and act upon enzymes that hydrolyse adenosine triphosphate (ATP) and guanosine triphosphate (GTP) (Bracher and Verghese, 2015; Packschies et al., 1997; Raimo et al., 1999). Despite this, there are currently no known NEFs that act upon SecA (Fak et al., 2004). Molecular machines, such

as SecA, can use ATP as a source of power. Hydrolysis of the γ-phosphate releases energy which is utilised to power processive conformational cycles of motor proteins. ATPases start off their cycle by binding to ATP. The γ-phosphate is hydrolysed, the phosphate group is released, and the protein remains bound to adenosine diphosphate (ADP). ADP is released allowing the cycle to continue upon rebinding of ATP.

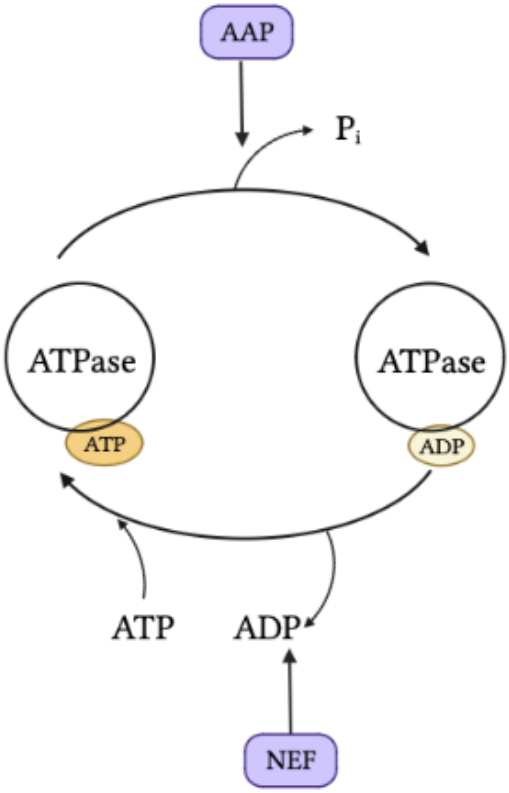

Figure 3 - General ATP cycle of an ATPase.

ATP-bound ATPase hydrolyses ATP, releasing inorganic phosphate. This step can be stimulated by ATPase activating proteins (AAP). The ATPase is then bound by ADP, which it must release in order to rebind another ATP. This step is stimulated by nucleotide exchange factors (NEFs).

The cycles of ATPases can be controlled by additional proteins. ATPase activating proteins (AAPs) improve the ATPase rate by directly improving the rate of hydrolysis of ATP. Conversely, nucleotide exchange factors decrease the affinity of ADP to the motor protein, increasing the rate at which ADP can dissociate, allowing ATP to rebind. In *E. coli*, the best characterised NEF is GrpE, which is a NEF for DnaK (Packschies et al., 1997) .

GrpE is essential for viability (Ang and Georgopoulos, 1989). GrpE interacts with DnaK as dimer and interacts with a large area across the face of DnaK. GrpE does not directly contact the nucleotide binding cleft. Instead, binding of GrpE induces conformational changes in DnaK which causes DnaK to 'open', which disrupts the nucleotide binding site (Harrison et al., 1997). The interaction between GrpE and Dnak stimulates the rate of ADP release 5000-fold (Packschies et al., 1997) .

1.3.3. SecB

SecB, a homotetrameric chaperone, is responsible for maintaining a subset of secretory proteins in an unfolded state. SecB is present in all α-, β- and γ-proteobacteria (van der Sluis and Driessen, 2006).

Crystal structures of SecB from *E. coli* and *Haemophilus influenzae* show that SecB assembles as a tetramer by forming a dimer of dimers (Dekker et al., 2003; Xu et al., 2000). The tertiary structure of SecB is comprised of 4 antiparallel β-sheets, with two α- helices connected by an 11-residue loop (Xu et al., 2000). Monomers assemble into dimers through an interaction of the first β-sheet with the first α- helix. The dimer is then stabilised through hydrogen bonds

between the two opposing β-sheets. Two dimers then form a tetramer *via* polar interactions of the side chains of amino acids from the first α- helix.

SecB binds almost exclusively to unfolded proteins, and does so with low specificity *in vitro*, but high affinity (Randall and Hardy, 2002). *In vivo,* however, SecB shows high specificity (Kumamoto and Francetic, 1993). SecB binds to hydrophobic patches in the mature region of preproteins, without recognising the signal sequence (Huang et al., 2016). SecB client proteins interact with SecB by wrapping around SecB, and the SecB client-binding regions can accommodate up to 250 interacting residues (Huang et al., 2016).

Early evidence indicated that SecB recognises substrates and transfers them to SecA for translocation through the SecYEG channel (Hartl et al., 1990). Indeed, SecB does interact with SecA (den Blaauwen et al., 1997). However, it has recently been shown that the interaction between SecB and nascent polypeptides is dependent on SecA interacting with the ribosome (Huber et al., 2017). This suggests that SecA interacts with nascent proteins before SecB, and may therefore explain why, *in vivo,* SecB shows high selectivity.

SecB mutants show defects in translocation, and a cold-sensitive phenotype (Francetic and Kumamoto, 1996; Wild et al., 1993). Interestingly, the translocation defects extend to proteins that are not usually SecB clients (Francetic and Kumamoto, 1996). When overexpressed, SecB rescues aggregation and temperature sensitive phenotypes of both DnaK and Trigger Factor mutants, indicating SecB may also function as a general chaperone (Ullers et al., 2004).

1.3.4. Signal Recognition Particle (SRP)

The SRP is a cytoplasmic ribonucleoprotein complex that consists of a GTPase subunit, fifty-four homologue (Ffh) and 4.5S RNA (Rosenblad et al., 2003). Ffh consists of three domains, G, N and M. The N- domain exists as a collection of 4 helices, adjacent to the G-domain, which confers GTPase activity. The M domain is located at the carboxy terminus, connected by a 30 amino acid linker and contains 5 α -helices which together form a binding site for the signal sequence (Freymann et al., 1997; Hainzl et al., 2011).

The SRP recognises and binds nascent chains with hydrophobic signal sequences as they emerge from the ribosome, forming a ribosome-nascent chain complex (RNC) (Janda et al., 2010). This interaction is mediated by Ffh. The SRP binds to the ribosome close to the ribosome exit tunnel. The NG domain of Ffh binds nearby ribosomal proteins uL23 and uL29. The M domain also interacts with uL23, and the 4.5S RNA makes contact with ribosomal protein bL32 (Jomaa et al., 2016; Schaffitzel et al., 2006).

The SRP recognises signal sequences that are highly hydrophobic (Lee and Bernstein, 2001). RNC-SRP complexes recruit and bind FtsY. FtsY, known as the SRP receptor, is a peripheral membrane protein that interacts with SecYEG (Angelini et al., 2005). FtsY contains three domains: an N-terminal A domain, as well as the N and G domains which are homologous to those present in FtsH (Luirink and Sinning, 2004). FfH interacts with FtsY to delivery RNCs to the membrane-bound SecYEG *via* the N-G domain present in both proteins (Egea et al., 2004).

1.3.5. YidC

In *E. coli,* SecYEG forms a super-complex in the cytoplasmic membrane with the integral membrane proteins SecD, SecF, YajC and YidC (Schulze et al., 2014). These proteins are non-core components that play various roles in assisting the translocation machinery (Martin et al., 2019).

YidC, a membrane protein insertase, and its homologues are conserved across all domains of life, though its function has not been fully elucidated (Zhang et al., 2009). As well as working in tandem with SecYEG, YidC can also function as membrane protein insertase with Sec-independent substrates (Serek et al., 2004). Independently, the YidC family are known to assist in the insertion of respiration-related proteins, including the F_1 F_0 ATP synthase subunit c (van der Laan et al., 2004). However, evidence shows SecYEG and YidC are both required for efficient insertion of subunits a and b of F_1F_0 ATP Synthase (Yi et al., 2004). Subunit a of cytochrome c oxidase also requires the Sec-dependent YidC pathway for insertion (du Plessis et al., 2006). Together, this points to an important role of YidC in assembling respiration-related complexes.

1.3.6. SecDF

SecD was discovered in a genetic screen which resulted in cold-sensitive phenotypes and defects in protein translocation (Gardel et al., 1987). It was later found, through complementation experiments, that the *secD* locus contains two different genes, *secD* and *secF* (Gardel et al., 1990).

The high-resolution structure of SecDF from *Thermus thermophilus* shows that SecDF is comprised of a single polypeptide that forms 12 transmembrane helices and 6 periplasmic

sections (P1-P6) (Tsukazaki et al., 2011). P1 and P4 form separate domains. P1 consists of a head and base region linked by a hinge, and the P4 domain consists of a ferredoxin-like domain. The head of P1 domain has been suggested to interact with preprotein to prevent backsliding (Tsukazaki et al., 2011). The interface between SecD and SecF contains charged residues which allows the flow of protons, and the flow protons through SecDF is essential for its function (Tsukazaki et al., 2011).

The SecDF complex catalyses translocation. The rate of translocation both *in vitro* and *in vivo* is slower in the absence of the SecDF complex (Nouwen et al., 2005; Pogliano and Beckwith, 1994a). The large periplasmic loop of SecD is important for stimulation of translocation. Deletion of this loop decreases the rate of proOmpA translocation *in vitro* (Nouwen et al., 2005).

1.3.7. YajC

yajC, located on the *secD* operon together with *secD* and *secF*, encodes a 12 kDa integral membrane protein (Pogliano and Beckwith, 1994b). YajC is found as part of the holotranslocon, a large super complex, consisting of SecYEG-SecDF-YajC-YidC (Komar et al., 2016). While the exact function of YajC remains unclear, it has been shown that YajC forms a functional complex with SecDF *in vivo* (Duong and Wickner, 1997). The SecDF-YajC complex has a functional interaction with SecG, enhancing its stabilisation (Kato et al., 2003).

1.4. The Role of Molecular Chaperones in Translocation

The majority of soluble periplasmic and outer membrane proteins are translocated through the uncoupled translocation pathway i.e., they are fully, or almost fully synthesised before

translocation. In the absence of chaperones, proteins tend to fold into their native states, or misfold and aggregate. Sec translocation is only permissible to unfolded proteins, which therefore necessitates the presence of chaperones, such as SecB, which bind to nascent substrates and prevent premature cytoplasmic folding.

To effectively deal with both folding and unfolding of nascent proteins, many cytoplasmic chaperones are present in bacteria with varying functions. Foldases, in an ATP-dependent manner, assist in the folding of proteins, and include GroEL/GroES and DnaK. In contrast deaggregases, such as ClpB, assist in the de-aggregation of protein aggregates (Schlee et al., 2001). Other chaperones, often referred to as holdases, exhibit anti-folding activity, and function in an ATP-independent manner to prevent folding, aggregation or proteolytic degradation.

In *E. coli*, the chaperone Trigger Factor interacts with the ribosome and can bind to many nascent Sec substrates, including maltose binding protein and β-lactamase (Hoffmann et al., 2012). The largest subset of Trigger Factor substrates is outer membrane proteins (Oh et al., 2011). Deletion of the *tig* gene *in vivo* accelerates the rate of translocation of SecB substrates. Indeed, overexpression of Trigger Factor delays the translocation of OmpA (Lee and Bernstein, 2002). This suggests Trigger Factor plays a role in delaying the entry of secretory proteins into the translocation pathway. Further to this, *tig* inactivation can supress the translocation defects of a *secB* mutant, likely by allowing earlier entry into the secretory pathway (Ullers et al., 2007).

The DnaK/DnaJ chaperone system is a generalised chaperone system in *E. coli*, responsible for assisting the folding of a myriad of cytoplasmic proteins. The chaperone system is also responsible for aiding refolding of non-native proteins and preventing protein aggregation. In

this system, DnaJ (Hsp40) delivers unfolded or misfolded client proteins to DnaK (Hsp70). The ATPase DnaK, once bound to DnaJ and substrate protein, can hydrolyse ATP. ATP hydrolysis stimulates a conformational change driving protein refolding. The homodimeric protein GrpE is responsible for regulating nucleotide exchange (Rosenzweig et al., 2019). The DnaK/J system also binds to aggregated clients, serving as a molecular crowbar to pry out individual polypeptides with the assistance of ClpB (Goloubinoff et al., 1999). Overexpression of DnaK can also increase the efficiency of export of Sec substrates (Phillips and Silhavy, 1990). Overexpression of DnaJ is also sufficient to supress the cold-sensitive phenotypes of secB mutants, highlighting the role of the chaperone system in maintaining Sec substrates in a translocation-competent state (Sakr et al., 2010).

The GroEL/GroES chaperone system is one of the best-characterised chaperone systems in *E. coli.* Non-native proteins bind a ring the cavity of the large subunit GroEL. Binding of the GroES cap to GroEL induces ATP hydrolysis and a conformational change, altering the chemical environment of the folding cavity, which is thought to promote protein folding (Horwich et al., 2006). Evidence suggests that this system is involved in Sec-dependent translocation. Overexpression of GroEL improves the efficiency of Sec-dependent export of LamB *in vivo* in a β-galactosidase assay (Phillips and Silhavy, 1990). GroEL and GroES mutants can also cause defects in Sec substrate export (Kusukawa et al., 1989).

1.5. Translocation Pathways

In bacteria, there are two principal Sec-translocation pathways: coupled translocation and uncoupled translocation (Oswald et al., 2021). Signal sequences are required for proteins entering the Sec translocation pathway. Sec substrates are sorted into the different secretory pathways by virtue of differences in the properties of the signal sequence. The hydrophobicity of the signal sequence is the principal determining factor in pathway entrance. The SRP recognises both highly hydrophobic signal sequences as well transmembrane helices (Tsirigotaki et al., 2017). If not recognised by the SRP, SecA and trigger factor then interact with the signal sequence. Recently, it has been discovered that some mature domains of preproteins are essential for translocation and may be recognised by SecA (Chatzi et al., 2017). Preproteins may completely evade ribosome-bound proteins and instead bind to cytoplasmic chaperones including SecB, which recognises a 9 amino acid motif that contains basic and aromatic side chains (Sala et al., 2014). Together with the protein machinery, translocation of nascent proteins is driven by the proton motive force (PMF) and the hydrolysis of ATP (Schiebel et al., 1991).

1.5.1. Coupled Translocation

Coupled translocation (Figure 4) is the mechanism whereby protein translation and protein translocation occur simultaneously. This pathway is principally mediated by the SRP. The SRP binds to the ribosome and recognises highly hydrophobic signal sequences, forming an RNC-SRP complex. The SRP delivers Sec substrates to the SecYEG by interacting with peripheral membrane protein FtsY (Draycheva et al., 2018). FtsY interacts with SecYEG on two cytosolic loops, C4 and C5 (Kuhn et al., 2011). This forms the SecYEG-FtsY-SRP-RNC quaternary

complex, which leads to GTPase activation. Hydrolysis of GTP ultimately allows for insertion of preproteins into the SecYEG channel, and SRP and FtsY dissociate and are recycled back into the cytoplasm (Saraogi et al., 2014).

1.5.2. Uncoupled Translocation

The second mechanism of protein transport through SecYEG is uncoupled translocation (Figure 4), which occurs independently of protein translation, and it is mediated by the ATPase SecA. In bacteria, the majority of Sec substrates are translocated *via* the uncoupled translocation pathway, including outer membrane proteins and periplasmic proteins (Cranford-Smith and Huber, 2018). Ribosome-bound SecA recognises nascent peptides cotranslationally through its interaction with ribosomal protein uL23, close to the ribosome exit channel (Huber et al., 2011; Jamshad et al., 2019). The molecular chaperone SecB is then recruited to nascent substrate proteins by SecA (Huber et al., 2017). SecB then delivers preproteins to SecA-bound SecYEG for translocation across the inner membrane.

The molecular chaperone Trigger Factor binds to ribosomes and scans for nascent substrates. Trigger Factor and the SRP can both be bound to the ribosome simultaneously and screen emerging preproteins (Bornemann et al., 2014). Trigger Factor binds to hydrophobic patches on emerging preproteins with adjacent positively charged amino acids, which weakens the SRP-RNC interaction, ultimately excluding these proteins from the coupled translocation pathway (Bornemann et al., 2014; Patzelt et al., 2001). It is not yet clear how preproteins bound by TF are then targeted to the Sec machinery.

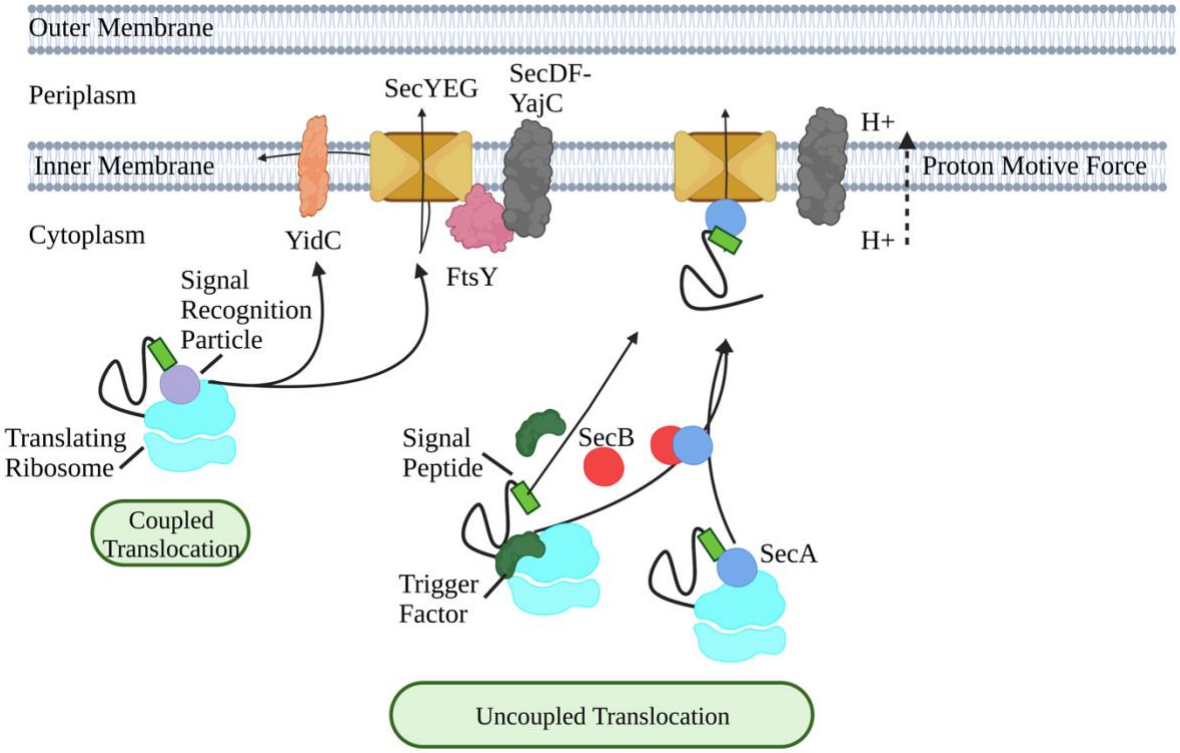

Figure 4 - Bacterial Sec secretion.

Coupled translation mediated by SRP (purple) delivers the RNC to SecYEG and YidC (orange) *via* its receptor FtsY. Substrates can pass through the SecYEG channel into the periplasm or enter the lipid phase through the lateral gate. Uncoupled translocation is often mediated by chaperones, including ribosome-bound Trigger Factor (green), and SecB (red) which binds to substrates in the cytoplasm. SecA (blue) binds to substrates whilst bound to the ribosome. Once delivered to the membrane, substrates are translocated in a SecA-dependent fashion. Figure adapted from (Tsirigotaki et al., 2016) and made in BioRender.

1.6. Quality Control

1.6.1. SecYEG Jamming

Substrates passing through the SecYEG can become stuck, blocking the channel (Bieker et al., 1990). Ribosome stalling also causes translocon jamming during coupled translocation. Jammed translocons are dealt with by the membrane embedded protease FtsH, which proteolytically degrades jammed SecYEG (van Stelten et al., 2009). The toxicity of SecYEG jamming is suppressed by the induction of the Cpx pathway, a two-component system that regulates gene expression in response to cell envelope stress, including expression of YccA (Cosma et al., 1995; Price and Raivio, 2009). YccA inhibits the protease FtsH, supressing the toxic effects of SecYEG degradation as a result of jamming (van Stelten et al., 2009).

1.6.2. Mislocalisation of Sec Substrates

Sec substrates can sometimes escape sorting pathways and become mislocalised in the cytoplasm. Sec substrates that accumulate in the cytoplasm can be degraded by Lon protease, including proOmpF and proOmpC (Sakr et al., 2010). Indeed, in the absence of Lon protease Sec substrates accumulate in the cytoplasm (Sakr et al., 2010).

1.6.3. SecY Proof Reading

SecY itself also has an intrinsic quality control mechanism. Suppressor mutants named prl were isolated which permitted export of preproteins that did not contain signal sequences (Smith et al., 2005). *PrlA* mutants in SecY were found to be capable of exporting signal sequence-less maltose binding protein (Derman et al., 1993). It has been demonstrated that outer membrane proteins OmpF and OmpC lacking a conserved motif are not fully translocated to the periplasm. When using the *PrlA* mutants, however, the translocation defect is supressed (Jung et al., 2020).

This suggests SecY plays a quality control role ensuring defective outer membrane porins do not reach the outer membrane.

1.6.4. Cell Stress Responses

Destruction of SecYEG complexes can lead to cell stress by causing an increase in concentration of untranslocated preprotein in the cytoplasm (Oswald et al., 2021). Temperature-induced stress can also lead to an accumulation of aggregated proteins (Arsene et al., 2000). In order to deal with this, cells express σ-32 – a sigma factor that enhances transcription of specific genes (Grossman et al., 1987). Mutations in the *secB* gene lead to the induction of the σ-32 pathway, due to the accumulation of Sec proteins in the cytoplasm (Wild et al., 1993). Upon induction, σ-32 dissociates from its usual state bound to DnaK/DnaJ and associates with RNA polymerase, promoting transcription of heat shock proteins including chaperones DnaK and GroEL (Chakraborty et al., 2014). The σ-32 pathway also modulates expression of FtsH and Lon protease, which play key roles in Sec quality control, including destruction of jammed SecYEG and degradation of accumulated Sec substrates (Jiang et al., 2021).

1.7. SecH (YecA)

SecH (Uniprot: P0AD05) is a protein of unknown function that contains a C-terminal MBD that is homologous to the C-terminal MBD in SecA that interacts with both SecB and ribosomes. Recent evidence suggests that SecH assists in Sec-dependent translocation (Smith et al., 2020). SecH contains two domains: The N-terminal domain of unknown function, UPF0149 and the C-terminal MBD which is nearly identical to the SecA MBD (Figure 5).

The structure of the UPF1049 in SecH is unknown. However, small angle x-ray scattering (SAXS) analysis of SecH suggests that, in solution, SecH is monomeric (Cranford-Smith, 2018). In contrast, high-resolution structural models of other UPF0149 domain proteins suggest that the UPF0149 domain forms homodimeric complexes (Michalska et al., 2012).

The UPF0149 domain is found in both SecH proteins and YgfB proteins. Though the function of YgfB remains unknown, it has been suggested to interact with RNA polymerase (Malecki et al., 2014). YgfB has also been suggested to be involved in multidrug resistance in *Pseudomonas aeuginosa,* by promoting expression of beta lactamase *ampC* (Sonnabend et al., 2020). *In vitro*, *E. coli* SecH prevents aggregation of porcine citrate synthase, suggesting it functions as a chaperone with holdase activity (Smith et al., 2020).

SecA interacts with SecB via the MBD on the extreme carboxyl-terminus of SecA, suggesting the MBD of SecH also interacts with SecB (Jamshad et al., 2019). Further, experiments using transposon-directed insertion-site sequencing (TraDIS) can identify which genes are essential for survival. A library of 500,000 mutants with the Tn5 transposon inserted at random sites was

created in a Δ*secH* mutant and was sequenced. No insertions were found in *secB,* indicating SecB becomes essential in the absence of SecH. This suggests SecB and SecH have overlapping functions. Indeed,

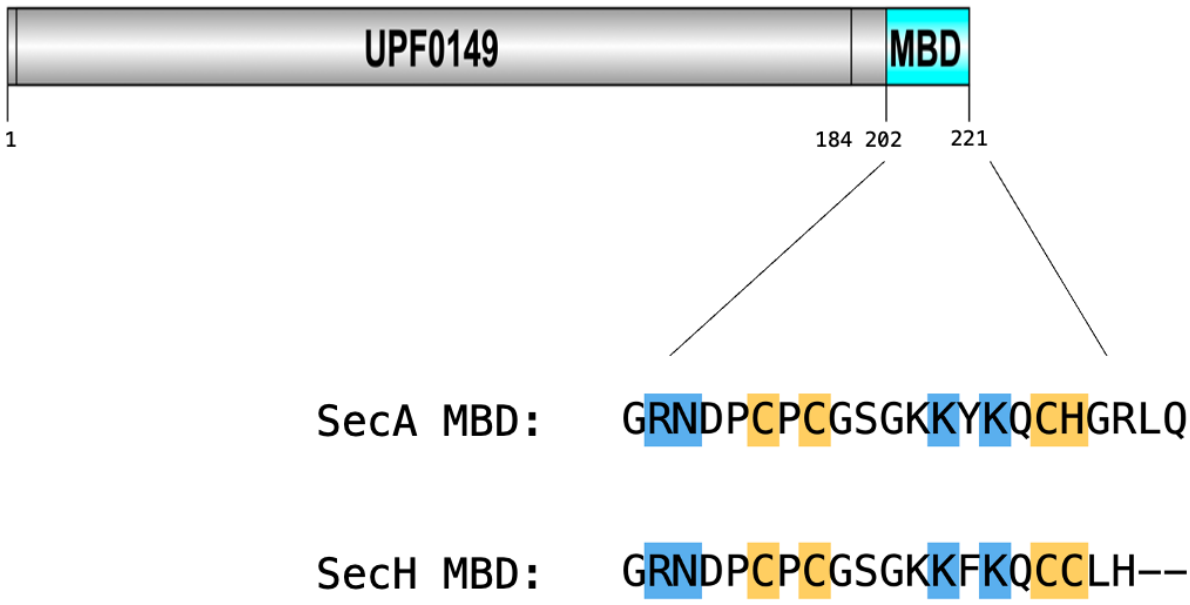

Figure 5 - Domain organisation of SecH

SecH contains 2 domains: an N-terminal UPF1049 domain from position 1 to 184 and a 20 amino C-terminal MBD from position 202 to 221. A sequence alignment of the MBD of SecA and SecH (CLUSTAL Omega) indicates the two domains have high sequence similarity. The amino acids in the SecA MBD that contact SecB (Zhou and Xu, 2003), highlighted in blue, are identical in SecH. The metal-coordinating residues (Zhou and Xu, 2003), highlighted in yellow ,are all identical, except for the replacement of histidine in SecA with cysteine in SecH.

in BW25113, a Δ*secH*Δ*secB* double mutant is not viable (Smith et al., 2020). However, a Δ*secH* Δ*secB* double mutant can be introduced in MG1655. In this mutant strain, both the cold-sensitive phenotype and the cell envelope defect are enhanced compared to a Δ*secB* mutant. These data indicate SecB and SecH have an overlapping role, giving credence to the idea that SecH is in fact a novel component of the Sec pathway.

SecH plays an unknown role in Sec-dependent translocation. In a β-galactosidase assay, LacZ is fused to MalE, which encodes MBP, a periplasmic Sec substrate, thereby targeting β-galactosidase to the periplasm and rendering it inactive. β-galactosidase activity is significantly increased in a Δ*secH* mutant compared to its parent strain, indicating deletion of SecH leads to translocation defects (Smith et al., 2020). Overexpression of SecH in this assay leads to a decrease in β-galactosidase activity, suggesting SecH assists in Sec-dependent translocation. However, in a Δ*secB* mutant, overexpression of SecH leads to an increase in β-galactosidase activity, suggesting SecH inhibits translocation in the absence of SecB. SecH increases the translocation-coupled ATPase activity of SecA, suggesting SecH may deliver substrate protein to SecA (Cranford-Smith, 2018).

1.8. Aims and Objectives

The aim of the work presented in this thesis was to investigate the function, structure and molecular mechanism of SecH. Data on both the function and structure of SecH is scarce. Although it is known that SecH assists Sec-dependent translocation, there is no current

understanding of its mechanism. The majority of SecH consists of a domain of unknown function, and therefore there is no information on its predicted function or interaction partners. The rest of SecH comprises a SecA-like MBD, however whether it functions in a similar manner or makes the same interacts as it does in SecA is currently unknown.

This study aims to further characterise the structure and function of SecH through investigations of its two domains. This study will first investigate the MBD of SecH to determine its similarity to the SecA MBD. Using structural modelling, the structure of the MBD and SecH as a whole will be investigated, with the aim to determine whether the protein: protein interactions made in the SecA MBD can be made in the SecH MBD. Further, the interactions of the SecH MBD will be investigated and characterised using biochemical and biophysical *in vitro* and *in vivo* assays.

Aided by structural insights, this study also aims to characterise the protein: protein interactions made by the UPF1049 domain using biochemical assays including photo-crosslinking. The oligomeric state of SecH will also be investigated, using *in vitro* and *in vivo* experiments together with structural modelling. Probing the structure and the interactions of the UPF0149 will aid in the understanding of the role of SecH in the Sec pathway and the substrates with which it interacts.

Chapter 2

Materials and Methods

2.1. Media and Growth Conditions

Lysogeny broth (LB) was used for all bacterial growth, comprising of NaCl 10 g/L, Tryptone 10 g/L and Yeast Extract 5 g/L. Overnight cultures were grown in 5 mL LB in 30 mL plastic universal containers. Cultures were then grown in 2 L plastic flasks in a shaking incubator at 180 rpm.

LB agar comprised of 1% (w/v) agar in LB. Bacteria on LB agar plates were grown at 37˚C unless otherwise stated. Antibiotics were used at concentrations of: Ampicillin 200 μg/mL, Kanamycin 50 μg/mL and Chloramphenicol 25 μg/mL.

2.2. Strains and Plasmids

Table 1- Strains used in this Study.

Name	**Description**	**Reference/ Source**
E. coli *DH*5α	F$^-$ *endA1 glnV44 thi-1 recA1 relA1 gyrA96 deoR nupG purB20* φ80d*lacZ*ΔM15 Δ(*lacZYA-argF*)U169, hsdR17($r_K^-m_K^+$), λ$^-$	Lab Stock
E. coli BL21(DE3)	*E. coli* str. B F$^-$ *ompT gal dcm lon hsdS*$_B$($r_B^-m_B^-$) λ(DE3 [*lacI lacUV5-T7p07 ind1 sam7 nin5*]) [*malB*$^+$]$_{K\text{-}12}$(λ^S)	Lab Stock
E. coli BTH101	*cyaA* mutant for Bacterial Two Hybrid screens	(Karimova et al., 1998)
MAW012	BL21(DE3) Δ*secB*	This study

Table 2 - Plasmids Used in this Study.

Name	Description	Reference/Source
pTCS070	pCA528-His6 -SUMO-*secH*	(Cranford-Smith, 2018)
pCS071	pCA528-His6 -SUMO-*secHΔMBD*	(Cranford-Smith, 2018)
pDRH625	pCA528-His6-SUMO-*secA*	(Huber et al., 2011)
pDRH585	pCA528-His6-SUMO-*secB*	(Huber et al., 2011)
pKT25	Expresses T25 fragment of *Bordetella pertussis* adenylate cyclase	(Karimova et al., 1998)
pUT18C	Expresses T18 fragment of *Bordetella pertussis* adenylate cyclase	(Karimova et al., 1998)
pMAW002	pKT25-*secB*	This study
pMAW003	pUT18C-*secH*	This study
pMAW004	pUT18C-*upf0149*	This study
pMAW005	pUT18C-*secHMBD*	This study
pMAW010	pUT18C-*secACTT*	This study
pCP20	Contains FLP recombinase	(Datsenko and Wanner, 2000)
pSUP-BpaRS-6TRN	Contains gene encoding amber suppressor tRNA and mutant tyrosyl-tRNA synthetase required for incorporation of Bpa.	(Datsenko and Wanner, 2000)
pMAW017	pCA528-His6-SUMO- *secH*-W13Am-AviTag	This study
pMAW018	pCA528-His6-SUMO- *secH*-H25Am-AviTag	This study

pMAW019	pCA528-His6-SUMO- *secH*-W52Am-AviTag	This study
pMAW020	pCA528-His6-SUMO- *secH*-Y63Am-AviTag	This study
pMAW021	pCA528-His6-SUMO- *secH*-F80Am-AviTag	This study
pMAW022	pCA528-His6-SUMO- *secH*-N91Am-AviTag	This study
pMAW023	pCA528-His6-SUMO- *secH*-F101Am-AviTag	This study
pMAW024	pCA528-His6-SUMO- *secH*-D129Am-AviTag	This study
pMAW025	pCA528-His6-SUMO- *secH*-L146Am-AviTag	This study
pMAW026	pCA528-His6-SUMO- *secH*-M159Am-AviTag	This study
pMAW027	pCA528-His6-SUMO- *secH*-L173Am-AviTag	This study
pMAW028	pCA528-His6-SUMO- *secH*-R203Am-AviTag	This study
pMAW029	pCA528-His6-SUMO- *secH*-K214Am-AviTag	This study

2.3. Buffers

Table 3 - Buffers Used in This Study

Use	**Name**	**Components**
Protein Purification	Lysis Buffer	20 mM HEPES, 25 mM KOAc, 10 mM Mg $(OAc)_2$ 1 mM TCEP, Dnase I (Sigma), cOmplete™ EDTA-free Protease Inhibitor Cocktail (Roche) and Lysozyme (Thermofisher)
	High Salt Wash Buffer	20 mM HEPES, 500 mM KOAc, 10 mM Mg $(OAc)_2$, 50 mM Imidazole and 1 mM TCEP

	Low Salt Wash Buffer	20 mM HEPES, 25 mM KOAc, 10 mM Mg $(OAc)_2$, 50 mM Imidazole and 1 mM TCEP
	Elution Buffer	20 mM HEPES, 25 mM KOAc, 10 mM Mg $(OAc)_2$, 500 mM Imidazole and 1 mM TCEP
	Buffer A	20 mM HEPES, 25 mM KOAc, 10 mM Mg $(OAc)_2$ 1 mM TCEP
	Buffer B	20 mM HEPES, 500 mM KOAc, 10 mM Mg $(OAc)_2$ and 1 mM TCEP
Incubation Buffer	Protein Assays	20 mM HEPES, 25 mM KOAc, 10 mM Mg $(OAc)_2$
Z Buffer	β-galactosidase assays	60 µM Na_2HPO_4, 40µM NaH_2PO_4, 10 µM KCl and 1 µM $MgSO_4$
TKM Buffer	ATP-assays	10 mM Tris-Cl pH 7.6, 50 mM KCl, 2 mM $MgCl_2$
TAE Buffer	Agarose Gel Electrophoresis	40 mM Tris, 20 mM glacial acetic acid, 1 mM EDTA
5X Laemmli Sample Buffer	SDS-PAGE Sample Buffer	0.02% (w/v) bromophenol-blue, 30% (v/v) glycerol, 10% (w/v) SDS and 250 mM Tris-HCL (pH 6.8)
SDS Running Buffer	SDS-PAGE	25 mM Tris, 192 mM glycine, 0.1 % (w/v) SDS
Transfer Buffer	Western Blotting	25 mM Tris, 192 mM glycine, 20% methanol
Pull Down Binding Buffer	Biotin Pull Down Assays	50 mM Tris-HCL pH 7.5, 150 mM NaCl, 1 mM EDTA, 2% Triton X-100

2.4. Molecular Genetics

2.4.1. **Plasmid Purification**

DNA was prepared from 5 mL overnight cultures in LB grown at 37˚C overnight and shaken at 180 rpm, supplemented with the appropriate antibiotics. The DNA was extracted using a QIAprep Spin Miniprep Kit (Qiagen). Cells were pelleted at 17,000 x g for 5 minutes and resuspended in 250 μL Buffer P1. 250 μL of buffer P2 was added and mixed by inversion 5 times to allow cell lysis. Cell lysis was stopped by addition of 350 μL buffer N3 and inversion 5 times. Lysates were centrifuged for 10 minutes at 17,000 x g to remove cellular debris. 800 μL of supernatant was applied to a QIAprep Spin Column, and columns were centrifuged for 1 minute. 750 μL buffer PB was added to the column and the column was centrifuged for 1 minute. The column was centrifuged again for 1 minute to remove residual ethanol. DNA was eluted with the addition of 50 μL dH_2O, allowed to stand for 1 minute and centrifuged for 1 minute.

2.4.2. **DNA Separation and Visualisation**

DNA fragments were separated using agarose gel electrophoresis. 1% w/v agarose was suspended in TAE buffer and SYBR Safe stain (APExBIO) was added at 1:10000 ratio. Fragments were mixed with 6X loading buffer (New England Biolabs). Gels were run in TAE buffer until the samples were fully resolved. MassRuler Mix (Thermofisher) was used at the DNA ladder. Gels were imaged using a Gel Doc XR+ (Bio-Rad).

2.4.3. **DNA Amplification**

Genes to be amplified for plasmid construction (Table 2) were amplified by Phusion® High-Fidelity DNA Polymerase (New England Biolabs) or Q5® High-Fidelity DNA Polymerase (New England Biolabs). The polymerase chain reaction was carried out using the components and conditions in Table 4 and Table 5.

Table 4 – Components for PCR DNA Amplification

Component	**Volume**	**Final Concentration**
5X Buffer	10 μL	1X
Template DNA	< 250 ng	< 250 ng
10 μM Forward Primer	2.5 μL	0.5 μM
10 μM Reverse Primer	2.5 μL	0.5 μM
10 mM dNTP Mix	1 μL	200 μM
100 % DMSO	1.5 μL	3%
Nuclease-free H_2O	to 50 μL final volume	
DNA polymerase	0.5 μL	1 unit/50 μL reaction

Table 5 – PCR Steps

Step	Cycles	Temperature	Time
Initial Denaturation	1	98˚C	30 seconds
Denaturation Annealing Extension	30	98˚C 45˚C – 72˚C 72˚C	10 seconds 30 seconds 30 seconds per kb
Final Extension	1	72˚C	10 minutes
Hold	1	4˚C	

2.4.4. **Colony PCR**

For colony PCR, MyTaq Red Mix (Bioline) was used. Each single colony was picked using a sterile 20 μL pipette tip and resuspended in 20 μL nuclease free dH_2O. 10 μL of the resuspended colony was boiled for 10 minutes before 2 μL was added to the reaction mixture.

2.4.5. **DNA Precipitation**

DNA precipitation was used to remove salts from DNA buffer prior to electrotransformation of bacteria. 100% Ammonium acetate was added at 1:1 volume to the suspended DNA. Isopropanol was then added at 2:1 volume. The reaction was mixed and centrifuged for 15 minutes at room temperature. The supernatant was removed and a 2:1 volume of 70% ethanol was added followed by centrifugation for 10 minutes at room temperature. The supernatant was again removed, and the residual ethanol was evaporated in the Concentrator 5301 (Eppendorf). 15 μL of nuclease-free sterile water was used to resuspend the pellet and the mixture was incubated at 50˚C for 10 minutes to ensure resuspension of DNA.

2.4.6. **DNA Purification**

PCR products needed for downstream applications were purified using the QIAquick PCR Purification Kit (Qiagen). All centrifugation steps were at 17,000 x g for 1 minute. 5 volume of Buffer PB were added to 1 volume of PCR reaction and mixed by pipetting. The sample was applied to QIAquick column and centrifuged. 750 μL Buffer PE was added to wash the column and was centrifuged for 1 minute. Residual ethanol was removed by centrifugation for 1 minute. The column was placed in a fresh 1.5 mL microcentrifuge tube and 50 μL of dH_2O was added to the column to elute the DNA. The column was allowed to stand for 1 minute and was then centrifuged.

2.4.7. **Molecular Cloning**

Plasmids were constructed from amplified PCR fragments either by restriction digestion and ligation or NEBuilder® HiFi DNA Assembly (New England Biolabs). For restriction enzyme-based cloning, 1 μg of DNA of the SecA CTT and pUT18c were digested using 1 μL high fidelity restriction endonucleases SmaI and BamHI in rCutSmart Buffer™ (New England Biolabs). The digested plasmid and digested SecA CTT were ligated using a molar ratio of vector to insert at 1:3, with the vector at a concentration of 0.0.2 pmol. 2 μL of T4 DNA Ligase (New England Biolabs) was used in T4 DNA ligase buffer, and the reaction was incubated at 4˚C overnight. Excess salt was then removed for downstream transformations as described in section 2.4.5 DNA Precipitation.

All other plasmids were constructed using NEBuilder® HiFi DNA Assembly. The desired DNA for insertion into plasmids was amplified by PCR and the vector was linearised and amplified by PCR. The vector was digested with 1 μL DpnI (New England Biolabs) and incubated for 1 hour at 37˚C to remove methylated host DNA. The vector and insert were added at a molar ratio of 1:2, with a maximum of 0.2 pmol of DNA. The DNA fragments were incubated with NEBuilder® HiFi DNA Assembly Master Mix at 50˚C for 15 minutes. 1 μL of the assembly product was used in the subsequent transformation.

2.5. Bacterial Transformation

2.5.1. **Electroporation**

2.5.1.3. PREPARATION OF ELECTROCOMPETENT CELLS

Electrocompetent cells were prepared according to (Sambrook et al., 2006). 5 mL of overnight culture were diluted 1:100 in LB and grown at 37˚C until the cultures OD_{600} reached 0.5. The cells were centrifuged at 2000 x g for 10 minutes at 4˚C. The supernatant was removed, and the cells were resuspended in the same volume of ice-cold dH_2O. This step was repeated, resuspending in 1/3 the volume of dH_2O. The pellet was then washed with 1/50 of the original volume with ice-cold sterile 10% glycerol. Finally, the cells were centrifuged and resuspended with 1/100 of the original volume with 10% glycerol and split into individual 100 μL aliquots. The aliquots were snap-frozen in liquid nitrogen and stored at -80˚C.

2.5.1.4. ELECTROPORATION

A 30 μL aliquot of electrocompetent cells was mixed with 1 μL of product DNA in a 1mm gap electroporation cuvette (Scientific Laboratory Supplies) and electroporated at 1750 V. 970 μL of LB was immediately added, and the recovered cells were incubated at 37˚C and shaken at

180 rpm for 1 hour. 100 μL of the cells were then plated on LB agar plates supplemented with the appropriate antibiotics and incubated overnight at 37˚C.

2.5.2. Chemical Transformation

50 μL aliquots of chemically competent cells (New England Biolabs) were thawed on ice. 1 μL of plasmid DNA was added to the cells, mixed by gentle pipetting, and incubated on ice for 30 minutes. The mixture was heat-shocked in a 42˚C water bath for 30 seconds before being placed on ice for 2 minutes. 950 μL of LB was added, and the cells were incubated at 37˚C and shaken at 180 rpm for 1 hour. 100 μL of the cells were plated on LB agar selection plates containing the appropriate antibiotics and incubated overnight at 37˚C.

2.6. P1 Transduction

P1 lysates were used to transduce a *secB* mutant from the Keio collection to the chromosome of *E. coli* BL21 by using bacteriophage to package the disrupted gene from the donor strain and recombine it into the recipient strain (Baba et al., 2006; Miller, 1972). 50 μL of overnight culture of strain DRH959 (MG1655 Δ*secB::*kan), which contains a *secB* allele that has been replaced with a kanamycin cassette flanked by FLP recognition target sites, was incubated with 5 mL LB and supplemented with 25 mM $CaCl_2$ and varying volumes of P1 phage (1μL – 5 μL). Cultures were grown until lysis was visible and were then centrifuged at 4000 x g for 10 minutes. 100 μL of chloroform was added to the supernatant to kill any remaining bacteria.

1 mL of overnight culture containing the recipient strain was centrifuged at 4000 x g for 1 minute and the supernatant was discarded. The resulting pellet was resuspended in 500 μL resuspension buffer (100 mM $CaCl_2$, 10 mM $MgCl_2$). 100 μl of resuspended cells was incubated with 20 μL of P1 lysate and 80 μL LB for 20 minutes at 37˚C in a static incubator. 200 μL of sodium citrate was added to kill the P1 phage and 500 μL of LB was added and incubated at 37˚C in a shaking incubator for 1.5 hours to allow recovery of the bacteria. The transductants were centrifuged at 4000 x g for 1 minute and resuspended in 200 μL sodium citrate and plated on selective media containing kanamycin. Resulting colonies were screened by colony PCR to ensure the loss of the *secB* gene.

2.6.1. **Removal of Kanamycin Cassette**

The kanamycin cassette was removed using the FLP recombinase plasmid pCP20 (Baba et al., 2006). Δ*secB::kan* BL21 electrocompetent cells were transformed with plasmid pCP20 and recovered with 1 mL LB for 1.5 hours at 30˚C. The transformants were centrifuged at 4000 x g for 1 minute and resuspended in 100 μL LB, plated on selective media containing both kanamycin and ampicillin, and incubated overnight at 30˚C. Resulting colonies were restreaked on LB plates and incubated at 42˚C to induce the FLP recombinase. Resulting colonies were restreaked on LB, kanamycin, and ampicillin plates to screen for colonies sensitive to both antibiotics. Colonies sensitive to both antibiotics were grown overnight and stored in glycerol stocks at -80˚C.

2.7. Protein Expression and Purification

2.7.1. **Protein Expression**

Plasmids containing genes for protein expression were transformed into the *E. coli* expression strain BL21 (DE3) which carries the T7 RNA polymerase under the control of a lac promoter. When grown from glycerol stocks, the desired strain was streaked onto an LB agar plate with the appropriate antibiotics and incubated at 37˚C overnight. An individual colony was used to inoculate a 5 mL LB culture with the appropriate antibiotics and was incubated overnight at 37˚C. The overnight culture was then subcultured 1:200 into 1L of LB. Cultures were grown to an OD_{600} of 0.8 and then the temperature was reduced to 18˚C. Protein expression was induced with 1 mM isopropyl β-D-1-thiogalactopyranoside (IPTG) and incubated overnight. Cells were harvested by centrifugation at 4500 x g for 30 minutes at 4˚C with a JLA-8.1000 rotor (Beckman Coulter).

2.7.2. **Protein Purification**

Cell pellets were resuspended in lysis buffer and incubated on a rolling incubator at 4˚C until cells were fully resuspended. Cells were lysed by cell disruption using a C3 Emulsiflex (Avestin) high pressure homogeniser. Resuspended cells were cycled 3 times through the homogeniser at 17,000 psi. Lysed cells were centrifuged at 27,000 x g for 20 minutes at 4˚C to remove cell debris, using a JA-20 rotor (Beckman Coulter). The lysate was cycled through a HisTrap™ (Cytiva) column overnight using a peristaltic pump at 4˚C. The bound protein was washed with 5 column volumes (CVs) of high salt wash buffer followed by 5 CVs of low salt wash buffer. The protein was eluted in 25 1 mL fractions collected in 1.5 mL microcentrifuge tubes, using elution buffer. Protein-containing fractions were determined by adding 2 μL of

each fraction to 198 μL 1X Bradford Reagent (Sigma) and looking for the appearance of a blue colour. Protein-containing fractions were pooled and dialysed (SnakeSkin 10 kDa MWCO) against buffer A at 4˚C overnight. The eluted protein was incubated with SUMO protease (purified in the lab) to remove the N-terminal 6xHis-SUMO fusion tag. The tag was subsequently removed from the sample by running the sample through a His column, allowing the tag to bind to the column and the cleaved protein to flow through.

2.7.3. **Anion Exchange Chromatography**

The cleaved protein was concentrated using a 10 kDa MWCO protein concentrator spin column (Vivaspin®). The concentrated protein was run through a 1 mL Resource™ Q anion exchange column, using an ÅKTA™ pure (GE Healthcare). The protein was eluted using a salt gradient with Buffer B. The protein was eluted in 2 mL fractions.

2.7.4. **Size Exclusion Chromatography**

Size exclusion chromatography was the last step in purification, performed using a Superdex 75 10/300 GL column (GE Healthcare). The column was equilibrated, and the protein was eluted using buffer A. Proteins were eluted in 2 mL fractions. Fractions containing purified protein were pooled and concentrated. The purified protein was aliquoted, snap frozen in liquid nitrogen and stored at -80˚C.

2.7.5. **Protein Concentration Determination**

Protein concentration was determined using an extinction coefficient calculated using ExPASy, part of online resource ProtParam, assuming all cysteine residues were reduced. Concentration of protein was determined using a Nanodrop (ThermoFisher), measuring light absorbance at

280 nm and calculated according to the Beer-Lambert Law $A = \varepsilon cl$, where A = absorbance, ε= extinction coefficient, c= concentration and l = path length.

2.7.6. **SDS -PAGE**

Protein samples were mixed with 5X Laemmli sample buffer at a ratio of 4:1 and boiled for 5 minutes. Proteins were analysed by SDS-PAGE according to (Sambrook et al., 2006). Proteins were separated using a 12 % resolving gel. In 10 mL, this consisted of 2.5 mL 1.5 M Tris (pH 8.8), 100 µL 10% (w/v) sodium dodecyl sulphate (SDS), 100 µL 10% (w/v) ammonium persulfate (APS), 5 mL 30% (w/v) acrylamide and 4 µL tetramethylethylenediamine (TEMED). 5 mL of stacking buffer consisted of 630 µL 1.0M Tris (pH 6.8), 50 µL 10% (w/v) SDS, 50 µL 10% (w/v) APS, 830 µL 30% (w/v) acrylamide and 5 µL TEMED. The gels were cast in 0.75 mm Mini-PROTEAN spacer plates. Gels were run in SDS running buffer until the loading dye reached the end of the gel. Gels were fixed with 50% (v/v) ethanol and 10% (v/v) acetic acid in dH_2O. Gels were then washed with 50% (v/v) methanol and 10% acetic acid. Gels were stained with 0.1% (w/v) Coomassie R250, 20% (v/v) methanol and 10% (v/v) acetic acid. Gels were destained with 50% (v/v) methanol and 10% acetic acid.

2.7.7. **Silver Staining**

To stain gels using silver staining, gels were washed twice in ultrapure water for 5 minutes before being stained with a silver stain kit (Pierce). Gels were fixed in 30% (v/v) ethanol and 10 % (v/v) acetic acid. Gels were then washed twice in 10% (v/v) ethanol for 5 minutes followed by twice in deionised water for 5 minutes. Gels were incubated with sensitiser solution for 1 minute, washed with ultrapure water for 1 minute before being incubated with silver stain for

30 minutes. Gels were rinsed twice with deionised water before being incubated with developer solution. The developing reaction was stopped using a stop solution of 5% (v/v) acetic acid.

2.7.8. **Western Blotting**

Proteins in SDS PAGE gels were transferred to nitrocellulose membranes (Amersham™ Protran™, 0.45 μm) according to (Sambrook et al., 2006). The proteins were transferred to the membrane using a wet transfer with a sandwich consisting of sponge and blotting filter paper (ThermoFisher) in transfer buffer. Proteins were transferred at 50 V for 3 hours or overnight at 15 V. Membranes were blocked with 5% (w/v) casein in TBS (Skimmed milk powder (Sainsbury's), 50 mM Tris-HCL, 150 mM NaCl) for 1 hour. Membranes were rinsed 3 times with TBS, and then incubated with the appropriate primary antibody in TBS at room temperature for 1 hour on an orbital shaker. The membrane was then washed 3 times for 15 minutes with TBST (TBS + 0.1% (v/v) Tween-20) then incubated with an anti-rabbit- HRP-linked secondary antibody in TBS for 1 hour on an orbital shaker. The membrane was washed twice in TBST for 15 minutes and rinsed with TBS before being developed with ECL™ Prime Western Blotting Detection Reagent (Cytiva Amersham™). Chemiluminescence was detected with a Gel Doc XR+ (Bio-Rad).

2.8. Mass Spectrometry Analysis

Proteins samples to be analysed by mass spectroscopy were excised from Coomassie-stained SDS-PAGE gels and submitted for liquid chromatography mass spectrometry (LC-MS/MS) analysis. The mass spectrometry data was filtered to include proteins that had a score sequest of 10 or more. The score sequest is a measure of how well the MS/MS spectrum for each peptide

matches the theoretical MS/MS spectrum. The higher the score, the better the confidence in identification of the protein.

2.9. Ribosome Cosedimentation Assay

Ribosome sedimentation assays were performed according to (Jamshad et al., 2019). 1 μM of purified 70S ribosomes were incubated with SecH and SecHΔMBD at varying concentrations in incubation buffer. Samples were incubated at 25˚C for 15 minutes, before being layered on a 30% sucrose cushion (60% (v/v) sucrose made up in incubation buffer). Samples were ultracentrifuged at 200,000 x g for 2 hours at 4˚C. Ribosomal pellets were resuspended in 1X SDS sample buffer and analysed by SDS-PAGE and western blotting.

2.10. Microscale Thermophoresis (MST)

Purified SecB was labelled using an NT-647-NHS labelling kit (NanoTemper). 160 nM labelled SecB was incubated with serial dilutions of SecH or SecHΔMBD from 200 μM to 6 nM in incubation buffer with 0.05% Tween. MST was performed using Monolith Premium Capillaries (NanoTemper), with a Monolith NT.115 (Nanotemper). The K_D was determined by fitting the curve to a non-linear regression one site total binding equation:

Y=Bmax*X/(Kd+X) + NS*X + Background

Where Bmax = maximum specific binding, K_D = equilibrium dissociation constant, NS = slope of non-specific binding and background = amount of nonspecific binding.

2.11. Bacterial Two Hybrid Assay

Plasmids for bacterial two hybrid assay (pMAW002, pMAW003, pMAW004 and pMAW005) were designed and constructed using NEB HIFIBuilder. pMAW010 was constructed using restriction digestion and ligation. All plasmids were co-transformed with pMAW002 into BTH101 electrocompetent cells.

Overnight cultures were diluted 1:100 into fresh LB and grown until exponential phase. Cultures were then cooled on ice for 20 minutes, and $O.D_{600}$ was measured. 500 µL of culture was mixed with 500 µL of Z buffer. Cells were lysed with 25 µL chloroform and 15 µL 0.1% SDS and vortexed. Cultures were warmed at 28˚C in a water bath for 5 minutes and 200 µL ONPG was added. The reaction was stopped after appearance of deep-yellow colour with 500 µL Na_2CO_3. Absorbance was then measured at 420 nm. Miller units were then calculated by the given equation:

$$\text{Miller Units} = \frac{OD420}{OD600\ X\ Culture\ vol.\ (mL)\ X\ Time\ of\ incubation\ (minutes)}\ x\ 1000$$

The resulting data was analysed statistically using a one-way ANOVA. The null hypothesis was rejected, and the data was analysed using *post-hoc* t-tests which correct the p-value for multiple comparisons.

2.12. Structural Modelling

The **P**rotein **H**omology/analog**Y** **R**ecognition **E**ngine V 2.0 (Phyre2) server was used to model the structure of SecH. SecH was modelled against UPF0149 domain protein lpg0076 from *Legionella pnuemophilia*, structure 4GYT (RSCB PDB). The modelled protein was visualised using the pyMOL Molecular Graphics System (Version 2.5.2, Schrödinger, LLC). AlphaFold2 and AlphaFold2 Multimer were used to model SecH and SecH in complex with SecB as well as oligomeric SecH complexes (Mirdita et al., 2022). Using Google Colaboratory, models can be created using both AlphaFold2 and AlphaFold Multimer. The AlphaFold online database was also used for single protein models (Jumper et al., 2021).

2.13. DSP Crosslinking

Purified SecB was incubated with purified SecH at both 2 µM and 4 µM at 25˚C for 30 minutes. Dithiobis (succinimidyl propionate) (DSP) (ThermoFisher) was added at concentrations of 0.2 mM, 1 mM and 5 mM to induce crosslinking and the reactions were incubated at 25˚C for 30 minutes. The crosslinking reaction was quenched with Tris-HCl at a final concentration of 50 mM. Samples were mixed with 5X SDS loading buffer and 10 µL of each sample was separated by SDS PAGE and analysed by western blotting.

2.14. Site-Specific Crosslinking

2.14.1. **Strain Construction**

Plasmids pMAW017-pMAW029 were designed using Snapgene® (Insightful Science). The genes were synthesised, and the plasmids constructed by GENEWIZ. Each plasmid was electroporated into *E. coli* BL21 containing pSUP-BpaRS-6TRN.

2.14.2. **Protein Expression and Purification**

Proteins were expressed as previously described and grown in the presence of 1 mM 4-Benzoyl-L-phenylalanine (Bpa, Bachem). Cultures were grown in covered flasks to reduce excess light that may activate Bpa crosslinking. Proteins were purified as previously described, using only the HisTrap™ step with the columns covered to reduce excess light. The eluted proteins were cleaved using SUMO protease (Sigma-Aldrich), and incubated overnight at 4˚C. The SUMO tag was removed by flowing the cleaved protein through a HisTrap column. The polyhistidine-SUMO tag bound to the column and the cleaved protein flowed through and was collected. The proteins were buffer exchanged to remove imidazole using a 10 kDa MWCO protein concentrator spin column.

2.14.3. **Photo-Crosslinking**

SecB at 2 µM was mixed with mutant Bpa-labelled proteins at a final concentration of 2 µM in incubation buffer and incubated at 25 ˚C for 30 minutes. 200 µL of each reaction was added to a round-bottom 96 well plate and exposed to UV light with a wavelength of 365 nm for 30 minutes on ice.

For photo-crosslinking of cell lysates, harvested cells were resuspended in lysis buffer. Buffer volume was adjusted to ensure an equal $O.D._{600}$ across samples. Resuspended cells were lysed

as previously described in section 2.7.2. 200 µL of each cell lysate was added to a round-bottom 96 well plate and exposed to UV light with a wavelength of 265 nm for 30 minutes on ice.

2.15. ATPase Activity Assay

The SecA ATPase activity assay was used according to (Cranford-Smith, 2018). The SecA ATPase activity was measured indirectly by coupling ATP hydrolysis to the oxidation of NADH to NAD+. On hydrolysis of ATP to ADP by SecA, pyruvate kinase produces pyruvate from ADP and phosphoenolpyruvate. Lactate dehydrogenase reduces pyruvate into lactate whilst simultaneously oxidising NADH, and the depletion of NADH is followed using absorbance at 340 nm. Each reaction contained with 20 units/mL Lactate dehydrogenase, 100 units/mL pyruvate kinase, 1 µM SecA and varying concentrations of SecH and SecHΔMBD. Reactions were incubated at room temperature before 1 mM ATP, 500 µM phosphoenolpyruvate and 200 µM NADH were added and mixed by pipetting. The absorbance was followed at 340 nm using Zenith 304rt Spectrophotometer. Rates were determined by using a linear regression on the depletion of NADH to determine the slope ($\Delta A_{340}.min^{-1}$). The rate was then divided by the extinction coefficient of NADH at 340 (6220 M^{-1}) and the concentration of SecA to yield the specific activity. Resulting data was analysed using a one-way ANOVA.

2.16. MANT-ADP Fluorescence

The rate of ADP dissociation from SecA was measured, according to (D'Lima and Teschke, 2014) using Förster Resonance Energy Transfer (FRET) between the tryptophan's in SecA as the donor and 2'-(or-3')-O-(N-Methylanthraniloyl) Adenosine 5'-Diphosphate (MANT-ADP)

as the acceptor (Robson et al., 2009). 0.5 µM SecA was preincubated with 1.2 µM MANT-ADP in the presence and absence of 0.5 µM SecH. Reactions were set up in TKM buffer and the measurements were taken in a quartz cuvette maintained at 20˚C. Tryptophans were excited at 295 nm and the emission of the MANT-ADP was measured at 450 nm, both with a 5 nm bandpass. The reaction was followed at 20˚C upon addition of excess ATP (1mM) in order to prevent rebinding of MANT-ADP. The dissociation constant was determined by fitting the curves to a one phase exponential decay equation:

$$Y = (Y0 - NS) * \exp(-K * X) + NS$$

Where K is the rate constant, Y0 is the fluorescence at time zero and NS is the background fluorescence.

2.17. Size Exclusion Chromatography

100 µL of 17.5 µM SecH and SecB were injected into a Superdex 20 10/300 GL column at a flow rate of 0.4 mL.min^{-1} and eluted with incubation buffer. Protein was eluted and collected in 250 µL fractions and further analysed by SDS PAGE and western blotting.

2.18. Pull-Down Assay

Hydrophilic streptavidin beads (New England Biolabs) were resuspended by gentle shaking before being vortexed for 1 minute. 50 µL of beads were aliquoted into sterile microcentrifuge tubes. A magnet was applied to separate the beads from the supernatant and the supernatant was removed. Beads were washed three times in 500 µL pull-down binding buffer. The beads were mixed with 5 mL biotinylated samples and incubated on a rolling mixer for 30 minutes. The magnet was applied to the beads and the supernatant was removed. The beads were washed 3 times as before, before being resuspended in 50 µL 1X SDS buffer.

Chapter 3

Bioinformatic Analysis of SecH

3.1. Introduction

SecH, initially named YecA, is a protein of unknown function which was first identified by the SecA-like Metal Binding Domain (MBD) (InterPro: IPR004027). The MBD in SecA interacts with SecB, which suggests SecH also makes this interaction with SecB and is therefore involved in Sec-dependent translocation. SecH consists of two domains: an N-terminal UPF1049 domain and the C-terminal metal binding domain. The UPF0149 domain is found in SecH and YgfB proteins and forms a principally alpha-helical secondary structure. The UPF0149 domain is typically present only in gamma proteobacteria (Blum et al., 2021).

In SecA, the MBD is a well conserved domain. The MBD is found at the extreme C- terminal end of SecA and interacts with SecB and the ribosome (Jamshad et al., 2019; Patel et al., 2006). The MBD is highly conserved amongst SecA proteins, however MBD sequences in YecA family proteins are more variable (Jiang et al., 2021). The conserved motif in SecA is $CXCXSX_3\Omega X_2C(H/C)$ where Ω corresponds to aromatic amino acids (Jamshad et al., 2019). N-terminal to this motif are a highly conserved arginine and asparagine. Both of these residues contact SecB (Zhou and Xu, 2003).

The SecB-SecA interaction occurs *via* amino acids in the SecA MBD that are conserved in the SecH MBD, suggesting SecH also interacts with SecB. In the *H. influenzae* co-crystal structure of SecB-SecA, the side chains of amino acids corresponding to R878, N879, K889 and K891 of the SecA MBD are involved in the interaction (Zhou and Xu, 2003). The amino acids at these positions are identical in the MBD of SecH, suggesting that SecH might physically interact with SecB.

The SecA MBD also interacts with the ribosome (Jamshad et al., 2019). The ribosomal surface, and particularly the ribosomal exit tunnel, are negatively charged and the SecA MBD contains many well conserved positively charged lysines which may electrostatically interact with the ribosomal surface (Jamshad et al., 2019; Lu et al., 2007). Indeed, SecA binds to ribosomal protein uL23 which is close to the entrance of the ribosomal exit tunnel (Jamshad et al., 2019). Alteration of the cysteines involved in metal coordination disrupt the ribosomal interaction, indicating correct folding of the MBD is required for the interaction (Jamshad et al., 2019).

The physiological metal ligand of the MBD was first thought to be zinc but has now been suggested to be iron (Cranford-Smith et al., 2020). In a co-crystal structure of SecB and the SecA C-terminus from *Haemophilus influenzae*, a single zinc ion is coordinated by the three cysteines and a histidine (Zhou and Xu, 2003). However, recently it has been suggested that *in vivo*, the MBD binds to iron (Cranford-Smith et al., 2020). Mass spectrometry analysis indicates that the MBD binds to iron as well as zinc, and NMR spectroscopy suggests the MBD preferentially binds to iron.

In this chapter, computational methods were used to investigate the structure and function of SecH, and the complex that may form between SecH and SecB. To this end, the co-occurrence of SecB and SecH was investigated to determine whether the two proteins may interact. Homology modelling and *de novo* modelling was used to investigate the tertiary structure of SecH, with particular focus on the metal binding domain to understand its similarity to the SecA MBD. AlphaFold Multimer was also used to model the multimeric interface between SecH and SecB in comparison to known structures of the SecA-SecB interaction.

3.2. Results

3.2.1. Metal Binding Domain Conservation

To investigate whether the SecH MBD could be capable of interacting with SecB, the consensus sequence of the SecH MBD was compared against the consensus sequence of the SecA MBD from species containing SecH (Figure 6). If the amino acids known to interact with SecB in the SecA MBD are conserved in the SecH MBD, it would suggest that SecH also interacts with SecB. 156 representative phylogenetic families were analysed, from a previous investigation into the SecA MBD as a basis for comparison (Jamshad et al., 2019).

The amino acids in SecA that contact SecB are fully conserved in the SecA MBD and are also identical in the SecH MBD (Figure 6). In *E. coli* SecA, the SecB-interacting residues are R881, N882 K892 and K894 (Zhou and Xu, 2003). The metal coordinating residues in *E. coli* SecA are C885, C887, C896 and H897 (Zhou and Xu, 2003). Almost all of these are identical in the SecH MBD. In SecA, the fourth metal-coordinating residue is either a histidine or cysteine, in SecH this amino acid is more likely to be a cysteine (Figure 6b). Indeed, H897 is replaced by a fourth cysteine in *E. coli* SecH.

The SecA MBD contains an invariant serine (S889) that is also conserved in the SecH MBD (Figure 6). This serine is important for the overall structure of the MBD, likely forming a hydrogen bond with the third cysteine (C896) (Dempsey et al., 2004). As well as this, S889 is involved in metal coordination and mediates the preference of the MBD for iron-binding (Cranford-Smith et al., 2020).

The SecA MBD has a well conserved tyrosine residue in between the two lysines involved in SecB binding, which has been suggested to be important for MBD stabilisation (Zhou and Xu, 2003). In the SecH MBD, this residue is replaced by phenylalanine, conserving its aromatic property.

The SecA MBD has 3 positively charged lysines and one arginine that may be important for its interaction with ribosome (Jamshad et al., 2019). These charged amino acids are fully conserved in the SecH MBD, indicating SecH binds to the ribosome.

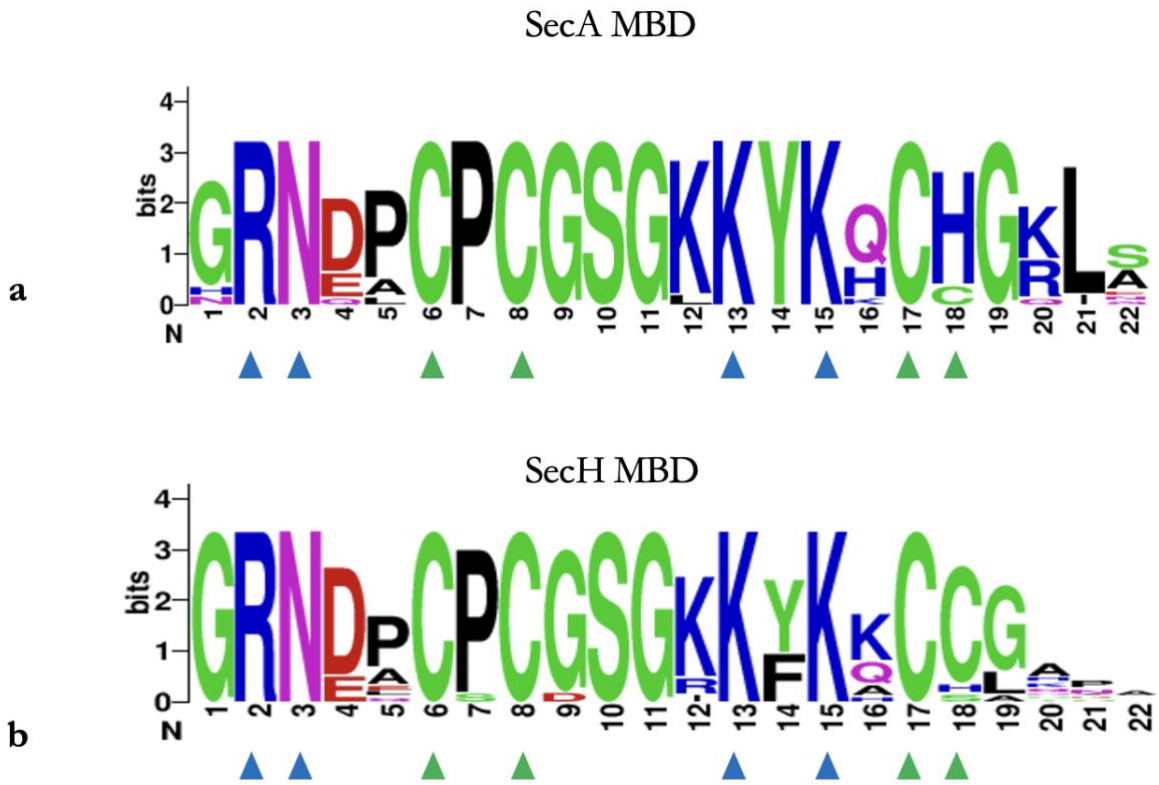

Figure 6- Logo of consensus sequence of the SecA MBD and SecH MBD.

The list of representative bacterial species (Jamshad et al., 2019) was manually searched for SecH-containing species. The SecA and SecH sequence from each resulting species was taken (Uniprot) and a logo was created (Crooks et al., 2004). Residues involved in SecB binding highlighted with blue arrow. Metal-coordinating residues highlighted with green arrow (Zhou and Xu, 2003).

3.2.2. SecH-SecB Co-Occurrence

The similar sequence of the SecA MBD and the SecH MBD suggested that the SecH might interact with SecB. If SecH interacts with SecB, it would be expected that SecB is present in SecH-containing species. To investigate this, the co-occurrence of SecH and SecB was analysed using the list of 156 representative phylogenetic families (Figure 7).

It was found that SecH proteins are present predominantly in Proteobacteria, principally in β - and γ -proteobacteria (Figure 7). In addition, one SecH species is also present in *Chlorobaculum tepidum* and *Pelobacter propionicus*. SecB is present in all but *Chlorobaculum tepidum* and *Pelobacter propionicus*. With the exception of the two species lacking SecB, all SecH-containing species are α-, β-and - γ -Proteobacteria. This distribution of SecH is similar to SecB, where SecB is present in almost all α- , β-and - γ -Proteobacteria and is sparsely distributed elsewhere (Sala et al., 2013).

Within the SecH- containing species, the amino acids involved in metal coordination and SecB binding are all perfectly conserved. This co-occurrence suggests that the two proteins interact with one another.

Class	Species	SecH Accession Number	SecB Accession Number	MBD Sequence
α - Proteobacteria	*Magnetococcus Marinus*	AOLBK9	AOLD65	GRNEPCPCGSGKKFKKCCGNPANSVH
β - Proteobacteria	*Janthinobacterium sp.*	A6SW96	A6T312	GRNDECSCGSGKKYKKCCGAATEGGAE
	Rhodoferax ferrireducens	Q220H9	Q21YV7	GRNDPCPCGSGKKYKKCCGA
	Chromobacterium violaceum	Q7NWQ1	Q7NYZ5	GRNDACPCGSGKKYKACCGAN
	Nisseria meningitidis	Q9JZG0	Q9JY16	GRNDPCPCGSGRKYKACCGKN
	Dechloromonas aromatica	Q47EU0	Q4YIG1	GRNDPCPCGSGKKFKQCCGSPEKLN
	Aromatoleum aromaticum	Q5P0Q8	Q5P7N1	GRNEACPCGSGKKYKKCCGAPR
	Azoarcus sp.	A1K5N6	A1K9C3	GRNEPCPCGSGKKYKKCHGADA
γ- Proteobacteria	*Escherichia coli*	P0AD05	P10408	GRNDPCPCGSGKKFKQCCLH
	Salmonella typhimurium	Q8ZNU3	Q7CPH8	GRNDPCPCGSGKKFKQCCLH

	Hahella chejuensis	Q2SEB0	Q2SMA3	GRNDPCPCGSGKKFKKCCL
	Vibrio cholera	Q9KSZ9	Q9KNS8	GRNDACPCDSGKKFKQCCGQ
δ/ ε-Proteobacteria	*Pelobacter propionicus*	A1AQ56	-	GRNDPCPCGSGIKYKKCCGK
Chlorobia	*Chlorobaculum tepidum*	Q8KA93	-	GRNDLCPCGSGKKYKKCSGQ

Figure 7 - Table of SecH containing species and co-occurring SecB.

From the list of 156 representative phylogenetic families (Jamshad et al., 2019), SecH-containing species were manually identified using UniProt. These species were then investigated to determine whether they contain SecB. The sequence of the metal binding domain is displayed, and the metal-binding residues are underlined. Accession numbers refer to UniProt Accession Numbers.

3.2.3. Structural Modelling

Understanding the structure of SecH is important to gain insight into its function. To investigate the structure of SecH, in the absence of experimentally determined structures of entire SecH family proteins, homology modelling and artificial intelligence- based structural modelling was used to predict the tertiary structure of SecH.

Two methods were used to predict the structure of SecH: Phyre2, a homology modelling tool (Figure 8a) and AlphaFold2 (Figure 8b). Homology modelling uses the primary structure of a protein together with the previously determined structures of homologous proteins to model the tertiary structure of a novel protein. There are two high resolution structural models of UPF0149 domain-containing proteins, the structure 4GYT (PDBe) was chosen given its higher degree of sequence similarity. The first 170 amino acids, representing 77% coverage were modelled with 99.9% confidence. The C-terminal tail and metal binding domain were not modelled because there are no existing high-resolution structures of SecH family proteins containing both the UPF1049 domain and metal binding domain. AlphaFold2, unlike Phyre2, was able to predict the entire structure of SecH including the MBD. AlphaFold2 uses neural networks to create a model based on primary sequence alone. The neural network uses a multiple sequence alignment together with calculations of spatial information from a distance matrix to construct a final 3D model (Jones and Thornton, 2022; Jumper et al., 2021).

The models from both methods were largely consistent. Similar to known structures of UPF0149 domain -containing proteins, the SecH predicted structures contain 7 alpha helices, comprising of 4 helices at the N-terminus, and 3 C-terminal helices in an up-down-up

orientation (Galkin et al., 2004). A small 5-residue helix between helices 5 and 6 is present in structure 4GYT. The other UPF0149 structure from YgfB (PDBe: 1izm) also contains this helix, though it is directly adjacent to helix 5 (Galkin et al., 2004). This additional helix is not present in the modelled structures and is replaced by a linker. The connecting loop between helix 3 and 4 in structure 4GYT comprises of 6 amino acids and 8 amino acids in structure 1IZM. The modelled structures suggest this loop in SecH is extended, comprising of 12 amino acids, which may confer additional structural flexibility.

Despite the similarities in the two models, the AlphaFold2 model has some differences compared to the Phyre2 model. In the AlphaFold model, helix 5 of SecH is broken up by a β-hairpin motif. This is two antiparallel β-sheets linked by 4 amino acids. There is a 12 amino acid linker between helix 3 and 4 in the Phyre2 model, though in the AlphaFold2 model a 3-residue helix is present in the middle of this linker. In agreement with the determined structures, the Phyre2 model predicts a linker region between helix 6 and 7. The AlphaFold2 model, however, predicts a small 9 residue helix in between these two helices.

AlphaFold2 could also be used to model the SecH MBD. Amino acids 189-198 were predicted with low confidence (Per-residue confidence score (pLDDT) between 70 and 50). These residues consist of a long, disordered region linking the UPF0149 domain to the MBD. The lack of secondary structure in this region gives doubt about the location of the MBD relative to the UPF0149 domain. The MBD itself was predicted with high confidence (pLDDT > 90). The entirety of the UPF0149 domain was predicted with very high confidence, except for the β-hairpin motif on helix 5 which was predicted with lower confidence (pLDDT between 90 and 70).

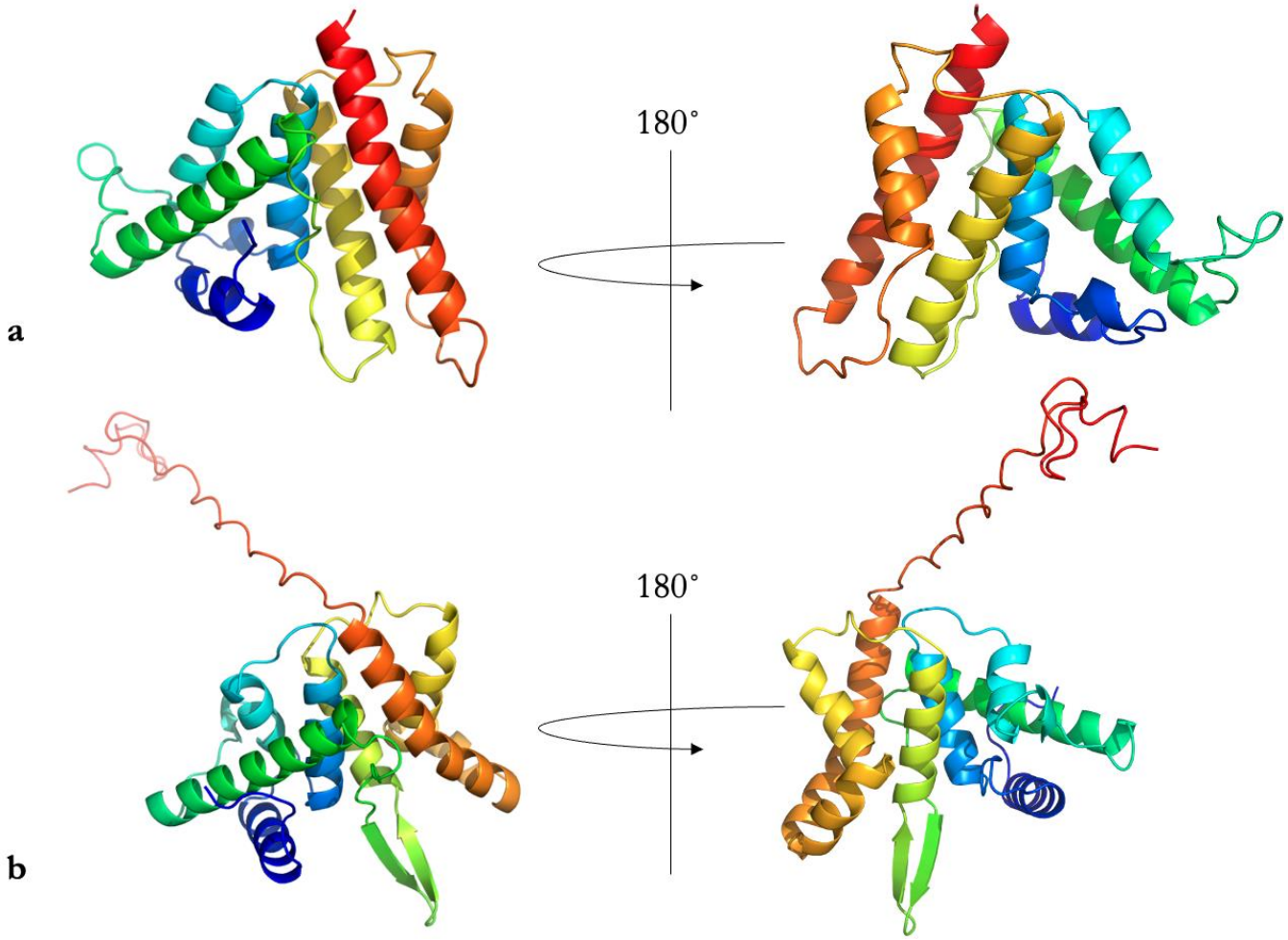

Figure 8 - Structural Modelling of SecH.

Structures are colour-coded from N- to C-terminus by rainbow. **a**) Homology models of SecH using Phyre2 – front and 180˚ reverse angles. The SecH sequence was inputted, and homologous structural models were searched. 4GYT was used as the template structure as it had the highest percentage sequence identity. **b**) Forward and 180˚ reverse angle of SecH AlphaFold artificial intelligence-based model from the E. coli K12 SecH sequence.

3.2.4. Metal Binding Domain Model

To investigate the structure of the SecH MBD and its structural similarity to the SecA MBD, its structure was modelled using homology modelling and compared to a crystal structure of the SecA MBD. The *E. coli* SecA MBD structure determined by NMR shows the MBD coordinating a zinc ion *via* amino acids corresponding to C885, C887, C896 and H897 in a tetrahedral geometry (Figure 9a) (Dempsey et al., 2004).

Phyre 2 was used to model the SecH MBD as, in the absence of a metal, AlphaFold predicted the formation of disulphide bonds between the side chains of the 4 cysteine amino acids. The solution NMR structure of the SecA MBD was used as the template (PDBe: 1sx1) as it had the highest degree of sequence similarity. The domain was modelled with 99.3% confidence and 67% sequence coverage. It is not possible to model the structure in the presence of a metal ion.

The modelled structure (Figure 9b) shows large similarity to the determined structure, which is expected given the high degree of conservation (Figure 9a). C207 and C209 of SecH (corresponding to C885 and C887 in SecA) are in close proximity with the invariant serine in-between. These residues are located above where the metal would be coordinated. C218 and C219 in SecH (corresponding to C896 and H897 in SecA) are located below the pocket pointing towards the binding region. C218 in the SecH MBD has a different geometry compared to C896 in SecA. In the NMR structure, C896 of SecA faces inwards towards the metal, whereas the model depicts C218 of SecH facing outwards towards the solution. The aromatic F215 (Y893 in SecA) is proximal to the metal binding site in the same orientation as in SecA. S889 in SecA hydrogen bonds with C896, with a distance of 3.6 Å between the two residues. The SecH MBD

model places S211 and C218 in a similar conformation with a distance of 3.4 Å between the two residues which would allow for hydrogen bond formation.

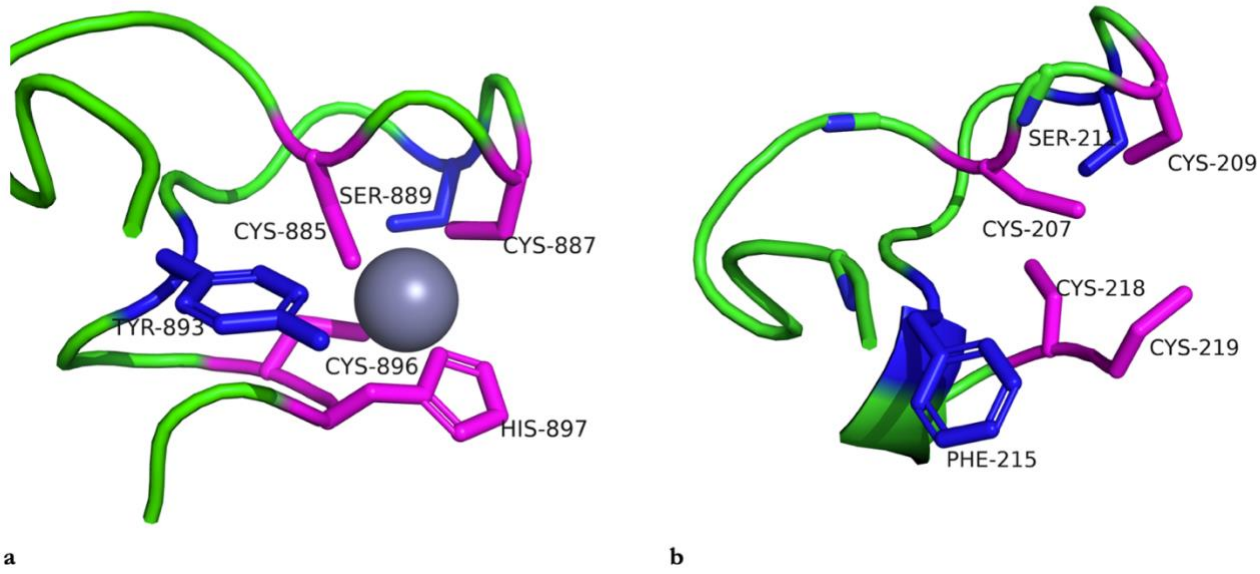

Figure 9 - Determined structure SecA metal binding domain (PDB:1SX1), and modelled SecH metal binding domain.

a) Structure of SecA metal binding domain coordinating a zinc ion, determined by NMR. Residues involved in metal coordination are highlighted in magenta. Potential iron binding residues coloured in blue. **b)** Modelled structure of SecH metal binding domain from Phyre2. The SecH MBD sequence was inputted, and homologous structural models were searched. 1sx1 was used as the template structure as it had the highest percentage sequence identity. Residues suspected to be involved in metal coordination are coloured in magenta. Potential iron binding residues coloured in blue. Structures modelled in Pymol.

3.2.5. SecB-SecH Model

The sequence conservation of the SecH MBD and the co-occurrence of SecB in SecH-containing species suggests the two proteins interact. To investigate the structure of this interaction, and whether the MBD of SecH is capable of interacting with SecB in a similar fashion to the SecA MBD, AlphaFold-Multimer was used to predict the structure of a SecB-SecH MBD complex in comparison to the determined structure of SecB – SecAMBD. AlphaFold-Multimer is an extension of AlphaFold, which models protein chains and is able to predict multimer interfaces of complexes with known stoichiometry (Evans et al., 2022).

In the SecA MBD-SecB complex, the SecA MBD is located at the interface of a homodimeric SecB (Figure 10a). The SecA MBD interacts primarily with amino acids on the first β- sheet of both SecB protomers (Zhou and Xu, 2003). The quaternary structure of the AlphaFold-Multimer model (Figure 10b) is consistent with the determined SecA-SecB structure (Figure 10a). The model predicts the same interaction of the two SecB protomers, with the first β- sheet of each monomer parallel to each other. The SecH MBD, as with the SecA MBD, is predicted to interact with SecB at the interface between the two monomers.

In *H. influenzae,* SecA binds to SecB at the interface of the SecB homodimer through four conserved residues in the MBD: R878, N879, K889 and K891 (Figure 10c– Magenta). R878 forms a salt bridge with E31. N879 hydrogen bonds with both V28 and D27. K889 also forms two salt bridges with E31 and E86, although this is on protomer B of SecB. Finally, K891 of SecA hydrogen bonds with S29.

The interface between the SecH MBD and SecB in the AlphaFold Multimer model (Figure 10d) is mostly similar to the known SecA-SecB structure (Figure 10c). R203 of SecH (R878 in SecA) is still in proximity to the conserved glutamic acid residue on subunit A, but in the model it may be hydrogen bonding to E77 on subunit B. N204 of SecH (N879 in SecA) is also in close proximity to the conserved aspartic acid residue, but not close enough to form a hydrogen bond. The valine in *H. influenzae* is replaced by an isoleucine in the *E. coli* SecB but is not located in proximity to N204. K214 of SecH (K889 in SecA) is in close proximity to the two conserved glutamic acid residues in the SecB subunit B. K216 of SecH (K891 in SecA) is positioned in close proximity to S22 (S29 in *H. influenzae),* close enough to form a hydrogen bond.

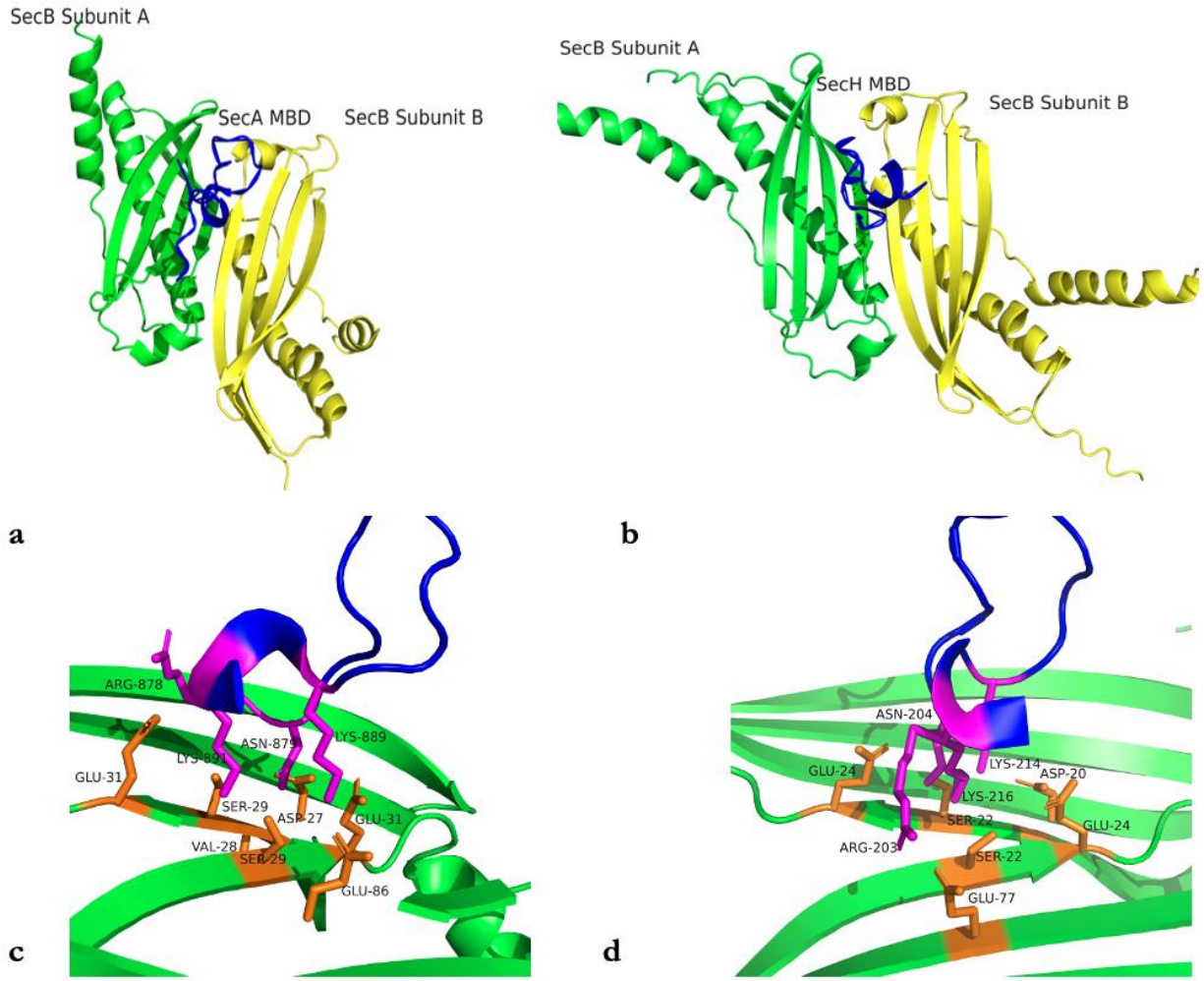

Figure 10 - Structures of SecA and SecH metal binding domains interacting with SecB.

a) Quaternary structure overview of *Haemophilus influenzae* (*H. influenzae)* SecB dimer with SecA MBD bound at the interface of two dimers (PDB:1OZB). **b)** AlphaFold predicted structure of two *E. coli* SecB protomers with SecH MBD. **c)** Structure of *H. influenzae* SecA metal binding domain when in complex with *H. influenzae* SecB (PBD:1OZB), coordinating a zinc ion. Residues involved in SecB binding are highlighted in magenta. **d)** AlphaFold predicted structure of *E. coli* SecH metal binding domain in complex with *E. coli* SecB, coordinating no metal. Amino acids corresponding to SecB-binding residues in Figure 10c are highlighted in magenta.

3.3. Discussion

This chapter firstly set out to investigate the relationship between SecB and SecH. Sequence analysis indicates that the MBD of SecH is well-conserved and almost identical to that of SecA. The residues involved in the SecB interaction are fully conserved in SecH, suggesting SecH and SecB should also interact. The positively charged lysines and arginines are fully conserved in the SecH MBD, suggesting the MBD interacts with the ribosome.

Although the co-occurrence analysis suggests an interaction between SecH and SecB, SecH is found in two species that lack SecB. Although there is no SecB in *Pelobacter propionicus*, a SecB protein is present in close relative *Pelobacter carbinolicus*, though there is no SecH present in this species suggesting that this species recently lost SecB and may be in the process of losing SecH. One SecB species in *Chlorobaculum tepidum* is also present. However, in this species the fourth metal coordinating cysteine is replaced with a serine, which is not seen in any other SecH MBD sequence suggesting that SecH might interact with another component of the Sec machinery in addition to SecB. This likely disrupts metal coordination and may alter its ability to bind to SecB.

Homology modelling and AlphaFold modelling were used in conjunction to predict the overall structure of SecH. The UPF0149 domain was modelled with high confidence and is in broad agreement between the two methods. The UPF0149 domain model is broadly consistent with the two determined UPF0149 domain structures. However, the AlphaFold2 model predicts helix 5 is broken up by a β- sheet that is not seen in any other known UPF0149 structure. This β- sheet is surface exposed and could therefore be functionally important. However, this sheet

was modelled with lower confidence than the rest of the domain, indicating a β- sheet may not be the true fold. Between helix 5 and 6 in the two high-resolution determined structures is a small helix. However, in both the Phyre2 and AlphaFold2 model, no helix is present. The lack of a helix may destabilise the structure with a linker making the SecH UPF0149 domain more flexible. This region of the protein is also surface exposed which could alter protein function if the helix is involved in protein: protein interactions.

The SecH MBD was modelled by both AlphaFold2 (Figure 8b) and homology modelling (Figure 9b) and showed significant similarities to the determined structure of the SecA MBD. The AlphaFold2 model could only model the region between the UPF0149 domain and the MBD with low confidence. This indicates that this region is intrinsically disordered. SecA contains a flexible linker domain (FLD) N-terminal to the MBD. This model suggests that SecH also contains an FLD linking the UPF0149 domain to the MBD. This may have implications for the function of SecH and may also explain the difficulties in crystalising the protein. The homology model of the SecH MBD indicates the conserved metal-coordinating residues are arranged similarly to the SecA MBD, permissive for coordination of a metal ion.

AlphaFold multimer was used to predict the quaternary structure of the SecB-SecHMBD interaction. The SecH MBD is predicted to bind in the same location as that of the SecA MBD, with the same amino acid side chains in SecB in close proximity to the conserved amino acid side chains in the MBD of SecH. However, the structural model predicts a loss of the asparagine hydrogen bond in the MBD to SecB as well as an alternate hydrogen bond of the arginine residue in the SecH MBD. The loss of these interactions may alter the affinity of the SecH MBD for SecB compared to the SecA MBD-SecB interaction. The entire structure of SecH was

initially used in the multimer prediction. However, the flexibility of the linker domain means the predicted position of the UPF0149 domain relative to the MBD is highly unreliable. Therefore, the location of the UPF0149 domain when SecB is in contact with the MBD is difficult to model and renders the resulting models unreliable and variable.

The results in this chapter indicate the MBD of SecH is a protein: protein interaction domain that can bind to the ribosome and SecB. The data also suggest that the function of SecH involves interaction with SecB. However, these results are predictions and require experimental confirmation. To test these hypotheses, in the next chapter, the interactions of SecH with the ribosome and SecB are explored.

Chapter 4

Investigation of the Interactions of the Metal-Binding Domain of SecH

4.1. Introduction

The MBD of SecA binds to SecB and ribosomes (Jamshad et al., 2019; Zhou and Xu, 2003). SecA interacts with the ribosome and this interaction has been suggested to be mediated by the conserved positively charged amino acids in the MBD (Jamshad et al., 2019). These amino acids are conserved in the SecH MBD, suggesting that SecH also interacts with the ribosome (Figure 6). Ribosome cosedimentation assays indicate that the SecA MBD alone cosediments with ribosomes and altering the conserved cysteines in the MBD disrupts the SecA-ribosome interaction (Jamshad et al., 2019). Crosslinking experiments suggest that this interaction occurs close to the polypeptide exit tunnel of the ribosomes (Jamshad et al., 2019).

Sequence analysis and co-occurrence analysis (Figure 6 and Figure 7) indicate that the MBD of SecH also interacts with SecB and ribosomes, and this is further evidenced by structural modelling of SecH and SecB (Figure 10d), suggesting the MBD of SecH interacts with SecB in a similar fashion to SecA. Taken together, these results suggest that the MBD of SecH is an interaction domain that is able to bind to SecB and ribosomes to facilitate the function of the rest of the protein.

In this chapter, Microscale Thermophoresis (MST), chemical crosslinking and a two-hybrid assay were used to investigate the interaction between SecB and SecH. MST follows the migration of a fluorescently labelled protein down a temperature gradient. One protein is fluorescently labelled, and the second protein of interest is titrated in, and a temperature gradient is induced. The resulting signal is impacted by both Temperature-Related Intensity Change (TRIC) and thermophoresis. TRIC refers to the changes in fluorophore signal which

occur depending on the temperature of the solution. The thermophoresis signal is affected by thermophoresis of the proteins, which is the movement of proteins in a temperature gradient. This property is affected by size, charge and hydration shell. The second protein of interest is added to the fluorescently labelled protein and heat is applied. Protein binding alters the thermophoretic ability of the complex which can be detected by a change in MST signal. MST can be used to detect the interaction of two proteins *in vitro* and to calculate the equilibrium dissociation constant (K_D). For example, MST has been used to measure the SecA-SecYEG interaction in lipid nanodiscs, showing a dependence in binding on the presence of anionic lipids (Koch et al., 2016).

Protein-protein interactions can also be detected *in vitro* using crosslinking agents. The addition of a crosslinker will cause nearby and interacting proteins to form covalent inter-protein crosslinks. If the two proteins interact, in the presence of chemical crosslinker dithiobis (succinimidyl propionate) (DSP) they should form a covalent link, increasing their overall mass. DSP contains an N-Hydroxysuccinimide (NHS) ester at each end, with an 8-carbon spacer arm in-between which corresponds to 11.4Å. The NHS ester is highly reactive and forms amide bonds by reacting with primary amines. Primary amines are found at the N-termini of proteins as well as the side chains of lysines. The reaction is shown in Figure 11. This method has been used to investigate the interactions of SecYEG with YidC and SecD (Schulze et al., 2014).

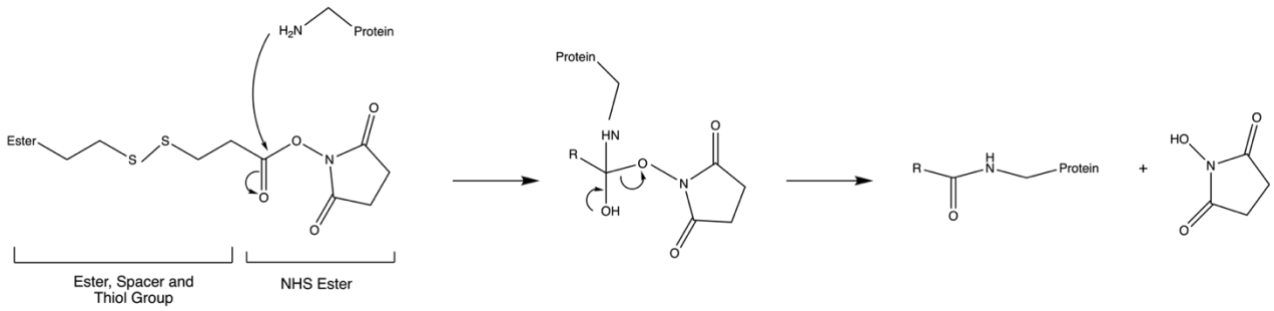

Figure 11 - DSP reaction scheme.

One half of DSP is shown, with its 8-carbon spacer arm and NHS ester group. The primary amine of the reacting protein attacks the carbonyl group of the NHS ester. An unstable tetrahedral intermediate is formed, which results in the loss of the NHS group to be lost and the formation of an amide bond to the remainder of the crosslinker. Figure drawn with Chemdraw 21.0.0

A bacterial two hybrid (BTH) screen was used to investigate the SecB- SecH interaction *in vivo* (Figure 12). The assay functions by using the catalytic domain of adenylate cyclase from *Bordetella pertussis*, which consists of two separate components, T25 and T18. These two fragments separately have no catalytic activity, but their catalytic activity is restored if the two fragments interact with each other. Each fragment can be fused to two separate proteins of interest. If the two proteins of interest interact, the two fragments of adenylate cyclase are brought into close proximity with each other, restoring the catalytic activity of adenylate cyclase. The active adenylate cyclase produces cyclic AMP (cAMP), which binds to the catabolite activator protein (CAP). The CAP/cAMP complex activates the expression of the lactose and maltose utilisation pathways. Maltose metabolism can be indirectly visualised by the breakdown of maltose on McConkey agar plates, causing a pH change, resulting in the formation of red colonies. Lactose metabolism can be visualised by the breakdown of X-gal by β-galactosidase on LB agar, forming blue colonies. β-galactosidase expression can also be detected through the breakdown of lactose mimic ortho-Nitrophenyl- β-galactosidase (ONPG). β-galactosidase hydrolyses ONPG into galactose and ortho-nitrophenol which forms a yellow colour that can be measured spectrophotometrically. These screens can be used in both yeast and bacteria and have been used to investigate many different protein interactions. For example, bacterial two hybrid screens have been used to demonstrate interactions between EntC and EntB, two proteins involved in the production of iron chelator enterobactin (Ouellette et al., 2022).

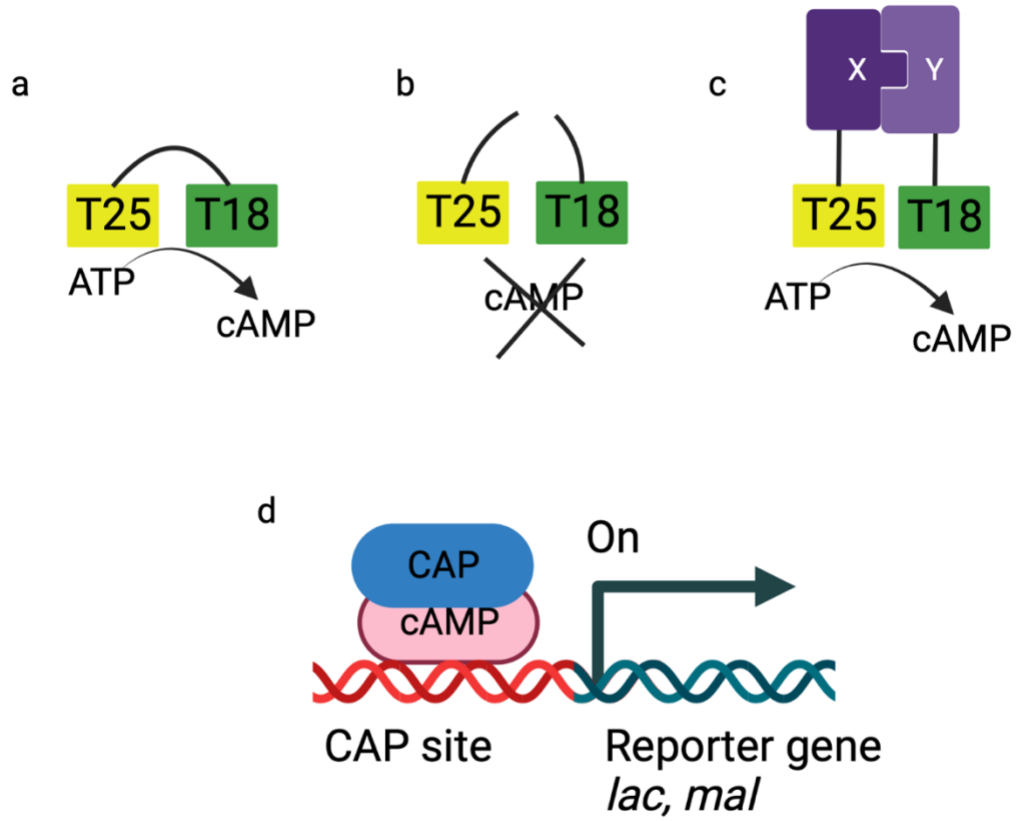

Figure 12 – Schematic of the bacterial two hybrid assay.

a) The T25 and T18 fragments of adenylate cyclase are active when fused together, producing cAMP from ATP. **b)** When the two fragments of adenylate cyclase are not interacting, no cAMP is produced. **c)** When T25 and T18 are separately fused to two interacting proteins X and Y, the interaction of X and Y brings T25 and T18 into close proximity, activating the catalytic activity and results in the production of cAMP. **d)** cAMP interacts with CAP, forming the CAP/cAMP complex which binds to DNA and promotes the transcription of reporter genes including β-galactosidase.

To investigate the interaction between the SecH MBD and the ribosome, a ribosome cosedimentation was used. Purified ribosomes were incubated with purified SecH. The incubated solution was layered on a 30% sucrose and ultracentrifuged. The density of ribosomes results in more rapid sedimentation compared to other cellular proteins. As a result, any proteins interacting with the ribosome will sediment along with the ribosomes. The resulting ribosomal pellet was probed by western blotting for the presence of SecH.

In this chapter, a number of protein: protein interaction assays were used in order to probe the interactions the MBD of SecH makes. The interaction of the MBD with the ribosome was investigated using a ribosome cosedimentation assay. The interaction of the MBD and SecB was then investigated using both *in vitro* and *in vivo* methods. This chapter presents the first evidence indicating the MBD of SecH makes the same interactions as that of the SecA MBD, interacting with both SecB and ribosomes.

4.2. Results

4.2.1. **SecH – Ribosome Interaction**

The analysis in Chapter 3 indicated the SecH MBD contains the same amino acids thought to be involved in the interaction in SecA with the ribosome. A ribosome cosedimentation assay was used to investigate the interaction between SecH and ribosomes *in vitro*. To determine whether wild type SecH can bind to ribosomes, SecH was incubated with ribosomes, with SecH at concentrations ranging from 1 μM to 32 μM, and the resulting pellet was probed with an antibody against SecH (Figure 13a). Incubating the ribosome alone resulted in no detectable SecH in the pellet (lane 1). Upon adding increasing concentrations of SecH, SecH began to cosediment, and SecH saturated at 16 μM (lane 7).

To determine whether the MBD was required for ribosome binding, cosedimentation assays were repeated using SecHΔMBD (Figure 13b). When the MBD was removed (lanes 5 and 6), cosedimentation with the ribosome was severely disrupted. Signal quantification indicates that the signal fell by 64%. The loading control signal between 8 μM SecH and 8 μM SecHΔMBD remain consistent (lanes 3 and 5), as do the 16 μM lanes (lanes 4 and 6), indicating the reduction in signal was not due to issues in antibody detection of SecH lacking the MBD.

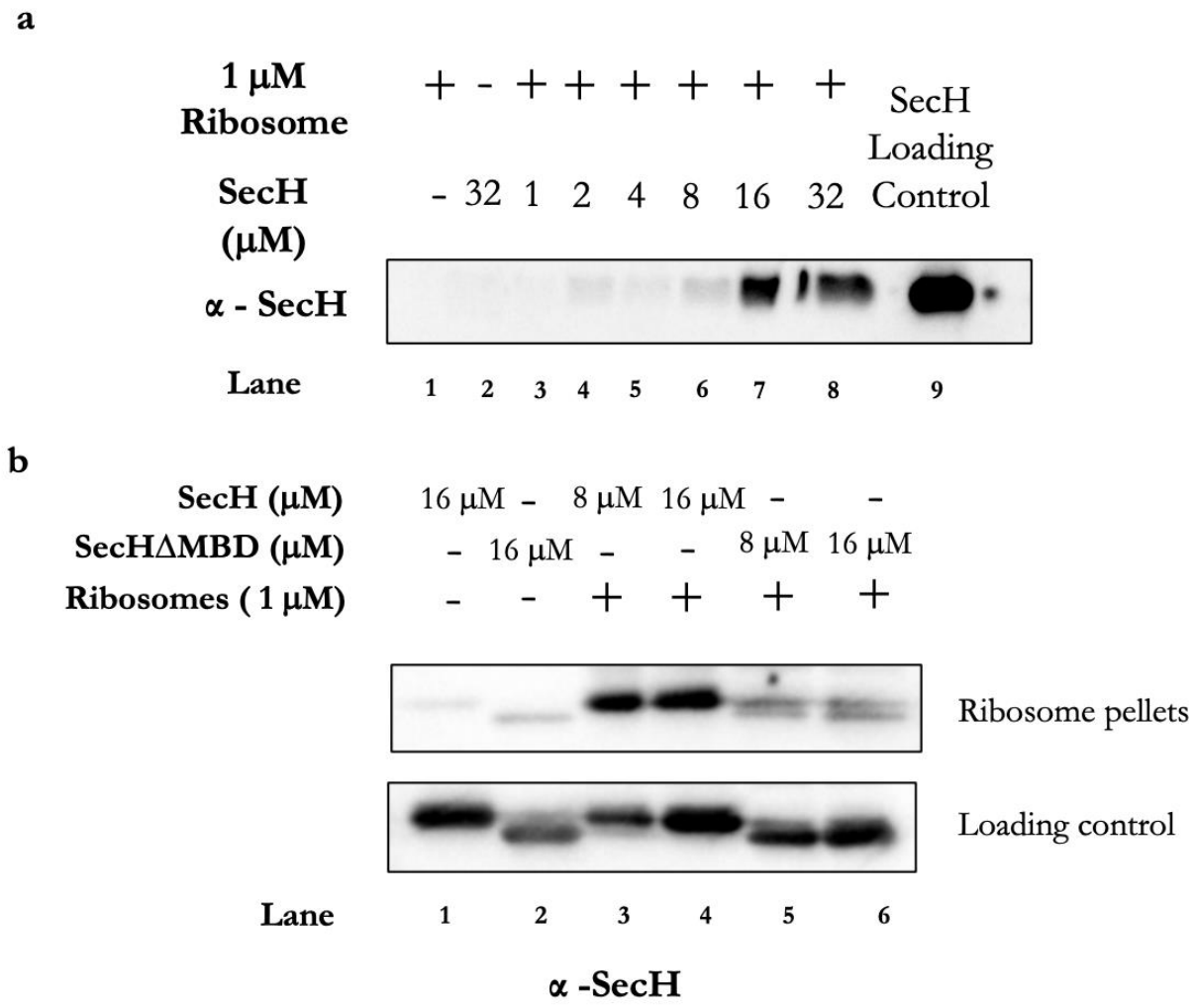

Figure 13 - Cosedimentation of SecH with vacant 70S ribosomes.

1 µM ribosomes were incubated at 25˚C for 15 minutes with indicated concentrations of SecH (0.5 – 512 pmol). Incubated solutions were layered on top of a 30% sucrose cushion and centrifuged for 2 hours at 75,000 rpm. Ribosomal pellets were resuspended in binding buffer. Samples were mixed with SDS loading buffer and 10 µL of sample was loaded onto a 12% SDS-PAGE gel. Proteins were transferred onto a nitrocellulose membrane and western blotted. **a)** α- SecH western blot of wild type SecH cosedimentation assay with increasing concentrations of SecH. 32 pmol SecH used as loading control and 3 pmol ribosomes were loaded **b)** α- SecH western blot of cosedimentation assay with both SecH and SecHΔMBD. Loading control contained 8 pmol (in 8 µM lane) or 16 pmol (in 16 µM lane) of respective SecH variant.

4.2.2. **SecB- SecH Interaction – Microscale Thermophoresis**

MST was used to further confirm the SecB-SecH interaction *in vitro* and to calculate the affinity of SecH for SecB. Increasing concentrations of SecH were titrated into 160 nM SecB which was fluorescently labelled with the NT-647-NHS dye.

When increasing the concentration of SecH in the presence of SecB, the fluorescence change followed a characteristic dose-response relationship characteristic of binding in an MST experiment (Figure 14a). The curve was fitted using non-linear regression one site binding equation and allowed for a calculation of apparent K_D = 129 nM. The characteristic dose-response relationship was not seen when increasing the concentration of SecHΔMBD in the presence of SecB (Figure 14b). The mean response to the addition of SecH and SecHΔMBD was also plotted (Figure 14c). This was calculated as the difference between the minimum and maximum response from each individual experiment. The addition of SecH to SecB had a large impact on the thermophoresis of SecB. However, when SecHΔMBD was added, there was a negligible change in SecB thermophoresis. The difference between SecH and SecHΔMBD response was statistically significant ($p<0.01$) (unpaired T-test).

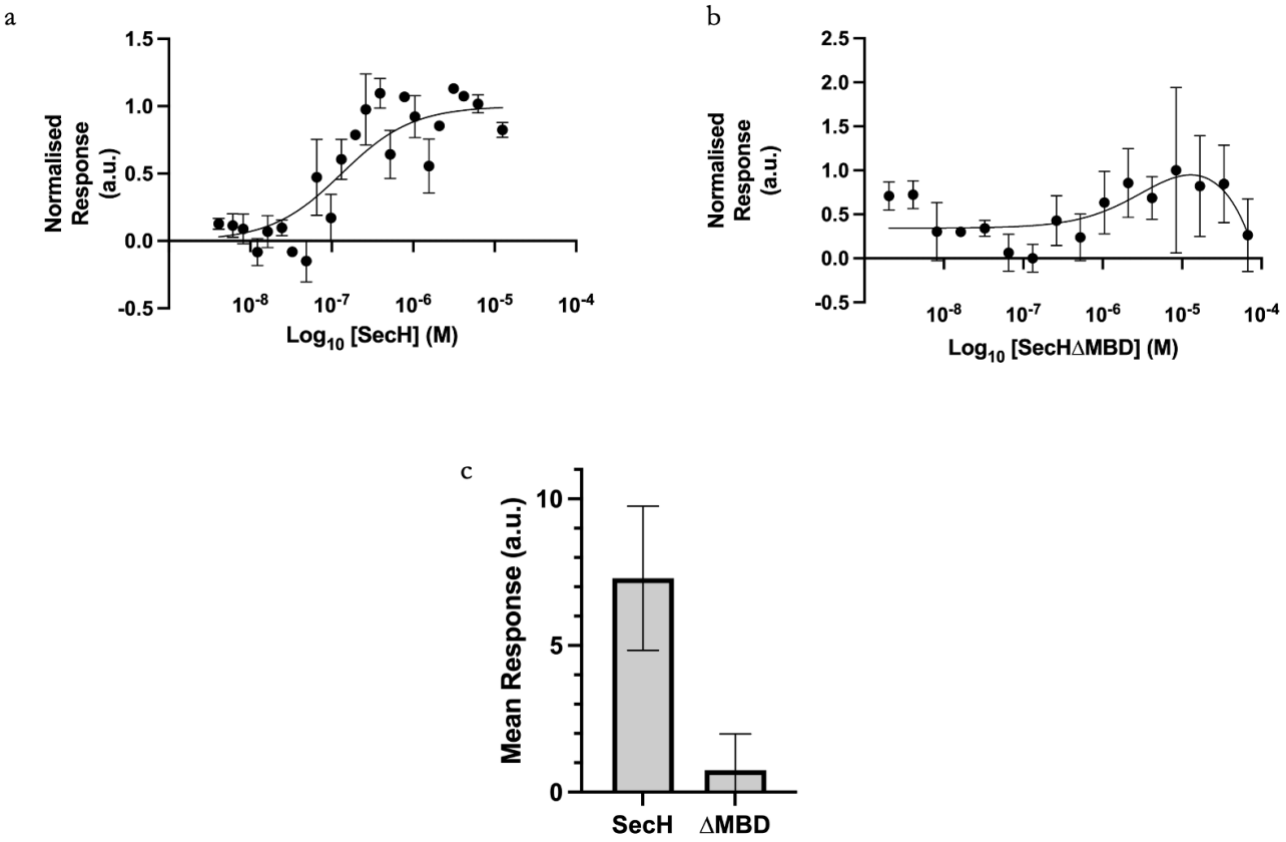

Figure 14 – SecB – SecH interaction measured using microscale thermophoresis.

SecB was labelled with NT-647-NHS labelling kit. 160 nM labelled SecB was incubated with concentrations of SecH or SecHΔMBD ranging from 6 nM to 200 µM at 25˚C for 30 minutes in the presence of 0.05% Tween and loaded into capillaries. MST was performed with a Monolith NT.115 at 100% power. Error bars are representative of 1 standard deviation. Experiments were performed 5 times for SecH and in triplicate for SecHΔMBD. The response was normalised to the maximum value for each individual experiment. **a)** Binding curve of SecB with SecH being titrated in at increasing concentrations. **b)** Binding curve of SecB with SecHΔMBD being titrated in at increasing concentrations. **c)** Magnitude of the response of fluorescently labelled SecB on addition of unlabelled SecH and SecHΔMBD.

4.2.3. **SecB – SecH Interaction – DSP Crosslinking**

The results presented in Chapter 3 indicated that SecH could interact with SecB. To further investigate whether the two proteins interact, chemical crosslinking using DSP was used. If SecH binds to SecB, it should be possible to create a chemical crosslink between the two proteins.

2 μM and 4 μM SecH were incubated with 2 μM and 4 μM SecB in the presence of 0.2 mM DSP. SecB and SecH were also incubated in the presence of 0.05% Tween, as the presence of Tween had been important for measuring the interaction of SecB and SecH using MST.
Purified SecB incubated in the presence of DSP showed 3 distinct bands at 17 kDa, 34 kDa and ≈ 50 kDa (Figure 15a lane 1). These bands likely correspond to the SecB monomer, dimer and tetramer respectively. Purified SecH showed a strong band at 26 kDa (lane 2). A small band at ≈ 50 kDa appeared indicating some SecH may dimerise. When SecB and SecH were incubated together and DSP is added, a band at ≈ 43 kDa appeared (indicated by an asterisk, lanes 3-6), corresponding to a SecH monomer and SecB monomer, indicating a heterodimeric crosslink. To confirm these bands were crosslinks, the samples were blotted against both SecB and SecH (Figure 15b). The four crosslinking bands cross reacted against antisera directed against SecB and SecH (lanes 3-6), apart from the first crosslinking band against the SecH antibody. The appearance of the bands against both antibodies suggested that the band is the crosslinking adduct. The strongest signal was seen in the sample containing Tween, suggesting Tween contributes to the interaction between SecB and SecH.

To determine the effect of the MBD on the interaction of the SecB and SecH, purified SecHΔMBD was used to crosslink with SecB (Figure 15c). SecB and SecH together in the presence of DSP formed the same crosslinking adduct (lane 4). However, when the MBD was removed from SecH, the discernible crosslinking adduct disappeared (lane 5). This suggests that SecB and SecH interact *in vitro,* and the interaction is dependent on the SecH MBD.

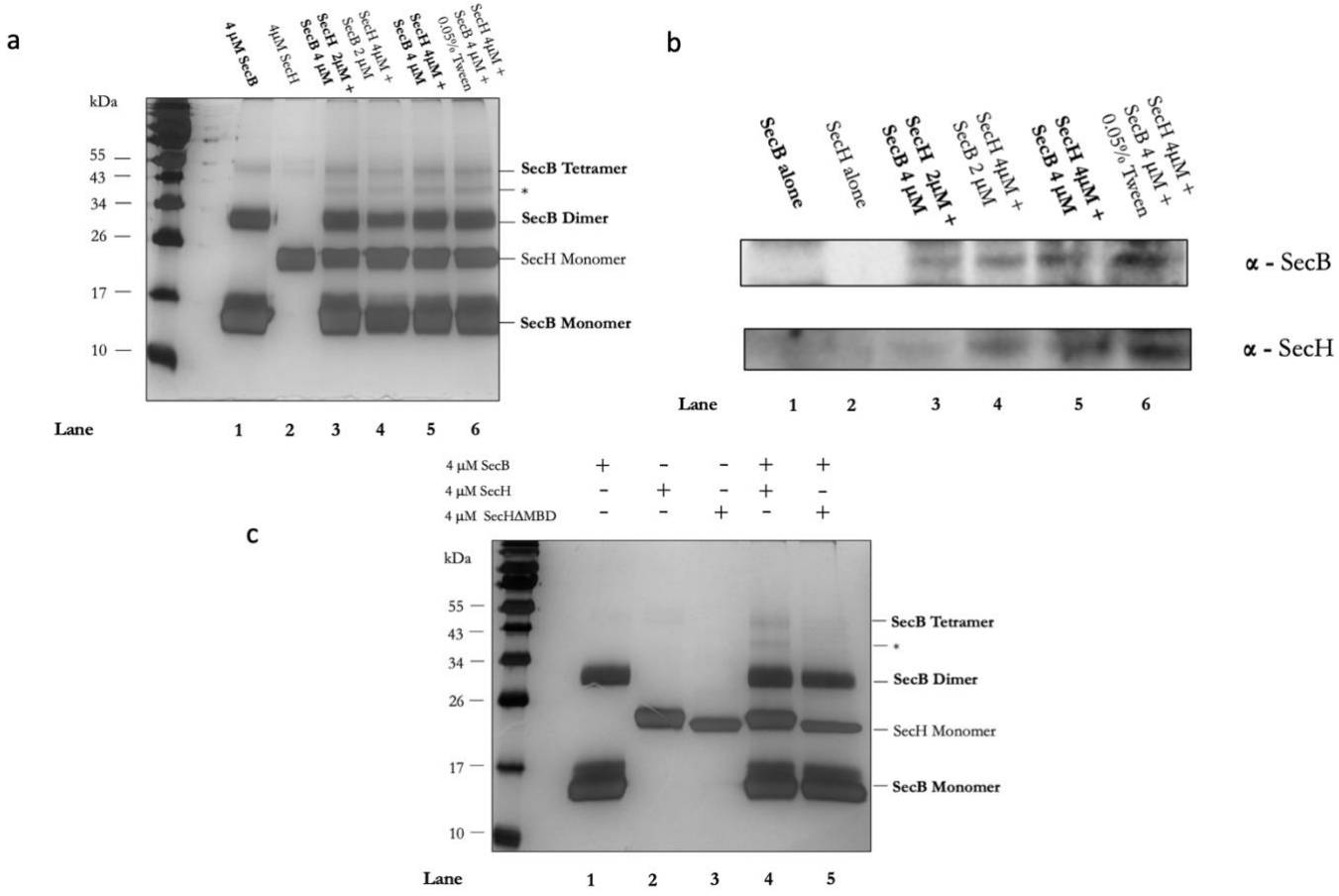

Figure 15 - DSP-mediated crosslinking of SecB and SecH.

Proteins at their indicated concentrations were incubated at 25˚C for 30 minutes before addition of 0.2 mM DSP. The reaction was allowed to proceed at room temperature for 1 hour before being quenched with 1 µL of 50 mM Tris-HCL. Samples were mixed with SDS loading buffer and 10 µL was loaded onto an SDS PAGE gel. **a)** Silver stain of DSP-mediated crosslinking between SecH and SecB. Asterisk represents running position of band containing possible crosslink. **b)** Western blot of band containing possible crosslink between SecB and SecH. The sample was blotted against SecB and SecH. **c)** Silver stain of DSP mediated crosslinking between SecB and both SecH and SecHΔMBD. Asterisk represents running position of the protein band containing the SecB-SecH crosslink.

4.2.4. **SecB- SecH Interaction – Bacterial Two Hybrid Screen**

To determine whether the SecH MBD could interact with SecB *in vivo,* a bacterial two hybrid screen was used to probe the interaction. SecB was fused to the T25 fragment of adenylate cyclase, and the interacting proteins to be investigated were expressed as a fusion protein with the T18 fragment of adenylate cyclase. The pUT18c plasmid alone, containing just the T18 fragment with no fusion protein, was used as a negative control. The SecA C-terminal tail (SecACTT), which is well established to interact with SecB, was used as a positive control. The plasmids were transformed into strain BTH101, expressed, and the resulting β-galactosidase activity was assayed (Figure 16).

Compared to the negative control, SecACTT displayed the strongest β-galactosidase activity with SecB (44 Miller Units). Full length SecH had the next strongest interaction with SecB (15 Miller Units), and this interaction compared to the negative control was statistically significant ($p<0.01$). The MBD alone had a β-galactosidase activity with similar intensity to full length SecH (14 Miller Units), and this interaction compared to the negative control was also statistically significant ($p<0.05$). The UPF0149 domain alone, i.e., SecHΔMBD (12 Miller Units), showed a similar β-galactosidase activity compared to the control (11 Miller Units). This data suggests that *in vivo* SecH interacts with SecB, and the interaction is dependent on the MBD.

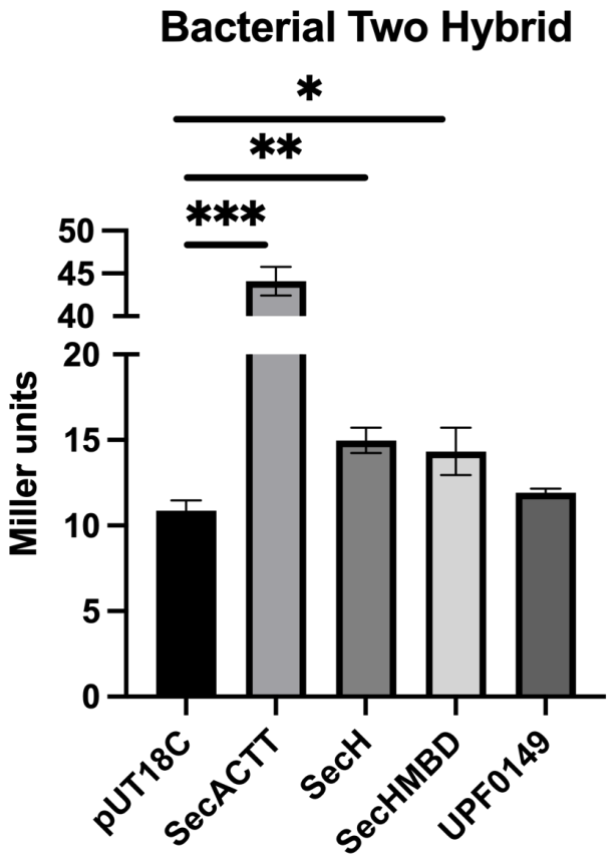

Figure 16- Bacterial two hybrid screen between SecB and SecH.

Each strain was cultured overnight and diluted 1:100 into LB and grown until exponential phase. Cultures were chilled on ice for 20 minutes and the OD_{600} was recorded. 500 mL culture was mixed 1:1 with Z buffer. Lysis was induced by addition of 25 µL chloroform and 0.1% SDS. The solutions were incubated at 28˚C for 5 minutes at 200 µL ONPG was added. The time taken for appearance of deep-yellow colour was measured and the reaction was quenched by addition of 500 µL Na_2CO_3. Absorbances were then measured at 420 nm and the resulting miller units for each reaction was calculated. Error bars represented as 1 standard deviation. Statistical analyses used ANOVA to determine there was a statistically significant difference between the means ($p<0.0001$). Multiple unpaired t-tests, which corrects the p-value for multiple hypothesis testing were then used.

4.3. Discussion

The results in this chapter suggest that SecH interacts with SecB, *via* the MBD, *in vitro* and *in vivo.* The results also indicate that SecH binds to ribosomes, and the interaction is dependent on the MBD. These data suggest that SecH is a Sec protein.

This chapter first set out to demonstrate that SecH interacts with the ribosome. The cosedimentation experiments indicate that SecH, *via* the MBD, interacts with the ribosome. Removal of the MBD does not completely disrupt cosedimentation. This could indicate that other regions of SecH contact the ribosome, as is the case with SecA. In the future, repeating this experiment with the MBD alone would help to determine the contribution of the UPF0149 domain to cosedimentation. It may also be the case that a proportion of the purified ribosomes still contains nascent chains, which then may be bound by the UPF0149 domain of SecH. When investigating the effect of removing the MBD, SecH and SecHΔMBD without ribosomes cosediment in very small amounts. This is likely due to the propensity of SecH to increasingly aggregate after purification and after very few freeze-thaw cycles.

This chapter also set out to investigate the interaction between SecB and SecH. MST experiments suggest SecH does bind to SecB. However, SecH was only able to detectably affect the thermophoretic property of SecB in the presence of 0.05% Tween, which was added due to concerns of surface adsorption to capillaries. Western blotting of the DSP-crosslinked SecB-SecH complex indicated the strongest signal came from the sample that contained 0.05% Tween. This suggests Tween stabilises the interaction between the two proteins.

MST also allowed for determination of K_D for the SecB-SecH interaction, which was measured to be 130 nM. This affinity is in the expected range; *in vitro* the SecA- SecB $K_D \approx$ 1-2 µM, and when SecA is membrane-bound this increases to 30 nM (den Blaauwen et al., 1997; Hartl et al., 1990). This K_D is notably higher than the SecB-SecA interaction in solution - 1.7 µM and even higher than the SecACTT-SecB interaction - 2.7 µM (Patel et al., 2006). In contrast, the bacterial two hybrid screen shows *in vivo* that the SecH-SecB interaction is much weaker than the SecACTT-SecB interaction. However, the bacterial two hybrid screen may not be a useful tool for determination of the strength of an interaction. Many factors can influence the interaction in this assay, including steric hindrance of the T18 and T25 fragments.

As described in Chapter 3, the amino acids involved in SecB binding in the SecA MBD are identical in SecH. Given that the K_D for the SecB-SecH interaction *in vitro* is higher than for SecA-SecB, it is possible that other amino acids from the UPF0149 domain contribute to the interaction. Indeed, in the bacterial two hybrid screen, the β-galactosidase activity in the SecH-SecB assay was slightly higher than in the SecHMBD- SecB assay, indicating the UPF0149 may contribute partly to this interaction.

Despite the apparent higher affinity of SecH for SecB *in vitro*, *in vivo* the bacterial two hybrid screen indicates the SecH interaction is much weaker than the SecACTT-SecB interaction. This may be explained by the SecHMBD-SecB model in Chapter 3. This model suggests that some of the interactions made by the SecA MBD are not made in the SecH MBD with SecB, which may contribute to the reduced strength of the interaction.

The data in this chapter suggest that the MBD of SecH, similar to SecA, can interact with the ribosome as well as SecB *in vitro* and *in vivo.* This indicates that SecH may play a role in Sec-substrate recognition and delivery of nascent substrates from the ribosome to SecB and SecA. That the MBD makes these interactions in both SecA and SecH may signify an existence of a subset of Sec proteins that play an as of yet unknown role in Sec-dependent translocation. The interactions with the ribosome and SecB place SecH in the Sec-dependent pathway. However, the role it plays in this pathway is unknown. In the next chapter, the function of the UPF0149 domain is investigated to shed light on the potential role of SecH as a Sec protein.

Chapter 5

Investigation of the Function of the UPF0149 Domain

All data was acquired and analysed by Max Wynne, with the exception of native mass spectrometry data which was acquired and analysed by Kish Adoni.

5.1. Introduction

The UPF0149 domain is present in YgfB- and YecA-family proteins. Though structures have been determined for two of these proteins (PDB: 4GYT, 1IZM), the ultimate function of the domain remains unknown (Galkin et al., 2004; Michalska et al., 2012).

SecH has an apparent effect on translocation. A *secH* knockout inhibits translocation of maltose binding protein (MBP), and overexpression of SecH increases the efficiency of MBP translocation. Further, overexpression of SecH in strains lacking *secB* inhibits translocation of MBP, suggesting SecH passes client proteins to SecB (Smith et al., 2020).

SecH has holdase chaperone activity. SecH prevents the aggregation of porcine citrate synthase *in vitro* (Smith et al., 2020). *In vivo,* SecH promiscuously binds to many proteins, suggesting it has chaperone activity (Smith et al., 2020). However, the mechanism of client binding and recognition is currently unknown.

SecH modulates the ATPase activity of SecA *in vitro.* In the presence of SecYEG and substrate protein, SecH significantly increases the SecA ATPase rate by almost 40% (Cranford-Smith, 2018). It is not currently clear whether this occurs due to a direct interaction of SecH with SecA, or if the chaperone activity of SecH functions to increase the concentration of substrate protein for SecA.

In this chapter, the function of the UPF1049 domain was investigated. Site specific crosslinking was used to capture the interaction of SecH with Sec substrates. *In vitro* assays were also used to probe the direct effect of SecH on the ATPase activity of SecA. Size exclusion chromatography, photo-crosslinking and native mass spectrometry were used to probe the oligomerisation of SecH. Structural modelling was used to predict the interaction interface of SecH oligomers as well as the interactions between SecH and SecA. This chapter provides evidence that SecH does not directly interact with SecA in the absence of SecYEG and substrate protein. This chapter also provides the first evidence of SecH oligomerising *in vivo.*

5.2. Results

5.2.1. Site-Specific Crosslinking Protein Design

SecH, *in vivo*, promiscuously interacts with a large number of proteins (Smith et al., 2020). Further, the MBD of SecA binds to ribosomes to aid the interaction of SecA with nascent proteins, suggesting SecH may also interact with substrate proteins (Jamshad et al., 2019). In order to investigate the interactions that the UPF1049 domain makes, the unnatural amino acid p-benzoyl-l-phenylalanine (Bpa) was incorporated at different positions across the surface of SecH (Figure 17). Bpa is an unnatural amino acid that can form covalent bonds with CH, NH, SH and OH chemical groups, which is enhanced by UV light. (Schwarz et al., 2016). The structural model of SecH (Figure 8) was explored to select residues for incorporation of Bpa. Amino acids that are surface-exposed, near hydrophobic patches and residues on loops were considered for incorporation. In total, 11 amino acids were selected: W13, H25, W52, Y63, F80, N91, D129, F101, L146, M159 and L173 (Figure 18). At the N-terminus, W13 protrudes into the solvent from the first helix. H25 is present on the loop connecting helix 1 to helix 2. W52 is located in the middle of helix 3. Y63 sits in the long connecting loop between helix 3 and 4. F80 protrudes into the solvent from the middle of helix 4. Next, the hydrophobic N91 is situated at the C-terminal end of helix 4. F101 is located at the surface of helix 5 and protrudes into the solvent. Negatively charged D129 is located on the loop between helices 5 and 6. L146 is located at the end of helix 6. The connecting loop to helix 7 contains M159, and the middle of helix 7 holds L173.

The mutant proteins were designed to include an N-terminal 6x-His tag and SUMO tag and a C-terminal AviTag which allows for biotinylation of the protein (Jamshad et al., 2019). Bpa is incorporated at the amber codon, which would normally cause termination of translation. Bpa incorporation therefore allows translation of the remainder of the protein, including the C-terminal AviTag. Therefore, Bpa-incorporated proteins can be detected by western blotting using HRP-conjugated streptavidin, which binds to biotin.

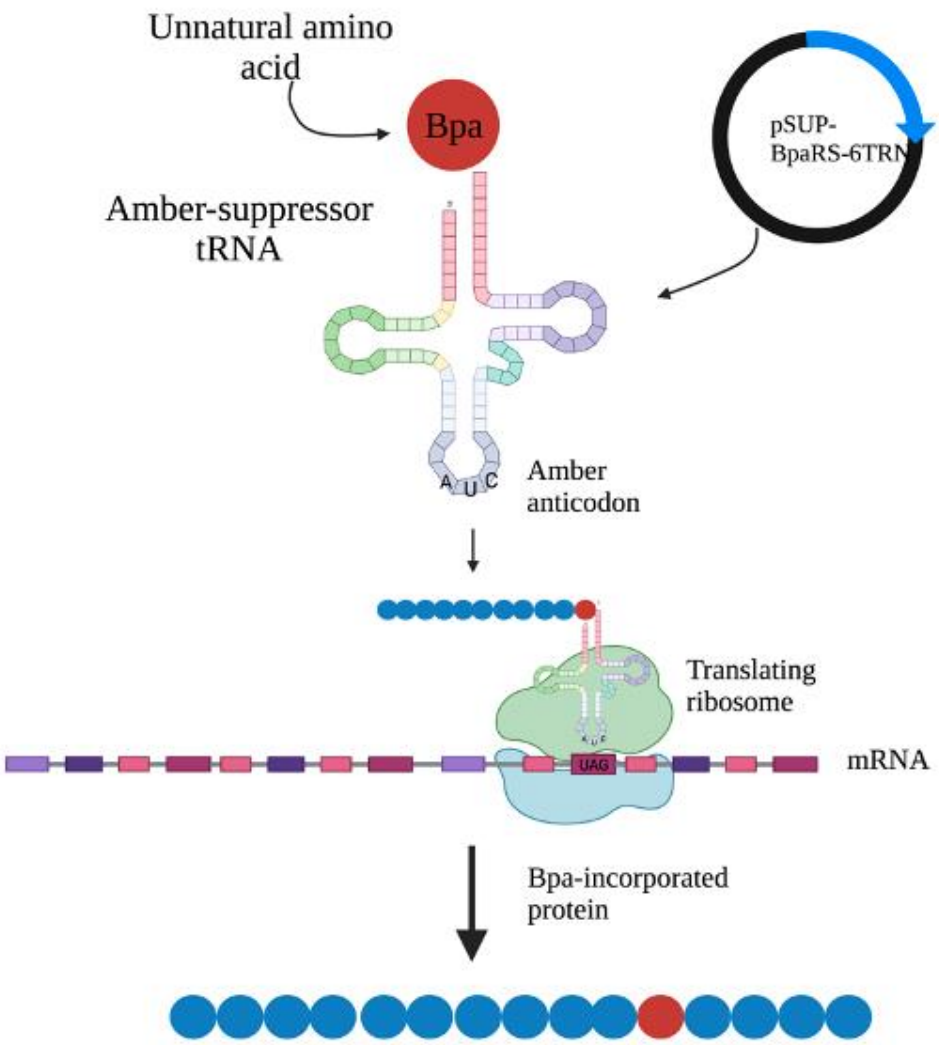

Figure 17 – Schematic of Bpa-incorporation into proteins.

The plasmid pSUP-BpaRS-6TRN expresses a mutant tRNA/tRNA synthetase from *M. jannaschii,* which recognises amber stop codons (TAG). Recognition of the amber stop mRNA codon UAG normally results in termination of translation. The suppressor tRNA, however, incorporates the unnatural amino acid Bpa, allowing for continuation of translation. Figure made using BioRender.

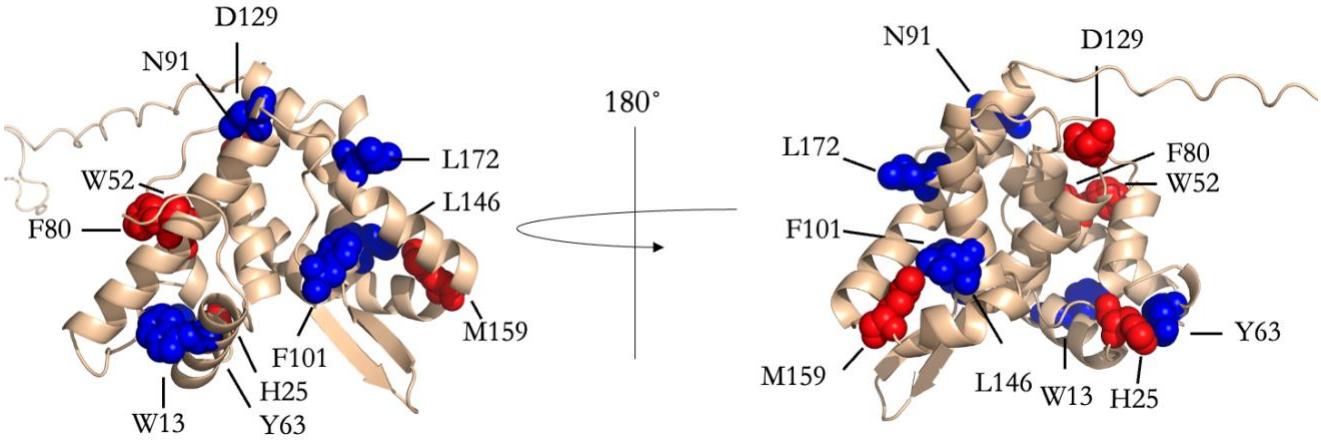

Figure 18- SecH structural model with residues chosen for Bpa incorporation.

SecH was modelled as described in Chapter 3. The structural model is presented with positions chosen for Bpa incorporation highlighted as spheres. Residues were chosen to effectively cover a large amount of the surface of the protein to increase the probability of capturing interacting surfaces of the protein. Positions showing possible crosslinks are coloured in blue, and positions showing no potential crosslinks are coloured in red. Model visualised in pyMOL.

5.2.2. SecH- SecB Photo-Crosslinking

The results in chapter 4 suggested that some amino acids in the UPF0149 domain of SecH may contribute to the interaction of SecH with SecB. In order to identify residues in the UPF0149 that may contact SecB, the Bpa-incorporated mutant proteins were purified using a HisTrap column and incubated with SecB to determine whether crosslinks form. Each mutant was incubated with SecB and exposed to UV light at 365 nm. These samples were blotted against biotin (Figure 19).

The majority of the mutant proteins were expressed, with a band visible at 25 kDa. However, H25, W52, F80 were not produced in detectable amounts. A crosslink between SecH and SecB would yield a crosslinking adduct at around 42 kDa as seen previously in section 4.2.3. Purified $SecH^{W13Bpa}$, $SecH^{Y63Bpa}$, $SecH^{N91Bpa}$, $SecH^{F101Bpa}$, $SecH^{L146Bpa}$ and $SecH^{L173Bpa}$ contained many bands at a wide range of different sizes suggesting these mutants are crosslinking to many different proteins, which may include SecB, and this occurs either during growth or during preparation and purification.

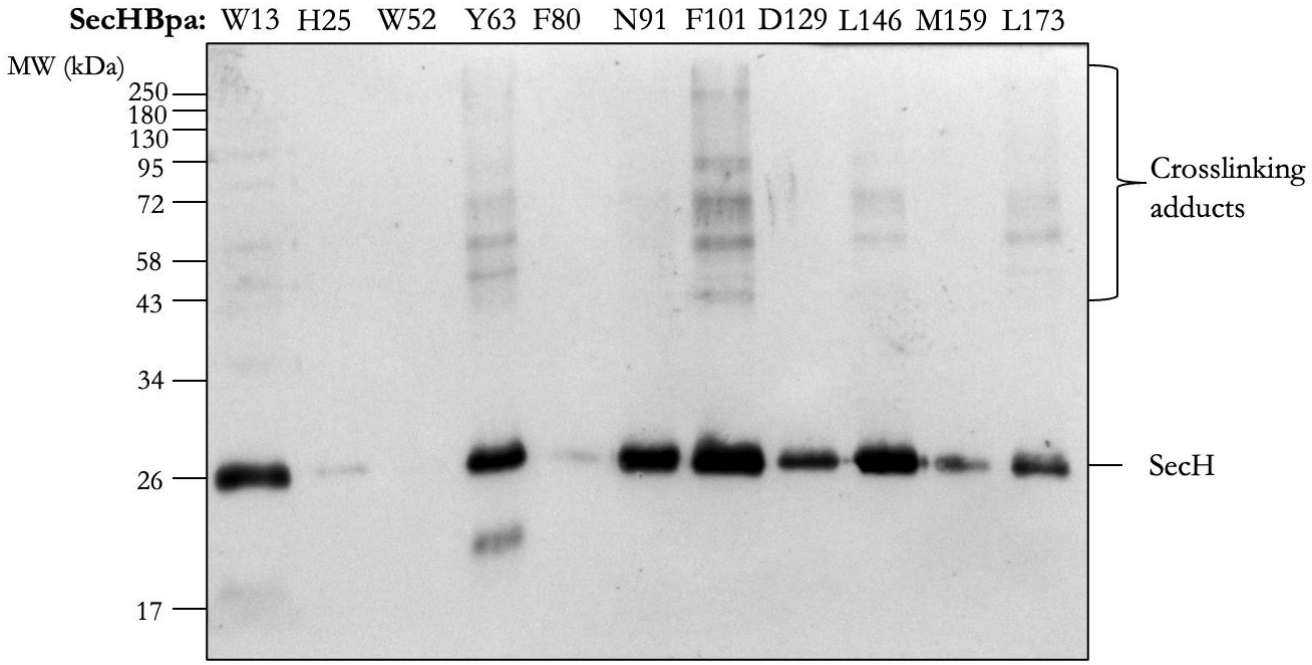

Figure 19 – Western blot of Bpa-incorporated SecH mutants incubated with SecB and exposed to UV light.

2 µM SecB was incubated with each SecH mutant at a concentration of 2 µM in binding buffer. 200 µL of each incubation reaction was exposed to UV light at 365 nm on ice for 30 minutes in a round bottom- 96 well plate. 10 µL of each sample was loaded onto an SDS-PAGE gel and then western blotted against biotin.

From these experiments, 6 SecH mutants contained banding patterns that could possibly contain a SecB crosslink: W13Bpa, Y63Bpa, N91Bpa, F101Bpa, L146Bpa and L173Bpa. To further probe for a crosslink, these 6 mutants were incubated both with and without SecB and exposed to UV light to determine whether a SecB crosslinking band appears when crosslinking is induced (Figure 20).

Except for SecH mutant W13Bpa, all other mutants displayed the wide variety of bands that cross-react with biotin in the absence of SecB, indicating that the mutant proteins had already formed these crosslinks *in vivo*. The sizes of the crosslinking bands varied, suggesting the mutants are crosslinking to many different proteins. On addition of SecB, no SecH mutant contained an additional band at 42 kDa, suggesting that none of the SecH mutants crosslink to SecB.

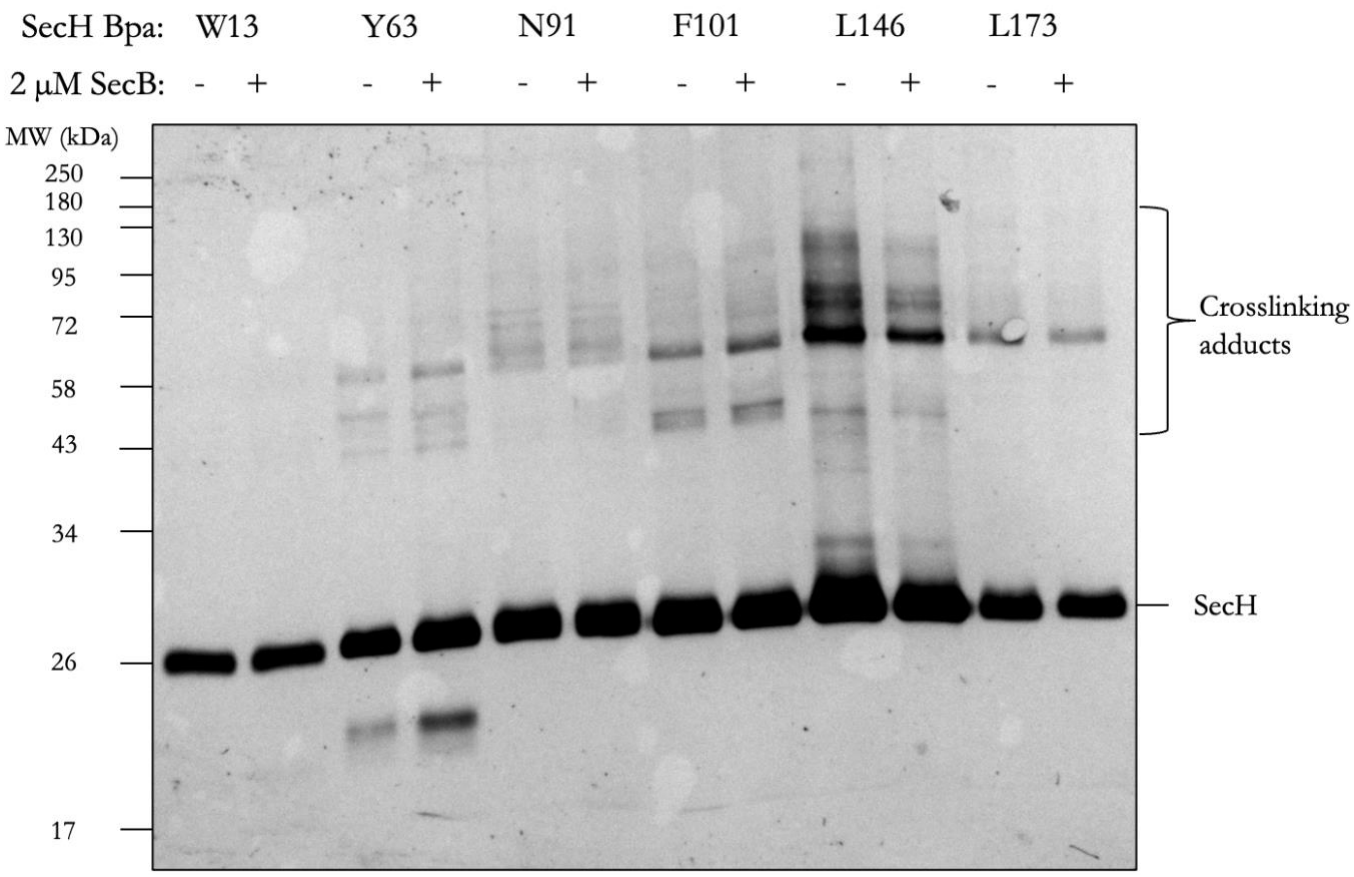

Figure 20- Anti-biotin western blot of potential SecB-crosslinking mutants.

2 μM of each mutant was incubated either alone or 2 μM of SecB. 200 μL of each sample was crosslinked by exposure to UV light at 365 nm for 20 minutes on ice. 10 μL of each sample was loaded onto an SDS PAGE gel and then western blotted against biotin.

5.2.3. Photo-Crosslinking of SecH Mutant Lysates

Western blotting of purified SecH mutants suggested that the SecH mutants are forming crosslinks to many different proteins either during growth or purification. To confirm that the suspected crosslinking bands seen were occurring *in vivo*, and to identify the crosslinked proteins, lysates of cells producing mutant proteins were exposed to UV light to induce crosslinking. N91Bpa and F101Bpa mutants were chosen as they were the most consistent in showing a variety of crosslinking bands. Cells were grown and lysed as previously described in the presence of 1 mM Bpa and the cell lysates were exposed to UV light at 365 nm for 30 minutes on ice and then blotted against biotin (Figure 21). Both mutants had two distinct bands. The higher band at 45 kDa represents the expressed mutant protein with the SUMO tag (and 6x-His tag) still attached to the N-terminus and the AviTag, which is biotinylated, at the C-terminus. The smaller band is likely the mutant protein that has had the SUMO tag cleaved *in vivo* through non-specific cleavage.

Both the N91Bpa and F101Bpa samples contained faint bands at high molecular weights that reacted with anti-biotin antibody, indicating low levels of crosslinking without direct exposure to UV light. On exposure to 365 nm UV light, these bands became more prominent, especially with mutant N91Bpa. This indicates that both N91Bpa and F101Bpa crosslink to a variety of different proteins *in vivo* both spontaneously but largely on direct exposure to UV light.

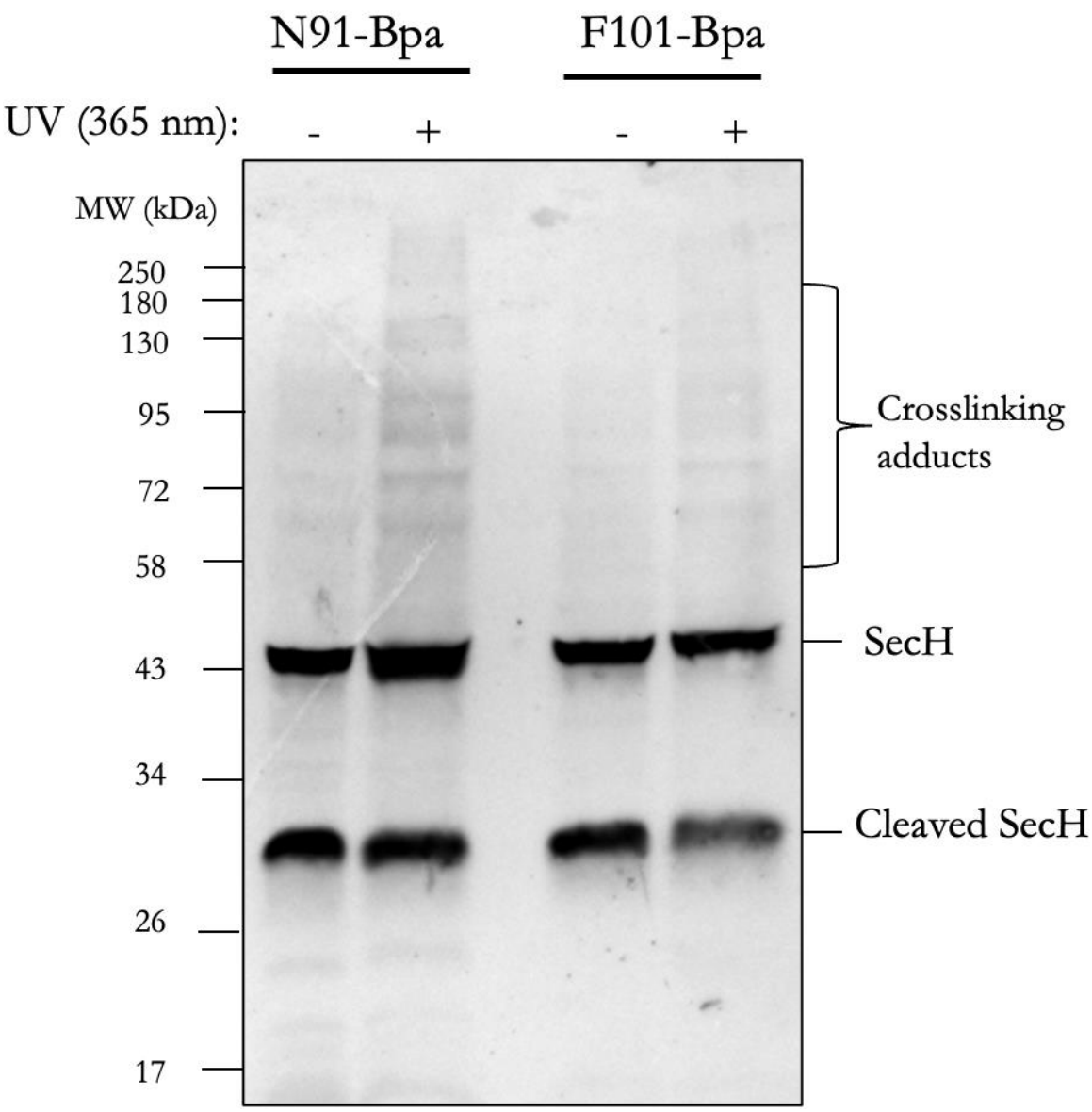

Figure 21 – Western blot of mutant N91 and F101 lysates before and after exposure to 365 nm UV light.

Mutant proteins were grown as previously described in the presence of 1mM Bpa, 1 mM IPTG and appropriate antibiotics. Cells were lysed using a C3 Emulsiflex homogeniser and clarified by centrifugation to remove cellular debris. 200 µL of each lysate was exposed to 365 nm UV light for 30 minutes on ice. 10 µL of each sample was loaded on to an SDS PAGE gel before being blotted against biotin.

5.2.4. Identification of Crosslinked Proteins

Identifying the proteins that crosslink to the mutant SecH proteins could give insight into the function of the UPF0149 domain by elucidating its substrate specificity. As the mutant N91Bpa protein showed a large representative banding pattern, the purified protein was run on an SDS-PAGE gel, together with W13Bpa as a negative control. W13Bpa was used as a negative control as no crosslinking bands were seen (Figure 20). Sections of the gel where the banding patterns occurred were excised and sent for protein identification by mass spectrometry. 3 sections of the gel were excised containing crosslinking bands: 34-43 kDa, 43 kDa – 65 kDa and 65 kDa-100 kDa. Several constraints were used to filter the identified proteins in order to reduce the likelihood of false positive results and only identify crosslinked proteins: (i) Only proteins with 2 or more unique peptides were included (ii) Only proteins with a score sequest result of 10 or more were included (iii) the molecular weight from each gel slice was filtered to include only crosslinking proteins by subtracting the molecular weight of SecH (25 kDa), given that on an SDS PAGE gel, proteins that are covalently linked to SecH will resolve with a molecular weight that is 25 kDa greater than their actual molecular weight.

Mass spectrometry analysis identified 116 proteins in the N91Bpa sample compared to 29 proteins with W13Bpa (Appendix Table 7-Table 12), consistent with the wide range of adducts produced by N91Bpa *in vivo* (Figure 21). This suggested the N91Bpa mutant protein is crosslinking to more proteins compared to W13Bpa. These proteins identified in the N91Bpa sample were analysed for enrichments to determine similarities between them using the Database for Annotation, Visualisation and Integrated Discovery (DAVID). Gene Ontology (GO) was used to annotate these proteins based on their molecular function. This analysis found

that the proteins identified in the N91Bpa sample were enriched for non-specific functions including proteins with catalytic activity (p=0.0000002) and protein-binding proteins (p = 0.0000048) (Table 6). The identified proteins were also enriched for nucleotide-binding proteins. However, closer inspection of the proteins within the enriched categories did not reveal any common sequence or structural motif, consistent with previous data that *in vivo* SecH interacts promiscuously with a wide range of proteins (Smith et al., 2020). In addition, SecA was among the proteins identified in N91Bpa (11 peptides and 12 peptide spectral matches (PSMs)) and W13Bpa (5 peptides and 5 PSMs), suggesting that SecA interacts with SecH *in vivo.*

Molecular Function Term	Number of Proteins	P-value	Number of Secretory Proteins
Catalytic Activity	30	0.0000002	2
Nucleotide Binding	34	0.0000024	2
Protein Binding	54	0.0000048	9

Table 6 – Molecular Function Enrichment of identified crosslinking adducts.

Proteins identified as potential crosslinking adducts were analysed using DAVID. The GO Molecular Function Database is an annotated database that contains GO terms for each protein, which describes its molecular function. Using this database, the GO terms for each of the inputted proteins were analysed to determine any enrichment. The above table contains the GO term, the number of proteins that are annotated with this term, the p value and the number of secretory proteins associated with each enrichment. The null hypothesis states that the inputted list of proteins being enriched for the particular GO term is due to random chance. The full list of identified proteins can be found in the Appendix (Table 7-Table 12).

5.2.5. SecH Pull-Down from Mutant Protein Lysates in Cells Lacking SecB

In vivo, SecH inhibits translocation in cells lacking SecB, suggesting that it may interact with Sec substrates before SecB. Therefore, to investigate the interaction of SecH with Sec substrates, *secB* was removed from the chromosome of *E. coli* BL21 to increase the probability of SecH interacting with Sec substrates. The SecH Bpa mutant proteins were expressed in the presence of 2% maltose to induce the expression of the mal regulon, including Sec substrate LamB. SecH Bpa mutants which showed the largest number of crosslinking adducts, SecH $N91^{Bpa}$ and SecH $F101^{Bpa}$, as well WT SecH, were then overexpressed and exposed to UV light to induce crosslinking. The WT SecH and the two mutant SecH proteins were pulled down from the lysate using streptavidin-coated magnetic beads, which binds to the C-terminal biotin tag, and washed with binding buffer containing 2% Triton X-100 and western blotted against biotin (Figure 22).

The full-length tagged SecH resolved with a molecular weight of 45 kDa. In both the N91Bpa and F101Bpa samples, two bands with a strong signal resolved with approximate molecular weights of 100 and 150 kDa. Finally, a large band was present in the F101Bpa sample at 200 kDa. To identify the proteins in the bands, the 45, 100, 150 and 200 kDa bands present in the F101Bpa sample were excised and sent for identification by mass spectrometry (Appendix Table 13 - Table 16).

In the protein band corresponding to 45 kDa, the most abundant protein identified was SecH (6 Peptides, 15 PSMs). Elongation factor Tu (43 kDa – 2 peptides, 2 PSMs), Cysteine desulfurase

(45 kDa – 2 peptides 2 PSMs), 3-dehydroquinate synthase (39 kDa- 1 peptides, 1 PSM) and transcription termination factor Rho (47 kDa – 1 peptide 1 PSM) were also present in trace amounts in this band.

In the 100 kDa band, SecH was the most abundant protein, with 4 peptides identified and 18 PSMs. Bifunctional aspartokinase/homoserine dehydrogenase (89 kDa) and Glyceraldehyde-3-phosphate dehydrogenase (36 kDa) were also identified, however these two proteins had a significantly lower abundance, with 2 peptides and 2 PSMS, and 1 peptide with 1 PSM respectively. If the excised band contained a SecH-protein crosslink, it would be expected that the crosslinked protein would be found in a similar abundance to SecH. This suggests that the excised band at 100 kDa is likely a SecH dimer.

The protein band excised at 150 kDa also contained SecH (4 peptides, 13 PSMs). The only other protein identified was Apartokinase (49 kDa). This protein was also at significantly lower abundance, with only 1 peptide identified and 1 PSM, indicating it is likely a contaminating protein. The protein band that resolved at 200 kDa contained SecH (4 peptides, 6 PSMs). The other protein present was Elongation Factor Tu. This protein was also at significantly lower abundance (2 peptides and 2 PSMs). Taken together, this suggests that the excised band at 150 kDa and 250 kDa contain higher order SecH multimers, consistent with the molecular weight of a trimer and tetramer.

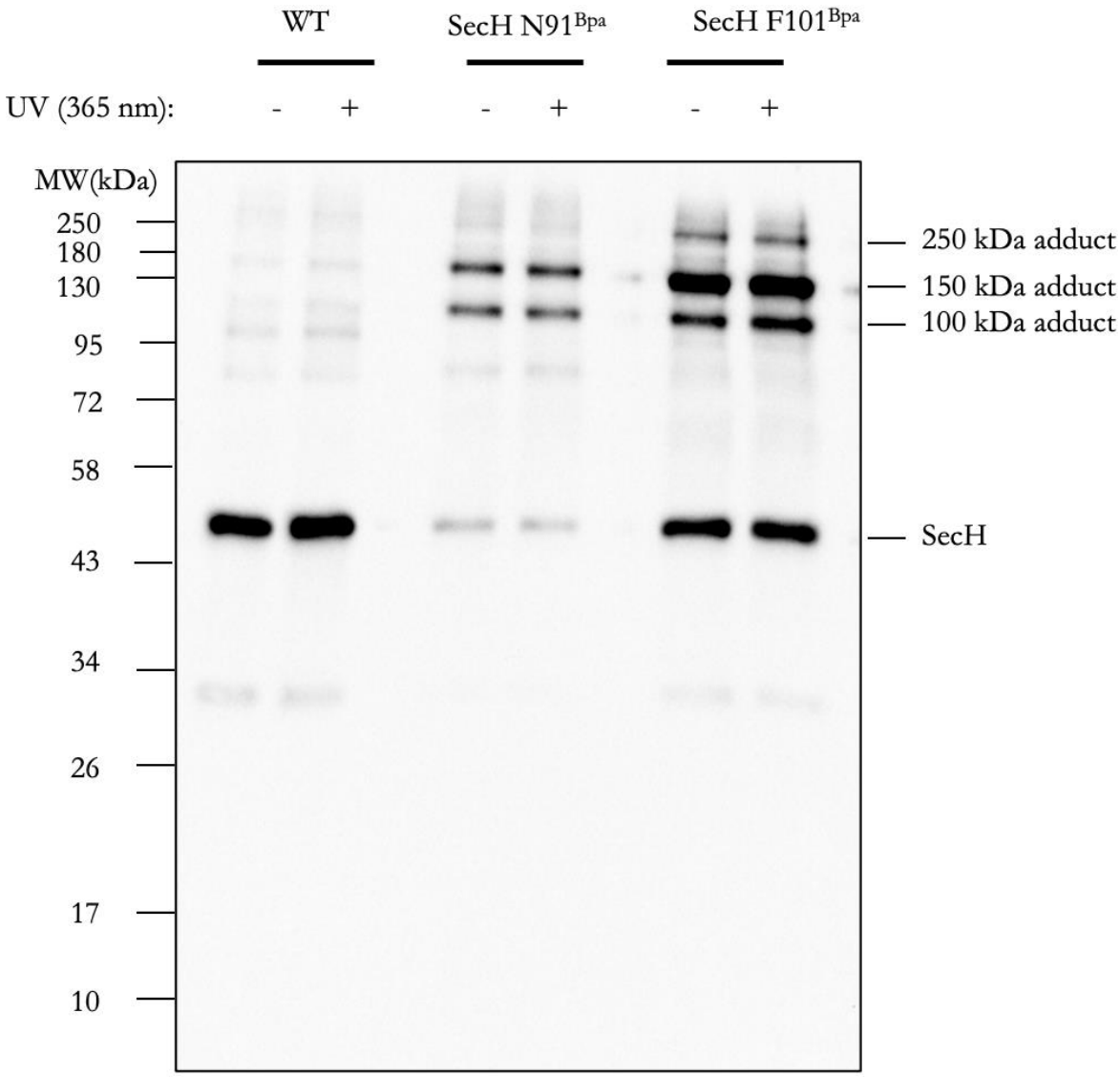

Figure 22 - Anti-biotin western blot of proteins SecH mutants pulled down from lysates using streptavidin.

Mutant proteins were grown as previously described in the presence of 1mM Bpa, 1 mM IPTG and appropriate antibiotics. Cells were lysed using a C3 Emulsiflex homogeniser and clarified by centrifugation to remove cellular debris. Biotinylated SecH and crosslinked proteins were pulled down using streptavidin beads. 50 µL beads were washed in pull-down binding buffer three times, before being incubated with 5 mL lysate for 30 minutes. The beads were then washed three times and bound proteins were eluted by resuspension in 50 µL 1X SDS buffer and were boiled for 5 minutes. Samples were separated by SDS PAGE and western blotted against biotin.

5.2.6. SecH Co-Purification from Mutant Protein Lysates

The data in the previous section suggested that in the absence of SecB, both F101Bpa and N91Bpa crosslink to form higher order SecH oligomers. However, pull-down assays in the presence of 2% Triton disrupts the interaction of copurifying proteins with the SecH mutant proteins. To investigate which proteins copurify with SecHF101^{Bpa} and SecHN91^{Bpa} in the absence of SecB, these mutant proteins were pulled down from lysates of cells lacking SecB as previously described, with binding buffer that did not contain Triton and analysed by mass spectrometry (Appendix Table 17-Table 19). In the WT SecH sample, where SecH oligomers had not been stabilised, WT SecH copurified with 176 proteins (Table 17). In contrast, N91Bpa copurified with 474 proteins (Table 18) and F101Bpa copurified with 310 proteins **(**Table 19). This suggests that oligomeric SecH interacts more strongly with proteins than WT SecH.

The identified copurifying proteins were analysed for enrichments by DAVID to investigate the molecular function of the copurifying proteins (Figure 23). The proteins copurifying with WT SecH, SecHN91^{Bpa} and SecHF101^{Bpa} were all found to be significantly enriched for ribosomal proteins, consistent with results from Chapter 4 that SecH binds to the ribosome. Further, all samples were enriched for RNA binding proteins. In all cases, the majority of the RNA-binding proteins were ribosomal subunit proteins. Indeed, WT SecH and SecHF101^{Bpa} were both enriched for rRNA binding proteins. These results suggest in the absence of SecB, SecH copurifies strongly with ribosomes.

WT SecH

Molecular Function Term	Number of Proteins	P-value	Number of Secretory Proteins
Protein-binding	116	$3.9*10^{-19}$	**26**
Structural constituent of ribosome	25	$1.1*10^{-16}$	
RNA binding	37	$1.9*10^{-14}$	
rRNA binding	22	$6.0*10^{-13}$	

SecHN91^{Bpa}

Molecular Function Term	Number of Proteins	P-value	Number of Secretory Proteins
Ribosomal Protein	40	$9.6*10^{-26}$	**47**
Ribonucleoprotein	40	$2.7*10^{-25}$	
rRNA-binding	34	$1.5*10^{-19}$	
RNA binding	54	$3.2*10^{-19}$	

SecHF101^{Bpa}

Molecular Function Term	Number of Proteins	P-value	Number of Secretory Proteins
Protein-binding	148	$1.4*10^{-20}$	**52**
Identical protein binding	74	$1.2*10^{-12}$	
Structural constituent of ribosome	24	$1.5*10^{-12}$	
RNA binding	36	$1.1*10^{-9}$	

Figure 23 - Molecular Function Enrichment of identified copurifying proteins.

Identified copurifying proteins were analysed using DAVID to identify enrichments. Using this database, the GO terms for each of the inputted proteins were analysed to determine any enrichment. The above table contains the GO term, the number of proteins that are annotated with this term the p value and the number of secretory proteins copurifying with each mutant. The null hypothesis states that the inputted list of proteins being enriched for the particular GO term is due to random chance. The full list of proteins can be found in the appendix (Table 17 - Table 19).

Cells were grown in the presence of 2% maltose to induce expression of Sec substrate LamB. It was found that LamB was one of the most strongly enriched proteins that copurified due to cross-linked stabilisation of SecH multimers. LamB copurified more strongly with both N91Bpa (9 peptides and 10 PSMs) and F101Bpa (7 peptides and 9 PSMs) compared to WT SecH (1 peptide and 1 PSM), suggesting LamB interacts more strongly with oligomerised SecH in the absence of SecB.

To confirm these mass spectrometry results, the SecH pull-down samples were western blotted using antibodies directed against LamB (Figure 24). The LamB signal was significantly stronger in the N91Bpa and F101Bpa samples compared to WT SecH. This suggests that LamB copurifies with SecH and may do so more strongly with oligomerised SecH.

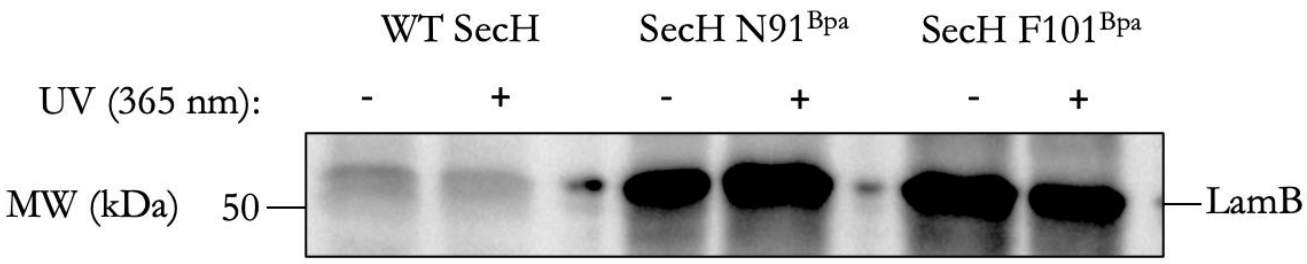

Figure 24 – Western blot against LamB of proteins copurifying with SecH mutant proteins in cells lacking SecB.

Strains were grown as previously described in the presence of 1mM Bpa, 1 mM IPTG, 2% maltose and appropriate antibiotics. Cells were lysed using a C3 Emulsiflex homogeniser and clarified by centrifugation to remove cellular debris. Biotinylated SecH and copurifying proteins were pulled down using streptavidin beads. 50 µL beads were washed in pull-down binding buffer lacking Triton three times, before being incubated with 5 mL lysate for 30 minutes. The beads were then washed three times and bound proteins were eluted by resuspension in 50 µL 1X SDS buffer and were boiled for 5 minutes. Samples were separated by SDS PAGE and western blotted against the

SecH increases the ATPase activity of SecA in translocation-coupled ATPase assays, suggesting SecH may interact with SecA. SecA copurified in similar abundance with both WT SecH and the two SecH mutant proteins, suggesting SecH interacts with SecA *in vivo* in the absence of SecB. To confirm these results, the SecH-pull down samples were blotted using antibodies directed against SecA (Figure 25). The strongest signal was detected at 100 kDa in the $N91^{Bpa}$ sample both before and after exposure to UV light. There was a weaker signal detected in the WT SecH sample, and no signal detected in the F101Bpa sample. This indicates SecA copurifies with WT SecH, and more strongly copurifies with N91Bpa, suggesting SecA interacts with SecH *in vivo.*

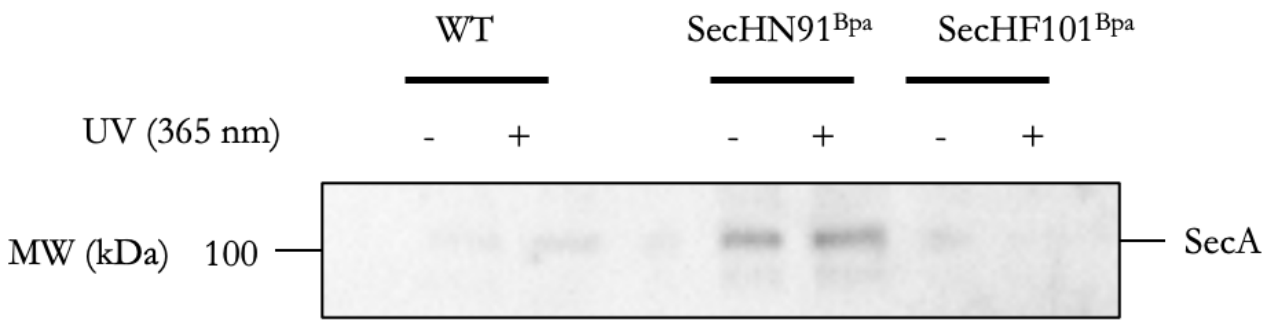

Figure 25 - Western blot against SecA of proteins copurifying with SecH mutant proteins in cells lacking SecB.

Mutant proteins were grown as previously described in the presence of 1mM Bpa, 1 mM IPTG, 2% maltose and appropriate antibiotics. Cells were lysed using a C3 Emulsiflex homogeniser and clarified by centrifugation to remove cellular debris. Biotinylated SecH and copurifying proteins were pulled down using streptavidin beads. 50 µL beads were washed in pull-down binding buffer lacking Triton three times, before being incubated with 5 mL lysate for 30 minutes. The beads were then washed three times and bound proteins were eluted by resuspension in 50 µL 1X SDS buffer and were boiled for 5 minutes. Samples were separated by SDS PAGE and western blotted against SecA.

5.2.7. Size Exclusion Chromatography

To investigate the possibility that SecH oligomerises, size exclusion chromatography was used (Figure 26). Size exclusion chromatography is used to separate proteins in a solution by their size. Within a size exclusion column, there is a porous resin consisting of beads. Smaller proteins are able to diffuse into these beads whereas larger proteins cannot. As a result, larger proteins have a smaller volume to navigate and therefore elute earlier, whilst smaller proteins travel through the beads and elute later. If SecH dimerises, this complex (50 kDa) would have a similar size to SecB, which forms a 68 kDa tetramer, and could be detected using size exclusion chromatography.

Purified SecH was run through a Superdex 200 column, represented as a cyan trace (Figure 26). SecH eluted as a larger peak at around 16 mL, with a peak that spans from 16 mL – 14 mL. Western blotting of the fractions corresponding to both peaks with antisera directed against SecH indicated both peaks contain SecH. This peak suggests that in solution SecH adopts both monomeric and dimeric conformations.

Next, purified SecB, which is a 68 kDa tetramer in solution, was passed through the column, represented as magenta trace. The protein eluted as a sharp peak at roughly 14 mL. This peak eluted at a similar volume to the broad SecH peak, suggesting SecH forms a dimer with a similar, but slightly smaller molecular weight, which is consistent with a SecH dimer (50 kDa).

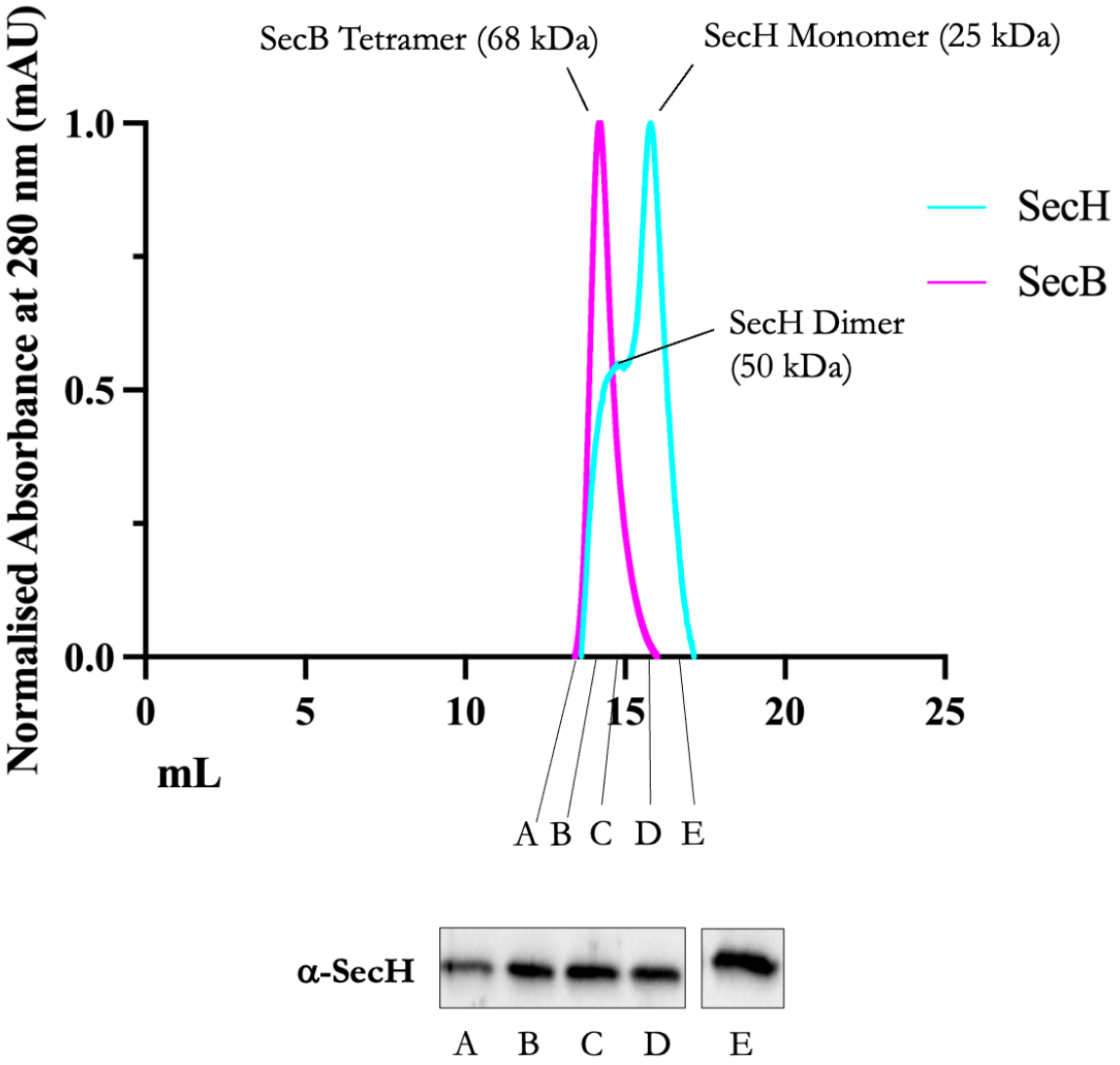

Figure 26 - SecB and SecH size exclusion chromatogram.

Purified proteins were diluted to desired concentrations in 20 mM HEPES, 25 mM $KOAc_2$, 10 mM $Mg(OAc)_2$ 100 µL of .70 µM SecB and 17.5 µM SecH were run through a Superdex 200 10/300 GL column at a flow rate of 0.4 $mL.min^{-1}$. Fractions were collected and diluted in SDS loading buffer. 15 µL of each sample was loaded on an SDS PAGE gel and subsequently western blotted. SecB represented by a magenta trace and SecH is represented by a cyan trace.

5.2.8. Native Mass Spectrometry

The results in the previous section suggested that SecH dimerises. To confirm that SecH dimerises in solution, purified SecH was analysed by native mass spectrometry (MS). By maintaining proteins in their native conformation, native mass spectrometry can be used to analyse intact proteins and the non-covalent interactions they make.

SecH was identified by calculating the charge states for each peak, allowing calculation of the mass corresponding to each charge state distribution. Under the conditions used for native MS, the most abundant species had a molecular weight consistent with monomeric SecH (Figure 27). However, dimeric SecH was also present in detectable quantities indicating that SecH does form homodimers in solution with low affinity between protomers (Figure 28).

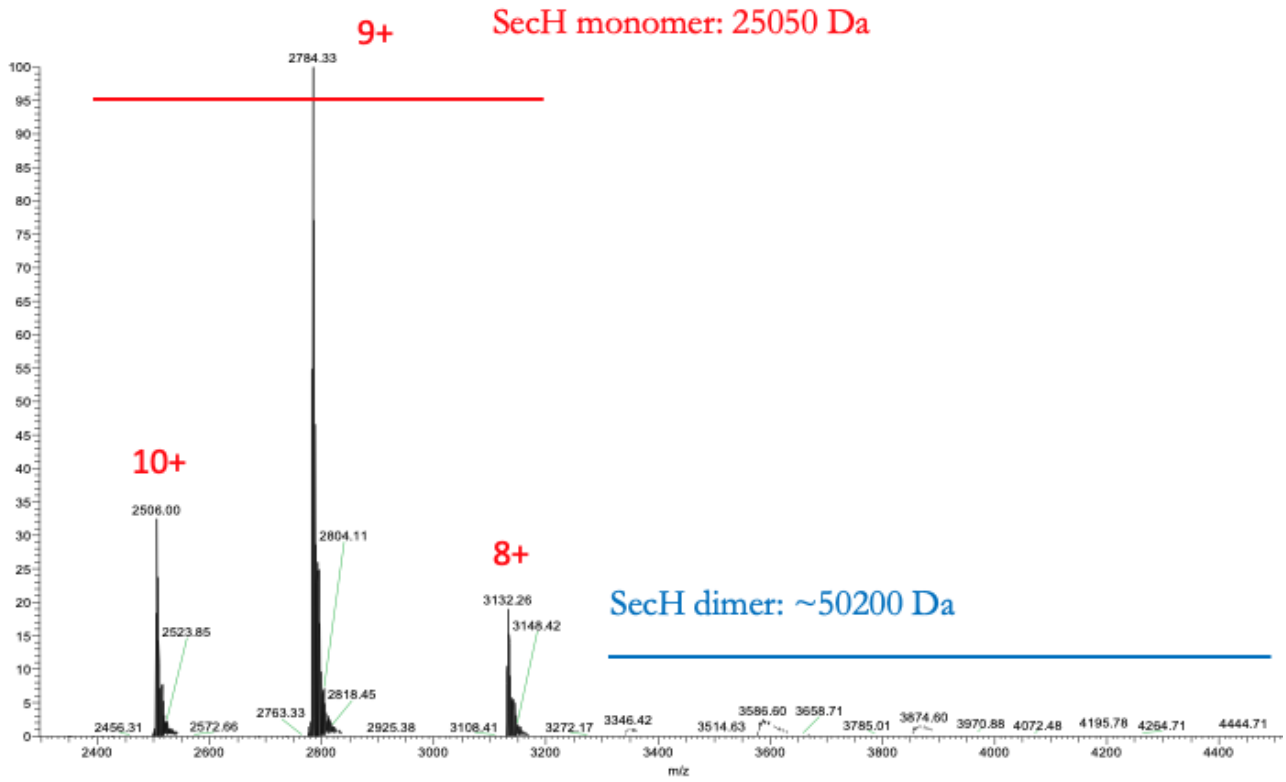

Figure 27- Native Mass spectrum of purified SecH.

5 µM SecH in 100 mM ammonium acetate was analysed by native mass spectrometry. The large peaks correspond to different charge states of SecH monomers. The monomeric charge states of SecH, between m/z 2400 and 3200 are highlighted in red, and the dimeric charge states of SecH, between m/z 3400 and 4100are highlighted in blue. Small amounts of SecH dimers are detectable.

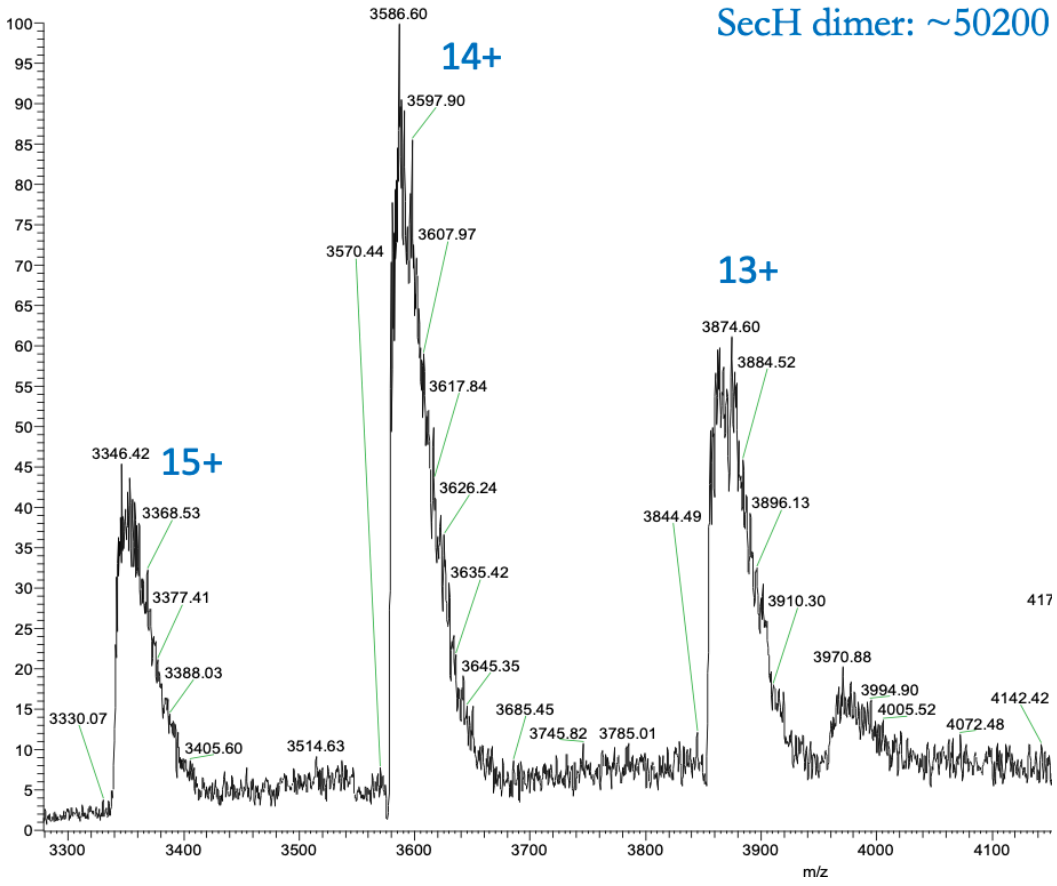

Figure 28 - Native Mass spectrum of SecH dimers.

5 µM SecH in 100 mM ammonium acetate was analysed by native mass spectrometry. The peaks corresponding to SecH dimers between m/z 3300 and 4100 are poorly resolved due to low abundance but indicate presence of SecH dimers. The charge states of each peak are highlighted in blue.

5.2.9. SecH-Mediated Stimulation of ATPase Activity

The finding that SecH copurifies with SecA, and other ATPases, suggested that it might enhance the ATPase activity of SecA by interacting with it directly. To investigate this possibility, an NADH-coupled ATPase was used to determine the effect of SecH on the ATPase activity of SecA. This assay couples ATP hydrolysis to pyruvate kinase, which generates ATP from ADP, converting phosphoenolpyruvate to pyruvate. Lactate dehydrogenase catalyses the conversion of pyruvate to lactate, whilst oxidising NADH to NAD+. The oxidation of NADH can be measured spectrophotometrically by the decrease in absorbance at 340 nm (Figure 29).

SecH and SecHΔMBD were added at 2:1, 1:1, and decreasing stoichiometries with SecA to probe its effect on the ATPase activity of SecA (Figure 30). SecA alone was measured and used as the control. In the presence of both WT SecH and SecHΔMBD, there was no discernible difference in the specific activity of SecA at any stoichiometry. There is no significant different between the means of the different samples (One-way ANOVA $p>0.05$).

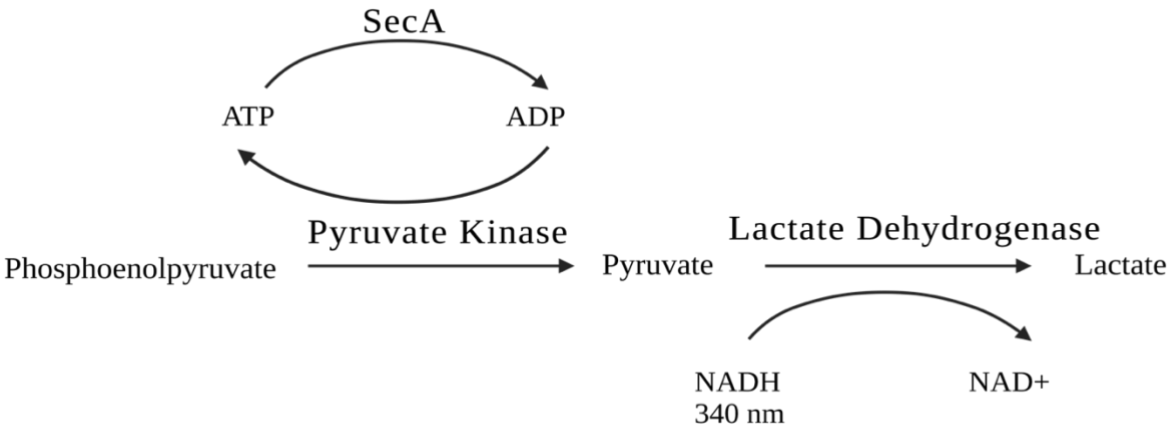

Figure 29- Reaction scheme of NADH-coupled ATPase assay.

SecA ATP hydrolysis generates ADP, which is used by pyruvate kinase to catalyse the formation of pyruvate from phosphoenolpyruvate. Lactate dehydrogenase then catalyses the reduction of pyruvate to lactate by oxidising NADH to NAD+. The reaction is followed spectrophotometrically as NADH absorbs light at 340 nm.

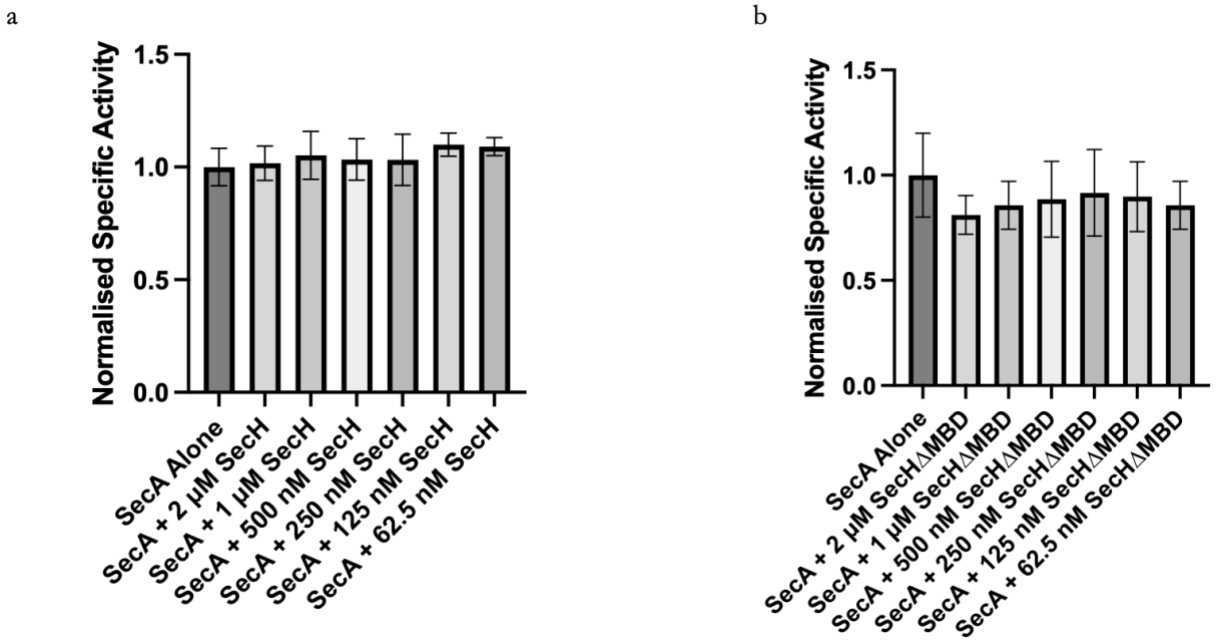

Figure 30 – ATPase assays of SecA in the presence of SecH.

Reactions were run in the presence of TKM buffer (20 mM Tris-HCl, 50 mM KCl, 2 mM $MgCl_2$ and 0.05% Tween). Reactions were made up with 500 µM phosphoenolpyruvate, 200 µM NADH, 20 units/mL lactate dehydrogenase and 100 units/mL pyruvate kinase and 1 µM SecA and varying concentrations of SecH. Reactions were started by addition of 1 mM ATP and absorbance at 340 nm was immediately measured at 10 second intervals. Linear regressions were used to determine the rate from each individual experiment. Each rate was used to calculate the specific activity of SecA. Specific activities were normalised to SecA alone. Data is representative of 9 independent experiments. Error bars represent 1 standard deviation.

5.2.10. SecH -Mediated Stimulation of Nucleotide Exchange

Nucleotide exchange, which occurs after ATP hydrolysis, is the rate limiting step in the SecA ATPase cycle (Fak et al., 2004). Therefore, the inability of SecH to increase the ATPase activity of SecA suggested that it was not a nucleotide exchange factor for SecA. However, in many cases nucleotide exchange factors may increase the exchange rate for both ADP and ATP, raising the possibility that the increased rate of exchange of ATP in the presence of SecH could compete with ATP hydrolysis. This may explain the small decrease in ATPase activity caused by SecHΔMBD.

The effect of SecH on the rate of nucleotide exchange was investigated by the use of fluorescent nucleotide analogue MANT-ADP. MANT-ADP binding to proteins causes an increase in Förster Resonance Energy Transfer (FRET) at 440 nm. Dissociation of MANT-ADP can be measured spectrophotometrically by following the decrease of this fluorescence on the addition of ATP.

Firstly, the dissociation rate of MANT-ADP was measured with SecA alone and in the presence of WT SecH (Figure 31a). The dissociation constant of MANT-ADP with SecA alone was 0.050 $s^{-1,}$ compared with 0.051 s^{-1} in the presence of SecH. There was no significant difference between the means of the two groups (two tailed t-test, $p> 0.05$).

Next, the dissociation of MANT-ADP was measured with SecA alone and in the presence of SecHΔMBD to determine how the UPF0149 domain alone impacts MANT-ADP dissociation (Figure 31b). The dissociation constant of MANT-ADP with SecA alone in these experiments was 0.026 s^{-1}. In the presence of SecHΔMBD, the dissociation constant was 0.030 s^{-1}. Again, there was no significant difference between the means of the two groups (two tailed t-test, $p>0.05$).

These results suggest that SecH does not directly modulate the affinity of SecA for MANT-ADP.

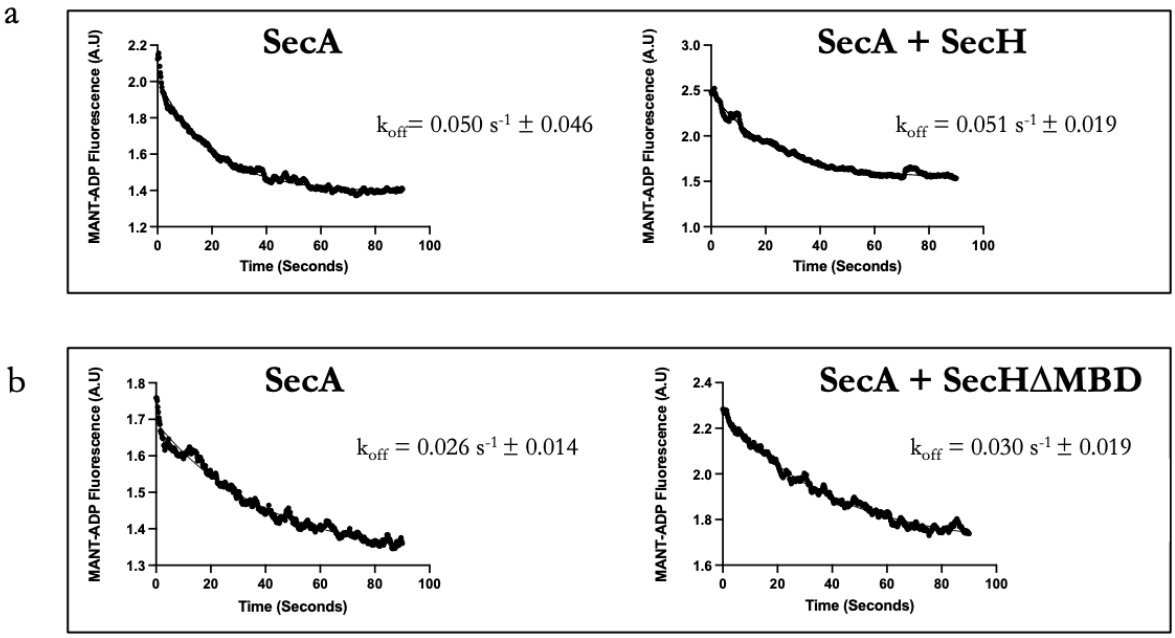

Figure 31 -Fluorescence of MANT-ADP dissociation from SecA.

0.5 µM SecA was incubated either alone or with 0.5 µM of a SecH variant in the presence of 1.2 µM MANT-ADP, buffered with TKM buffer. Measurements were taken in a quartz cuvette maintained at 25˚C. Tryptophans were excited at 295 nm and the emission of MANT-ADP was measured at 450 nm, both with a 5 nm bandpass. **a)** Left panel represents dissociation curve of MANT-ADP in the presence of only SecA. Right panel represents dissociation curve of MANT-ADP in the presence of SecA and WT SecH. **b)** Right panel represents dissociation curve of MANT-ADP in the presence of SecA. Left panel represents dissociation curve of MANT-ADP in the presence of SecA and SecHΔMBD. Data includes 3 replicates for WT SecH experiments and 5 replicates for SecHΔMBD.

5.2.11. Structural Models of SecH Oligomers

The size exclusion experiments, together with native mass spectrometry data and photo-crosslinking data all suggest that SecH forms dimers and possibly higher order oligomers. To investigate whether this was structurally plausible, AlphaFold2 Multimer was used to model the structure of SecH oligomers. SecH was modelled as a dimer, with 4 of the 5 resulting models predicting the same dimerisation interface (Figure 32c). In this model, helix 3 of protomer 1 (cyan) makes many interactions with helix 4 of protomer 2 (green). This includes hydrogen bonds of E50 of helix 3 in one protomer with T73 of helix 4 in the second protomer, as well as hydrophobic interactions of A60 of helix 3 with the carbon atoms in the side chain of E69. The same interactions are made with the helix 3 of protomer 2 and helix 4 of protomer 1. In UPF0149 domain protein lpg0076, dimerisation also occurs with helix 3, however this helix interacts with helix 5 of the second protomer (Figure 32b) (PDB: 4GYT) (Michalska et al., 2012). In the UPF0149 domain protein from *Haemophilus influenzae*, dimerisation occurs *via* helices 6 and 7 of two protomers (Figure 32a). Figure 32d shows the SecH dimer model with amino acids N91 and F101 highlighted in green. When Bpa is incorporated at these positions in the absence of SecB, crosslinks form between the two protomers forming stabilised dimers *in vivo* (section 5.2.5).

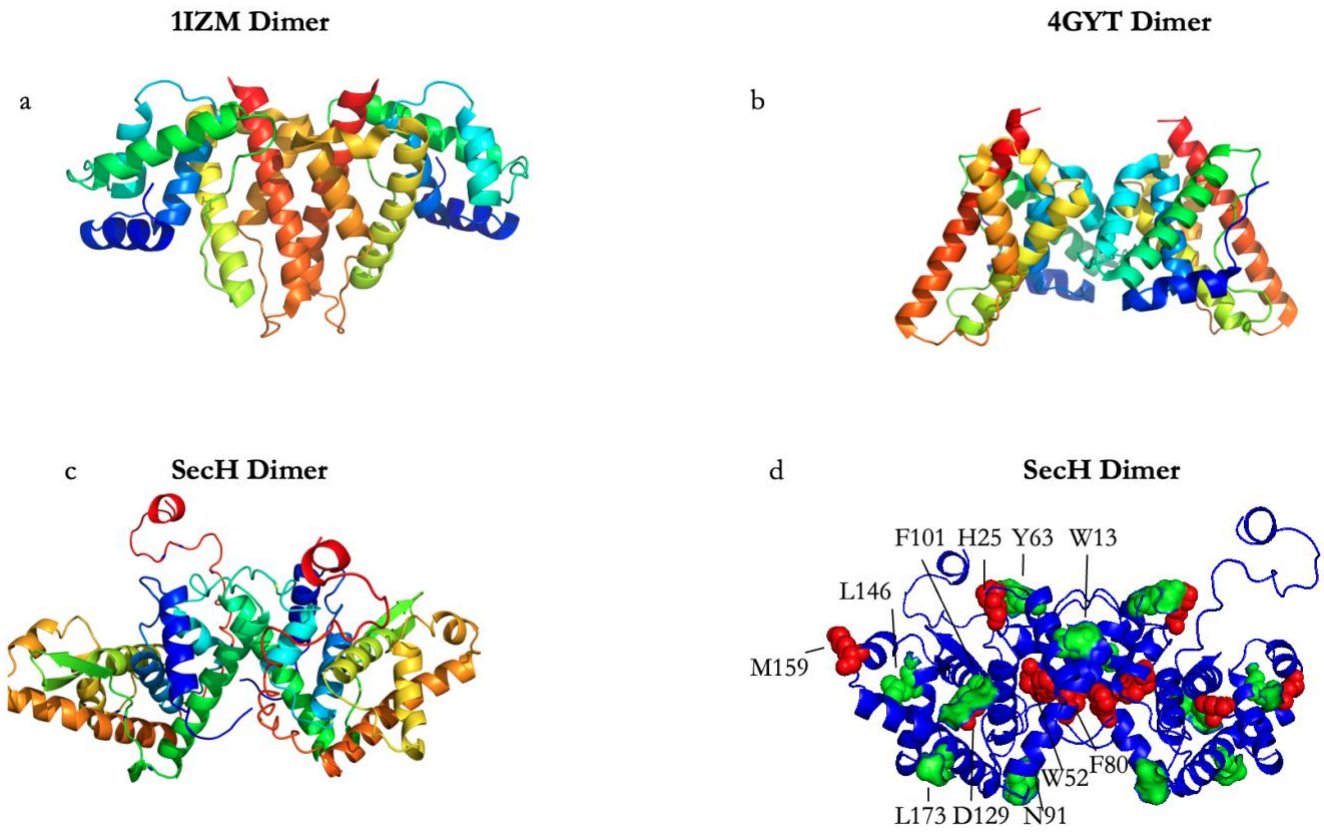

Figure 32- Structural models of UPF1049 dimers.

a) Model of UPF0149 domain-containing protein YgfB from *Haemophilus influenzae* (PBD:1IZM). Each protomer coloured by rainbow. **b)** Model of UPF0149 domain-containing protein YgfB from *Legionella pneumophila* (PBD:4GYT). Each protomer coloured by rainbow. **c)** Model of two SecH protomers forming a homodimer. Each monomer coloured by rainbow. **d)** Model of two SecH protomers forming a homodimer. Positions showing crosslinks are coloured in green and those that did not are coloured in red. Models visualised in pyMOL.

To investigate the structure of higher order oligomers, AlphaFold2 was used to model a SecH trimer and tetramer. In all models of a SecH trimer, 3 protomers of SecH were not predicted to contact each other at the same time, suggesting SecH may form tetrameric complexes by interacting as a 'dimer of dimers'. Indeed, in the AlphaFold models of tetrameric SecH, SecH forms a 'dimer of dimers', with a two-fold symmetry (Figure 33a). The interface between the two dimers consists of packing between helix 6 and 7 of one protomer on the first dimer with another protomer on the second dimer. This interface between two UPF0149 domain protomers occurs in protein HI0807 in *H. influenzae* (Figure 32c). Notably, the surface between the two dimers contains many negatively charged amino acids. This suggests positively charged amino acids may bind in this region, causing dissociation of tetramers into dimers. Figure 33b shows the locations of positions 91 and 101, in which Bpa was incorporated and resulting crosslinking formed stabilised SecH homotetrameric complexes in the absence of SecB (section 5.2.5). Position 91 is located at interface of tetrameric SecH and is in close proximity to each protomer. Position 101, though further away from the tetramer interface, is in close proximity to the SecH protomer on the opposite SecH dimer.

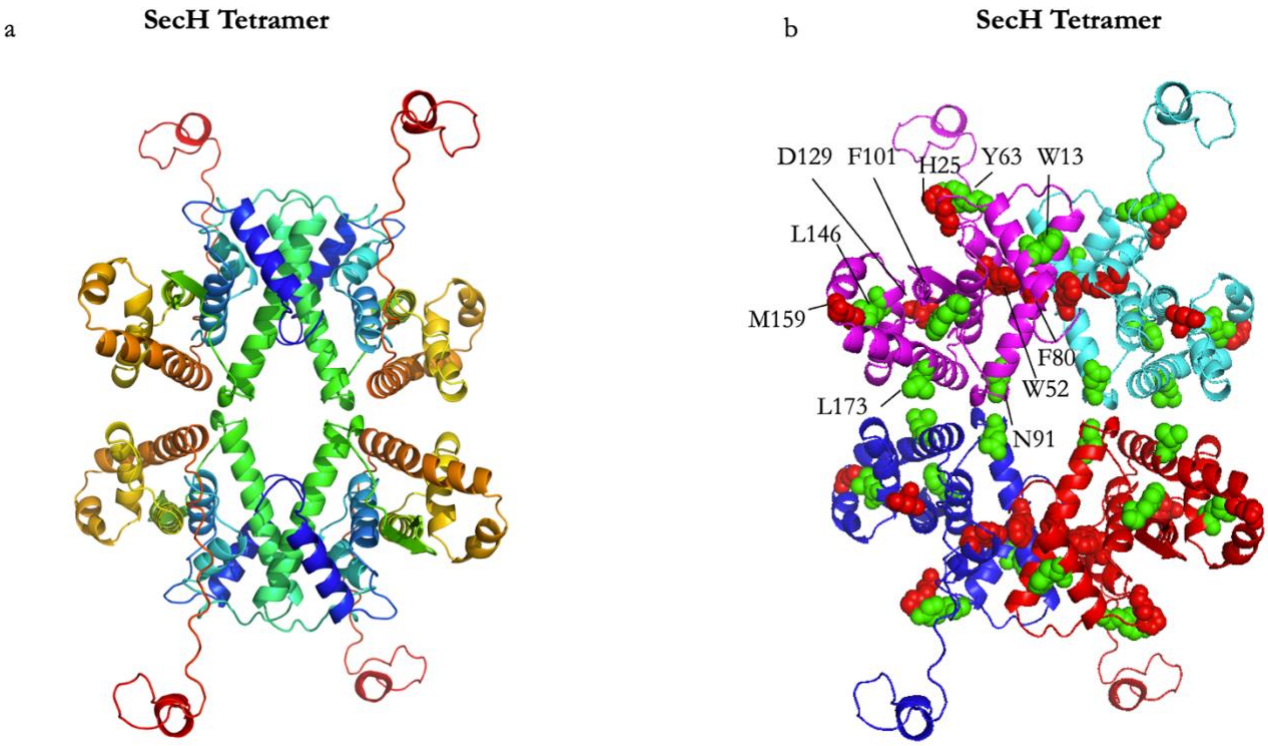

Figure 33 – Structural model of SecH tetramers.

AlphaFold2 Multimer model of SecH tetramer, formed by two interacting dimers. **a)** Each monomer is coloured by rainbow. **b)** AlphaFold2 Multimer model with each promoter coloured separately. Positions showing crosslinks are coloured in green and those that did not are coloured in red. Models were visualised in pyMOL.

The results in section 5.2.5 suggested that SecH mutants F101Bpa and N91Bpa crosslink to SecH protomers to form dimeric complexes. Using AlphaFold2 SecH with the C-terminal 6xHis and SUMO tag, together with the N-terminal biotin tag was modelled (Figure 34). In this model, the asparagine at position 91 is adjacent to the SUMO tag from the second protomer, which would allow for photo-crosslinking of Bpa. Bpa-incorporated proteins can crosslink to amino acids over distances up to 20 Å (Forne et al., 2012). The side chain of phenylalanine at position 101 faces the second protomer and is approximately 20 Å away from the closest side chain on the second protomer. Accounting for the size of Bpa, which spans at least 10 Å, the model is consistent with both SecHN91^{Bpa} and SecHF101^{Bpa} protomers crosslinking to form dimeric complexes.

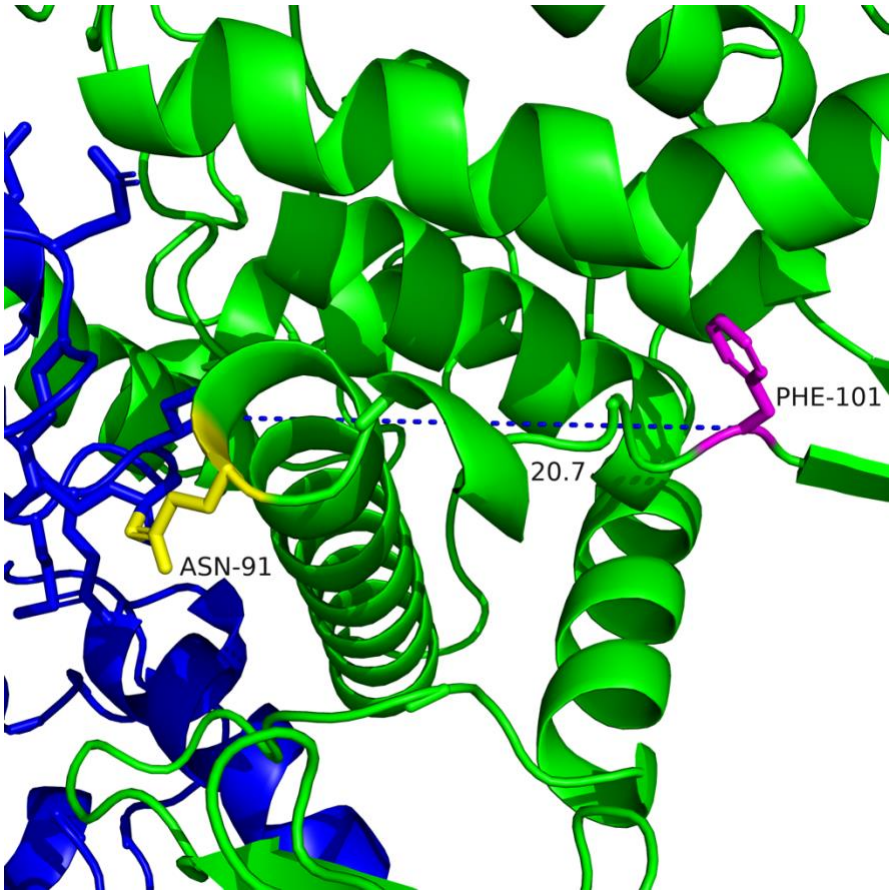

Figure 34 - AlphaFold2 model of dimeric SecH with SUMO, 6x-His and AviTag.

Two SecH promoters modelled by AlphaFold2 Multimer. Two protomers are coloured in blue and green. The F101 residues are coloured in magenta and the N91 residues are coloured in red. The distance from amino acid F101 to the closest amino acid on the second protomer is measured from the α-carbon of F101 to the closest atom on the second promoter. Model visualised in pyMOL.

5.2.12. SecH-SecA Structural Model

The results in the section 5.2.4 suggested that SecH interacts with a variety of proteins. SecH also increases the ATPase activity of SecA in the presence of SecYEG and preprotein. Taken together, these data suggest SecH could directly interact with SecA. To investigate the potential interaction with SecH and SecA, AlphaFold2 Multimer was used to model the interaction between the two proteins (Figure 35). Monomeric and dimeric SecH were both modelled with SecA. Two SecH protomers were not predicted by AlphaFold2 to both interact with SecA. The AlphaFold2 models of monomeric SecH with SecA predict a SecH monomer makes the majority of its interactions with NBD2 of SecA (Figure 35b). Some contacts are also made with the HSD and to a lesser extent NBD1.

The β-hairpin motif that precedes helix 5 of SecH contacts the intersection of NBD2 and the HSD (Figure 35c). R104 of SecH is in close contact with the H620 of NBD2 and P621 at the N-terminus of the HSD. This arginine may form like-charged interactions with H620 if the histidine is protonated (Heyda et al., 2010). In this model, the nitrogen atom of the arginine side chain interacts with the nitrogen on the main chain of P621. F101, which was replaced with Bpa, is adjacent to this arginine residue in SecH. However, the model predicts that F101 faces away from SecA. It is not possible to model the structure with Bpa instead of natural amino acids.

Amino acids from the linker region between helices 1 and 2 as well as the linker region between helices 6 and 7 in SecH also contact SecA (Figure 35d). E150 of SecH forms a salt bridge between the anionic carboxy group of glutamic acid and the cationic ammonium group of SecA

K609 in NBD2. F153 of SecH is in close proximity to form interactions with M606 of SecA. Methionine interactions with aromatic residues frequently stabilise protein structures (Weber and Warren, 2019). Another salt bridge is formed between D24 of SecH and R602 of SecA. R602 of SecA contributes to ribosome binding, interacting with 23S RNA H7 (Wang et al., 2019). Y63 was replaced by Bpa in crosslinking experiments, and this residue is present on a flexible loop between helices 4 and 5. This residue sits in close proximity to the SecA-SecH interaction surface. This model suggests SecH interacts with SecA in close proximity to the substrate-binding region of SecA, suggesting SecH could pass substrate protein to SecA.

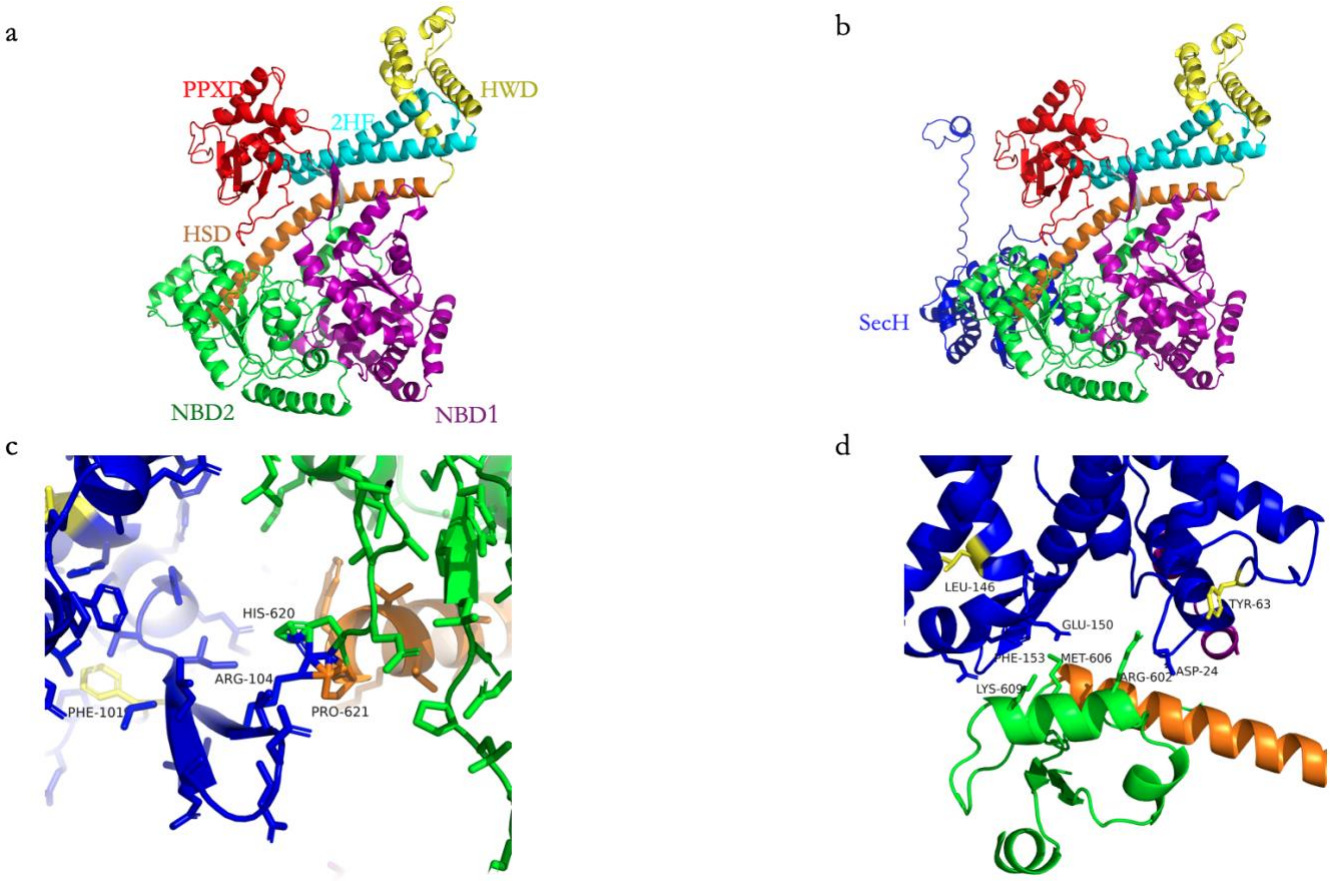

Figure 35 – AlphaFold2 structural modelling of SecH with SecA.

Using AlphaFold2 Multimer, the SecA and SecH sequences were used to model their interaction. **a)** AlphaFold2 model of SecA coloured by domain. **b)** Overall view of model with SecH (blue) bound to SecA. **c)** Image of residue interaction of SecH with the N-terminus of the HSD. **d)** View of SecH residues interacting with helix of NBD2. Residues replaced by Bpa in crosslinking experiments in SecH highlighted in yellow. NBD1 – Purple, NBD2 – Green, HSD- orange, HWD – Yellow, 2HF- Cyan. Models visualised in pyMOL.

5.3. Discussion

This chapter set out to investigate both the function and mechanism of the UPF0149 domain of SecH. Photo-crosslinking experiments suggested that the UPF1049 domain *in vivo* interacts promiscuously with many proteins. Together with evidence that SecH increases the translocation-coupled ATPase rate of SecA, it was reasoned SecH may play a role in directly altering the ATPase cycle of SecA. NADH-coupled ATPase assays and MANT-ADP dissociation assays indicate SecH does not directly alter the ATPase rate of SecA or alter its rate of ADP release. Pull down assays of photo-crosslinked SecH suggest that *in vivo*, in the absence of SecB, SecH oligomerises. Oligomerisation of SecH is also evidenced by size exclusion experiments and native mass spectrometry. Copurification analysis of SecH in the absence of SecB also suggests SecH interacts with Sec substrate LamB and SecA.

11 mutant SecH proteins containing photo-inducible crosslinker Bpa were purified in order to investigate the protein: protein interactions of SecH. Mass spectrometry analysis of overexpressed N91Bpa suggested that SecH interacts with a wide variety of proteins. This data is consistent with SecH having molecular chaperone activity.

SecH increases the ATPase rate of SecA in translocation-coupled ATPase assays. However, the data in this chapter suggest SecH does not do this in the absence of SecYEG and substrate protein. This raises the possibility that SecH passes substrate protein to SecA, which then increases the SecA ATPase rate. In the AlphaFold2 model of the SecH -SecA complex, SecH interacts with SecA adjacent to the substrate binding domain, suggesting SecH could pass substrate protein directly to SecA.

Photo-crosslinking experiments, size exclusion chromatography and native mass spectrometry experiments all suggest that SecH oligomerises. Size exclusion chromatography analysis suggests that a proportion of SecH elutes at a similar volume as SecB (68 kDa), suggesting that SecH dimerises. Native spectrometry analysis of purified SecH also identified monomeric and dimeric SecH. Photo-crosslinking experiments suggest that *in vivo*, SecH forms oligomers which may include trimers and tetramers. Western blotting of the pulled-down photo-crosslinked SecH mutants in the absence of SecB (Figure 22) indicates a greater proportion of SecH is in an oligomeric form compared to native mass spectrometry, suggesting that substrate binding promotes oligomerisation of SecH. These SecH mutants, however, contained an N-terminal SUMO tag. Structural modelling of dimeric SecH with the SUMO tag indicated that the SUMO moiety could be involved in the dimer interface. This suggests the SUMO tag may influence the oligomerisation of SecH.

Structural modelling of SecH oligomers predict a dimer interface that is consistent with high-resolution structural models of known UPF0149 domain proteins. The modelled SecH dimerisation interface is similar to the determined structure of the UPF0149 domain protein from *Legionella pnuemophilia,* with helix 3 of each protomer at the site of dimerisation. Pull down assays suggested SecH may form tetramers. Structural models of SecH tetramers suggest this may be plausible. In the predicted tetramer interface, helix 6 and 7 of one protomer interact with helix 6 and 7 on the corresponding dimer, which is also seen in the dimer interface of UP0149 domain -containing protein from *Haemophilus influenzae.*

The results in this chapter suggest that *in vivo* SecH oligomerises, and oligomeric SecH may interact more strongly with other proteins, including Sec substrate LamB. The results in this chapter suggest that SecH does not directly alter the ATPase activity of SecA, but SecH does interact with SecA *in vivo.* Structural modelling suggests that SecH *via* the UPF1049 domain, can also directly interact with SecA.

Concluding Remarks

In this thesis, the structure and function of SecH was investigated. The results presented suggest that the MBD of SecH interacts with both SecB and ribosomes. The results also suggest that SecH may interact with SecA. Results in this thesis also suggest that SecH in solution is in both monomeric and dimeric states and forms higher-order complexes *in vivo.* Taken together, the results presented in this thesis suggest that SecH is a novel component of the Sec machinery.

6.1. SecH in the Sec pathway

The last component of the Sec machinery to be discovered was YidC, more than 20 years ago. This study indicates SecH, *via* its SecA-like MBD, interacts with components of the Sec pathway. The identification of a novel Sec protein, and a domain that interacts with components of the Sec pathway, suggests there may be even more unidentified accessory Sec proteins. Indeed, in *E. coli,* protein of unknown function YchJ also contains the SecA-like MBD at its C-terminus. At the N-terminus it contains another domain of unknown function UPF0225, suggesting the existence of other unidentified Sec proteins with unknown functions.

The results in this study indicate that SecH binds to both ribosomes and SecB *via* the MBD. Therefore, it possible that SecH interacts with Sec substrates as they are emerging from the ribosome and passes them to SecB. Consistent with this, overexpression of SecH decreases translocation efficiency in the absence of SecB, indicating SecH interacts with substrates and passes client to protein to SecB (Smith et al., 2020).

Previous data also indicates that SecH interacts with SecA, increasing the translocation-coupled ATPase activity of SecA. However, *in vitro* assays suggest that there is no functional interaction between SecA and SecH in the absence of substrate protein or SecYEG. This indicates that as

well as passing substrate to SecB, SecH may also pass substrate protein directly to SecA which would explain the increase in ATPase activity of SecA in the presence of SecH, SecYEG and preprotein, but not in the presence of only SecH. Structural models generated in this thesis suggest that SecH interacts with SecA *via* the NBD2, close to the preprotein binding region, suggesting it is structurally feasible for SecH to pass preprotein directly to SecA.

The substrate specificity of SecH remains unknown. Consistent with many molecular chaperones, SecH has been found to promiscuously bind to many proteins *in vivo* (Smith et al., 2020). This study was unable to directly identify a specific subset of secretory proteins that SecH interacts with. However, mass spectrometry analysis of proteins copurifying with SecH in strains with a Sec defect indicates that SecH copurifies strongly with Sec substrates including LamB and OmpF. An investigation into gene expression in *S. typhimurium* found that the expression of SecH under anaerobic shock increases 4-fold (Kroger et al., 2013). Therefore, SecH may bind to a specific subset of secretory proteins that are expressed under anaerobic conditions. To investigate this, future studies could use ribosome profiling under different conditions, including anaerobic stress, to identify the substrate pool of SecH.

6.2. Mechanism of SecH

The UPF0149 domain remains a domain of unknown function, despite the presence of two high-resolution structural models of this domain. Both of these structural models indicate that the UPF0149 domain has a preference for forming homodimeric complexes (Galkin et al., 2004; Michalska et al., 2012). However, initial studies of SecH *in vitro* found that purified SecH is principally monomeric (Cranford-Smith, 2018). This study provides evidence that suggests the

UPF0149 domain of SecH dimerises in solution and forms higher order oligomers *in vivo*. In a strain lacking *secB,* SecH formed oligomeric complexes consistent with dimers and tetramers. The absence of *secB* causes an accumulation of Sec substrates in the cytoplasm. The formation of higher order oligomers of SecH in this strain suggests that SecH may bind to client proteins in an oligomeric form.

In contrast, modelling of SecH in complex with SecA and SecB suggests SecH interacts with both proteins in a monomeric form. This indicates a potential dimer-monomer transition. In the future, the structure of SecH could be investigated using cryo-electron microscopy to analyse the structure of a complex of SecH in the presence of unfolded protein as well as SecA and SecB. Using Cryo-electron microscopy would be particularly advantageous in the case of SecH as it has proven difficult to crystalise, likely due in part to the flexibility of the MBD. Experiments in this thesis probing the oligomerisation of SecH, including size exclusion chromatography and native mass spectrometry, could be repeated with SecH in the presence of Sec substrate to investigate the effect of substrate protein on the oligomerisation of SecH.

6 of the Bpa-incorporated SecH mutants showed large banding patterns when western blotted against Biotin after purification, suggesting these positions may be substrate binding regions. However, as shown in Figure 18, these residues are largely spread across the face of SecH, suggesting SecH may not have one substrate binding region. It may be the case that SecH interacts with substrates in a similar way to SecB, with a small motif that is repeated across the primary sequence of the protein. In the future, after identification of SecH substrates, a peptide scan could be used to characterise a potential SecH binding motif – as was used to identify the SecB substrate binding motif (Knoblauch et al., 1999).

Taken together, the data in this thesis demonstrates that the MBD of SecH binds to SecB and the ribosome. The results also suggest that SecH copurifies with many proteins *in vivo*, consistent with results that SecH has molecular chaperone activity. In strains with a Sec defect, SecH copurifies with Sec substrates as well as SecA, suggesting it plays a role in the Sec-dependent translocation pathway. The results also indicate that SecH oligomerises both *in vitro* and *in vivo.* These results have investigated the function, structure and mechanism of SecH and provides a foundation for further structural and functional elucidation of SecH in the future.

Bibliography

Allen, W.J., R.A. Corey, P. Oatley, R.B. Sessions, S.A. Baldwin, S.E. Radford, R. Tuma, and I. Collinson. 2016. Two-way communication between SecY and SecA suggests a Brownian ratchet mechanism for protein translocation. *Elife*. 5.

Allen, W.J., R.A. Corey, D.W. Watkins, A.S.F. Oliveira, K. Hards, G.M. Cook, and I. Collinson. 2022. Rate-limiting transport of positively charged arginine residues through the Sec-machinery is integral to the mechanism of protein secretion. *Elife*. 11.

Ang, D., and C. Georgopoulos. 1989. The heat-shock-regulated grpE gene of Escherichia coli is required for bacterial growth at all temperatures but is dispensable in certain mutant backgrounds. *J Bacteriol*. 171:2748-2755.

Angelini, S., S. Deitermann, and H.G. Koch. 2005. FtsY, the bacterial signal-recognition particle receptor, interacts functionally and physically with the SecYEG translocon. *EMBO Rep.* 6:476-481.

Arsene, F., T. Tomoyasu, and B. Bukau. 2000. The heat shock response of Escherichia coli. *Int J Food Microbiol.* 55:3-9.

Baba, T., T. Ara, M. Hasegawa, Y. Takai, Y. Okumura, M. Baba, K.A. Datsenko, M. Tomita, B.L. Wanner, and H. Mori. 2006. Construction of Escherichia coli K-12 in-frame, single-gene knockout mutants: the Keio collection. *Mol Syst Biol.* 2:2006 0008.

Bauer, B.W., T. Shemesh, Y. Chen, and T.A. Rapoport. 2014. A "push and slide" mechanism allows sequence-insensitive translocation of secretory proteins by the SecA ATPase. *Cell.* 157:1416-1429.

Bieker, K.L., G.J. Phillips, and T.J. Silhavy. 1990. The sec and prl genes of Escherichia coli. *J Bioenerg Biomembr*. 22:291-310.

Blum, M., H.Y. Chang, S. Chuguransky, T. Grego, S. Kandasaamy, A. Mitchell, G. Nuka, T. Paysan-Lafosse, M. Qureshi, S. Raj, L. Richardson, G.A. Salazar, L. Williams, P. Bork, A. Bridge, J. Gough, D.H. Haft, I. Letunic, A. Marchler-Bauer, H. Mi, D.A. Natale, M. Necci, C.A. Orengo, A.P. Pandurangan, C. Rivoire, C.J.A. Sigrist, I. Sillitoe, N. Thanki, P.D. Thomas, S.C.E. Tosatto, C.H. Wu, A. Bateman, and R.D. Finn. 2021. The InterPro protein families and domains database: 20 years on. *Nucleic Acids Res*. 49:D344-D354.

Bornemann, T., W. Holtkamp, and W. Wintermeyer. 2014. Interplay between trigger factor and other protein biogenesis factors on the ribosome. *Nat Commun*. 5:4180.

Bracher, A., and J. Verghese. 2015. The nucleotide exchange factors of Hsp70 molecular chaperones. *Front Mol Biosci.* 2:10.

Catipovic, M.A., B.W. Bauer, J.J. Loparo, and T.A. Rapoport. 2019. Protein translocation by the SecA ATPase occurs by a power-stroke mechanism. *EMBO J.* 38.

Chakraborty, A., S. Mukherjee, R. Chattopadhyay, S. Roy, and S. Chakrabarti. 2014. Conformational adaptation in the E. coli sigma 32 protein in response to heat shock. *J Phys Chem B.* 118:4793-4802.

Chatzi, K.E., M.F. Sardis, A. Tsirigotaki, M. Koukaki, N. Sostaric, A. Konijnenberg, F. Sobott, C.G. Kalodimos, S. Karamanou, and A. Economou. 2017. Preprotein mature domains contain translocase targeting signals that are essential for secretion. *J Cell Biol.* 216:1357-1369.

Cosma, C.L., P.N. Danese, J.H. Carlson, T.J. Silhavy, and W.B. Snyder. 1995. Mutational activation of the Cpx signal transduction pathway of Escherichia coli suppresses the toxicity conferred by certain envelope-associated stresses. *Mol Microbiol.* 18:491-505.

Cranford-Smith, T. 2018. Genetic, biochemical and structural characterisation of YecA, a novel component of the bacterial Sec machinery. *In* School of Bioscience. Vol. PhD. University of Birmingham, Birmingham.

Cranford-Smith, T., and D. Huber. 2018. The way is the goal: how SecA transports proteins across the cytoplasmic membrane in bacteria. *FEMS Microbiol Lett.* 365.

Cranford-Smith, T., M. Jamshad, M. Jeeves, R.A. Chandler, J. Yule, A. Robinson, F. Alam, K.A. Dunne, E.H. Aponte Angarita, M. Alanazi, C. Carter, I.R. Henderson, J.E. Lovett, P. Winn, T. Knowles, and D. Huber. 2020. Iron is a ligand of SecA-like metal-binding domains in vivo. *J Biol Chem.* 295:7516-7528.

Crooks, G.E., G. Hon, J.M. Chandonia, and S.E. Brenner. 2004. WebLogo: a sequence logo generator. *Genome Res.* 14:1188-1190.

D'Lima, N.G., and C.M. Teschke. 2014. ADP-dependent conformational changes distinguish Mycobacterium tuberculosis SecA2 from SecA1. *J Biol Chem.* 289:2307-2317.

Datsenko, K.A., and B.L. Wanner. 2000. One-step inactivation of chromosomal genes in Escherichia coli K-12 using PCR products. *Proc Natl Acad Sci U S A.* 97:6640-6645.

Dekker, C., B. de Kruijff, and P. Gros. 2003. Crystal structure of SecB from Escherichia coli. *J Struct Biol.* 144:313-319.

Dempsey, B.R., M. Wrona, J.M. Moulin, G.B. Gloor, F. Jalilehvand, G. Lajoie, G.S. Shaw, and B.H. Shilton. 2004. Solution NMR structure and X-ray absorption analysis of the C-terminal zinc-binding domain of the SecA ATPase. *Biochemistry*. 43:9361-9371.

den Blaauwen, T., E. Terpetschnig, J.R. Lakowicz, and A.J. Driessen. 1997. Interaction of SecB with soluble SecA. *FEBS Lett*. 416:35-38.

Derman, A.I., J.W. Puziss, P.J. Bassford, Jr., and J. Beckwith. 1993. A signal sequence is not required for protein export in prlA mutants of Escherichia coli. *EMBO J*. 12:879-888.

Draycheva, A., S. Lee, and W. Wintermeyer. 2018. Cotranslational protein targeting to the membrane: Nascent-chain transfer in a quaternary complex formed at the translocon. *Sci Rep*. 8:9922.

Driessen, A.J., and N. Nouwen. 2008. Protein translocation across the bacterial cytoplasmic membrane. *Annu Rev Biochem*. 77:643-667.

du Plessis, D.J., G. Berrelkamp, N. Nouwen, and A.J. Driessen. 2009. The lateral gate of SecYEG opens during protein translocation. *J Biol Chem*. 284:15805-15814.

du Plessis, D.J., N. Nouwen, and A.J. Driessen. 2006. Subunit a of cytochrome o oxidase requires both YidC and SecYEG for membrane insertion. *J Biol Chem*. 281:12248-12252.

Duong, F., and W. Wickner. 1997. Distinct catalytic roles of the SecYE, SecG and SecDFyajC subunits of preprotein translocase holoenzyme. *EMBO J*. 16:2756-2768.

Egea, P.F., S.O. Shan, J. Napetschnig, D.F. Savage, P. Walter, and R.M. Stroud. 2004. Substrate twinning activates the signal recognition particle and its receptor. *Nature*. 427:215-221.

Erlandson, K.J., S.B. Miller, Y. Nam, A.R. Osborne, J. Zimmer, and T.A. Rapoport. 2008. A role for the two-helix finger of the SecA ATPase in protein translocation. *Nature*. 455:984-987.

Evans, R., M. O'Neill, A. Pritzel, N. Antropova, A. Senior, T. Green, A. Žídek, R. Bates, S. Blackwell, J. Yim, O. Ronneberger, S. Bodenstein, M. Zielinski, A. Bridgland, A. Potapenko, A. Cowie, K. Tunyasuvunakool, R. Jain, E. Clancy, P. Kohli, J. Jumper, and D. Hassabis. 2022. Protein complex prediction with AlphaFold-Multimer. *bio*R*xiv*:2021.2010.2004.463034.

Fak, J.J., A. Itkin, D.D. Ciobanu, E.C. Lin, X.J. Song, Y.T. Chou, L.M. Gierasch, and J.F. Hunt. 2004. Nucleotide exchange from the high-affinity ATP-binding site in SecA is the rate-limiting step in the ATPase cycle of the soluble enzyme and occurs through a specialized conformational state. *Biochemistry*. 43:7307-7327.

Fekkes, P., and A.J. Driessen. 1999. Protein targeting to the bacterial cytoplasmic membrane. *Microbiol Mol Biol Rev*. 63:161-173.

Fekkes, P., C. van der Does, and A.J. Driessen. 1997. The molecular chaperone SecB is released from the carboxy-terminus of SecA during initiation of precursor protein translocation. *EMBO J.* 16:6105-6113.

Fikes, J.D., G.A. Barkocy-Gallagher, D.G. Klapper, and P.J. Bassford, Jr. 1990. Maturation of Escherichia coli maltose-binding protein by signal peptidase I in vivo. Sequence requirements for efficient processing and demonstration of an alternate cleavage site. *J Biol Chem.* 265:3417-3423.

Forne, I., J. Ludwigsen, A. Imhof, P.B. Becker, and F. Mueller-Planitz. 2012. Probing the conformation of the ISWI ATPase domain with genetically encoded photoreactive crosslinkers and mass spectrometry. *Mol Cell Proteomics.* 11:M111 012088.

Francetic, O., and C.A. Kumamoto. 1996. Escherichia coli SecB stimulates export without maintaining export competence of ribose-binding protein signal sequence mutants. *J Bacteriol.* 178:5954-5959.

Freymann, D.M., R.J. Keenan, R.M. Stroud, and P. Walter. 1997. Structure of the conserved GTPase domain of the signal recognition particle. *Nature.* 385:361-364.

Galkin, A., E. Sarikaya, C. Lehmann, A. Howard, and O. Herzberg. 2004. X-ray structure of HI0817 from Haemophilus influenzae: protein of unknown function with a novel fold. *Proteins.* 57:874-877.

Gardel, C., S. Benson, J. Hunt, S. Michaelis, and J. Beckwith. 1987. secD, a new gene involved in protein export in Escherichia coli. *J Bacteriol.* 169:1286-1290.

Gardel, C., K. Johnson, A. Jacq, and J. Beckwith. 1990. The secD locus of E. coli codes for two membrane proteins required for protein export. *EMBO J.* 9:4205-4206.

Goloubinoff, P., A. Mogk, A.P. Zvi, T. Tomoyasu, and B. Bukau. 1999. Sequential mechanism of solubilization and refolding of stable protein aggregates by a bichaperone network. *Proc Natl Acad Sci U S A.* 96:13732-13737.

Greenfield, J.J., and S. High. 1999. The Sec61 complex is located in both the ER and the ER-Golgi intermediate compartment. *J Cell Sci.* 112 (Pt 10):1477-1486.

Grossman, A.D., D.B. Straus, W.A. Walter, and C.A. Gross. 1987. Sigma 32 synthesis can regulate the synthesis of heat shock proteins in Escherichia coli. *Genes Dev.* 1:179-184.

Hainzl, T., S. Huang, G. Merilainen, K. Brannstrom, and A.E. Sauer-Eriksson. 2011. Structural basis of signal-sequence recognition by the signal recognition particle. *Nat Struct Mol Biol.* 18:389-391.

Harrison, C.J., M. Hayer-Hartl, M. Di Liberto, F. Hartl, and J. Kuriyan. 1997. Crystal structure of the nucleotide exchange factor GrpE bound to the ATPase domain of the molecular chaperone DnaK. *Science.* 276:431-435.

Hartl, F.U., S. Lecker, E. Schiebel, J.P. Hendrick, and W. Wickner. 1990. The binding cascade of SecB to SecA to SecY/E mediates preprotein targeting to the E. coli plasma membrane. *Cell.* 63:269-279.

Hartmann, E., T. Sommer, S. Prehn, D. Gorlich, S. Jentsch, and T.A. Rapoport. 1994. Evolutionary conservation of components of the protein translocation complex. *Nature.* 367:654-657.

Heyda, J., P.E. Mason, and P. Jungwirth. 2010. Attractive interactions between side chains of histidine-histidine and histidine-arginine-based cationic dipeptides in water. *J Phys Chem B.* 114:8744-8749.

Hoffmann, A., A.H. Becker, B. Zachmann-Brand, E. Deuerling, B. Bukau, and G. Kramer. 2012. Concerted action of the ribosome and the associated chaperone trigger factor confines nascent polypeptide folding. *Mol Cell.* 48:63-74.

Horwich, A.L., G.W. Farr, and W.A. Fenton. 2006. GroEL-GroES-mediated protein folding. *Chem Rev.* 106:1917-1930.

Huang, C., P. Rossi, T. Saio, and C.G. Kalodimos. 2016. Structural basis for the antifolding activity of a molecular chaperone. *Nature.* 537:202-206.

Huber, D., M. Jamshad, R. Hanmer, D. Schibich, K. Doring, I. Marcomini, G. Kramer, and B. Bukau. 2017. SecA Cotranslationally Interacts with Nascent Substrate Proteins In Vivo. *J Bacteriol.* 199.

Huber, D., N. Rajagopalan, S. Preissler, M.A. Rocco, F. Merz, G. Kramer, and B. Bukau. 2011. SecA interacts with ribosomes in order to facilitate posttranslational translocation in bacteria. *Mol Cell.* 41:343-353.

Hunt, J.F., S. Weinkauf, L. Henry, J.J. Fak, P. McNicholas, D.B. Oliver, and J. Deisenhofer. 2002. Nucleotide control of interdomain interactions in the conformational reaction cycle of SecA. *Science.* 297:2018-2026.

Jamshad, M., T.J. Knowles, S.A. White, D.G. Ward, F. Mohammed, K.F. Rahman, M. Wynne, G.W. Hughes, G. Kramer, B. Bukau, and D. Huber. 2019. The C-terminal tail of the bacterial translocation ATPase SecA modulates its activity. *Elife.* 8.

Janda, C.Y., J. Li, C. Oubridge, H. Hernandez, C.V. Robinson, and K. Nagai. 2010. Recognition of a signal peptide by the signal recognition particle. *Nature.* 465:507-510.

Jiang, C., M. Wynne, and D. Huber. 2021. How Quality Control Systems AID Sec-Dependent Protein Translocation. *Front Mol Biosci.* 8:669376.

Jomaa, A., D. Boehringer, M. Leibundgut, and N. Ban. 2016. Structures of the E. coli translating ribosome with SRP and its receptor and with the translocon. *Nat Commun.* 7:10471.

Jones, D.T., and J.M. Thornton. 2022. The impact of AlphaFold2 one year on. *Nat Methods.* 19:15-20.

Jumper, J., R. Evans, A. Pritzel, T. Green, M. Figurnov, O. Ronneberger, K. Tunyasuvunakool, R. Bates, A. Zidek, A. Potapenko, A. Bridgland, C. Meyer, S.A.A. Kohl, A.J. Ballard, A. Cowie, B. Romera-Paredes, S. Nikolov, R. Jain, J. Adler, T. Back, S. Petersen, D. Reiman, E. Clancy, M. Zielinski, M. Steinegger, M. Pacholska, T. Berghammer, S. Bodenstein, D. Silver, O. Vinyals, A.W. Senior, K. Kavukcuoglu, P. Kohli, and D. Hassabis. 2021. Highly accurate protein structure prediction with AlphaFold. *Nature.* 596:583-589.

Jung, S., V. Bader, A. Natriashvili, H.G. Koch, K.F. Winklhofer, and J. Tatzelt. 2020. SecY-mediated quality control prevents the translocation of non-gated porins. *Sci Rep.* 10:16347.

Karimova, G., J. Pidoux, A. Ullmann, and D. Ladant. 1998. A bacterial two-hybrid system based on a reconstituted signal transduction pathway. *Proc Natl Acad Sci U S A.* 95:5752-5756.

Kato, Y., K. Nishiyama, and H. Tokuda. 2003. Depletion of SecDF-YajC causes a decrease in the level of SecG: implication for their functional interaction. *FEBS Lett.* 550:114-118.

Kimura, E., M. Akita, S. Matsuyama, and S. Mizushima. 1991. Determination of a region in SecA that interacts with presecretory proteins in Escherichia coli. *J Biol Chem.* 266:6600-6606.

Knoblauch, N.T., S. Rudiger, H.J. Schonfeld, A.J. Driessen, J. Schneider-Mergener, and B. Bukau. 1999. Substrate specificity of the SecB chaperone. *J Biol Chem.* 274:34219-34225.

Koch, S., J.G. de Wit, I. Vos, J.P. Birkner, P. Gordiichuk, A. Herrmann, A.M. van Oijen, and A.J. Driessen. 2016. Lipids Activate SecA for High Affinity Binding to the SecYEG Complex. *J Biol Chem.* 291:22534-22543.

Komar, J., S. Alvira, R.J. Schulze, R. Martin, A.N.J.A. Lycklama, S.C. Lee, T.R. Dafforn, G. Deckers-Hebestreit, I. Berger, C. Schaffitzel, and I. Collinson. 2016. Membrane protein insertion and assembly by the bacterial holo-translocon SecYEG-SecDF-YajC-YidC. *Biochem J.* 473:3341-3354.

Kroger, C., A. Colgan, S. Srikumar, K. Handler, S.K. Sivasankaran, D.L. Hammarlof, R. Canals, J.E. Grissom, T. Conway, K. Hokamp, and J.C. Hinton. 2013. An infection-relevant transcriptomic compendium for Salmonella enterica Serovar Typhimurium. *Cell Host Microbe.* 14:683-695.

Kuhn, P., B. Weiche, L. Sturm, E. Sommer, F. Drepper, B. Warscheid, V. Sourjik, and H.G. Koch. 2011. The bacterial SRP receptor, SecA and the ribosome use overlapping binding sites on the SecY translocon. *Traffic*. 12:563-578.

Kumamoto, C.A., and O. Francetic. 1993. Highly selective binding of nascent polypeptides by an Escherichia coli chaperone protein in vivo. *J Bacteriol*. 175:2184-2188.

Kusters, I., and A.J. Driessen. 2011. SecA, a remarkable nanomachine. *Cell Mol Life Sci*. 68:2053-2066.

Kusukawa, N., T. Yura, C. Ueguchi, Y. Akiyama, and K. Ito. 1989. Effects of mutations in heat-shock genes groES and groEL on protein export in Escherichia coli. *EMBO J*. 8:3517-3521.

Lee, H.C., and H.D. Bernstein. 2001. The targeting pathway of Escherichia coli presecretory and integral membrane proteins is specified by the hydrophobicity of the targeting signal. *Proc Natl Acad Sci U S A*. 98:3471-3476.

Lee, H.C., and H.D. Bernstein. 2002. Trigger factor retards protein export in Escherichia coli. *J Biol Chem*. 277:43527-43535.

Lill, R., W. Dowhan, and W. Wickner. 1990. The ATPase activity of SecA is regulated by acidic phospholipids, SecY, and the leader and mature domains of precursor proteins. *Cell*. 60:271-280.

Lu, J., W.R. Kobertz, and C. Deutsch. 2007. Mapping the electrostatic potential within the ribosomal exit tunnel. *J Mol Biol*. 371:1378-1391.

Luirink, J., and I. Sinning. 2004. SRP-mediated protein targeting: structure and function revisited. *Biochim Biophys Acta*. 1694:17-35.

Lycklama a Nijeholt, J.A., J. de Keyzer, I. Prabudiansyah, and A.J. Driessen. 2013. Characterization of the supporting role of SecE in protein translocation. *FEBS Lett*. 587:3083-3088.

Malecki, M., C. Barria, and C.M. Arraiano. 2014. Characterization of the RNase R association with ribosomes. *BMC Microbiol*. 14:34.

Martin, R., A.H. Larsen, R.A. Corey, S.R. Midtgaard, H. Frielinghaus, C. Schaffitzel, L. Arleth, and I. Collinson. 2019. Structure and Dynamics of the Central Lipid Pool and Proteins of the Bacterial Holo-Translocon. *Biophys J*. 116:1931-1940.

Michalska, K., X. Xu, H. Cui, A. Savchenko, and A. Joachimiak. 2012. Crystal structure of lpg0076 protein from Legionella pneumophila (PDB ID: 4GYT).

Miller, A., L. Wang, and D.A. Kendall. 2002. SecB modulates the nucleotide-bound state of SecA and stimulates ATPase activity. *Biochemistry.* 41:5325-5332.

Miller, J.H. 1972. Experiments in molecular genetics. Cold Spring Harbor Laboratory, Cold Spring Harbor, N.Y. xvi, 466 p. pp.

Mirdita, M., K. Schutze, Y. Moriwaki, L. Heo, S. Ovchinnikov, and M. Steinegger. 2022. ColabFold: making protein folding accessible to all. *Nat Methods.* 19:679-682.

Mitchell, C., and D. Oliver. 1993. Two distinct ATP-binding domains are needed to promote protein export by Escherichia coli SecA ATPase. *Mol Microbiol.* 10:483-497.

Musial-Siwek, M., S.L. Rusch, and D.A. Kendall. 2007. Selective photoaffinity labeling identifies the signal peptide binding domain on SecA. *J Mol Biol.* 365:637-648.

Nishiyama, K., M. Hanada, and H. Tokuda. 1994. Disruption of the gene encoding p12 (SecG) reveals the direct involvement and important function of SecG in the protein translocation of Escherichia coli at low temperature. *EMBO J.* 13:3272-3277.

Nouwen, N., M. Piwowarek, G. Berrelkamp, and A.J. Driessen. 2005. The large first periplasmic loop of SecD and SecF plays an important role in SecDF functioning. *J Bacteriol.* 187:5857-5860.

Oh, E., A.H. Becker, A. Sandikci, D. Huber, R. Chaba, F. Gloge, R.J. Nichols, A. Typas, C.A. Gross, G. Kramer, J.S. Weissman, and B. Bukau. 2011. Selective ribosome profiling reveals the cotranslational chaperone action of trigger factor in vivo. *Cell.* 147:1295-1308.

Oswald, J., R. Njenga, A. Natriashvili, P. Sarmah, and H.G. Koch. 2021. The Dynamic SecYEG Translocon. *Front Mol Biosci.* 8:664241.

Ouellette, S., P. Pakarian, X. Bin, and P.D. Pawelek. 2022. Evidence of an intracellular interaction between the Escherichia coli enzymes EntC and EntB and identification of a potential electrostatic channeling surface. *Biochimie.*

Packschies, L., H. Theyssen, A. Buchberger, B. Bukau, R.S. Goody, and J. Reinstein. 1997. GrpE accelerates nucleotide exchange of the molecular chaperone DnaK with an associative displacement mechanism. *Biochemistry.* 36:3417-3422.

Paetzel, M., A. Karla, N.C. Strynadka, and R.E. Dalbey. 2002. Signal peptidases. *Chem Rev.* 102:4549-4580.

Patel, C.N., V.F. Smith, and L.L. Randall. 2006. Characterization of three areas of interactions stabilizing complexes between SecA and SecB, two proteins involved in protein export. *Protein Sci.* 15:1379-1386.

Patzelt, H., S. Rudiger, D. Brehmer, G. Kramer, S. Vorderwulbecke, E. Schaffitzel, A. Waitz, T. Hesterkamp, L. Dong, J. Schneider-Mergener, B. Bukau, and E. Deuerling. 2001. Binding specificity of Escherichia coli trigger factor. *Proc Natl Acad Sci U S A*. 98:14244-14249.

Phillips, G.J., and T.J. Silhavy. 1990. Heat-shock proteins DnaK and GroEL facilitate export of LacZ hybrid proteins in E. coli. *Nature*. 344:882-884.

Pogliano, J.A., and J. Beckwith. 1994a. SecD and SecF facilitate protein export in Escherichia coli. *EMBO J*. 13:554-561.

Pogliano, K.J., and J. Beckwith. 1994b. Genetic and molecular characterization of the Escherichia coli secD operon and its products. *J Bacteriol*. 176:804-814.

Price, N.L., and T.L. Raivio. 2009. Characterization of the Cpx regulon in Escherichia coli strain MC4100. *J Bacteriol*. 191:1798-1815.

Raimo, G., M. Masullo, and V. Bocchini. 1999. The interaction between the archaeal elongation factor 1alpha and its nucleotide exchange factor 1beta. *FEBS Lett*. 451:109-112.

Randall, L.L., and S.J. Hardy. 2002. SecB, one small chaperone in the complex milieu of the cell. *Cell Mol Life Sci*. 59:1617-1623.

Robson, A., V.A. Gold, S. Hodson, A.R. Clarke, and I. Collinson. 2009. Energy transduction in protein transport and the ATP hydrolytic cycle of SecA. *Proc Natl Acad Sci U S A*. 106:5111-5116.

Rosenblad, M.A., J. Gorodkin, B. Knudsen, C. Zwieb, and T. Samuelsson. 2003. SRPDB: Signal Recognition Particle Database. *Nucleic Acids Res*. 31:363-364.

Rosenzweig, R., N.B. Nillegoda, M.P. Mayer, and B. Bukau. 2019. The Hsp70 chaperone network. *Nat Rev Mol Cell Biol*. 20:665-680.

Sakr, S., A.M. Cirinesi, R.S. Ullers, F. Schwager, C. Georgopoulos, and P. Genevaux. 2010. Lon protease quality control of presecretory proteins in Escherichia coli and its dependence on the SecB and DnaJ (Hsp40) chaperones. *J Biol Chem*. 285:23506-23514.

Sala, A., P. Bordes, and P. Genevaux. 2014. Multitasking SecB chaperones in bacteria. *Front Microbiol*. 5:666.

Sala, A., V. Calderon, P. Bordes, and P. Genevaux. 2013. TAC from Mycobacterium tuberculosis: a paradigm for stress-responsive toxin-antitoxin systems controlled by SecB-like chaperones. *Cell Stress Chaperones*. 18:129-135.

Sambrook, J., D.W. Russell, and J. Sambrook. 2006. The condensed protocols from Molecular cloning : a laboratory manual. Cold Spring Harbor Laboratory Press, Cold Spring Harbor, N.Y. v, 800 p. pp.

Saraogi, I., D. Akopian, and S.O. Shan. 2014. Regulation of cargo recognition, commitment, and unloading drives cotranslational protein targeting. *J Cell Biol.* 205:693-706.

Schaffitzel, C., M. Oswald, I. Berger, T. Ishikawa, J.P. Abrahams, H.K. Koerten, R.I. Koning, and N. Ban. 2006. Structure of the E. coli signal recognition particle bound to a translating ribosome. *Nature.* 444:503-506.

Schiebel, E., A.J. Driessen, F.U. Hartl, and W. Wickner. 1991. Delta mu H+ and ATP function at different steps of the catalytic cycle of preprotein translocase. *Cell.* 64:927-939.

Schlee, S., Y. Groemping, P. Herde, R. Seidel, and J. Reinstein. 2001. The chaperone function of ClpB from Thermus thermophilus depends on allosteric interactions of its two ATP-binding sites. *J Mol Biol.* 306:889-899.

Schulze, R.J., J. Komar, M. Botte, W.J. Allen, S. Whitehouse, V.A. Gold, A.N.J.A. Lycklama, K. Huard, I. Berger, C. Schaffitzel, and I. Collinson. 2014. Membrane protein insertion and proton-motive-force-dependent secretion through the bacterial holo-translocon SecYEG-SecDF-YajC-YidC. *Proc Natl Acad Sci U S A.* 111:4844-4849.

Schwarz, R., D. Tanzler, C.H. Ihling, and A. Sinz. 2016. Monitoring Solution Structures of Peroxisome Proliferator-Activated Receptor beta/delta upon Ligand Binding. *PLoS One.* 11:e0151412.

Serek, J., G. Bauer-Manz, G. Struhalla, L. van den Berg, D. Kiefer, R. Dalbey, and A. Kuhn. 2004. Escherichia coli YidC is a membrane insertase for Sec-independent proteins. *EMBO J.* 23:294-301.

Sianidis, G., S. Karamanou, E. Vrontou, K. Boulias, K. Repanas, N. Kyrpides, A.S. Politou, and A. Economou. 2001. Cross-talk between catalytic and regulatory elements in a DEAD motor domain is essential for SecA function. *EMBO J.* 20:961-970.

Smith, M.A., W.M. Clemons, Jr., C.J. DeMars, and A.M. Flower. 2005. Modeling the effects of prl mutations on the Escherichia coli SecY complex. *J Bacteriol.* 187:6454-6465.

Smith, T.C., M. Wynne, C. Carter, C. Jiang, M. Jamshad, M.T. Milner, Y. Djouider, E. Hutchinson, P.A. Lund, I. Henderson, and D. Huber. 2020. AscA (YecA) is a molecular chaperone involved in Sec-dependent protein translocation in *Escherichia coli*. *bioRxiv*:2020.2007.2021.215244.

Sonnabend, M.S., K. Klein, S. Beier, A. Angelov, R. Kluj, C. Mayer, C. Gross, K. Hofmeister, A. Beuttner, M. Willmann, S. Peter, P. Oberhettinger, A. Schmidt, I.B. Autenrieth, M. Schutz, and E. Bohn. 2020. Identification of Drug Resistance Determinants in a Clinical

Isolate of Pseudomonas aeruginosa by High-Density Transposon Mutagenesis. *Antimicrob Agents Chemother*. 64.

Tanaka, Y., Y. Sugano, M. Takemoto, T. Mori, A. Furukawa, T. Kusakizako, K. Kumazaki, A. Kashima, R. Ishitani, Y. Sugita, O. Nureki, and T. Tsukazaki. 2015. Crystal Structures of SecYEG in Lipidic Cubic Phase Elucidate a Precise Resting and a Peptide-Bound State. *Cell Rep*. 13:1561-1568.

Tsirigotaki, A., J. De Geyter, N. Sostaric, A. Economou, and S. Karamanou. 2017. Protein export through the bacterial Sec pathway. *Nat Rev Microbiol*. 15:21-36.

Tsukazaki, T., H. Mori, Y. Echizen, R. Ishitani, S. Fukai, T. Tanaka, A. Perederina, D.G. Vassylyev, T. Kohno, A.D. Maturana, K. Ito, and O. Nureki. 2011. Structure and function of a membrane component SecDF that enhances protein export. *Nature*. 474:235-238.

Ullers, R.S., D. Ang, F. Schwager, C. Georgopoulos, and P. Genevaux. 2007. Trigger Factor can antagonize both SecB and DnaK/DnaJ chaperone functions in Escherichia coli. *Proc Natl Acad Sci U S A*. 104:3101-3106.

Ullers, R.S., J. Luirink, N. Harms, F. Schwager, C. Georgopoulos, and P. Genevaux. 2004. SecB is a bona fide generalized chaperone in Escherichia coli. *Proc Natl Acad Sci U S A*. 101:7583-7588.

Van den Berg, B., W.M. Clemons, Jr., I. Collinson, Y. Modis, E. Hartmann, S.C. Harrison, and T.A. Rapoport. 2004. X-ray structure of a protein-conducting channel. *Nature*. 427:36-44.

van der Laan, M., P. Bechtluft, S. Kol, N. Nouwen, and A.J. Driessen. 2004. F1F0 ATP synthase subunit c is a substrate of the novel YidC pathway for membrane protein biogenesis. *J Cell Biol*. 165:213-222.

van der Sluis, E.O., and A.J. Driessen. 2006. Stepwise evolution of the Sec machinery in Proteobacteria. *Trends Microbiol*. 14:105-108.

van Stelten, J., F. Silva, D. Belin, and T.J. Silhavy. 2009. Effects of antibiotics and a proto-oncogene homolog on destruction of protein translocator SecY. *Science*. 325:753-756.

Veenendaal, A.K., C. van der Does, and A.J. Driessen. 2004. The protein-conducting channel SecYEG. *Biochim Biophys Acta*. 1694:81-95.

Vlasuk, G.P., S. Inouye, H. Ito, K. Itakura, and M. Inouye. 1983. Effects of the complete removal of basic amino acid residues from the signal peptide on secretion of lipoprotein in Escherichia coli. *J Biol Chem*. 258:7141-7148.

von Heijne, G. 1990. The signal peptide. *J Membr Biol*. 115:195-201.

von Heijne, G. 1994. Membrane proteins: from sequence to structure. *Annu Rev Biophys Biomol Struct*. 23:167-192.

Wang, S., A. Jomaa, M. Jaskolowski, C.I. Yang, N. Ban, and S.O. Shan. 2019. The molecular mechanism of cotranslational membrane protein recognition and targeting by SecA. *Nat Struct Mol Biol*. 26:919-929.

Weber, D.S., and J.J. Warren. 2019. The interaction between methionine and two aromatic amino acids is an abundant and multifunctional motif in proteins. *Arch Biochem Biophys*. 672:108053.

Wild, J., W.A. Walter, C.A. Gross, and E. Altman. 1993. Accumulation of secretory protein precursors in Escherichia coli induces the heat shock response. *J Bacteriol*. 175:3992-3997.

Xu, Z., J.D. Knafels, and K. Yoshino. 2000. Crystal structure of the bacterial protein export chaperone secB. *Nat Struct Biol*. 7:1172-1177.

Yi, L., N. Celebi, M. Chen, and R.E. Dalbey. 2004. Sec/SRP requirements and energetics of membrane insertion of subunits a, b, and c of the Escherichia coli F1F0 ATP synthase. *J Biol Chem*. 279:39260-39267.

Zhang, Y.J., H.F. Tian, and J.F. Wen. 2009. The evolution of YidC/Oxa/Alb3 family in the three domains of life: a phylogenomic analysis. *BMC Evol Biol*. 9:137.

Zhou, J., and Z. Xu. 2003. Structural determinants of SecB recognition by SecA in bacterial protein translocation. *Nat Struct Biol*. 10:942-947.

Zimmer, J., Y. Nam, and T.A. Rapoport. 2008. Structure of a complex of the ATPase SecA and the protein-translocation channel. *Nature*. 455:936-943.

Zimmer, J., and T.A. Rapoport. 2009. Conformational flexibility and peptide interaction of the translocation ATPase SecA. *J Mol Biol*. 394:606-612.

Appendix

Table 7 – Mass spectrometry results from Section 5.2.4 – W13Bpa 33-43 kDa

UniProt Accession ID	Gene Name	Coverage [%]	Peptides	PSMs	Unique Peptides	AAs	MW [kDa]	Score Sequest
P0A6B7	iscS	68	22	42	22	404	45.1	125.27
Q57261	truD	74	20	38	20	349	39.1	118.51
P0CE47	tufA	69	20	33	20	394	43.3	97.95
P00370	gdhA	62	19	29	19	447	48.6	89.44
P25539	ribD	67	19	28	19	367	40.3	93.4
P03023	lacI	60	16	28	16	360	38.6	85.16
P06987	hisB	48	16	27	16	355	40.3	90.22
P75863	ycbX	63	16	26	16	369	40.6	78.04
P0A9J8	pheA	46	16	26	16	386	43.1	61.71
P0AD05	yecA	57	8	25	8	221	25	73.22
P0ADV5	yhbW	50	14	24	14	335	37.1	70.43
Q46851	gpr	80	19	24	19	346	38.8	79.19
P0ACP7	purR	50	15	23	15	341	38.2	69.38
P0A825	glyA	46	14	21	14	417	45.3	55.03
P0ACI0	rob	63	15	20	15	289	33.1	52.82
P60390	rsmH	61	15	19	15	313	34.9	56.45
P30177	ybiB	61	14	18	14	320	35	60.57
P00887	aroH	43	12	17	12	348	38.7	45.42
P76291	cmoB	56	13	17	13	323	37	45.96
P67910	hldD	50	14	17	14	310	34.9	43.59
P0ABQ0	coaBC	47	14	16	14	406	43.4	44.86
P69797	manX	44	10	16	10	323	35	34.53
P0ABD5	accA	55	13	16	13	319	35.2	47.79
P77398	arnA	25	14	15	14	660	74.2	29.53
P0A7Z4	rpoA	51	13	15	13	329	36.5	38.63
P76116	yncE	32	10	14	10	353	38.6	35.88
P21151	fadA	45	10	14	10	387	40.9	44.57
P28631	holB	46	10	13	10	334	36.9	39.67
P63883	amiC	35	11	13	11	417	45.6	23.25
P75876	rlmI	37	11	13	11	396	44.3	33.47
P0A847	tgt	34	11	13	11	375	42.6	33.65
P39286	rsgA	47	12	13	12	350	39.2	33.93
P17802	mutY	31	9	12	9	350	39.1	20.16
P37661	eptB	27	10	12	10	563	63.8	32.86
P0A9B2	gapA	39	11	12	11	331	35.5	21.45
P0A6U3	mnmG	21	8	11	8	629	69.5	14.02
P77690	arnB	27	7	11	7	385	42.2	34.28
P0A717	prs	40	9	10	9	315	34.2	22.79
P0A910	ompA	37	9	10	9	346	37.2	33.82
P12008	aroC	33	7	9	7	361	39.1	27.4
P29680	hemE	29	8	9	8	354	39.2	17.52
P76373	ugd	24	8	9	8	388	43.6	16.25
P0A9S5	gldA	26	6	8	6	367	38.7	19.09
A0A1V1IFM5	gsk-4	24	7	8	7	434	48.4	13.36
P0ADG7	guaB	13	4	8	4	488	52	10.84
P0ADR8	ppnN	20	8	8	8	454	50.9	16.59
P17115	gutQ	29	8	8	8	321	34	13.52
P0AB91	aroG	31	8	8	8	350	38	25.37
P37651	bcsZ	22	7	7	7	368	41.7	10.46
P33643	rluD	30	6	7	6	326	37.1	16.63
P0AC41	sdhA	14	7	7	7	588	64.4	16.21
P37051	purU	25	5	6	5	280	31.9	4.14
P0A6Y5	hslO	27	6	6	6	292	32.5	13.72
P22188	murE	12	5	6	5	495	53.3	9.85
P60716	lipA	21	5	6	5	321	36	7.49
P37631	yhiN	19	6	6	6	400	43.7	12.06
P0A9K3	ybeZ	23	6	6	6	346	39	14.91

P23003	trmA	14	5	6	5	366	41.9	12.6
P0AG40	ribF	22	5	5	5	313	34.7	9.68
P0AEI4	rimO	15	4	5	4	441	49.6	15.1
P0ABH7	gltA	9	3	5	3	427	48	1.68
P0ACR4	yeiE	19	4	5	4	293	32.7	8.64
P06959	aceF	10	5	5	5	630	66.1	7.13
P0ABK5	cysK	23	5	5	5	323	34.5	8.5
P0A8J8	rhlB	10	4	4	4	421	47.1	8.7
P21645	lpxD	24	4	4	4	341	36	6.72
P60757	hisG	18	4	4	4	299	33.3	2.64
P76193	ynhG	16	4	4	4	334	36.1	10.69
P33030	yeiR	17	4	4	4	328	36.1	4.55
P0ABZ6	surA	11	4	4	4	428	47.3	8.68
P28630	holA	12	3	4	3	343	38.7	12.09
P0ADQ2	fabY	16	4	4	4	329	37.1	11.19
P0A8E1	ycfP	18	3	4	3	180	21.2	8.07
P09831	gltB	3	4	4	4	1486	163.2	6.95
P0A9S3	gatD	12	4	4	4	346	37.4	9.69
P39451	adhP	13	3	4	3	336	35.4	4.69
P0A855	tolB	11	4	4	4	430	45.9	4.33
P0A705	infB	4	4	4	4	890	97.3	8.71
P0A9B6	epd	11	4	4	4	339	37.3	7.19
P0A6W0	glsA2	18	4	4	4	308	33.5	9.53
P0AFG6	sucB	12	4	4	4	405	44	10.87
P66948	bepA	10	3	3	3	487	53.9	3.19
P39406	rsmC	18	3	3	3	343	37.6	1.68
P28304	qorA	9	2	3	2	327	35.2	1.87
P27306	sthA	11	3	3	3	466	51.5	8.41
P37610	tauD	10	3	3	3	283	32.4	6.78
P0A935	mltA	11	3	3	3	365	40.4	8.53
P76422	thiD	16	2	3	2	266	28.6	7.88
P0A7B3	nadK	20	3	3	3	292	32.5	3.03
P0ACP1	cra	11	3	3	3	334	38	7.92
P0A722	lpxA	13	3	3	3	262	28.1	8.22
P0ABH9	clpA	9	3	3	3	758	84.2	2.35
P37692	rfaF	9	3	3	3	348	39	2.02
P0ACN7	cytR	11	3	3	3	341	37.8	3.42
P0AES6	gyrB	6	3	3	3	804	89.9	5.02
P0CG19	rph	11	2	3	2	228	24.4	8.76
P14294	topB	4	1	3	1	653	73.2	0
P02931	ompF	9	3	3	3	362	39.3	6.46
P68187	malK	13	3	3	3	371	41	1.87
P0AE18	map	9	2	2	2	264	29.3	5.62
P0A9K9	slyD	10	2	2	2	196	20.8	4.97
P02943	lamB	7	2	2	2	446	49.9	3.96
P06710	dnaX	2	2	2	2	643	71.1	0
P0AD70	ampH	8	2	2	2	385	41.8	6.34
P0A850	tig	5	2	2	2	432	48.2	0
P04036	dapB	11	2	2	2	273	28.7	2.13
P0AEX9	malE	7	2	2	2	396	43.4	0
P0A7B5	proB	7	2	2	2	367	39	0
P0ACC7	glmU	5	2	2	2	456	49.2	4.73
P0A7G6	recA	7	2	2	2	353	38	4.35
P64588	yqjI	8	2	2	2	207	23.4	4.3
P0C0V0	degP	5	2	2	2	474	49.3	5.14
P0ACP5	gntR	9	2	2	2	331	36.4	2.17
P0ADR6	rlmM	5	2	2	2	366	41.9	0
P06992	rsmA	16	2	2	2	273	30.4	2.09
P0ADG4	suhB	10	2	2	2	267	29.2	2.54
P67660	yhaJ	9	2	2	2	298	33.2	1.64
P12295	ung	10	2	2	2	229	25.7	5.66
P0ABC3	hflC	5	2	2	2	334	37.6	2.1
P0AC53	zwf	4	2	2	2	491	55.7	4.97
P75825	hcp	4	1	2	1	550	60	0
P07023	tyrA	6	2	2	2	373	42	0
P0AB71	fbaA	8	2	2	2	359	39.1	4.67
P0A9F3	cysB	7	2	2	2	324	36.1	4.12
P77581	astC	11	2	2	2	406	43.6	2.29
P46139	dgcN	5	1	2	1	408	46	0
P75913	ghrA	9	2	2	2	312	35.3	0
P07639	aroB	10	2	2	2	362	38.9	2.31
P36999	rlmA	6	1	1	1	269	30.4	2.5
P76215	astE	4	1	1	1	322	35.8	1.61

P06721	metC	5	1	1	1	395	43.2	2.28
P33225	torA	4	1	1	1	848	94.4	0
P00393	ndh	3	1	1	1	434	47.3	2.41
P42641	obgE	6	1	1	1	390	43.3	0
P36672	treB	5	1	1	1	473	51	0
P77774	bamB	3	1	1	1	392	41.9	0
P0C0L7	proP	3	1	1	1	500	54.8	0
P08390	usg	4	1	1	1	337	36.3	0
P0A9Q5	accD	4	1	1	1	304	33.3	2.21
P0ACB7	hemY	2	1	1	1	398	45.2	0
P07913	tdh	2	1	1	1	341	37.2	0
P76237	dgcJ	2	1	1	1	496	56.6	0
P76055	ttcA	2	1	1	1	311	35.5	0
P0AAD6	sdaC	3	1	1	1	429	46.9	0
P77434	alaC	2	1	1	1	412	46.2	1.8
P37313	dppF	5	1	1	1	334	37.5	0
P61889	mdh	4	1	1	1	312	32.3	0
P39835	gntT	5	1	1	1	438	45.9	0
P0A853	tnaA	2	1	1	1	471	52.7	2.45
P24188	trhO	2	1	1	1	350	39.8	0
P0A749	murA	6	1	1	1	419	44.8	0
P21599	pykA	2	1	1	1	480	51.3	2.15
P13482	treA	2	1	1	1	565	63.6	0
P30748	moaD	26	1	1	1	81	8.8	4.56
P29018	cydD	1	1	1	1	588	65	0
P45577	proQ	4	1	1	1	232	25.9	2.48
P77737	oppF	3	1	1	1	334	37.2	1.6
P21513	rne	2	1	1	1	1061	118.1	1.95
P0AG30	rho	3	1	1	1	419	47	1.97
P33232	lldD	3	1	1	1	396	42.7	0
P0A8I5	trmB	5	1	1	1	239	27.3	0
P0A7S9	rpsM	11	1	1	1	118	13.1	3.09
P25535	ubiI	3	1	1	1	400	44.2	1.95
P77743	prpR	1	1	1	1	528	58.6	0
P41069	traV	4	1	1	1	171	18.6	0
P0A836	sucC	3	1	1	1	388	41.4	0
P0ABC7	hflK	3	1	1	1	419	45.5	0
P0A817	metK	3	1	1	1	384	41.9	0
P0AFX4	rsd	6	1	1	1	158	18.2	1.85
P0A6A6	leuC	2	1	1	1	466	49.9	0
P09030	xthA	3	1	1	1	268	31	0
P0DMC5	rcsC	1	1	1	1	949	106.4	1.98
P0A6F1	carA	3	1	1	1	382	41.4	1.75
P06961	cca	4	1	1	1	412	46.4	0
P0AF08	mrp	5	1	1	1	369	39.9	0
P0ABB4	atpD	3	1	1	1	460	50.3	0
P0A9P0	lpdA	2	1	1	1	474	50.7	1.91
P00954	trpS	7	1	1	1	334	37.4	0
P0A6U5	rsmG	5	1	1	1	207	23.4	2.66
P0A9A9	fur	9	1	1	1	148	16.8	3.68
P06612	topA	2	1	1	1	865	97.3	2.38
P23908	argE	3	1	1	1	383	42.3	2.42
P05020	pyrC	3	1	1	1	348	38.8	1.61
P36659	cbpA	5	1	1	1	306	34.4	0
P45395	kdsD	2	1	1	1	328	35.2	1.72
P0AG86	secB	13	1	1	1	155	17.3	0
P69776	lpp	18	1	1	1	78	8.3	0
P76177	ydgH	5	1	1	1	314	33.9	0

Table 8 - Mass spectrometry results from Section 5.2.4 – W13Bpa 42-65 kDa

UniProt Accession ID	Gene Name	Coverage [%]	Peptides	PSMs	Unique Peptides	AAs	MW [kDa]	Score Sequest
P0A825	glyA	71	28	96	28	417	45.3	310
P00370	gdhA	74	27	71	27	447	48.6	208.42
P0ADR8	ppnN	77	30	61	30	454	50.9	161.08
P0A6B7	iscS	73	26	61	26	404	45.1	167.53
P0ABZ6	surA	59	21	51	21	428	47.3	158.36
P0CE47	tufA	77	21	51	21	394	43.3	151.32
P0ADG7	guaB	75	26	49	26	488	52	154
P0A847	tgt	73	25	43	25	375	42.6	138.71
P0ACC7	glmU	59	20	40	20	456	49.2	122.31
P27306	sthA	69	22	38	22	466	51.5	117.59
P21599	pykA	62	22	37	22	480	51.3	97.62
P0AC53	zwf	62	27	36	27	491	55.7	97.96
P0A850	tig	56	21	34	21	432	48.2	86.61
P0A8J8	rhlB	71	19	31	19	421	47.1	112.92
P0AD05	yecA	57	8	30	8	221	25	87.53
P0ABQ0	coaB	53	16	27	16	406	43.4	72.32
P77398	rnA	33	19	26	19	660	74.2	66.02
P06987	hisB	50	15	24	15	355	40.3	67.63
P0AG30	rho	45	18	24	18	419	47	60.39
P25552	gppA	42	14	23	14	494	54.8	65.06
P06720	melA	36	12	21	12	451	50.6	43.56
P03023	lacI	57	14	21	14	360	38.6	62.9
P36929	rsmB	50	13	21	13	429	48.3	47.71
P0AAZ4	rarA	51	17	21	17	447	49.6	56.35
P21513	rne	23	18	20	18	1061	118.1	47.92
P0ABH7	gltA	50	13	20	13	427	48	52.1
P0A9P0	lpdA	39	14	20	14	474	50.7	71.67
P76273	rsmF	35	12	20	12	479	53.2	55.01
P24182	accC	35	12	20	12	449	49.3	63.66
A0A1V1IFM5	gsk-4	49	14	18	14	434	48.4	44.29
Q57261	truD	60	15	17	15	349	39.1	37.93
P0A9J8	pheA	37	11	16	11	386	43.1	39.69
P0AFL6	ppx	32	13	16	13	513	58.1	37.73
P06961	cca	40	13	15	13	412	46.4	36.94
P25539	ribD	41	12	14	12	367	40.3	29.85
P32131	hemN	33	12	13	12	457	52.7	33.33
P0A9P6	deaD	23	11	12	11	629	70.5	30.18
P31806	nnr	28	10	12	10	515	54.6	33.24
P75863	ycbX	33	9	12	9	369	40.6	31.53
P0ACP7	purR	35	11	12	11	341	38.2	26.77
P0ABB0	atpA	28	11	11	11	513	55.2	29.9
P77434	alaC	38	11	11	11	412	46.2	28.31
P30871	ygiF	26	9	11	9	433	48.4	19.27
P06710	dnaX	14	7	10	7	643	71.1	18.44
P23845	cysN	23	9	10	9	475	52.5	23.82
P33643	rluD	43	8	10	8	326	37.1	32.24
P0AFG6	sucB	20	7	10	7	405	44	32.36
P02943	lamB	39	10	10	10	446	49.9	29.24
P66948	bepA	22	8	9	8	487	53.9	25.86
P0AC41	sdhA	17	8	9	8	588	64.4	18.95
P76403	trhP	25	8	9	8	453	51.2	19.5
P39099	degQ	32	9	9	9	455	47.2	26.21
P0A6P9	eno	20	7	8	7	432	45.6	17.66
P22188	murE	19	6	8	6	495	53.3	15.71
P11880	murF	18	6	8	6	452	47.4	24.09
P0A705	infB	9	7	8	7	890	97.3	11.54
P0AEI4	rimO	23	7	8	7	441	49.6	25.57
P0A6A6	leuC	28	8	8	8	466	49.9	16.6
P0ACI0	rob	35	7	8	7	289	33.1	5.34
P60906	hisS	23	7	8	7	424	47	17.33
P38051	menF	23	7	7	7	431	48.7	9.68
P0A7Z4	rpoA	26	7	7	7	329	36.5	11.34
P23830	pssA	18	6	6	6	451	52.8	8.02

P0A6F3	glpK	14	6	6	6	502	56.2	12.95
P21151	fadA	19	5	6	5	387	40.9	19.44
P0AFU4	glrR	18	6	6	6	444	49.1	10.94
P0ABB4	atpD	21	6	6	6	460	50.3	16.86
P0A6C5	argA	15	5	6	5	443	49.2	5.74
P08660	lys	16	5	6	5	449	48.5	12.45
P33599	nuoC	9	5	5	5	596	68.2	6.96
P0A6U8	glgA	14	4	5	4	477	52.8	14.17
P0A8M3	thrS	6	4	5	4	642	74	8.09
P0A6T5	folE	24	5	5	5	222	24.8	6.74
P00887	aroH	15	4	5	4	348	38.7	9.07
P30177	ybiB	23	5	5	5	320	35	7.41
P04036	dapB	18	4	5	4	273	28.7	10
P75876	rlmI	18	5	5	5	396	44.3	9.64
P00914	phrB	8	4	4	4	472	53.6	2.4
P0AES6	gyrB	5	4	4	4	804	89.9	7.74
P0A749	murA	9	4	4	4	419	44.8	3.55
P0C0V0	degP	13	4	4	4	474	49.3	2.05
P05042	fumC	9	4	4	4	467	50.5	3.71
P17315	cirA	3	1	4	1	663	73.9	0
P07639	aroB	12	3	4	3	362	38.9	9.73
P0C8J8	gatZ	10	4	4	4	420	47.1	3.19
P37675	yiaN	9	1	4	1	425	45.3	0
P39286	rsgA	15	4	4	4	350	39.2	4.84
P33360	yehX	8	1	4	1	308	34.4	0
P0A8N3	lysS	7	4	4	4	505	57.6	1.74
P37631	yhiN	13	4	4	4	400	43.7	7.81
P37051	purU	18	4	4	4	280	31.9	6.15
P12295	ung	21	4	4	4	229	25.7	4.72
P52097	tilS	10	4	4	4	432	48.2	10.45
P45577	proQ	11	3	3	3	232	25.9	5.02
P0A8E1	ycfP	14	2	3	2	180	21.2	5.52
P76046	ycjX	8	3	3	3	465	52.6	2.91
P0ABC7	hflK	10	3	3	3	419	45.5	6.15
P04335	frsA	7	3	3	3	414	47	0
P0A722	lpxA	13	3	3	3	262	28.1	7.52
P08200	icd	9	3	3	3	416	45.7	0
P31979	nuoF	7	3	3	3	445	49.3	5.55
P42641	obgE	11	3	3	3	390	43.3	7.21
P76291	cmoB	11	3	3	3	323	37	3.02
P77581	astC	8	3	3	3	406	43.6	6.25
P76422	thiD	16	2	3	2	266	28.6	6.7
P0A717	prs	14	3	3	3	315	34.2	4.89
P35340	ahpF	9	3	3	3	521	56.1	2.58
P55135	rlmD	7	2	3	2	433	48	5.02
P08192	folC	8	3	3	3	422	45.4	4.14
Q46851	gpr	12	3	3	3	346	38.8	4.03
P06959	aceF	5	3	3	3	630	66.1	5.12
P09831	gltB	2	3	3	3	1486	163.2	0
P09832	gltD	10	3	3	3	472	52	6.2
P00579	rpoD	3	2	3	2	613	70.2	4.83
P0A910	mpA	9	2	2	2	346	37.2	3.28
P0ABJ9	cydA	4	2	2	2	522	58.2	2.3
P0AE18	map	7	2	2	2	264	29.3	1.97
P00490	malP	2	2	2	2	797	90.5	0
P0A9S5	gldA	8	2	2	2	367	38.7	0
P0A7V8	rpsD	11	2	2	2	206	23.5	2.57
P0A6H1	clpX	5	2	2	2	424	46.3	5.23
P0A6U5	rsmG	10	2	2	2	207	23.4	2.47
P0A9Q7	adhE	2	2	2	2	891	96.1	1.99
P0A6E4	argG	4	2	2	2	447	49.9	1.92
P0ADV5	yhbW	9	2	2	2	335	37.1	0
P0AG67	rpsA	5	2	2	2	557	61.1	2.6
P77690	arnB	9	2	2	2	385	42.2	3.85
P02930	tolC	5	2	2	2	493	53.7	2.01
P0A9K9	slyD	12	2	2	2	196	20.8	2.65
P43672	uup	5	2	2	2	635	72	3.96
Q47622	sapA	5	2	2	2	547	61.5	6.92

P71242	wcaK	4	2	2	2	426	47.3	1.86
P0AEX9	malE	3	1	1	1	396	43.4	0
P12008	aroC	4	1	1	1	361	39.1	2.55
P0A9W9	yrdA	8	1	1	1	184	20.2	0
P30958	mfd	1	1	1	1	1148	129.9	2.58
P23893	hemL	2	1	1	1	426	45.3	0
P04995	sbcB	3	1	1	1	475	54.5	0
P28631	holB	3	1	1	1	334	36.9	0
P76373	ugd	2	1	1	1	388	43.6	2.07
P0A9B2	gapA	5	1	1	1	331	35.5	0
P0AFG8	aceE	1	1	1	1	887	99.6	2.84
P0A7B1	ppk	1	1	1	1	688	80.4	0
P0AB89	purB	2	1	1	1	456	51.5	0
P10902	nadB	2	1	1	1	540	60.3	1.94
P75780	fiu	3	1	1	1	760	81.9	0
P30845	eptA	1	1	1	1	547	61.6	1.88
P04994	xseA	3	1	1	1	456	51.8	2.82
P30748	moaD	26	1	1	1	81	8.8	5.36
P0A6V1	glgC	4	1	1	1	431	48.7	0
P0ACR4	yeiE	5	1	1	1	293	32.7	0
P0AEI1	miaB	5	1	1	1	474	53.6	0
P24228	dacB	3	1	1	1	477	51.8	0
P64588	yqjI	4	1	1	1	207	23.4	1.99
P31677	otsA	5	1	1	1	474	53.6	0
P37773	mpl	2	1	1	1	457	49.8	2.16
P0A8V2	rpoB	1	1	1	1	1342	150.5	0
P60390	rsmH	4	1	1	1	313	34.9	1.61
P41069	traV	4	1	1	1	171	18.6	0
P27431	roxA	3	1	1	1	373	42.6	0
P0A6J5	dadA	4	1	1	1	432	47.6	2.06
P0DMC5	rcsC	1	1	1	1	949	106.4	1.66
P0AG40	ribF	5	1	1	1	313	34.7	0
P0A817	metK	2	1	1	1	384	41.9	1.63
P23865	prc	1	1	1	1	682	76.6	2.3
P23003	trmA	2	1	1	1	366	41.9	0
P75906	pgaB	1	1	1	1	672	77.4	0
P0ABH9	clpA	3	1	1	1	758	84.2	0
P09127	hemX	3	1	1	1	393	42.9	2.79
P33136	mdoG	3	1	1	1	511	57.9	2.57
P0A7E5	pyrG	3	1	1	1	545	60.3	1.73
P0ABD5	accA	4	1	1	1	319	35.2	2.16
P0CG19	rph	5	1	1	1	228	24.4	2.24
P0A9A9	fur	9	1	1	1	148	16.8	3.66
P06612	topA	1	1	1	1	865	97.3	0
P05041	pabB	3	1	1	1	453	50.9	0
P77173	zipA	2	1	1	1	328	36.5	0
P39410	yjjJ	3	1	1	1	443	49.7	2.04
P0AEA8	cysG	4	1	1	1	457	49.9	2.31
P23908	argE	2	1	1	1	383	42.3	0
P17115	gutQ	2	1	1	1	321	34	1.65
P0AB91	aroG	3	1	1	1	350	38	0
P13009	metH	2	1	1	1	1227	135.9	0
P0AG63	rpsQ	10	1	1	1	84	9.7	1.68
P0A6U3	mnmG	1	1	1	1	629	69.5	0
P06992	rsmA	4	1	1	1	273	30.4	2.24
P0ADG4	suhB	5	1	1	1	267	29.2	0
P00393	ndh	3	1	1	1	434	47.3	0
P75817	rlmC	6	1	1	1	375	41.9	0
P19934	tolA	3	1	1	1	421	43.1	0
P0A8I5	trmB	5	1	1	1	239	27.3	0

Table 9 - Mass spectrometry results from Section 5.2.4 – W13Bpa 65-100 kDa

UniProt Accession ID	Gene Name	Coverage [%]	Peptides	PSMs	Unique Peptides	AAs	MW [kDa]	Score Sequest
P00490	malP	56	33	55	33	797	90.5	123.53
P77398	arnA	57	29	47	29	660	74.2	132.33
P0AFG8	aceE	48	34	46	34	887	99.6	97.56
P06612	topA	49	32	42	32	865	97.3	109.49
P23865	prc	50	27	33	27	682	76.6	67.5
P0A8M3	thrS	50	27	33	27	642	74	70.72
P06959	aceF	51	23	28	23	630	66.1	67.31
P0AES4	gyrA	29	22	27	22	875	96.9	72
P09831	gltB	20	22	25	22	1486	163.2	52.46
P0CE47	tufA	60	17	23	17	394	43.3	36.89
P0AES6	gyrB	36	21	23	21	804	89.9	54.36
P0A9Q7	adhE	27	19	23	19	891	96.1	61.73
P0AFG3	sucA	25	17	22	17	933	105	36.42
P30958	mfd	19	20	21	20	1148	129.9	41.55
P0AC41	sdhA	35	16	19	16	588	64.4	43.2
P30850	rnb	34	17	19	17	644	72.4	41.69
P33602	nuoG	22	15	17	15	908	100.2	38.4
P0A705	infB	24	14	16	14	890	97.3	19.07
P00562	metL	21	14	15	14	810	88.8	30.43
P00452	nrdA	22	14	14	14	761	85.7	25.09
P0A825	glyA	40	11	13	11	417	45.3	32.98
P00370	gdhA	38	12	13	12	447	48.6	34.07
P0ABH9	clpA	20	12	13	12	758	84.2	20.28
P0A6B7	iscS	36	12	12	12	404	45.1	25.74
P0AC53	zwf	27	12	12	12	491	55.7	22.52
P0A9M8	pta	22	11	11	11	714	77.1	22.29
P0ADG7	guaB	35	9	10	9	488	52	15.62
P00579	rpoD	22	10	10	10	613	70.2	17.23
P0AD05	yecA	28	4	10	4	221	25	24.45
P0A698	uvrA	13	10	10	10	940	103.8	15.52
P0ADR8	ppnN	24	10	10	10	454	50.9	22.26
P0A6U3	mnmG	19	9	9	9	629	69.5	12.89
P27249	glnD	11	8	8	8	890	102.3	12.9
P0A8V2	rpoB	5	7	7	7	1342	150.5	10.7
P76562	tmcA	11	6	6	6	671	74.8	6.31
P23909	mutS	9	6	6	6	853	95.2	6.84
P04036	dapB	21	4	6	4	273	28.7	18.55
P09546	putA	5	5	6	5	1320	143.7	2.36
P15977	malQ	13	6	6	6	694	78.5	6.7
P02931	ompF	16	6	6	6	362	39.3	15.24
P77182	mnmC	13	5	5	5	668	74.4	6.29
P10408	secA	8	5	5	5	901	102	7.58
P36683	acnB	8	5	5	5	865	93.4	5.1
P06987	hisB	15	5	5	5	355	40.3	8.15
P08660	lysC	12	4	5	4	449	48.5	10.16
P00582	polA	9	4	5	4	928	103.1	0
P21599	pykA	11	4	4	4	480	51.3	3.75
P76422	thiD	19	3	4	3	266	28.6	9.26
P60785	lepA	10	4	4	4	599	66.5	2.68
P0A6Y8	dnaK	9	4	4	4	638	69.1	5.46
Q57261	truD	14	4	4	4	349	39.1	4.34
P33599	nuoC	7	4	4	4	596	68.2	1.66
P27306	sthA	17	4	4	4	466	51.5	2.44
P30870	glnE	5	3	3	3	946	108.4	3.99
P0A9A9	fur	30	3	3	3	148	16.8	6.33
P0A850	tig	11	3	3	3	432	48.2	3.34
P0A9P0	lpdA	9	3	3	3	474	50.7	4.38
P05055	pnp	5	3	3	3	711	77.1	2.08
P25539	ribD	10	3	3	3	367	40.3	0
P0A9J8	pheA	5	2	2	2	386	43.1	1.65
P17169	glmS	4	2	2	2	609	66.9	4.51

P0A9C5	glnA	4	1	2	1	469	51.9	0
P07639	aroB	9	2	2	2	362	38.9	0
P00957	alaS	3	2	2	2	876	96	1.75
P0AEI4	rimO	8	2	2	2	441	49.6	2.88
P0ABQ0	coaBC	8	2	2	2	406	43.4	0
P0A6M8	fusA	3	2	2	2	704	77.5	3.78
P03018	uvrD	3	2	2	2	720	81.9	0
P0A9K9	slyD	10	2	2	2	196	20.8	4.43
P28903	nrdD	5	2	2	2	712	80	0
P21189	polB	3	2	2	2	783	90	4.37
P0A847	tgt	5	1	1	1	375	42.6	0
B8LFD5	lacI	4	1	1	1	363	38.9	2.04
P06710	dnaX	2	1	1	1	643	71.1	0
P0AG30	rho	5	1	1	1	419	47	2.18
P25907	ydbD	2	1	1	1	768	86.7	0
P18775	dmsA	1	1	1	1	814	90.3	0
P0AAI3	ftsH	3	1	1	1	644	70.7	0
P0A8N3	lysS	2	1	1	1	505	57.6	0
P21177	fadB	2	1	1	1	729	79.5	0
P45577	proQ	4	1	1	1	232	25.9	2.38
P42907	agaS	4	1	1	1	384	41.8	0
P24182	accC	3	1	1	1	449	49.3	2.5
P52126	abpB	2	1	1	1	729	83	0
P76273	rsmF	4	1	1	1	479	53.2	0
P11880	murF	5	1	1	1	452	47.4	0
P00887	aroH	4	1	1	1	348	38.7	0
P15286	flk	10	1	1	1	331	36.6	0
P0A8E1	ycfP	7	1	1	1	180	21.2	2.48
P39385	yjiN	7	1	1	1	426	48.2	0
P69776	lpp	18	1	1	1	78	8.3	0
P42632	tdcE	4	1	1	1	764	85.9	0
P76578	yfhM	1	1	1	1	1653	181.5	0
P0A8J8	rhlB	2	1	1	1	421	47.1	0
P30748	moaD	26	1	1	1	81	8.8	4.06
P0A910	ompA	4	1	1	1	346	37.2	2.78
P32176	fdoG	2	1	1	1	1016	112.5	0
P35340	ahpF	4	1	1	1	521	56.1	3.13
P21179	katE	1	1	1	1	753	84.1	0
P0AG20	relA	3	1	1	1	744	83.8	0
P21645	lpxD	2	1	1	1	341	36	1.95

Table 10 - Mass spectrometry results from Section 5.2.4– N91Bpa 34-43 kDa

UniProt Accession ID	Gene Name	Coverage [%]	Peptides	PSMs	Unique Peptides	AAs	MW [kDa]	Score Sequest
P0CE47	tufA	90	32	263	32	394	43.3	522.06
P0A6B7	iscS	60	21	56	21	404	45.1	178.08
P77581	astC	64	18	34	18	406	43.6	128.47
P06987	hisB	50	17	33	17	355	40.3	117.32
P21151	fadA	55	13	31	13	387	40.9	106.51
P0A9J8	pheA	48	16	30	16	386	43.1	93.04
P02931	ompF	53	15	29	15	362	39.3	78.17
P69797	manX	56	16	28	16	323	35	89.34
P75876	rlmI	53	17	25	17	396	44.3	71.65
P75863	ycbX	73	19	24	19	369	40.6	84.68
P23908	argE	61	12	23	12	383	42.3	89.85
P25539	ribD	56	15	22	15	367	40.3	75.02
P0A847	tgt	61	17	22	17	375	42.6	65.55
P03023	lacI	53	13	21	13	360	38.6	73.41
Q57261	truD	66	16	21	16	349	39.1	62.22
P0ABH7	gltA	51	12	21	12	427	48	68.3
P33030	yeiR	53	14	20	14	328	36.1	57.4
P17169	glmS	35	14	20	14	609	66.9	55.56
P0ACP7	purR	45	13	19	13	341	38.2	61.68
A0A1V1IFM5	gsk-4	43	13	18	13	434	48.4	51.62
P66948	bepA	32	10	17	10	487	53.9	49.5
P0A855	tolB	39	11	17	11	430	45.9	50.61
P0A7Z4	rpoA	57	14	17	14	329	36.5	34.06
P29680	hemE	47	13	16	13	354	39.2	35.69
P0AB91	aroG	58	12	15	12	350	38	56.05
P0C0V0	degP	36	11	15	11	474	49.3	43.32
P0A910	ompA	43	10	15	10	346	37.2	56.84
P0ADV5	yhbW	35	9	13	9	335	37.1	42.59
P30177	ybiB	43	11	13	11	320	35	42.75
P0ABQ0	coaBC	32	9	13	9	406	43.4	50.74
P76291	cmoB	36	10	13	10	323	37	41.88
P0AG30	rho	33	12	13	12	419	47	31.89
P77398	arnA	24	12	13	12	660	74.2	26.41
P25888	rhlE	33	10	13	10	454	50	40.01
P33643	rluD	52	11	13	11	326	37.1	41.21
P39451	adhP	38	8	13	8	336	35.4	34.63
P0AE06	acrA	42	11	12	11	397	42.2	29.18
P0ACI0	rob	39	9	12	9	289	33.1	26.6
P0A7G6	recA	28	8	12	8	353	38	37.56
P76116	yncE	32	9	12	9	353	38.6	36.71
P00490	malP	18	12	12	12	797	90.5	26.05
P28631	holB	45	9	12	9	334	36.9	40.46
P35340	ahpF	28	10	11	10	521	56.1	31.94
P39286	rsgA	33	8	11	8	350	39.2	32.46
P0A825	glyA	31	9	11	9	417	45.3	26.13
P02943	lamB	35	9	11	9	446	49.9	39.31
P0A9P0	lpdA	32	10	11	10	474	50.7	37.09
P22188	murE	28	9	11	9	495	53.3	31.82
P0A9B2	gapA	39	9	10	9	331	35.5	20.77
P24188	trhO	32	10	10	10	350	39.8	15.41
P13033	glpB	22	7	10	7	419	45.3	26.86
P0ADG7	guaB	20	5	10	5	488	52	18.7
P67910	hldD	27	8	9	8	310	34.9	17.93
P67660	yhaJ	27	7	9	7	298	33.2	26.37
P0A9S3	gatD	19	8	8	8	346	37.4	24
P21599	pykA	22	8	8	8	480	51.3	23.59
P60716	lipA	27	6	8	6	321	36	25.25
P77690	arnB	24	6	7	6	385	42.2	24.59
P0A786	pyrB	30	6	7	6	311	34.4	16.25
P09831	gltB	5	6	7	6	1486	163.2	14.66

P13039	fes	26	7	7	7	400	45.6	17.25
P39099	degQ	25	6	7	6	455	47.2	9.87
P77434	alaC	26	7	7	7	412	46.2	16.28
P0A9A6	ftsZ	31	7	7	7	383	40.3	13.7
P0AD05	yecA	42	5	6	5	221	25	17.55
P37661	eptB	11	4	6	4	563	63.8	14.23
P0AF08	mrp	18	4	6	4	369	39.9	14.39
P00963	asnA	25	6	6	6	330	36.6	19.26
P0A6F1	carA	27	6	6	6	382	41.4	21.59
P0A6Y8	dnaK	14	6	6	6	638	69.1	15.23
P08390	usg	28	5	6	5	337	36.3	13.53
P28304	qorA	23	4	6	4	327	35.2	12.93
P0AB71	fbaA	26	6	6	6	359	39.1	14.77
P0A903	bamC	25	6	6	6	344	36.8	17.78
P0A6Y5	hslO	21	4	5	4	292	32.5	12.67
P0A6W0	glsA2	16	4	5	4	308	33.5	10.63
P0AEI4	rimO	17	5	5	5	441	49.6	10.75
P76035	yciW	15	5	5	5	375	42.2	15.24
P0A6A3	ackA	16	4	5	4	400	43.3	14.34
P0ACP1	cra	17	5	5	5	334	38	10.89
P42596	rlmG	13	4	4	4	378	42.3	10.3
P0AFG3	sucA	6	4	4	4	933	105	6.85
P37692	rfaF	17	4	4	4	348	39	8.06
P63883	amiC	11	3	4	3	417	45.6	6.22
P0AF20	nagC	11	4	4	4	406	44.5	8.18
P0A850	tig	12	4	4	4	432	48.2	7.75
P64588	yqjI	18	4	4	4	207	23.4	8.84
P0ABH0	ftsA	17	3	4	3	420	45.3	2.45
P0A9X4	mreB	14	4	4	4	347	36.9	8.21
P0AC41	sdhA	9	4	4	4	588	64.4	11.27
P0ABD5	accA	19	4	4	4	319	35.2	10.04
P23524	garK	10	1	4	1	381	39.1	0
P17115	gutQ	19	4	4	4	321	34	7.26
P0AEB2	dacA	12	4	4	4	403	44.4	8.29
P0ABK5	cysK	20	4	4	4	323	34.5	12.79
P0A796	pfkA	11	4	4	4	320	34.8	8.17
P0A9B6	epd	14	4	4	4	339	37.3	8.61
P76373	ugd	16	4	4	4	388	43.6	7.52
P13009	metH	5	4	4	4	1227	135.9	6.69
P27306	sthA	15	4	4	4	466	51.5	14.4
P0A9F3	cysB	14	4	4	4	324	36.1	7.03
P0AFG6	sucB	15	4	4	4	405	44	12.13
P0AEX9	malE	14	4	4	4	396	43.4	5.38
P0ABC3	hflC	8	3	3	3	334	37.6	4.22
P0A817	metK	10	3	3	3	384	41.9	4.34
P27305	gluQ	10	2	3	2	308	34.8	6
P23003	trmA	13	3	3	3	366	41.9	7.96
P21179	katE	5	3	3	3	753	84.1	7.64
P37906	puuB	7	3	3	3	426	47.1	5.76
P0A705	infB	3	3	3	3	890	97.3	4.24
P0A9K9	slyD	22	3	3	3	196	20.8	9.34
P77774	bamB	12	3	3	3	392	41.9	9.6
P0AE18	map	13	3	3	3	264	29.3	8.87
P39298	yjfP	6	1	3	1	249	27.6	0
P23893	hemL	8	3	3	3	426	45.3	7.64
P17952	murC	11	3	3	3	491	53.6	7.98
P37651	bcsZ	9	3	3	3	368	41.7	3.74
P0AEP3	galU	11	3	3	3	302	32.9	8.42
P0A7V0	rpsB	15	3	3	3	241	26.7	6.1
P76422	thiD	16	2	3	2	266	28.6	9.95
P68187	malK	11	2	3	2	371	41	6.85
P16456	selD	7	2	3	2	347	36.7	3.24
P75949	nagZ	11	3	3	3	341	37.6	6.1
P00887	aroH	9	2	3	2	348	38.7	6.32
P0ABB4	atpD	5	2	2	2	460	50.3	5.1
P76193	ynhG	8	2	2	2	334	36.1	1.64
P24182	accC	5	2	2	2	449	49.3	4.29

P0AAI3	ftsH	6	2	2	2	644	70.7	2.26
P0ABZ6	surA	6	2	2	2	428	47.3	5.36
P06961	cca	6	2	2	2	412	46.4	0
P0ADY3	rplN	21	2	2	2	123	13.5	2.34
P0A7B5	proB	11	2	2	2	367	39	0
P36929	rsmB	3	1	2	1	429	48.3	0
P0ABH9	clpA	5	2	2	2	758	84.2	5.41
P77735	yajO	11	2	2	2	324	36.4	6.09
P0ACB7	hemY	8	2	2	2	398	45.2	3.96
P0C8J8	gatZ	5	2	2	2	420	47.1	4.59
P0A749	murA	5	2	2	2	419	44.8	3.94
P0A862	tpx	11	1	2	1	168	17.8	0
P04395	alkA	11	1	2	1	282	31.4	0
P64612	zapE	5	2	2	2	375	43	1.75
P21645	lpxD	6	2	2	2	341	36	4.89
P76177	ydgH	11	2	2	2	314	33.9	6.41
P0AE08	ahpC	18	2	2	2	187	20.7	3.61
P0A8E1	ycfP	14	2	2	2	180	21.2	5.22
P08200	icd	8	2	2	2	416	45.7	5.68
P00370	gdhA	6	1	2	1	447	48.6	2.44
P0A879	trpB	7	2	2	2	397	43	5.89
P21513	rne	3	2	2	2	1061	118.1	2.33
P09155	rnd	6	2	2	2	375	42.7	4.93
P03004	dnaA	3	1	2	1	467	52.5	0
P45395	kdsD	10	2	2	2	328	35.2	6.16
P0A7B3	nadK	5	1	1	1	292	32.5	3.01
Q46939	yqeF	7	1	1	1	393	41	0
P0A9S5	gldA	5	1	1	1	367	38.7	2.72
P25535	ubiI	3	1	1	1	400	44.2	1.67
P37773	mpl	2	1	1	1	457	49.8	1.75
P69874	potA	4	1	1	1	378	43	0
P32131	hemN	4	1	1	1	457	52.7	0
P0AGA2	secY	2	1	1	1	443	48.5	0
P21156	cysD	6	1	1	1	302	35.2	0
P0AE37	astA	3	1	1	1	344	38.4	2.19
P0A988	dnaN	5	1	1	1	366	40.6	0
P36672	treB	3	1	1	1	473	51	0
P00393	ndh	3	1	1	1	434	47.3	2.45
P0A9W9	yrdA	8	1	1	1	184	20.2	2.46
P67087	rsmI	6	1	1	1	286	31.3	2.65
P0ACN4	allR	14	1	1	1	271	29.3	0
P09053	avtA	2	1	1	1	417	46.7	0
P0A7I4	prfC	2	1	1	1	529	59.5	0
P0A6A8	acpP	12	1	1	1	78	8.6	0
P0A6P9	eno	4	1	1	1	432	45.6	0
P68767	pepA	2	1	1	1	503	54.8	0
P77808	yfaY	4	1	1	1	400	44.2	1.78
P0C0L7	proP	3	1	1	1	500	54.8	2.16
P75804	yliI	5	1	1	1	371	41	2.61
P0AC53	zwf	2	1	1	1	491	55.7	2.17
P30748	moaD	26	1	1	1	81	8.8	4.42
P0A8N3	lysS	2	1	1	1	505	57.6	0
P0ACR4	yeiE	3	1	1	1	293	32.7	0
P38051	menF	3	1	1	1	431	48.7	0
P07913	tdh	2	1	1	1	341	37.2	2.5
P08178	purM	4	1	1	1	345	36.8	3.25
P77357	abgA	5	1	1	1	436	46.6	3.57
P12295	ung	6	1	1	1	229	25.7	3.06
P02916	malF	4	1	1	1	514	57	0
P0A6K6	deoB	3	1	1	1	407	44.3	1.69
P0A836	sucC	3	1	1	1	388	41.4	0
P0AED7	dapE	3	1	1	1	375	41.2	0
P33937	napA	3	1	1	1	828	93	0
P0A6I3	coaA	3	1	1	1	316	36.3	1.65
P0AB74	kbaY	3	1	1	1	286	31.3	1.85
P30843	basR	5	1	1	1	222	25	2.09
P77757	arnC	4	1	1	1	322	36.3	0

P07117	putP	3	1	1	1	502	54.3	0
P0A717	prs	4	1	1	1	315	34.2	0
P0ADR8	ppnN	3	1	1	1	454	50.9	0
P11880	murF	2	1	1	1	452	47.4	2.71
Q46925	csdA	3	1	1	1	401	43.2	1.72
P0AAE0	cycA	3	1	1	1	470	51.6	3.05
Q47679	yafV	3	1	1	1	256	28.9	0
P36659	cbpA	5	1	1	1	306	34.4	3.49
P36979	rlmN	4	1	1	1	384	43.1	0
P0ADR6	rlmM	3	1	1	1	366	41.9	0
P0A7M2	rpmB	13	1	1	1	78	9	1.98
P37610	tauD	4	1	1	1	283	32.4	2.87
P0A6E4	argG	2	1	1	1	447	49.9	2.15
P08192	folC	2	1	1	1	422	45.4	2.02
P0ACJ8	crp	6	1	1	1	210	23.6	2.48
P0ADA3	nlpD	3	1	1	1	379	40.1	2.47
P61889	mdh	4	1	1	1	312	32.3	2.36
P62623	ispH	6	1	1	1	316	34.8	1.62
P0AB80	ilvE	6	1	1	1	309	34.1	2.57
P0A7J3	rplJ	7	1	1	1	165	17.7	0
P0ABC7	hflK	3	1	1	1	419	45.5	3.43
P77374	ynfE	3	1	1	1	808	89.7	0
P75913	ghrA	4	1	1	1	312	35.3	2.29
P0ADQ2	fabY	5	1	1	1	329	37.1	1.77
P37180	hybB	4	1	1	1	392	43.6	0
P75728	ubiF	4	1	1	1	391	42.9	1.99
P0AGJ5	yfiF	7	1	1	1	345	37.8	0
P40874	solA	5	1	1	1	372	40.9	3.05
P24202	mrr	6	1	1	1	304	33.5	3.17
P76102	insQ	4	1	1	1	382	43.3	0
P76273	rsmF	4	1	1	1	479	53.2	0
P41069	traV	4	1	1	1	171	18.6	1.61
P16688	phnJ	7	1	1	1	281	31.8	0

Table 11 - Mass spectrometry results from Section 5.2.4 – N91Bpa 43-65 kDa

UniProt Accession ID	Gene Name	Coverage [%]	Peptides	PSMs	Unique Peptides	AAs	MW [kDa]	Score Sequest
P0CE47	tufA	84	26	109	26	394	43.3	309.19
P0ADG7	guaB	73	24	75	24	488	52	248.97
P21599	pykA	81	29	74	29	480	51.3	249.16
P0A825	glyA	63	19	61	19	417	45.3	205.75
P0AG30	rho	68	27	61	27	419	47	183.57
P0A850	tig	65	29	58	29	432	48.2	164.14
P22188	murE	63	24	56	24	495	53.3	175.97
P35340	ahpF	67	26	53	26	521	56.1	174.72
P0A9P0	lpdA	58	24	49	24	474	50.7	161.8
P27306	sthA	72	24	47	24	466	51.5	151.54
P0ABZ6	surA	56	19	44	19	428	47.3	145.65
P0A6F3	glpK	61	26	42	26	502	56.2	104.55

P08192	folC	65	18	41	18	422	45.4	141.16
P0ABB0	atpA	68	26	39	26	513	55.2	116.91
P17169	glmS	59	26	38	26	609	66.9	128.94
P0AFG6	sucB	60	18	36	18	405	44	107.7
P24182	accC	56	20	35	20	449	49.3	109.79
P76403	trhP	54	17	34	17	453	51.2	122.24
P0ABH7	gltA	63	18	33	18	427	48	86.33
P0A7I4	prfC	50	20	33	20	529	59.5	100.63
P0ADR8	ppnN	59	22	31	22	454	50.9	75.98
P0AEI4	rimO	58	18	31	18	441	49.6	99.14
P77581	astC	64	17	28	17	406	43.6	86.68
P0AAZ4	rarA	65	21	28	21	447	49.6	81.43
P0A6B7	iscS	50	18	27	18	404	45.1	72.12
P0AC53	zwf	53	21	27	21	491	55.7	68.96
P0ABB4	atpD	70	19	26	19	460	50.3	67.3
P76273	rsmF	41	15	25	15	479	53.2	79.67
P25552	gppA	48	16	25	16	494	54.8	73.67
P39099	degQ	49	17	23	17	455	47.2	83.82
P11880	murF	39	11	23	11	452	47.4	65.59
P77357	abgA	48	14	22	14	436	46.6	54.05
P37773	mpl	37	10	21	10	457	49.8	64.73
P77398	arnA	33	18	21	18	660	74.2	48.2
P05042	fumC	58	16	21	16	467	50.5	49.2
Q47622	sapA	42	17	20	17	547	61.5	50.59
P23845	cysN	50	17	20	17	475	52.5	44.52
P0C0V0	degP	43	15	20	15	474	49.3	56.34
P31979	nuoF	52	17	19	17	445	49.3	55.74
P0AG67	rpsA	32	14	19	14	557	61.1	39.82
P66948	bepA	42	13	18	13	487	53.9	56.32
P21151	fadA	35	9	18	9	387	40.9	46.82
P0A6Y8	dnaK	31	15	18	15	638	69.1	49.68
P06987	hisB	43	13	17	13	355	40.3	38.36
P00861	lysA	50	10	17	10	420	46.1	68.92
P17952	murC	37	13	16	13	491	53.6	48.46
P0AEI1	miaB	45	13	16	13	474	53.6	45.07
A0A1V1IFM5	gsk-4	44	11	16	11	434	48.4	34.53
P0A9J8	pheA	37	12	16	12	386	43.1	44.65
P00490	malP	19	12	15	12	797	90.5	17.02
P0AC41	sdhA	28	13	15	13	588	64.4	35.4
P21513	rne	17	13	15	13	1061	118.1	39.2
P0ABQ0	coaBC	44	11	15	11	406	43.4	40.51
P77434	alaC	39	12	14	12	412	46.2	42.26
P32131	hemN	31	11	14	11	457	52.7	41.27
P40874	solA	41	11	13	11	372	40.9	21.7
P0A8J8	rhlB	37	12	13	12	421	47.1	35.84
P77804	ydgA	34	12	13	12	502	54.7	26.84
P0AFU4	glrR	31	11	13	11	444	49.1	32.41
P0AD61	pykF	33	12	12	12	470	50.7	30
P0A9P6	deaD	24	12	12	12	629	70.5	23.37
P02930	tolC	27	10	12	10	493	53.7	27.07
P02943	lamB	42	11	11	11	446	49.9	25.8
P31806	nnr	29	10	11	10	515	54.6	36.94
P33602	nuoG	18	11	11	11	908	100.2	28
P04079	guaA	29	10	11	10	525	58.6	33.59
P0A749	murA	26	10	11	10	419	44.8	21.12
P03023	lacI	44	10	11	10	360	38.6	23.38
P0A6H5	hslU	27	8	11	8	443	49.6	17.14
P0ACC7	glmU	24	7	10	7	456	49.2	22.7
P23003	trmA	34	8	10	8	366	41.9	21.93
P0A7V0	rpsB	51	8	10	8	241	26.7	23.82
P33029	yeiQ	25	10	10	10	488	54	27.74
P0AD05	yecA	50	6	10	6	221	25	28.85
P06961	cca	24	9	9	9	412	46.4	16.61
P0AFG3	sucA	14	9	9	9	933	105	13.86
P68767	pepA	22	9	9	9	503	54.8	20.81
P0A847	tgt	25	7	9	7	375	42.6	18.64
P36929	rsmB	23	7	8	7	429	48.3	11.69

P0A6A6	leuC	24	7	8	7	466	49.9	26.09
P0AAG8	mglA	17	7	8	7	506	56.4	15.94
P04805	gltX	20	8	8	8	471	53.8	18.4
P0A6P9	eno	19	6	8	6	432	45.6	17.21
P09831	gltB	5	7	7	7	1486	163.2	5.98
P0A8N3	lysS	15	6	7	6	505	57.6	1.9
P0A6C5	argA	21	7	7	7	443	49.2	9.38
P0A6E4	argG	16	5	7	5	447	49.9	11.2
P08660	lysC	17	6	7	6	449	48.5	16.14
P0C8J8	gatZ	12	5	6	5	420	47.1	12.5
P33599	nuoC	12	6	6	6	596	68.2	8.4
P75876	rlmI	17	5	6	5	396	44.3	16.38
P30871	ygiF	13	5	5	5	433	48.4	9.64
P09127	hemX	13	5	5	5	393	42.9	7.15
P06720	melA	15	5	5	5	451	50.6	7.48
P21179	katE	8	5	5	5	753	84.1	11.48
P55135	rlmD	16	4	5	4	433	48	13.2
P23830	pssA	18	5	5	5	451	52.8	11.93
P33940	mqo	10	5	5	5	548	60.2	10.95
P0A6U8	glgA	12	4	4	4	477	52.8	11.29
P0A9K9	slyD	17	3	4	3	196	20.8	11.09
P0ABC7	hflK	11	4	4	4	419	45.5	10.03
P00370	gdhA	16	4	4	4	447	48.6	5.7
P10902	nadB	7	4	4	4	540	60.3	6.6
P24228	dacB	10	3	4	3	477	51.8	4.67
P27434	rodZ	20	4	4	4	337	36.2	14.7
P36649	cueO	16	4	4	4	516	56.5	8.69
P06710	dnaX	7	4	4	4	643	71.1	12.31
P0DP90	ilvG	14	4	4	4	548	59.2	5.22
P0A705	infB	5	4	4	4	890	97.3	8.13
P07012	prfB	8	3	3	3	365	41.2	3.7
P0AAI3	ftsH	5	2	3	2	644	70.7	0
P15034	pepP	7	3	3	3	441	49.8	5.1
P07639	aroB	8	3	3	3	362	38.9	4.93
P33643	rluD	17	3	3	3	326	37.1	8.26
P60422	rplB	14	3	3	3	273	29.8	4.47
P23908	argE	7	2	3	2	383	42.3	4.51
P76422	thiD	16	2	3	2	266	28.6	9.15
P0AA53	qmcA	13	1	3	1	305	33.7	0
P0AFL6	ppx	3	1	2	1	513	58.1	2.34
P0AEA8	cysG	7	2	2	2	457	49.9	2.56
P13009	metH	2	2	2	2	1227	135.9	2.7
P08200	icd	6	2	2	2	416	45.7	2.04
P60906	hisS	7	2	2	2	424	47	6.57
P0AE18	map	13	2	2	2	264	29.3	4.15
P0ABJ9	cydA	4	2	2	2	522	58.2	3.8
P75863	ycbX	10	2	2	2	369	40.6	2.39
P23883	puuC	7	2	2	2	495	53.4	6.47
P0AGD7	ffh	6	2	2	2	453	49.8	1.78
P0ABH0	ftsA	7	2	2	2	420	45.3	0
P30850	rnb	4	2	2	2	644	72.4	4.02
P0A9J0	rng	7	2	2	2	489	55.3	4.17
P23524	garK	10	1	2	1	381	39.1	0
P25539	ribD	6	2	2	2	367	40.3	3.42
P09832	gltD	5	2	2	2	472	52	4.33
Q57261	truD	8	2	2	2	349	39.1	2.68
P0A9M8	pta	3	2	2	2	714	77.1	3.67
P0A6M8	fusA	2	1	1	1	704	77.5	2.48
P07001	pntA	2	1	1	1	510	54.6	1.7
P62399	rplE	6	1	1	1	179	20.3	0
P10384	fadL	3	1	1	1	446	48.5	0
P28631	holB	3	1	1	1	334	36.9	0
P64588	yqjI	4	1	1	1	207	23.4	1.89
P00934	thrC	4	1	1	1	428	47.1	2.55
P31473	ravA	3	1	1	1	498	56.4	2.18
P0A8M3	thrS	2	1	1	1	642	74	0
A0A0G3HHZ6	puuA	4	1	1	1	472	53.1	1.98

P25519	hflX	3	1	1	1	426	48.3	1.93
P0AB91	aroG	3	1	1	1	350	38	1.66
P0A8E1	ycfP	7	1	1	1	180	21.2	2.95
P04036	dapB	7	1	1	1	273	28.7	0
P03960	kdpB	2	1	1	1	682	72.2	0
Q00037	tnpA	1	1	1	1	1002	113.7	0
P00963	asnA	4	1	1	1	330	36.6	1.67
P05055	pnp	2	1	1	1	711	77.1	0
P00914	phrB	2	1	1	1	472	53.6	1.9
P07604	tyrR	2	1	1	1	513	57.6	0
P0AES6	gyrB	1	1	1	1	804	89.9	0
P0AB89	purB	2	1	1	1	456	51.5	1.69
P24174	manC	2	1	1	1	478	53	1.92
P0A7D4	purA	3	1	1	1	432	47.3	2.54
P77488	dxs	1	1	1	1	620	67.6	1.65
P30845	eptA	1	1	1	1	547	61.6	2.57
P77718	thiI	3	1	1	1	482	54.9	0
P60438	rplC	10	1	1	1	209	22.2	0
P0A786	pyrB	4	1	1	1	311	34.4	0
P06959	aceF	2	1	1	1	630	66.1	0
P28904	treC	3	1	1	1	551	63.8	2.09
P15288	pepD	3	1	1	1	485	52.9	2.16
P15639	purH	2	1	1	1	529	57.3	2.3
P13029	katG	2	1	1	1	726	80	0
P30748	moaD	26	1	1	1	81	8.8	3.95
P0A9C5	glnA	2	1	1	1	469	51.9	0
P0A6V1	glgC	4	1	1	1	431	48.7	0
P0AGI8	trkA	4	1	1	1	458	50.3	2.55
P30843	basR	5	1	1	1	222	25	1.69
P76046	ycjX	3	1	1	1	465	52.6	1.72
P75958	lolE	6	1	1	1	414	45.3	0
P13039	fes	5	1	1	1	400	45.6	0
P60293	mukF	3	1	1	1	440	50.5	0
P00393	ndh	3	1	1	1	434	47.3	0
P17802	mutY	6	1	1	1	350	39.1	2.98
P36680	zapD	4	1	1	1	247	28.3	0
P77649	selO	2	1	1	1	478	54.3	0
P42641	obgE	5	1	1	1	390	43.3	2.78
P0A6F5	groEL	2	1	1	1	548	57.3	1.81
P23865	prc	1	1	1	1	682	76.6	2.63

Table 12 - Mass spectrometry results from Section 5.2.4 – N91Bpa 65-100 kDa

UniProt	Gene	Coverage	Peptides	PSMs	Unique	AAs	MW	Score
P17169	glmS	81	47	158	47	609	66.9	579.02
P00490	malP	74	49	124	49	797	90.5	411.64
P0A6Y8	dnaK	74	50	95	50	638	69.1	327.66
P77398	arnA	73	39	91	39	660	74.2	324.3
P0AFG3	sucA	51	33	65	33	933	105	183.68
P0AC41	sdhA	75	32	62	32	588	64.4	197.31
P0AFG8	aceE	59	42	58	42	887	99.6	161.58
P33602	nuoG	56	37	56	37	908	100.2	193.52
P0A8N3	lysS	71	34	52	24	505	57.6	161.31
P05055	pnp	52	30	51	30	711	77.1	164.11

P21179	katE	51	34	50	34	753	84.1	168.71
P0CE47	tufA	84	24	50	24	394	43.3	150.93
P09831	gltB	33	37	45	37	1486	163.2	120.39
P0AG67	rpsA	55	30	45	30	557	61.1	159.12
P0A705	infB	44	29	44	29	890	97.3	135.6
P0A7I4	prfC	50	23	42	23	529	59.5	121.53
P06959	aceF	56	29	41	29	630	66.1	132.18
P30850	rnb	53	28	37	28	644	72.4	105.33
P23865	prc	50	26	34	26	682	76.6	86.05
P0A6F5	groEL	59	24	33	24	548	57.3	83.11
P0ADG7	guaB	72	21	30	21	488	52	95.29
P0A9M8	pta	46	22	28	22	714	77.1	92.17
P0AES6	gyrB	35	21	28	21	804	89.9	68.85
P00957	alaS	36	24	25	24	876	96	59.01
P33195	gcvP	33	19	25	19	957	104.3	63.99
P0A9P6	deaD	40	18	23	18	629	70.5	58.04
P27302	tktA	44	19	23	19	663	72.2	62.79
P17952	murC	40	13	23	13	491	53.6	73.46
P0ADY1	ppiD	43	21	22	21	623	68.1	59.44
P33599	nuoC	30	16	21	16	596	68.2	42.71
P35340	ahpF	46	18	21	18	521	56.1	60.92
P21599	pykA	49	17	20	17	480	51.3	61.96
P09373	pflB	30	16	19	16	760	85.3	49.35
P22188	murE	34	13	19	13	495	53.3	52.83
P0A8N5	lysU	33	17	19	7	505	57.8	38.75
P0A9P0	lpdA	39	14	18	14	474	50.7	56.09
P0A9W3	ettA	42	16	17	16	555	62.4	43.02
P00579	rpoD	26	13	17	13	613	70.2	36.98
P0A8M3	thrS	25	14	16	14	642	74	33.92
P00893	ilvI	32	12	16	12	574	62.9	31.36
P00562	metL	22	14	15	14	810	88.8	39.55
P76104	rlhA	25	13	15	13	653	72.7	41.26
P0A6P5	der	32	11	14	11	490	55	28.21
P10902	nadB	24	10	14	10	540	60.3	26.48
P0A6Z3	htpG	28	14	14	14	624	71.4	36.49
P13009	metH	12	13	13	13	1227	135.9	28.68
P0AES4	gyrA	15	12	13	12	875	96.9	29.13
P21170	speA	18	11	13	11	658	73.9	37.92
P0AC33	fumA	31	12	13	12	548	60.3	35.66
P09546	putA	11	10	12	10	1320	143.7	20.7
P0AC53	zwf	28	12	12	12	491	55.7	33.85
P77182	mnmC	28	11	12	11	668	74.4	22.83
P0A6M8	fusA	24	11	12	11	704	77.5	34.41
P10408	secA	18	11	12	11	901	102	32.01
P28903	nrdD	18	9	12	9	712	80	21.91
P0A9J8	pheA	29	10	12	10	386	43.1	24.13
P0AAI3	ftsH	22	11	12	11	644	70.7	32.24
P43672	uup	22	11	12	11	635	72	19.68
P21513	rne	16	11	11	11	1061	118.1	25.17
P0A7E5	pyrG	21	10	11	10	545	60.3	24.97
P0A9Q7	adhE	14	10	11	10	891	96.1	29.03
P15977	malQ	22	11	11	11	694	78.5	26.77
P00452	nrdA	17	10	11	10	761	85.7	22.1
P21151	fadA	26	7	10	7	387	40.9	28.04
P08192	folC	36	10	10	10	422	45.4	32.74
P32176	fdoG	14	8	9	8	1016	112.5	9.56
P76273	rsmF	27	7	9	7	479	53.2	14.17
P0A940	bamA	14	9	9	9	810	90.5	24.11
P05825	fepA	14	8	8	8	746	82.1	17.47
P08660	lysC	17	6	8	6	449	48.5	16.68
P27249	glnD	10	7	8	7	890	102.3	6.24
P27306	sthA	20	8	8	8	466	51.5	23.23
P0CB39	eptC	17	8	8	8	577	66.6	17.34
P28904	treC	16	8	8	8	551	63.8	22.02
P23538	ppsA	12	8	8	8	792	87.4	10.1
P0AD05	yecA	50	6	8	6	221	25	27.55
P0ABH9	clpA	16	7	8	7	758	84.2	9.64

P07762	glgB	12	8	8	8	728	84.3	13.85
P0ABB0	atpA	20	8	8	8	513	55.2	21.41
P37024	hrpB	13	8	8	8	809	89.1	14.77
P75864	rlmL	11	6	7	6	702	78.8	13.05
P0AGC3	slt	10	6	7	6	645	73.3	9.86
P0A6B7	iscS	19	7	7	7	404	45.1	16.56
P24182	accC	20	7	7	7	449	49.3	14.36
P06987	hisB	21	6	7	6	355	40.3	13.54
P0ABH7	gltA	22	6	7	6	427	48	13.36
P06149	dld	14	7	7	7	571	64.6	11.33
P30958	mfd	9	7	7	7	1148	129.9	16.96
P15639	purH	13	6	6	6	529	57.3	12.49
P0AFF6	nusA	18	6	6	6	495	54.8	12.46
P76403	trhP	19	5	6	5	453	51.2	18.01
P14081	selB	11	6	6	6	614	68.8	8.82
P77581	astC	20	5	6	5	406	43.6	15.31
P77488	dxs	11	6	6	6	620	67.6	7.41
P0A850	tig	17	6	6	6	432	48.2	11.34
P0A825	glyA	19	6	6	6	417	45.3	13.31
P11557	damX	9	3	5	3	428	46.1	7.19
P23367	mutL	14	5	5	5	615	67.9	4.91
P0A6F3	glpK	13	5	5	5	502	56.2	8.78
P23003	trmA	18	5	5	5	366	41.9	13.16
P04036	dapB	21	4	5	4	273	28.7	18.65
P0A8T7	rpoC	4	5	5	5	1407	155.1	6.14
P0AEI4	rimO	20	5	5	5	441	49.6	17.58
P36683	acnB	7	4	5	4	865	93.4	10.13
P39401	mdoB	4	3	5	3	763	85.4	6.6
P11880	murF	16	5	5	5	452	47.4	13.84
P33919	radD	9	4	4	4	586	66.4	8.97
P60785	lepA	8	4	4	4	599	66.5	5.06
P0AFG6	sucB	14	4	4	4	405	44	9.81
P0A9K9	slyD	36	4	4	4	196	20.8	6.77
P21889	aspS	6	4	4	4	590	65.9	7.6
P0A8V2	rpoB	3	4	4	4	1342	150.5	1.88
P11071	aceK	9	4	4	4	578	67.7	10.84
P75876	rlmI	9	3	4	3	396	44.3	2.07
P13029	katG	9	4	4	4	726	80	0
P0AG30	rho	10	4	4	4	419	47	8.69
P07604	tyrR	8	4	4	4	513	57.6	7.55
P23908	argE	10	3	4	3	383	42.3	1.61
P31449	yidL	8	1	4	1	297	33.9	0
Q47622	sapA	10	4	4	4	547	61.5	4.06
P0DP90	ilvG	12	4	4	4	548	59.2	7.64
P77748	ydiJ	5	3	4	3	1018	113.2	1.96
P0AG90	secD	8	4	4	4	615	66.6	11.01
P04079	guaA	12	3	4	3	525	58.6	11.78
P0ACE0	hybC	11	4	4	4	567	62.5	8.68
P25552	gppA	9	4	4	4	494	54.8	10.79
P0A6Z1	hscA	12	4	4	4	616	65.6	6.84
P22525	ycbB	9	3	3	3	615	67.8	8.08
P33136	mdoG	7	3	3	3	511	57.9	6.39
P37773	mpl	12	3	3	3	457	49.8	4.76
P0A6G7	clpP	11	1	3	1	207	23.2	0
P45464	lpoA	5	3	3	3	678	72.8	3.9
P0AAB4	ubiD	8	3	3	3	497	55.6	6.26
P07639	aroB	9	2	3	2	362	38.9	1.99
P17444	betA	7	3	3	3	556	61.8	6.18
P77567	nhoA	18	3	3	3	281	32.3	8.75
P15877	gcd	4	1	3	1	796	86.7	0
P00363	frdA	7	3	3	3	602	65.9	10.28
P17846	cysI	8	3	3	3	570	64	4.64
P76422	thiD	16	2	3	2	266	28.6	12.1
P0A9C5	glnA	9	2	2	2	469	51.9	0
P0DTT0	bipA	4	2	2	2	607	67.3	5.01
P05791	ilvD	4	2	2	2	616	65.5	4.67
P03018	uvrD	3	2	2	2	720	81.9	0

P0AD61	pykF	4	2	2	2	470	50.7	0
P0ACD4	iscU	16	2	2	2	128	13.8	2.55
B8LFD5	lacI	6	2	2	2	363	38.9	4.9
P0A6U3	mnmG	4	2	2	2	629	69.5	4.28
P00722	lacZ	3	2	2	2	1024	116.4	2.32
P00968	carB	3	2	2	2	1073	117.8	3.7
P69451	fadD	5	2	2	2	561	62.3	2.38
P60716	lipA	10	2	2	2	321	36	5.98
P33916	yejF	2	1	2	1	529	58.7	0
P0A7V0	rpsB	9	2	2	2	241	26.7	5.12
P75867	ycbZ	7	2	2	2	586	65.8	1.83
P00582	polA	5	2	2	2	928	103.1	2.66
P27298	prlC	3	2	2	2	680	77.1	1.76
P00864	ppc	3	2	2	2	883	99	1.97
P0AG20	relA	3	1	2	1	744	83.8	3.57
P27550	acs	4	2	2	2	652	72	4.94
P09323	nagE	4	2	2	2	648	68.3	0
P76578	yfhM	2	2	2	2	1653	181.5	0
P37127	aegA	5	2	2	2	659	71.8	1.78
P76562	tmcA	2	2	2	2	671	74.8	2.04
P77718	thiI	5	2	2	2	482	54.9	3.21
P23845	cysN	6	2	2	2	475	52.5	4.46
P25714	yidC	7	2	2	2	548	61.5	5.02
P0AEI1	miaB	7	2	2	2	474	53.6	4.41
P00861	lysA	7	2	2	2	420	46.1	4.76
P25539	ribD	3	1	1	1	367	40.3	0
P25718	malS	3	1	1	1	676	75.7	0
P67087	rsmI	6	1	1	1	286	31.3	2.5
P0A8E1	ycfP	7	1	1	1	180	21.2	2.45
P0AB91	aroG	3	1	1	1	350	38	0
P0AD14	btsS	4	1	1	1	561	62.1	0
P00961	glyS	2	1	1	1	689	76.8	0
P0AFV4	mepS	5	1	1	1	188	21	0
P00962	glnS	2	1	1	1	554	63.4	0
P77334	pdeR	3	1	1	1	661	74.6	0
P0ADR8	ppnN	2	1	1	1	454	50.9	1.67
P60422	rplB	6	1	1	1	273	29.8	0
P22523	mukB	0	1	1	1	1486	170.1	1.77
P63389	yheS	1	1	1	1	637	71.8	0
P08839	ptsI	2	1	1	1	575	63.5	0
P16659	proS	2	1	1	1	572	63.7	0
P0ADY3	rplN	7	1	1	1	123	13.5	0
P63284	clpB	2	1	1	1	857	95.5	3.26
P31554	lptD	2	1	1	1	784	89.6	1.77
P37051	purU	9	1	1	1	280	31.9	0
P20099	bisC	2	1	1	1	777	85.8	0
P77732	rhmR	4	1	1	1	260	28.9	0
P0A7Z4	rpoA	4	1	1	1	329	36.5	0
P30748	moaD	26	1	1	1	81	8.8	4.54
P0AE18	map	3	1	1	1	264	29.3	1.63
P05041	pabB	2	1	1	1	453	50.9	0
P0ABQ0	coaBC	4	1	1	1	406	43.4	0
P0A749	murA	3	1	1	1	419	44.8	0
P64588	yqjI	4	1	1	1	207	23.4	2.4
P0ABI8	cyoB	4	1	1	1	663	74.3	0
A0A1V1IFM5	gsk-4	5	1	1	1	434	48.4	0
P06710	dnaX	2	1	1	1	643	71.1	0
P60752	msbA	3	1	1	1	582	64.4	0
P0A853	tnaA	2	1	1	1	471	52.7	0
P38038	cysJ	4	1	1	1	599	66.2	0
P60566	fixA	12	1	1	1	256	27.1	0
Q46820	uacF	3	1	1	1	639	69	0
P46923	torZ	1	1	1	1	809	88.9	2.04
P0DM85	crfC	2	1	1	1	742	84.3	0
P13036	fecA	1	1	1	1	774	85.3	0
P06612	topA	2	1	1	1	865	97.3	0
P0AAN3	hypB	4	1	1	1	290	31.5	1.95

P0ABB8	mgtA	1	1	1	1	898	99.4	0
P33937	napA	2	1	1	1	828	93	2.28
P23524	garK	10	1	1	1	381	39.1	3.47

Table 13 – Mass spectrometry results of proteins in N91^{Bpa} 45 kDa band, from Section 5.2.5

Accession	Protein Name	Coverage [%]	Peptides	PSMs	Unique Peptides	AAs	MW [kDa]	Score Sequest
A0A140N953	SecH	39	6	15	6	221	25	48.77
A0A140N6W0	Elongation factor Tu	5	2	2	2	394	43.3	5.52
A0A140N9D5	Cysteine desulfurase	6	2	2	2	404	45.1	4.37
A0A140N784	3-dehydroquinate synthase	3	1	1	1	362	38.8	2.27
A0A140NF01	Transcription termination factor Rho	2	1	1	1	419	47	1.94

Table 14 - Mass spectrometry results of proteins in N91^{Bpa} 100 kDa band, from Section 5.2.5

Accession	Protein Name	Coverage [%]	Peptides	PSMs	Unique Peptides	AAs	MW [kDa]	Score Sequest
A0A140N953	SecH	27	4	18	4	221	25	56.69
A0A140NF74	Bifunctional aspartokinase/ homoserine dehydrogenase	3	2	2	2	810	88.9	4.24
A0A140N783	Glyceraldehyde-3-phosphate dehydrogenase	4	1	1	1	331	35.5	2.35

Table 15 - Mass spectrometry results of proteins in N91^{Bpa} 150 kDa band, from Section 5.2.5

Accession	Protein Name	Coverage [%]	Peptides	PSMs	Unique Peptides	AAs	MW [kDa]	Score Sequest
A0A140N953	SecH	27	4	13	4	221	25	38.48
A0A140NEC0	Aspartokinase	3	1	1	1	449	48.5	2.26

Table 16 - Mass spectrometry results of proteins in N91^{Bpa} 200 kDa band, from Section 5.2.5

Accession	Protein Name	Coverage [%]	Peptides	PSMs	Unique Peptides	AAs	MW [kDa]	Score Sequest
A0A140N953	SecH	27	4	6	4	221	25	18.17
A0A140N6W0	Elongation Factor Tu	7	2	2	2	394	43.3	4.6

Table 17 – Mass spectrometry results from Section 5.2.6– WT SecH

UniProt Accession ID	Gene Name	Coverage [%]	Peptides	PSMs	Unique Peptides	AAs	MW [kDa]	Score Sequest
P0AD05	yecA	65	8	130	8	221	25	472.55
P02931	ompF	93	22	77	22	362	39.3	274.53
P0CE47	tufA	76	21	78	21	394	43.3	252.05
P03023	lacI	55	14	46	14	360	38.6	166.31
P10408	secA	59	36	48	36	901	102	165.55
P0A6Y8	dnaK	58	29	42	29	638	69.1	160.77
P0AG67	rpsA	42	19	35	19	557	61.1	124.29
P0A850	tig	47	17	37	17	432	48.2	124.16
P0A705	infB	44	26	35	26	890	97.3	114.93

P0A9B2	gapA	57	11	28	11	331	35.5	103.65
P0A6Z3	htpG	48	24	30	24	624	71.4	92.6
P08660	lysC	25	8	28	8	449	48.5	90.68
P0A910	ompA	61	14	24	14	346	37.2	90.53
P0A6F5	groEL	41	16	24	16	548	57.3	77.35
P0A6M8	fusA	38	18	22	18	704	77.5	75.54
P36683	acnB	32	19	23	19	865	93.4	69.86
P62399	rplE	61	11	19	11	179	20.3	60.64
P0ABK5	cysK	59	13	16	13	323	34.5	57.62
P77398	arnA	30	16	19	16	660	74.2	55.97
P09373	pflB	27	12	16	12	760	85.3	52.49
P35340	ahpF	37	13	16	13	521	56.1	52.34
P04036	dapB	25	5	13	5	273	28.7	51.86
P0AE08	ahpC	39	5	16	5	187	20.7	51.57
P0A6H1	clpX	50	14	16	14	424	46.3	50.11
P0ABB4	atpD	40	12	15	12	460	50.3	49.81
P0A7Z4	rpoA	53	12	16	12	329	36.5	49
P12996	bioB	56	11	14	11	346	38.6	46.67
P0A7V3	rpsC	46	8	12	8	233	26	46.53
P00562	metL	23	14	15	14	810	88.8	45.1
P0A6P1	tsf	43	10	14	10	283	30.4	44.88
P60785	lepA	26	11	13	11	599	66.5	44.82
P76373	ugd	39	12	14	12	388	43.6	42.71
P0ACP7	purR	44	11	14	11	341	38.2	42.53
P23843	oppA	30	9	12	9	543	60.9	41.9
P05055	pnp	27	12	13	12	711	77.1	40.82
P0A6P9	eno	37	11	13	11	432	45.6	40.25
P0DTT0	bipA	27	11	12	11	607	67.3	38.49
P0A8N3	lysS	34	12	13	9	505	57.6	37.36
P45577	proQ	35	6	11	6	232	25.9	34.92
P08200	icd	29	9	12	9	416	45.7	34.88
P25665	metE	18	12	12	12	753	84.6	34.45
P0AFF6	nusA	33	9	10	9	495	54.8	34.17
P0A6H5	hslU	30	10	10	10	443	49.6	33.45
P0A6F3	glpK	23	10	11	10	502	56.2	33.06
P0A799	pgk	33	7	9	7	387	41.1	32.92
P08839	ptsI	25	9	10	9	575	63.5	32.86
P28635	metQ	46	7	9	7	271	29.4	32.84
P0A9P0	lpdA	29	9	10	9	474	50.7	32.77
P0ABD5	accA	31	7	9	7	319	35.2	32.52
P0AG55	rplF	67	9	10	9	177	18.9	32.38
P00561	thrA	20	9	10	9	820	89.1	31.59
P33602	nuoG	15	9	11	9	908	100.2	31.52
P0A7S9	rpsM	60	7	9	7	118	13.1	31.5
P0A836	sucC	32	10	11	10	388	41.4	31.42
P62620	ispG	32	9	10	9	372	40.7	31.27
P0A7V8	rpsD	34	7	10	7	206	23.5	31.2
P0A6B7	iscS	33	10	10	10	404	45.1	30.97
P07639	aroB	21	4	8	4	362	38.9	30.03
P0ACF8	hns	49	6	9	6	137	15.5	29.8
P0ABB0	atpA	25	9	9	9	513	55.2	29.6
P00350	gnd	30	9	10	9	468	51.4	29.54
P63284	clpB	14	8	9	8	857	95.5	28.05
P0A6E4	argG	38	10	10	10	447	49.9	27.97
P0A8M0	asnS	26	9	9	9	466	52.5	27.5
P0A9D8	dapD	29	7	8	7	274	29.9	27.31
P0AGD3	sodB	52	6	9	6	193	21.3	27.1
P0A9P6	deaD	21	8	9	8	629	70.5	26.91
P0AC41	sdhA	19	8	8	8	588	64.4	26.68
P00579	rpoD	19	9	9	9	613	70.2	26.49
P0ACF0	hupA	61	5	8	5	90	9.5	26.43
P0A9Q1	arcA	32	5	7	5	238	27.3	26.05
P60422	rplB	31	6	9	6	273	29.8	25.94
P00957	alaS	12	8	9	8	876	96	25.13
P0AAI3	ftsH	16	7	8	7	644	70.7	25.11
P0AFG6	sucB	25	7	7	7	405	44	24.8
P02359	rpsG	42	5	6	5	179	20	24.45

P0A7D4	purA	23	7	8	7	432	47.3	23.96
P02925	rbsB	26	6	7	6	296	30.9	23.76
P13009	metH	8	8	8	8	1227	135.9	23.75
P0C8J8	gatZ	30	7	8	7	420	47.1	23.74
P00509	aspC	25	7	7	7	396	43.5	23.69
P30843	basR	32	5	8	5	222	25	23.67
P0AEZ3	minD	38	8	8	8	270	29.6	23.67
P0A707	infC	37	4	6	4	180	20.6	23.37
P0A7L0	rplA	37	8	8	8	234	24.7	23.12
P60438	rplC	23	3	6	3	209	22.2	22.8
P23538	ppsA	12	7	7	7	792	87.4	22.77
P0A7G6	recA	29	7	7	7	353	38	22.62
P76422	thiD	20	3	6	3	266	28.6	22.46
P61889	mdh	31	7	8	7	312	32.3	22.32
P23893	hemL	31	8	8	8	426	45.3	22.15
P0AG30	rho	20	7	8	7	419	47	21.84
P0A7V0	rpsB	46	6	7	6	241	26.7	21.8
P30748	moaD	26	1	5	1	81	8.8	21.7
P0A917	ompX	44	6	6	6	171	18.6	21.52
P0ADY1	ppiD	16	7	7	7	623	68.1	21.29
P0A7W1	rpsE	47	5	6	5	167	17.6	21.2
P33599	nuoC	17	8	8	8	596	68.2	21.19
P0A9M8	pta	12	6	7	6	714	77.1	21.11
P0AAI5	fabF	23	5	5	5	413	43	20.91
P0A993	fbp	27	6	7	6	332	36.8	20.7
P0A940	bamA	14	7	7	7	810	90.5	20.6
P61175	rplV	48	5	6	5	110	12.2	20.51
P0ABC7	hflK	21	7	7	7	419	45.5	20.34
P04983	rbsA	21	7	7	7	501	55	20.26
P0AGE9	sucD	27	5	6	5	289	29.8	20.09
P0AE88	cpxR	19	3	6	3	232	26.3	19.93
P0A9Q5	accD	21	4	5	4	304	33.3	19.15
P23909	mutS	11	7	7	7	853	95.2	18.98
P60757	hisG	30	5	6	5	299	33.3	18.91
P62707	gpmA	30	6	7	6	250	28.5	18.83
P0A749	murA	21	6	7	6	419	44.8	18.82
P0AB91	aroG	23	6	6	6	350	38	18.5
P76658	hldE	20	7	7	7	477	51	17.7
P0A870	talB	23	5	6	5	317	35.2	17.61
P0ABU2	ychF	21	6	6	6	363	39.6	17.54
P0A7K6	rplS	43	4	6	4	115	13.1	17.48
P0A8L1	serS	18	6	6	6	430	48.4	17.31
P0A817	metK	17	4	5	4	384	41.9	17.02
P0A9W3	ettA	15	6	6	6	555	62.4	16.84
P30850	rnb	10	5	6	5	644	72.4	16.78
P31979	nuoF	14	4	5	4	445	49.3	16.66
P0A8V2	rpoB	6	6	6	6	1342	150.5	16.41
P0A8M3	thrS	10	6	6	6	642	74	16.41
P0A9X9	cspA	53	3	5	2	70	7.4	16.21
P23836	phoP	29	5	5	5	223	25.5	16.18
P0A9X4	mreB	24	6	6	6	347	36.9	16.13
P0A9V1	lptB	28	4	5	4	241	26.8	15.94
P06959	aceF	11	5	5	5	630	66.1	15.82
P02413	rplO	42	5	5	5	144	15	15.55
P05791	ilvD	11	5	5	5	616	65.5	15.47
P0AEX9	malE	20	6	6	6	396	43.4	15.1
P0AGJ9	tyrS	12	4	5	4	424	47.5	14.95
P0AA10	rplM	46	5	5	5	142	16	14.87
P04968	ilvA	14	5	5	5	514	56.2	14.58
P0A8F0	upp	30	4	5	4	208	22.5	14.51
P0AG44	rplQ	27	4	5	4	127	14.4	14.31
P69783	crr	35	3	4	3	169	18.2	14.24
P10121	ftsY	16	5	5	5	497	54.5	14.23
P0AFG8	aceE	8	5	5	5	887	99.6	14.19
P0CB39	eptC	11	4	5	4	577	66.6	14.1
P00934	thrC	19	5	5	5	428	47.1	13.84
P0A912	pal	24	3	5	3	173	18.8	13.57

P0A7R1	rplI	34	5	5	5	149	15.8	13.53
P0A7J7	rplK	33	4	5	4	142	14.9	13.5
P0AG63	rpsQ	32	2	4	2	84	9.7	13.49
P69441	adk	21	4	5	4	214	23.6	13.41
P0A862	tpx	38	4	4	4	168	17.8	13.34
P0AF08	mrp	15	3	5	3	369	39.9	13.3
P0A7J3	rplJ	32	4	4	4	165	17.7	13.27
P21599	pykA	12	5	5	5	480	51.3	13
P0A6R0	fabH	19	4	4	4	317	33.5	12.78
P0ABZ6	surA	12	4	4	4	428	47.3	12.68
P0AFG0	nusG	35	4	4	4	181	20.5	12.54
P24182	accC	10	5	5	5	449	49.3	12.52
P00961	glyS	9	4	4	4	689	76.8	12.46
P16659	proS	10	4	4	4	572	63.7	12.27
P0ABH9	clpA	10	5	5	5	758	84.2	12.22
P0A9Q9	asd	21	4	4	4	367	40	12.14
P0A6Z1	hscA	10	4	4	4	616	65.6	12.11
P60723	rplD	26	4	4	4	201	22.1	11.81
P0AE06	acrA	18	4	4	4	397	42.2	11.78
P0C0S1	mscS	22	4	4	4	286	30.9	11.69
P45523	fkpA	24	4	4	4	270	28.9	11.55
P0AES6	gyrB	6	4	4	4	804	89.9	11.54
P0AEK2	fabG	24	3	3	3	244	25.5	11.35
P0A7M2	rpmB	23	2	5	2	78	9	11.33
P0A9A6	ftsZ	17	4	4	4	383	40.3	11.26
P0A825	glyA	12	4	4	4	417	45.3	11.04
P00888	aroF	16	3	3	3	356	38.8	10.83
P68919	rplY	43	4	4	4	94	10.7	10.73
P02930	tolC	9	3	3	3	493	53.7	10.61
P08390	usg	23	3	3	3	337	36.3	10.45
P0A7T3	rpsP	37	2	3	2	82	9.2	10.25
P00370	gdhA	12	3	3	3	447	48.6	10.21
P60624	rplX	37	3	3	3	104	11.3	9.87
P00968	carB	5	4	4	4	1073	117.8	9.85
P07014	sdhB	16	3	3	3	238	26.8	9.81
P62623	ispH	16	4	4	4	316	34.8	9.7
P0A8N5	lysU	8	4	4	1	505	57.8	9.7
P0A8T7	rpoC	4	4	4	4	1407	155.1	9.68
P0A7L3	rplT	23	3	4	3	118	13.5	9.59
P27306	sthA	10	2	2	2	466	51.5	9.42
P0A955	eda	34	3	3	3	213	22.3	9.23
P0A953	fabB	12	3	3	3	406	42.6	9.21
P0AAX8	ybiS	21	3	3	3	306	33.3	9.13
P0A9U3	ybiT	12	3	3	3	530	59.8	9.11
P27302	tktA	7	3	3	3	663	72.2	9.1
P13029	katG	7	4	4	4	726	80	9.09
P21889	aspS	7	3	3	3	590	65.9	9
P0A7B5	proB	13	4	4	4	367	39	8.97
P0A7E5	pyrG	7	3	3	3	545	60.3	8.95
P09832	gltD	12	3	3	3	472	52	8.93
P77690	arnB	12	3	3	3	385	42.2	8.83
P0AB80	ilvE	13	3	3	3	309	34.1	8.81
P06612	topA	5	4	4	4	865	97.3	8.77
P0A7M6	rpmC	46	2	3	2	63	7.3	8.7
P0AA16	ompR	21	3	3	3	239	27.3	8.67
P0A7X3	rpsI	25	3	3	3	130	14.8	8.59
P0ADR8	ppnN	8	3	3	3	454	50.9	8.52
P0A7G2	rbfA	25	3	3	3	133	15.1	8.46
P0AEK4	fabI	15	3	3	3	262	27.8	8.44
P0A978	cspG	31	2	3	1	70	7.8	8.32
P0A6F9	groES	42	3	3	3	97	10.4	8.31
P0A9S3	gatD	9	3	3	3	346	37.4	8.24
P0A7R5	rpsJ	34	3	3	3	103	11.7	8.23
P77395	cnoX	12	3	3	3	284	31.8	8.16
P0A7W7	rpsH	33	4	4	4	130	14.1	8.16
P27248	gcvT	7	2	3	2	364	40.1	8.15
P76472	arnD	11	2	3	2	296	33.1	8.14

P0ABH7	gltA	7	2	2	2	427	48	8.1
P0AAA1	yagU	13	2	3	2	204	23	8.1
P0AEQ3	glnH	13	2	3	2	248	27.2	8.03
P00864	ppc	6	3	3	3	883	99	8
P09546	putA	4	3	3	3	1320	143.7	8
P37440	ucpA	14	3	3	3	263	27.8	7.89
P75990	bluF	8	3	3	3	403	45.3	7.86
P0AGD7	ffh	9	3	3	3	453	49.8	7.8
P0C0V0	degP	7	2	2	2	474	49.3	7.79
P00959	metG	6	3	3	3	677	76.2	7.76
P60716	lipA	12	2	2	2	321	36	7.68
P0AAB6	galF	14	3	3	3	297	32.8	7.39
P0A7U7	rpsT	36	3	3	3	87	9.7	7.16
P06992	rsmA	12	2	2	2	273	30.4	7.09
P14175	proV	8	2	3	2	400	44.1	7.08
P0A7M9	rpmE	41	2	2	2	70	7.9	7.05
P0AEP3	galU	11	3	3	3	302	32.9	7.04
P0ADY3	rplN	30	2	2	2	123	13.5	6.92
P0A7S3	rpsL	18	3	3	3	124	13.7	6.84
P0ABC3	hflC	8	3	3	3	334	37.6	6.78
P37902	gltI	9	2	2	2	302	33.4	6.7
P23830	pssA	7	2	2	2	451	52.8	6.67
P0AFG3	sucA	5	3	3	3	933	105	6.62
P0AG90	secD	5	2	2	2	615	66.6	6.58
P0ACF4	hupB	16	1	2	1	90	9.2	6.55
P0AGG8	tldD	7	2	2	2	481	51.3	6.4
P0A6S0	flgH	12	2	2	2	232	24.6	6.34
P06149	dld	7	2	2	2	571	64.6	6.33
P0ADG4	suhB	11	2	2	2	267	29.2	6.27
P25553	aldA	7	3	3	3	479	52.2	6.26
P0A805	frr	16	2	2	2	185	20.6	6.22
P0AEI1	miaB	6	2	2	2	474	53.6	6.22
P33218	yebE	17	2	2	2	219	23.7	6.15
P0AFU8	ribC	11	2	2	2	213	23.4	6.13
P0ADY7	rplP	22	2	2	2	136	15.3	6.07
P69776	lpp	33	2	2	2	78	8.3	6.03
P0A6Y5	hslO	10	2	2	2	292	32.5	6.02
P21170	speA	4	2	2	2	658	73.9	5.91
P07012	prfB	8	2	2	2	365	41.2	5.88
P77774	bamB	6	2	2	2	392	41.9	5.87
P06616	era	8	2	2	2	301	33.8	5.83
P0A959	alaA	6	1	2	1	405	45.5	5.82
P23845	cysN	7	2	2	2	475	52.5	5.82
P25437	frmA	8	2	2	2	369	39.3	5.77
P0A855	tolB	10	2	2	2	430	45.9	5.68
P60390	rsmH	11	2	2	2	313	34.9	5.63
P0A6F1	carA	7	2	2	2	382	41.4	5.6
P0AC69	grxD	28	2	2	2	115	12.9	5.59
P0AEI4	rimO	6	2	2	2	441	49.6	5.59
P22259	pckA	6	2	2	2	540	59.6	5.58
P0ABJ1	cyoA	13	2	2	2	315	34.9	5.56
P62768	yaeH	17	2	2	2	128	15.1	5.55
P0AB71	fbaA	8	2	2	2	359	39.1	5.54
P09127	hemX	7	2	2	2	393	42.9	5.51
P77737	oppF	13	2	2	2	334	37.2	5.46
P32176	fdoG	3	2	2	2	1016	112.5	5.4
P0ACE0	hybC	8	2	2	2	567	62.5	5.39
P0A7T7	rpsR	29	2	2	2	75	9	5.39
P0AB24	efeO	9	2	2	2	375	41.1	5.38
P60906	hisS	7	2	2	2	424	47	5.36
P0A7K2	rplL	17	2	2	2	121	12.3	5.35
P0ACA3	sspA	12	2	2	2	212	24.3	5.33
P0ACP5	gntR	6	1	2	1	331	36.4	5.19
P00909	trpC	5	2	2	2	453	49.5	5.18
P64588	yqjI	10	2	2	2	207	23.4	5.18
P25519	hflX	5	2	2	2	426	48.3	5.16
P39342	yjgR	6	2	2	2	500	54.3	5.11

P0A9K9	slyD	10	2	2	2	196	20.8	5.01
P0A6P5	der	6	2	2	2	490	55	5.01
P60595	hisH	11	2	2	2	196	21.6	4.95
P0AFC7	nuoB	10	2	2	2	220	25	4.91
P39835	gntT	5	1	2	1	438	45.9	4.86
P0C018	rplR	15	2	2	2	117	12.8	4.81
P0A9Q7	adhE	3	2	2	2	891	96.1	4.78
P30011	nadC	7	2	2	2	297	32.7	4.73
P0AAC8	iscA	24	2	2	2	107	11.5	4.7
P0A9J6	rbsK	7	1	2	1	309	32.3	4.63
P77804	ydgA	4	2	2	2	502	54.7	4.63
P07604	tyrR	4	2	2	2	513	57.6	4.62
P0ACC3	erpA	18	2	2	2	114	12.1	4.55
P0AES4	gyrA	3	2	2	2	875	96.9	4.53
P16456	selD	5	2	2	2	347	36.7	4.49
P0DP89	ilvG	6	1	1	1	327	34.5	4.48
P0A734	minE	25	2	2	2	88	10.2	4.46
P0A7N4	rpmF	26	1	1	1	57	6.4	4.43
P0A9P4	trxB	8	2	2	2	321	34.6	4.35
P0A6Q3	fabA	11	2	2	2	172	19	4.24
P39831	ydfG	7	1	1	1	248	27.2	4.15
P37665	yiaD	8	1	1	1	219	22.2	4.09
P33916	yejF	3	1	1	1	529	58.7	3.99
P0ADZ4	rpsO	34	1	1	1	89	10.3	3.97
P30744	sdaB	4	2	2	2	455	48.7	3.94
P10371	hisA	7	1	1	1	245	26	3.81
P0A9A9	fur	9	1	1	1	148	16.8	3.7
P31224	acrB	1	1	1	1	1049	113.5	3.69
P00803	lepB	4	1	1	1	324	35.9	3.68
P76034	yciT	7	1	1	1	249	27.6	3.63
P61714	ribE	12	1	1	1	156	16.1	3.61
P23847	dppA	2	1	1	1	535	60.3	3.6
P0A8M6	yeeX	15	1	1	1	109	12.8	3.59
P0A937	bamE	18	1	1	1	113	12.3	3.59
P25714	yidC	3	1	1	1	548	61.5	3.54
P0A9T0	serA	6	1	1	1	410	44.1	3.51
P61517	can	6	1	1	1	220	25.1	3.48
P0AA25	trxA	11	1	1	1	109	11.8	3.47
P56262	ysgA	7	1	1	1	271	29.4	3.43
P0AEQ1	glcG	16	1	1	1	134	13.7	3.41
P0A6A3	ackA	6	1	1	1	400	43.3	3.41
P17169	glmS	3	1	1	1	609	66.9	3.39
P37689	gpmI	3	1	1	1	514	56.2	3.36
P33363	bglX	2	1	1	1	765	83.4	3.36
P08142	ilvB	4	1	1	1	562	60.4	3.34
P76177	ydgH	5	1	1	1	314	33.9	3.33
P37051	purU	9	1	1	1	280	31.9	3.32
P36672	treB	5	1	1	1	473	51	3.27
P14081	selB	3	1	1	1	614	68.8	3.24
P21888	cysS	2	1	1	1	461	52.2	3.2
P0A7Z0	rpiA	7	1	1	1	219	22.8	3.18
P0A877	trpA	7	1	1	1	268	28.7	3.16
P0A8F8	uvrB	3	1	1	1	673	76.2	3.15
P0A887	ubiE	5	1	1	1	251	28.1	3.14
P77529	tcyP	3	1	1	1	463	48.6	3.14
P64624	yheO	5	1	1	1	240	26.8	3.13
P08395	sppA	2	1	1	1	618	67.2	3.13
P0AFR4	yciO	5	1	1	1	206	23.2	3.12
P09053	avtA	3	1	1	1	417	46.7	3.08
P37188	gatB	20	1	1	1	94	10.2	3.04
P0A6G7	clpP	10	1	1	1	207	23.2	3.03
P0A6D7	aroK	8	1	1	1	173	19.5	3.03
P0A7N9	rpmG	27	1	1	1	55	6.4	3.03
P09372	grpE	7	1	1	1	197	21.8	3.03
P17846	cysI	3	1	1	1	570	64	3.02
P0AC33	fumA	3	1	1	1	548	60.3	3.02
P0A8E7	yajQ	10	1	1	1	163	18.3	3.01

P0A9Y6	cspC	22	1	1	1	69	7.4	2.99
P0ADC1	lptE	9	1	1	1	193	21.3	2.99
P05793	ilvC	3	1	1	1	491	54	2.97
P0AG93	secF	4	1	1	1	323	35.4	2.96
P0C0L7	proP	3	1	1	1	500	54.8	2.96
P02943	lamB	3	1	1	1	446	49.9	2.95
P0AFM6	pspA	7	1	1	1	222	25.5	2.94
P0AGK8	iscR	9	1	1	1	162	17.3	2.94
P0A9L3	fklB	6	1	1	1	206	22.2	2.92
P0A6A8	acpP	21	1	1	1	78	8.6	2.91
P0A9D4	cysE	8	1	1	1	273	29.3	2.9
P38489	nfsB	5	1	1	1	217	23.9	2.89
P45565	ais	11	1	1	1	200	22.2	2.87
P77211	cusC	2	1	1	1	457	50.2	2.86
P69222	infA	17	1	1	1	72	8.2	2.84
P0A9L5	ppiC	11	1	1	1	93	10.2	2.84
P75937	flgE	4	1	1	1	402	42	2.83
P0AF93	ridA	10	1	1	1	128	13.6	2.83
P0AAC0	uspE	6	1	1	1	316	35.7	2.83
P0AAE0	cycA	3	1	1	1	470	51.6	2.83
P0AEB2	dacA	4	1	1	1	403	44.4	2.82
P16700	cysP	3	1	1	1	338	37.6	2.8
P27298	prlC	2	1	1	1	680	77.1	2.79
P69054	sdhC	9	1	1	1	129	14.3	2.77
P0A6U5	rsmG	5	1	1	1	207	23.4	2.76
P00954	trpS	7	1	1	1	334	37.4	2.76
P36879	yadG	4	1	1	1	308	34.6	2.75
P60340	truB	4	1	1	1	314	35.1	2.73
P27833	wecE	4	1	1	1	376	41.9	2.71
P22333	add	9	1	1	1	333	36.4	2.71
P0ABN1	dgkA	9	1	1	1	122	13.2	2.71
P0A8I3	yaaA	7	1	1	1	258	29.6	2.7
P0ABJ9	cydA	3	1	1	1	522	58.2	2.69
P0ADK0	yiaF	6	1	1	1	236	25.6	2.67
P07862	ddlB	5	1	1	1	306	32.8	2.66
P0A9G6	aceA	3	1	1	1	434	47.5	2.66
P37744	rfbA	4	1	1	1	293	32.7	2.63
P68679	rpsU	14	1	1	1	71	8.5	2.63
P0AF28	narL	5	1	1	1	216	23.9	2.63
P0A9K3	ybeZ	4	1	1	1	346	39	2.63
P75913	ghrA	4	1	1	1	312	35.3	2.63
P0A6T5	folE	5	1	1	1	222	24.8	2.62
P0A908	mipA	6	1	1	1	248	27.8	2.62
P0ABA0	atpF	8	1	1	1	156	17.3	2.62
P50465	nei	5	1	1	1	263	29.8	2.6
P23721	serC	4	1	1	1	362	39.8	2.59
P06983	hemC	4	1	1	1	313	33.8	2.57
P32131	hemN	3	1	1	1	457	52.7	2.56
P0A8J8	rhlB	3	1	1	1	421	47.1	2.56
P07001	pntA	4	1	1	1	510	54.6	2.54
P69503	apt	11	1	1	1	183	19.8	2.52
P28904	treC	3	1	1	1	551	63.8	2.52
P69828	gatA	13	1	1	1	150	16.9	2.51
P0ABD8	accB	13	1	1	1	156	16.7	2.5
P36979	rlmN	2	1	1	1	384	43.1	2.5
P0AAI9	fabD	6	1	1	1	309	32.4	2.49
P31120	glmM	3	1	1	1	445	47.5	2.49
P0AEU0	hisJ	7	1	1	1	260	28.5	2.48
P0A6I0	cmk	12	1	1	1	227	24.7	2.47
P77488	dxs	1	1	1	1	620	67.6	2.44
P0A6J8	ddlA	4	1	1	1	364	39.3	2.44
P0AC53	zwf	2	1	1	1	491	55.7	2.43
P00894	ilvH	7	1	1	1	163	18	2.43
P42641	obgE	6	1	1	1	390	43.3	2.42
P00887	aroH	4	1	1	1	348	38.7	2.42
P36938	pgm	3	1	1	1	546	58.3	2.42
P0AG48	rplU	12	1	1	1	103	11.6	2.41

P0ACC1	prmC	5	1	1	1	277	31	2.41
P0AF24	nagD	4	1	1	1	250	27.1	2.4
P37095	pepB	3	1	1	1	427	46.2	2.39
P15042	ligA	2	1	1	1	671	73.6	2.38
P28248	dcd	6	1	1	1	193	21.2	2.38
P0A9W9	yrdA	11	1	1	1	184	20.2	2.38
P28903	nrdD	2	1	1	1	712	80	2.38
P69831	gatC	2	1	1	1	451	48.3	2.34
P0AGE0	ssb	6	1	1	1	178	19	2.33
P0A6X7	ihfA	10	1	1	1	99	11.3	2.32
P0ADZ0	rplW	12	1	1	1	100	11.2	2.3
P08622	dnaJ	3	1	1	1	376	41.1	2.3
P30845	eptA	1	1	1	1	547	61.6	2.28
P03024	galR	6	1	1	1	343	37.1	2.28
P76268	kdgR	6	1	1	1	263	30	2.28
P52108	rstA	4	1	1	1	239	26.7	2.27
P30750	metN	4	1	1	1	343	37.8	2.27
P16095	sdaA	2	1	1	1	454	48.9	2.24
P33232	lldD	3	1	1	1	396	42.7	2.24
P69228	baeR	7	1	1	1	240	27.6	2.23
P17952	murC	2	1	1	1	491	53.6	2.23
P0ADG7	guaB	4	1	1	1	488	52	2.23
P26646	acuI	5	1	1	1	324	34.7	2.23
P00550	mtlA	2	1	1	1	637	67.9	2.22
P0A8A0	yebC	3	1	1	1	246	26.4	2.21
P0ABP8	deoD	5	1	1	1	239	25.9	2.2
P0A800	rpoZ	10	1	1	1	91	10.2	2.2
P0ABI8	cyoB	3	1	1	1	663	74.3	2.2
P0AFC3	nuoA	7	1	1	1	147	16.4	2.15
P68699	atpE	11	1	1	1	79	8.3	2.13
P0ACY1	ydjA	6	1	1	1	183	20	2.11
P0AGB6	rpoE	4	1	1	1	191	21.7	2.09
P0A7Q1	rpmI	20	1	1	1	65	7.3	2.07
P77757	arnC	4	1	1	1	322	36.3	2.06
P16703	cysM	4	1	1	1	303	32.6	2.06
P24232	hmp	3	1	1	1	396	43.8	2.05
P30178	hcxB	3	1	1	1	361	38.9	2.04
P0A853	tnaA	3	1	1	1	471	52.7	2.04
P04951	kdsB	4	1	1	1	248	27.6	2.03
P0AGA2	secY	4	1	1	1	443	48.5	2.01
P03004	dnaA	2	1	1	1	467	52.5	2
P0AG99	secG	16	1	1	1	110	11.4	2
P0ADI7	yecD	5	1	1	1	188	20.4	2
P14176	proW	5	1	1	1	354	37.6	2
P0A794	pdxJ	5	1	1	1	243	26.4	2
P08312	pheS	3	1	1	1	327	36.8	1.99
P00962	glnS	5	1	1	1	554	63.4	1.99
P0AB38	lpoB	6	1	1	1	213	22.5	1.98
P0ACE7	hinT	11	1	1	1	119	13.2	1.98
P64596	dolP	8	1	1	1	191	20	1.97
P40874	solA	3	1	1	1	372	40.9	1.97
P31433	yicH	2	1	1	1	569	62.2	1.96
P45578	luxS	6	1	1	1	171	19.4	1.95
P18843	nadE	4	1	1	1	275	30.6	1.95
P0AFX9	rseB	4	1	1	1	318	35.7	1.95
P0A7R9	rpsK	6	1	1	1	129	13.8	1.93
P02358	rpsF	6	1	1	1	135	15.7	1.91
P0A905	slyB	6	1	1	1	155	15.6	1.91
P25746	hflD	7	1	1	1	213	22.9	1.91

Table 18 - Mass spectrometry results from Section 5.2.6– SecHN91^{Bpa}

UniProt Accession	Gene Name	Coverage [%]	Peptides	PSMs	Unique Peptides	AA	MW [kDa]	Score Sequest
P0CE47	tufA	75	20	102	20	394	43.3	339.04
P0A6Y8	dnaK	68	42	84	42	638	69.1	312.1
P0AD05	yecA	65	8	84	8	221	25	301.3
P10408	secA	62	42	63	42	901	102	217.63
P0A6F5	groEL	72	25	63	25	548	57.3	213.26
P0A850	tig	54	21	68	21	432	48.2	211.41
P0A9B2	gapA	63	15	53	15	331	35.5	188.3
P0A6M8	fusA	57	25	52	25	704	77.5	185.03
P02931	ompF	79	18	52	18	362	39.3	183.57
P36683	acnB	60	32	50	32	865	93.4	162.58
P0AG67	rpsA	55	22	43	22	557	61.1	158.72
P0A6Z3	htpG	68	33	48	33	624	71.4	157.01
P03023	lacI	55	14	39	14	360	38.6	143.4
P0A910	ompA	66	17	34	17	346	37.2	123.95
P10121	ftsY	60	21	31	21	497	54.5	111.57
P09373	pflB	46	22	29	22	760	85.3	96.53
P0ABK5	cysK	78	16	26	16	323	34.5	92.53
P0AC41	sdhA	52	19	26	19	588	64.4	86.04
P0ABD5	accA	55	14	24	14	319	35.2	85.95
P05055	pnp	41	20	26	20	711	77.1	84.5
P33602	nuoG	35	21	25	21	908	100.2	84.42
P0A705	infB	37	23	28	23	890	97.3	84.33
P63284	clpB	35	21	26	21	857	95.5	81.55
P61889	mdh	87	17	23	17	312	32.3	78.29
P0A7Z4	rpoA	58	14	24	14	329	36.5	71.12
P0ACP7	purR	49	13	21	13	341	38.2	69.37
P02925	rbsB	52	12	19	12	296	30.9	67.13
P0AAI5	fabF	50	11	18	11	413	43	66.71
P0A6E4	argG	49	13	20	13	447	49.9	64.8
P0A8M0	asnS	43	15	21	15	466	52.5	64.69
P0AAI3	ftsH	38	18	20	18	644	70.7	64.6
P0AGE9	sucD	65	13	20	13	289	29.8	62.01
P0AEX9	malE	48	13	19	13	396	43.4	61.08
P00509	aspC	47	14	19	14	396	43.5	58.79
P0AFF6	nusA	45	14	17	14	495	54.8	57.78
P0ABB4	atpD	46	13	17	13	460	50.3	56.6
P00961	glyS	27	14	17	14	689	76.8	56.05
P0C8J8	gatZ	53	12	18	12	420	47.1	55.18
P0A8V2	rpoB	20	19	19	19	1342	150.5	54.88
P0AFG6	sucB	34	11	17	11	405	44	53.62
P08200	icd	43	13	18	13	416	45.7	52.52
P0A6H5	hslU	25	8	14	8	443	49.6	51.72
P0A8N3	lysS	30	13	17	13	505	57.6	51.67
P0A6P1	tsf	59	12	17	12	283	30.4	50.93
P0AFG3	sucA	24	15	17	15	933	105	50.86
P06959	aceF	36	13	16	13	630	66.1	50.83
P0AE08	ahpC	45	6	15	6	187	20.7	50.45
P0A836	sucC	41	13	17	13	388	41.4	49.74
P0A9P0	lpdA	38	12	15	12	474	50.7	49.22
P0ABB0	atpA	34	13	14	12	513	55.2	49.01
P0A870	talB	51	12	15	12	317	35.2	48.23
P00350	gnd	34	12	15	12	468	51.4	48.1
P22259	pckA	30	11	15	11	540	59.6	47.95

P00579	rpoD	30	12	15	12	613	70.2	47.79
P0A7V3	rpsC	37	6	13	6	233	26	47.25
P08660	lysC	24	8	14	8	449	48.5	46.09
P0A6P9	eno	35	10	15	10	432	45.6	45.9
P31979	nuoF	33	10	14	10	445	49.3	44.71
P04983	rbsA	29	12	14	12	501	55	43.62
P0A7D4	purA	42	12	15	12	432	47.3	43.5
P77398	arnA	24	12	14	12	660	74.2	41.98
P0A799	pgk	42	10	12	10	387	41.1	41.68
P0A7V0	rpsB	50	9	13	9	241	26.7	40.53
P28635	metQ	48	7	10	7	271	29.4	39.93
P0A6B7	iscS	25	8	13	8	404	45.1	38.7
P04036	dapB	28	5	10	5	273	28.7	38.54
P62620	ispG	39	11	12	11	372	40.7	38.38
P62399	rplE	49	8	12	8	179	20.3	38.32
P23843	oppA	31	8	10	8	543	60.9	38.15
P16659	proS	26	11	11	11	572	63.7	38.03
P25665	metE	22	14	14	14	753	84.6	37.99
P0ACF8	hns	49	6	11	6	137	15.5	37.89
P0A9Q5	accD	39	7	10	7	304	33.3	37.38
P0AFG8	aceE	24	14	14	14	887	99.6	37.37
P0A825	glyA	35	9	12	9	417	45.3	37.16
P0ABC7	hflK	37	11	12	11	419	45.5	36.4
P02943	lamB	37	9	10	9	446	49.9	36.37
P0AGD3	sodB	53	6	11	6	193	21.3	35.93
P27302	tktA	19	9	12	9	663	72.2	34.54
P0AEK4	fabI	43	8	11	8	262	27.8	34.44
P00957	alaS	16	10	11	10	876	96	34
P0DTT0	bipA	23	9	11	9	607	67.3	33.79
P06612	topA	20	11	12	11	865	97.3	33.42
P0A6F3	glpK	24	11	12	11	502	56.2	33.33
P60785	lepA	24	9	10	9	599	66.5	33.11
P0AEK2	fabG	45	8	10	8	244	25.5	32.96
P33599	nuoC	25	11	12	11	596	68.2	32.61
P0A9K3	ybeZ	40	9	9	9	346	39	32.07
P23538	ppsA	17	10	10	10	792	87.4	31.7
P00562	metL	15	10	11	10	810	88.8	31.67
P0A940	bamA	19	9	10	9	810	90.5	31.62
P0AFM6	pspA	35	6	8	6	222	25.5	31.11
P0A9A6	ftsZ	42	10	10	10	383	40.3	31.11
P35340	ahpF	30	10	10	10	521	56.1	30.04
P0ADY1	ppiD	22	9	10	9	623	68.1	30.04
P0AG30	rho	21	8	10	8	419	47	29.77
P0A7L0	rplA	42	9	10	9	234	24.7	29.73
P0A7S9	rpsM	53	5	8	5	118	13.1	29.57
P23893	hemL	30	9	10	9	426	45.3	29.44
P45523	fkpA	38	6	8	6	270	28.9	28.96
P0A7J3	rplJ	52	6	9	6	165	17.7	28.86
P0ACF0	hupA	61	6	9	6	90	9.5	28.74
P08839	ptsI	20	8	9	8	575	63.5	28.65
P0A6Z1	hscA	18	8	9	8	616	65.6	28.13
P77690	arnB	28	7	8	7	385	42.2	28.09
P0A9W3	ettA	25	9	10	9	555	62.4	28.07
P62707	gpmA	39	8	10	8	250	28.5	27.9
P0AG55	rplF	47	8	9	8	177	18.9	27.67
P60422	rplB	32	7	10	7	273	29.8	27.63
P45577	proQ	31	5	8	5	232	25.9	27.59
P0A9D8	dapD	39	8	9	8	274	29.9	27.24
P0A9Q1	arcA	26	4	7	4	238	27.3	26.82
P0A6H1	clpX	33	10	10	10	424	46.3	26.65
P0A707	infC	42	5	7	5	180	20.6	26.45
P0CB39	eptC	12	7	9	7	577	66.6	26.43
P0A817	metK	22	6	8	6	384	41.9	26.36
P0ABC3	hflC	29	7	9	7	334	37.6	26.25
P0A7V8	rpsD	38	8	9	8	206	23.5	26.01
P0A862	tpx	54	5	6	5	168	17.8	25.71
P61175	rplV	43	5	7	5	110	12.2	25.68

P0A9S3	gatD	23	8	9	8	346	37.4	25.6
P37095	pepB	26	8	8	8	427	46.2	25.58
P02359	rpsG	42	5	7	5	179	20	25.47
P0AEZ3	minD	40	8	8	8	270	29.6	23.96
P30843	basR	35	5	7	5	222	25	23.66
P77395	cnoX	41	7	8	7	284	31.8	23.57
P0A9K9	slyD	49	5	8	5	196	20.8	23.22
P69783	crr	41	5	7	5	169	18.2	22.9
P33195	gcvP	11	6	7	6	957	104.3	22.64
P60438	rplC	23	3	6	3	209	22.2	22.56
P00956	ileS	14	8	8	8	938	104.2	22.55
P0A8T7	rpoC	8	9	9	9	1407	155.1	22.43
P0A7W1	rpsE	37	4	7	4	167	17.6	22.38
P0AFG0	nusG	55	6	7	6	181	20.5	22.3
P60723	rplD	32	4	6	4	201	22.1	22.13
P24182	accC	22	8	8	8	449	49.3	21.96
P0ABH7	gltA	19	6	7	6	427	48	21.48
P0AAB6	galF	36	6	7	6	297	32.8	20.94
P30748	moaD	26	1	5	1	81	8.8	20.91
P0AA10	rplM	51	6	7	6	142	16	20.53
P13029	katG	15	7	7	7	726	80	20.48
P60624	rplX	56	5	6	5	104	11.3	20.46
P17169	glmS	18	6	6	6	609	66.9	20.3
P76658	hldE	22	8	8	8	477	51	20.02
P21170	speA	12	6	6	6	658	73.9	19.77
P69441	adk	31	6	7	6	214	23.6	19.57
P0A9Q9	asd	26	6	7	6	367	40	19.47
P0A7R1	rplI	43	6	7	6	149	15.8	19.31
P23836	phoP	44	6	6	6	223	25.5	19.27
P0A9M8	pta	11	6	7	6	714	77.1	19.26
P0AC38	aspA	15	6	7	6	478	52.3	19.06
P0ABI8	cyoB	9	4	6	4	663	74.3	18.6
P07014	sdhB	26	5	6	5	238	26.8	18.15
P76422	thiD	20	3	5	3	266	28.6	18.12
P0A917	ompX	36	5	5	5	171	18.6	18.1
P0AB91	aroG	25	6	6	6	350	38	18.02
P0A953	fabB	14	3	5	3	406	42.6	17.85
P0ABZ6	surA	15	5	6	5	428	47.3	17.79
P0A8F0	upp	34	5	6	5	208	22.5	17.79
P27248	gcvT	26	6	6	6	364	40.1	17.73
P02930	tolC	17	6	6	6	493	53.7	17.71
P62768	yaeH	45	6	6	6	128	15.1	17.63
P0A8L1	serS	18	6	6	6	430	48.4	17.35
P00864	ppc	9	7	7	7	883	99	17.32
P07639	aroB	21	4	5	4	362	38.9	16.98
P0A805	frr	45	6	6	6	185	20.6	16.85
P15042	ligA	10	5	6	5	671	73.6	16.81
P00959	metG	10	4	5	4	677	76.2	16.62
P0AB71	fbaA	18	4	5	4	359	39.1	16.4
P0AEB2	dacA	23	6	6	5	403	44.4	16.17
P00934	thrC	24	5	5	5	428	47.1	15.86
P15288	pepD	16	5	5	5	485	52.9	15.81
P05791	ilvD	11	5	5	5	616	65.5	15.52
P0AC33	fumA	14	5	5	5	548	60.3	15.34
P0AE88	cpxR	20	3	4	3	232	26.3	15.3
P17846	cysI	14	4	4	4	570	64	15.23
P0A6F9	groES	53	4	5	4	97	10.4	14.89
P00370	gdhA	15	4	4	4	447	48.6	14.88
P0AEQ3	glnH	19	3	4	3	248	27.2	14.84
P0C0L7	proP	10	4	5	4	500	54.8	14.84
P0ABU2	ychF	18	5	5	5	363	39.6	14.7
P30845	eptA	11	5	5	5	547	61.6	14.62
P0A7E5	pyrG	13	5	5	5	545	60.3	14.61
P0ABA4	atpH	30	3	4	3	177	19.3	14.47
P0A9Q7	adhE	9	6	6	6	891	96.1	14.4
P0A9C5	glnA	20	5	5	5	469	51.9	14.25
P0AG44	rplQ	27	3	5	3	127	14.4	14.24

P02413	rplO	34	4	5	4	144	15	14.11
P21889	aspS	8	4	5	4	590	65.9	14.06
P0A9X9	cspA	53	3	4	3	70	7.4	14.03
P0A7J7	rplK	33	4	5	4	142	14.9	13.98
P0A7G2	rbfA	38	4	5	4	133	15.1	13.73
P37440	ucpA	21	5	5	5	263	27.8	13.63
P0A8M3	thrS	8	5	5	5	642	74	13.58
P00968	carB	6	5	5	5	1073	117.8	13.53
P0A993	fbp	24	5	5	5	332	36.8	13.49
P16703	cysM	27	4	4	4	303	32.6	13.44
P0A9M2	hpt	18	3	4	3	178	20.1	13.41
P60716	lipA	14	3	4	3	321	36	13.33
P0A9U3	ybiT	11	5	5	5	530	59.8	13.27
P23721	serC	19	5	5	5	362	39.8	13.12
P09546	putA	5	5	5	5	1320	143.7	12.97
P27298	prlC	13	5	5	5	680	77.1	12.88
P03841	malM	31	5	5	5	306	31.9	12.84
P0ABJ1	cyoA	26	4	4	4	315	34.9	12.72
P25553	aldA	11	4	4	4	479	52.2	12.65
P0A6Y5	hslO	21	4	4	4	292	32.5	12.61
P76558	maeB	11	5	5	5	759	82.4	12.59
P61714	ribE	40	4	4	4	156	16.1	12.53
P25519	hflX	7	2	4	2	426	48.3	12.42
P0A6G7	clpP	20	2	3	2	207	23.2	12.4
P0A7W7	rpsH	40	5	5	5	130	14.1	12.26
P0A6Q3	fabA	30	5	5	5	172	19	12.26
P39342	yjgR	13	4	4	4	500	54.3	12.03
P0A912	pal	24	3	4	3	173	18.8	11.9
P37665	yiaD	26	3	3	3	219	22.2	11.75
P0AAA1	yagU	26	4	4	4	204	23	11.65
P08312	pheS	12	3	4	3	327	36.8	11.63
P76177	ydgH	21	4	4	4	314	33.9	11.63
P45565	ais	28	4	4	4	200	22.2	11.61
P0A6S0	flgH	21	4	4	4	232	24.6	11.57
P0A6C8	argB	16	2	4	2	258	27.1	11.53
P0C054	ibpA	33	4	4	4	137	15.8	11.53
P0ACP5	gntR	14	3	4	3	331	36.4	11.51
P0AED0	uspA	50	3	3	3	144	16.1	11.25
P04825	pepN	7	4	4	4	870	98.9	11.18
P0AGI1	rbsC	15	3	4	3	321	33.4	11.12
P0AG90	secD	7	4	4	3	615	66.6	11.1
P76472	arnD	22	4	4	4	296	33.1	11.09
P0A715	kdsA	19	3	3	3	284	30.8	10.96
P0A6R0	fabH	21	4	4	4	317	33.5	10.85
P0AGJ9	tyrS	16	4	4	4	424	47.5	10.75
P0C058	ibpB	35	4	4	4	142	16.1	10.73
P0AE06	acrA	16	4	4	4	397	42.2	10.64
P0AAI9	fabD	21	3	3	3	309	32.4	10.64
P0A7T3	rpsP	52	3	3	3	82	9.2	10.63
P30850	rnb	7	4	4	4	644	72.4	10.6
P77804	ydgA	9	4	4	4	502	54.7	10.57
P21599	pykA	10	3	3	3	480	51.3	10.48
P09127	hemX	10	3	4	3	393	42.9	10.37
P0A749	murA	12	4	4	4	419	44.8	10.32
P0A7R5	rpsJ	34	3	4	3	103	11.7	10.29
P76268	kdgR	21	4	4	4	263	30	10.28
P39831	ydfG	18	3	3	3	248	27.2	10.19
P0A7X3	rpsI	25	3	4	3	130	14.8	9.91
P0ADZ4	rpsO	42	3	3	2	89	10.3	9.88
P37188	gatB	47	2	3	2	94	10.2	9.76
P0AGB6	rpoE	16	2	3	2	191	21.7	9.76
P08390	usg	20	3	3	3	337	36.3	9.71
P0A858	tpiA	26	3	3	3	255	27	9.65
P0AF08	mrp	14	3	3	3	369	39.9	9.63
P33218	yebE	12	2	3	2	219	23.7	9.59
P69776	lpp	33	2	3	2	78	8.3	9.58
P07862	ddlB	17	4	4	4	306	32.8	9.56

P0A7L3	rplT	23	3	4	3	118	13.5	9.53
P0AB80	ilvE	15	3	3	3	309	34.1	9.41
P0AA16	ompR	21	3	3	3	239	27.3	9.34
P38489	nfsB	22	3	3	3	217	23.9	9.32
P0AF24	nagD	16	2	3	2	250	27.1	9.32
P60906	hisS	10	3	3	3	424	47	9.27
P09372	grpE	24	2	3	2	197	21.8	9.1
P0A7U7	rpsT	36	4	4	4	87	9.7	9.09
P33363	bglX	5	3	3	3	765	83.4	9.05
P0A7B8	hslV	18	2	3	2	176	19.1	9.04
P00448	sodA	17	2	3	2	206	23.1	9.02
P0ABD8	accB	33	3	3	3	156	16.7	9.01
P00561	thrA	8	4	4	4	820	89.1	8.99
P0AEU0	hisJ	17	3	3	3	260	28.5	8.95
P37051	purU	20	3	3	3	280	31.9	8.89
P77757	arnC	14	3	3	3	322	36.3	8.89
P0AEI1	miaB	12	3	3	3	474	53.6	8.83
P31224	acrB	4	3	3	3	1049	113.5	8.76
P0A6J8	ddlA	11	3	3	3	364	39.3	8.76
P68919	rplY	30	3	3	3	94	10.7	8.72
P00803	lepB	11	3	3	3	324	35.9	8.72
P0A8I3	yaaA	22	3	3	3	258	29.6	8.71
P0AEU7	skp	10	1	3	1	161	17.7	8.64
P07813	leuS	7	3	3	3	860	97.2	8.59
P0A908	mipA	17	3	3	3	248	27.8	8.46
P17117	nfsA	20	3	3	3	240	26.8	8.46
P76576	yfgM	26	3	3	3	206	22.2	8.45
P07913	tdh	11	3	3	3	341	37.2	8.42
P0ADY7	rplP	22	2	3	2	136	15.3	8.37
P0ABN1	dgkA	17	2	3	2	122	13.2	8.33
P77488	dxs	7	3	3	3	620	67.6	8.28
P61517	can	16	3	3	3	220	25.1	8.23
P27306	sthA	8	2	2	2	466	51.5	8.22
P0A855	tolB	18	3	3	3	430	45.9	8.16
P0ABA0	atpF	24	3	3	3	156	17.3	8.08
P0A7U3	rpsS	21	2	3	2	92	10.4	8.03
P0AEP3	galU	11	2	3	2	302	32.9	7.98
P0A6K3	def	15	2	3	2	169	19.3	7.88
P0AES4	gyrA	3	2	2	2	875	96.9	7.8
P76027	oppD	11	2	2	2	337	37.2	7.8
P0A9J6	rbsK	10	2	3	2	309	32.3	7.66
P40874	solA	12	3	3	3	372	40.9	7.57
P0AFD6	nuoI	18	3	3	3	180	20.5	7.56
P37902	gltI	14	3	3	3	302	33.4	7.55
P0A7M2	rpmB	13	1	3	1	78	9	7.49
P0AG63	rpsQ	23	1	2	1	84	9.7	7.48
P0ADY3	rplN	30	2	2	2	123	13.5	7.42
P0A9Y6	cspC	54	3	3	3	69	7.4	7.36
P05793	ilvC	9	3	3	3	491	54	7.35
P13009	metH	3	3	3	3	1227	135.9	7.32
P0A6F1	carA	10	3	3	3	382	41.4	7.32
P16095	sdaA	8	3	3	3	454	48.9	7.26
P00962	glnS	6	2	3	2	554	63.4	7.25
P0AES6	gyrB	5	3	3	3	804	89.9	7.24
P08622	dnaJ	9	3	3	3	376	41.1	7.19
P31120	glmM	9	3	3	3	445	47.5	7.16
P0AEQ1	glcG	16	1	2	1	134	13.7	7.12
P77774	bamB	7	2	2	2	392	41.9	7.12
P0A7M6	rpmC	46	2	2	2	63	7.3	7.09
P0AG27	yibN	20	2	2	2	143	15.6	7.06
P0A7M9	rpmE	41	2	2	2	70	7.9	6.93
P0A8E7	yajQ	17	2	2	2	163	18.3	6.91
P0ADG4	suhB	11	2	2	2	267	29.2	6.91
P30011	nadC	12	3	3	3	297	32.7	6.77
P46837	yhgF	4	3	3	3	773	85.1	6.73
P02358	rpsF	25	2	2	2	135	15.7	6.69
P0A9P4	trxB	9	2	2	2	321	34.6	6.66

P0A955	eda	15	2	2	2	213	22.3	6.61
P0AAX8	ybiS	12	2	2	2	306	33.3	6.57
P0A7B5	proB	8	2	2	2	367	39	6.55
P0A6A3	ackA	8	2	2	2	400	43.3	6.54
P75913	ghrA	11	2	2	2	312	35.3	6.51
P27434	rodZ	10	2	2	2	337	36.2	6.37
P63224	gmhA	15	2	2	2	192	20.8	6.29
P0A6L4	nanA	13	2	2	2	297	32.6	6.29
P60390	rsmH	11	2	2	2	313	34.9	6.27
P0A903	bamC	7	2	2	2	344	36.8	6.27
P0A6N4	efp	17	2	2	2	188	20.6	6.24
P0A7K6	rplS	23	2	2	2	115	13.1	6.19
P0ACA3	sspA	12	2	2	2	212	24.3	6.14
P0A6U5	rsmG	10	2	2	2	207	23.4	6.12
P0AC69	grxD	29	2	2	2	115	12.9	6.07
P0AFC7	nuoB	13	2	2	2	220	25	5.97
P31663	panC	10	2	2	2	283	31.6	5.94
P0A7C2	lexA	11	2	2	2	202	22.3	5.92
P0A9V1	lptB	14	2	2	2	241	26.8	5.86
P0A9L3	fklB	12	2	2	2	206	22.2	5.83
P36680	zapD	8	2	2	2	247	28.3	5.8
P0A763	ndk	26	2	2	2	143	15.5	5.72
P15034	pepP	3	1	2	1	441	49.8	5.7
P60651	speB	9	2	2	2	306	33.5	5.65
P04951	kdsB	9	2	2	2	248	27.6	5.57
P37613	panZ	20	2	2	2	127	14.5	5.52
P25437	frmA	9	2	2	2	369	39.3	5.51
P0AGG8	tldD	6	2	2	2	481	51.3	5.51
P0A7T7	rpsR	29	2	2	2	75	9	5.49
P0A6L2	dapA	11	2	2	2	292	31.3	5.49
P22333	add	8	2	2	2	333	36.4	5.47
P0A6I0	cmk	13	2	2	2	227	24.7	5.46
P0A780	nusB	22	2	2	2	139	15.7	5.43
P60757	hisG	9	2	2	2	299	33.3	5.4
P00490	malP	3	2	2	2	797	90.5	5.39
P0A7K2	rplL	17	2	2	2	121	12.3	5.34
P0AG48	rplU	21	2	2	2	103	11.6	5.34
P0ADK0	yiaF	9	2	2	2	236	25.6	5.31
P0A8V6	fadR	15	2	2	2	239	27	5.31
P36672	treB	7	2	2	2	473	51	5.3
P0AGE0	ssb	13	2	2	2	178	19	5.29
P21177	fadB	4	2	2	2	729	79.5	5.28
P32131	hemN	6	2	2	2	457	52.7	5.28
P28904	treC	5	2	2	2	551	63.8	5.27
P00582	polA	4	2	2	2	928	103.1	5.25
P17854	cysH	9	2	2	2	244	28	5.22
P09053	avtA	6	2	2	2	417	46.7	5.21
P0A6T1	pgi	5	2	2	2	549	61.5	5.16
P0AAQ2	yajD	23	2	2	2	115	13.4	5.16
P76372	wzzB	6	2	2	2	326	36.4	5.08
P0A734	minE	34	2	2	2	88	10.2	5.05
P07118	valS	4	2	2	2	951	108.1	5.01
P0A9T0	serA	6	2	2	2	410	44.1	4.96
P0AFK0	pmbA	6	2	2	2	450	48.3	4.96
P0AFC3	nuoA	18	2	2	2	147	16.4	4.95
P64624	yheO	8	2	2	2	240	26.8	4.93
P76046	ycjX	7	2	2	2	465	52.6	4.88
P23865	prc	3	2	2	2	682	76.6	4.87
P07395	pheT	4	2	2	2	795	87.3	4.83
P00452	nrdA	4	2	2	2	761	85.7	4.83
P39835	gntT	8	2	2	2	438	45.9	4.82
P0ACG1	stpA	10	1	2	1	134	15.3	4.81
P0ABA6	atpG	8	2	2	2	287	31.6	4.8
P03024	galR	8	2	2	2	343	37.1	4.77
P0A959	alaA	9	2	2	2	405	45.5	4.76
P0AC53	zwf	4	2	2	2	491	55.7	4.74
P0ABJ9	cydA	4	2	2	2	522	58.2	4.74

P0AAC8	iscA	24	2	2	2	107	11.5	4.72
P0A9L5	ppiC	22	2	2	2	93	10.2	4.72
P22524	mukE	18	2	2	2	234	27	4.68
P0C018	rplR	15	2	2	2	117	12.8	4.67
P0A6R3	fis	23	1	1	1	98	11.2	4.65
P0AA25	trxA	19	2	2	2	109	11.8	4.65
P0AFF2	nupC	6	1	2	1	400	43.4	4.61
P11557	damX	5	2	2	2	428	46.1	4.6
P17952	murC	5	2	2	2	491	53.6	4.6
P06992	rsmA	16	2	2	2	273	30.4	4.59
P04968	ilvA	4	2	2	2	514	56.2	4.56
P36938	pgm	6	1	1	1	546	58.3	4.49
P64596	dolP	13	2	2	2	191	20	4.48
P0AFM9	pspB	22	1	1	1	74	8.8	4.46
P69924	nrdB	9	2	2	2	376	43.5	4.42
P0C0V0	degP	6	1	2	1	474	49.3	4.41
P52108	rstA	8	2	2	2	239	26.7	4.38
P0A887	ubiE	10	2	2	2	251	28.1	4.38
P0AAG8	mglA	4	2	2	2	506	56.4	4.38
P0AGD7	ffh	6	2	2	2	453	49.8	4.37
P63020	nfuA	16	1	1	1	191	21	4.29
P04425	gshB	8	2	2	2	316	35.5	4.26
P69831	gatC	4	2	2	2	451	48.3	4.25
P31554	lptD	3	2	2	2	784	89.6	4.19
P37759	rfbB	6	2	2	2	361	40.5	4.13
P0A7Z0	rpiA	7	1	1	1	219	22.8	4.11
P0A877	trpA	7	1	1	1	268	28.7	4.08
P0AF28	narL	12	1	1	1	216	23.9	4.03
P0AGA2	secY	7	2	2	2	443	48.5	4.02
P0A937	bamE	18	1	1	1	113	12.3	3.96
P0ACF4	hupB	16	1	1	1	90	9.2	3.87
P16456	selD	9	1	1	1	347	36.7	3.73
P77211	cusC	4	1	1	1	457	50.2	3.73
P76034	yciT	7	1	1	1	249	27.6	3.69
P0AFX4	rsd	15	1	1	1	158	18.2	3.69
P26616	maeA	4	1	1	1	565	63.2	3.63
P0AE78	corC	6	1	1	1	292	33.3	3.59
P69503	apt	11	1	1	1	183	19.8	3.59
Q57261	truD	6	1	1	1	349	39.1	3.42
P60752	msbA	3	1	1	1	582	64.4	3.42
P0ADC1	lptE	9	1	1	1	193	21.3	3.37
P0AC02	bamD	5	1	1	1	245	27.8	3.33
P0A9D4	cysE	8	1	1	1	273	29.3	3.33
P0A794	pdxJ	6	1	1	1	243	26.4	3.28
P0A6D7	aroK	8	1	1	1	173	19.5	3.27
P0A6X7	ihfA	10	1	1	1	99	11.3	3.26
P69411	rcsF	10	1	1	1	134	14.2	3.24
P0A6T5	folE	5	1	1	1	222	24.8	3.23
P0ADB7	ecnB	40	1	1	1	48	4.8	3.22
P0AG59	rpsN	19	1	1	1	101	11.6	3.22
P0AFF0	nuoN	2	1	1	1	485	52	3.2
P0A6K6	deoB	3	1	1	1	407	44.3	3.17
P00894	ilvH	7	1	1	1	163	18	3.17
P62623	ispH	6	1	1	1	316	34.8	3.14
P0ADG7	guaB	4	1	1	1	488	52	3.1
P69054	sdhC	9	1	1	1	129	14.3	3.09
P39173	yeaD	5	1	1	1	294	32.6	3.08
P31802	narP	7	1	1	1	215	23.6	3.07
P0AGK8	iscR	14	1	1	1	162	17.3	3.06
P0A988	dnaN	5	1	1	1	366	40.6	3.03
P16700	cysP	3	1	1	1	338	37.6	3.03
P0ACA7	gstB	9	1	1	1	208	23.7	2.99
P45955	cpoB	10	1	1	1	263	28.2	2.99
P77258	nemA	7	1	1	1	365	39.5	2.98
P52643	ldhA	4	1	1	1	329	36.5	2.98
P23839	yicC	4	1	1	1	287	33.2	2.97
P76535	murQ	7	1	1	1	298	31.2	2.96

P68187	malK	6	1	1	1	371	41	2.95
P0AF93	ridA	10	1	1	1	128	13.6	2.93
P0AG93	secF	4	1	1	1	323	35.4	2.92
P0ACC3	erpA	11	1	1	1	114	12.1	2.92
P0AB24	efeO	4	1	1	1	375	41.1	2.91
P07012	prfB	4	1	1	1	365	41.2	2.91
P0AAS0	ylaC	10	1	1	1	156	18.3	2.9
P75990	bluF	3	1	1	1	403	45.3	2.87
P0A8E1	ycfP	7	1	1	1	180	21.2	2.87
P0ACE0	hybC	3	1	1	1	567	62.5	2.87
P04079	guaA	3	1	1	1	525	58.6	2.84
P07117	putP	3	1	1	1	502	54.3	2.84
P0A9A9	fur	8	1	1	1	148	16.8	2.83
P36879	yadG	5	1	1	1	308	34.6	2.78
P0A6N8	yeiP	7	1	1	1	190	21.5	2.77
P0ACB7	hemY	3	1	1	1	398	45.2	2.76
P23847	dppA	5	1	1	1	535	60.3	2.76
P21888	cysS	2	1	1	1	461	52.2	2.76
P0A7S3	rpsL	10	1	1	1	124	13.7	2.74
P04982	rbsD	10	1	1	1	139	15.3	2.72
P0AB38	lpoB	7	1	1	1	213	22.5	2.72
P00954	trpS	7	1	1	1	334	37.4	2.72
P29012	dadX	3	1	1	1	356	38.8	2.72
P0A7N9	rpmG	27	1	1	1	55	6.4	2.72
P0AFD1	nuoE	11	1	1	1	166	18.6	2.71
P45578	luxS	8	1	1	1	171	19.4	2.7
P0A8A0	yebC	5	1	1	1	246	26.4	2.68
P06149	dld	4	1	1	1	571	64.6	2.68
P00722	lacZ	1	1	1	1	1024	116.4	2.66
P60340	truB	4	1	1	1	314	35.1	2.59
P43672	uup	2	1	1	1	635	72	2.55
P0A6S3	flgI	5	1	1	1	365	38.1	2.52
P64604	mlaD	4	1	1	1	183	19.6	2.51
P11880	murF	2	1	1	1	452	47.4	2.51
P75849	gloC	6	1	1	1	215	23.8	2.51
P0AD61	pykF	3	1	1	1	470	50.7	2.5
P24251	crl	9	1	1	1	133	15.6	2.49
P25714	yidC	3	1	1	1	548	61.5	2.48
P07001	pntA	4	1	1	1	510	54.6	2.48
P0A9N4	pflA	4	1	1	1	246	28.2	2.47
P04805	gltX	3	1	1	1	471	53.8	2.46
P0ADA3	nlpD	3	1	1	1	379	40.1	2.46
P69829	ptsN	10	1	1	1	163	17.9	2.46
P0AFX9	rseB	4	1	1	1	318	35.7	2.46
P0ADE8	ygfZ	3	1	1	1	326	36.1	2.45
P0A9W9	yrdA	7	1	1	1	184	20.2	2.41
P31808	yciK	5	1	1	1	252	27.9	2.41
P0AF70	yjeI	16	1	1	1	117	12	2.41
P60595	hisH	5	1	1	1	196	21.6	2.4
P10371	hisA	7	1	1	1	245	26	2.4
P0A7H6	recR	7	1	1	1	201	21.9	2.4
P30844	basS	4	1	1	1	363	41	2.38
P0AG51	rpmD	24	1	1	1	59	6.5	2.37
P0ACN4	allR	4	1	1	1	271	29.3	2.37
P77529	tcyP	3	1	1	1	463	48.6	2.37
P76270	msrC	6	1	1	1	165	18.1	2.37
P30744	sdaB	2	1	1	1	455	48.7	2.36
P0ABS1	dksA	6	1	1	1	151	17.5	2.35
P0AAG3	gltL	5	1	1	1	241	26.6	2.34
P38038	cysJ	2	1	1	1	599	66.2	2.33
P0AF12	mtnN	10	1	1	1	232	24.3	2.33
P77239	cusB	3	1	1	1	407	44.3	2.33
P0A8G6	wrbA	9	1	1	1	198	20.8	2.32
P25516	acnA	2	1	1	1	891	97.6	2.32
P0AFI7	pdxH	7	1	1	1	218	25.5	2.32
P0A8J4	ybeD	17	1	1	1	87	9.8	2.32
P0A8W0	nanR	5	1	1	1	263	29.5	2.31

P04846	nlpA	5	1	1	1	272	29.4	2.29
P69222	infA	17	1	1	1	72	8.2	2.28
P0AAY6	ybjN	8	1	1	1	158	17.7	2.27
P0A8A8	rimP	7	1	1	1	150	16.6	2.27
P33136	mdoG	2	1	1	1	511	57.9	2.26
P0AED7	dapE	2	1	1	1	375	41.2	2.26
P25748	galS	3	1	1	1	346	37.3	2.25
P08395	sppA	2	1	1	1	618	67.2	2.25
P0AG99	secG	16	1	1	1	110	11.4	2.24
P69828	gatA	13	1	1	1	150	16.9	2.21
P69797	manX	4	1	1	1	323	35	2.21
P05852	tsaD	4	1	1	1	337	36	2.19
P09323	nagE	3	1	1	1	648	68.3	2.19
P0AE18	map	4	1	1	1	264	29.3	2.17
P30178	hcxB	3	1	1	1	361	38.9	2.16
P60546	gmk	8	1	1	1	207	23.6	2.15
P21513	rne	1	1	1	1	1061	118.1	2.13
P0AEG4	dsbA	4	1	1	1	208	23.1	2.12
P77202	dsbG	6	1	1	1	248	27.5	2.12
P12758	udp	5	1	1	1	253	27.1	2.12
P77330	borD	10	1	1	1	97	10.4	2.1
P24224	acpS	12	1	1	1	126	14	2.09
P00960	glyQ	3	1	1	1	303	34.8	2.09
P29131	ftsN	4	1	1	1	319	35.8	2.09
P0ACC1	prmC	5	1	1	1	277	31	2.09
P06715	gor	2	1	1	1	450	48.7	2.09
P0A8D3	yaiI	10	1	1	1	152	17	2.06
P77737	oppF	3	1	1	1	334	37.2	2.06
P0AE01	trmJ	4	1	1	1	246	27	2.06
P0A800	rpoZ	10	1	1	1	91	10.2	2.04
P68699	atpE	11	1	1	1	79	8.3	2.03
P0ACL2	exuR	4	1	1	1	258	29.8	2.01
P18843	nadE	4	1	1	1	275	30.6	2.01
P0ADI7	yecD	5	1	1	1	188	20.4	2.01
P0A9Z1	glnB	7	1	1	1	112	12.4	2
P0A6V8	glk	5	1	1	1	321	34.7	2
P0AEE5	mglB	6	1	1	1	332	35.7	1.98
P68679	rpsU	11	1	1	1	71	8.5	1.98
P0AC44	sdhD	9	1	1	1	115	12.9	1.97
P30860	artJ	7	1	1	1	243	26.8	1.95
P0AFR4	yciO	5	1	1	1	206	23.2	1.95
P0AFH8	osmY	6	1	1	1	201	21.1	1.93
P23869	ppiB	7	1	1	1	164	18.1	1.93
P05042	fumC	2	1	1	1	467	50.5	1.93
P0AE52	bcp	9	1	1	1	156	17.6	1.93
P75838	ycaO	3	1	1	1	586	65.6	1.91
P0A8F8	uvrB	2	1	1	1	673	76.2	1.9

Table 19 - Mass spectrometry results from Section 5.2.6– SecHF101^{Bpa}

UniProt Accession	Gene Name	Coverage [%]	Peptides	PSMs	Unique Peptides	AAs	MW [kDa]	Score Sequest
P0A6Y8	dnaK	67	45	106	45	638	69.1	412.33
P0CE47	tufA	78	21	120	21	394	43.3	400.18
P0AD05	yecA	65	8	87	8	221	25	316.15
P0A6F5	groEL	73	27	77	27	548	57.3	277.14
P0A6M8	fusA	55	25	63	25	704	77.5	224.76
P0AG67	rpsA	49	24	57	24	557	61.1	207.49
P0A850	tig	54	22	60	22	432	48.2	188.64
P10408	secA	55	34	51	34	901	102	187.66
P02931	ompF	88	20	51	20	362	39.3	172.33
P36683	acnB	53	29	48	29	865	93.4	160.96
P0A9B2	gapA	63	13	43	13	331	35.5	153.19
P0A6Z3	htpG	58	30	45	30	624	71.4	151.84
P0A705	infB	42	27	36	27	890	97.3	124.84
P0A8V2	rpoB	36	33	40	33	1342	150.5	124.59
P0A910	ompA	66	17	33	17	346	37.2	123.95
P03023	lacI	55	14	29	14	360	38.6	107.69
P63284	clpB	44	24	32	24	857	95.5	105.55
P0ABD5	accA	59	15	30	15	319	35.2	102.06
P0A8T7	rpoC	27	25	30	25	1407	155.1	98.97
P61889	mdh	81	16	26	16	312	32.3	94.89
P02925	rbsB	62	13	25	13	296	30.9	92.98
P10121	ftsY	54	18	25	18	497	54.5	92.38
P0ABK5	cysK	68	15	25	15	323	34.5	91.17
P05055	pnp	37	17	25	17	711	77.1	88.39
P0AAI5	fabF	50	12	21	12	413	43	84.23
P0ABB4	atpD	56	15	22	15	460	50.3	81.85
P62399	rplE	56	10	24	10	179	20.3	79.71
P0A6P1	tsf	62	16	24	16	283	30.4	78.87
P09373	pflB	36	17	23	17	760	85.3	78.05
P0AE08	ahpC	57	8	20	8	187	20.7	71.47
P00350	gnd	46	15	21	15	468	51.4	70.98
P0A7V3	rpsC	52	9	18	9	233	26	70.49
P0A7Z4	rpoA	54	13	23	13	329	36.5	69.53
P02359	rpsG	43	7	17	7	179	20	67.45
P0AC41	sdhA	43	16	20	16	588	64.4	66.2
P0A8N3	lysS	49	17	21	14	505	57.6	64.73
P0A9P0	lpdA	41	13	18	13	474	50.7	64.4
P0ACP7	purR	48	12	19	12	341	38.2	64.22
P0A836	sucC	54	15	22	15	388	41.4	63.24
P0ABB0	atpA	37	13	17	12	513	55.2	61.84
P0AFG8	aceE	33	19	20	19	887	99.6	61.46
P00509	aspC	48	14	19	14	396	43.5	61.28
P06959	aceF	43	15	18	15	630	66.1	60.96
P0A7V0	rpsB	68	11	19	11	241	26.7	60.62
P0A6H5	hslU	36	12	17	12	443	49.6	60.25
P0AFF6	nusA	46	14	17	14	495	54.8	58.96
P0AAI3	ftsH	32	12	16	12	644	70.7	58.08
P0A6B7	iscS	40	13	19	13	404	45.1	57.91
P0AGE9	sucD	58	11	17	11	289	29.8	57.21
P00961	glyS	31	14	16	14	689	76.8	56.48
P0A7L0	rplA	54	12	19	12	234	24.7	56.15
P08200	icd	42	13	17	13	416	45.7	54.78
P33602	nuoG	23	13	15	13	908	100.2	54.5
P06612	topA	24	14	17	14	865	97.3	54.31
P0A8M0	asnS	37	12	16	12	466	52.5	52.36
P0ACF8	hns	55	7	15	7	137	15.5	52.27
P0AFG6	sucB	41	12	16	12	405	44	52.04
P0A6F3	glpK	32	16	18	16	502	56.2	51.82
P22259	pckA	32	12	16	12	540	59.6	51.65
P08660	lysC	20	8	16	8	449	48.5	51.07

P0A799	pgk	45	11	15	11	387	41.1	50.61
P00957	alaS	19	12	16	12	876	96	50.21
P23843	oppA	36	9	12	9	543	60.9	48.4
P0DTT0	bipA	32	12	14	12	607	67.3	48.36
P0A7D4	purA	38	13	16	13	432	47.3	47.74
P61175	rplV	62	9	14	9	110	12.2	47.12
P0A870	talB	46	11	15	11	317	35.2	46.91
P60422	rplB	38	8	15	8	273	29.8	46.66
P00579	rpoD	28	11	15	10	613	70.2	46.1
P00956	ileS	19	12	15	12	938	104.2	45.91
P0A862	tpx	59	6	12	6	168	17.8	45.74
P0AFG3	sucA	22	13	14	13	933	105	45.11
P0AEX9	malE	34	9	14	9	396	43.4	44.29
P0A6P9	eno	30	8	13	8	432	45.6	44.1
P62620	ispG	42	11	14	11	372	40.7	43.39
P0AG30	rho	26	10	14	10	419	47	43.11
P0AEK2	fabG	45	8	12	8	244	25.5	42.45
P0ACF0	hupA	61	6	13	6	90	9.5	41.87
P0AG55	rplF	60	8	12	8	177	18.9	41.44
P28635	metQ	56	8	10	8	271	29.4	41.02
P0AGD3	sodB	66	6	12	6	193	21.3	40.97
P0A9D8	dapD	48	10	12	10	274	29.9	39.73
P27302	tktA	27	11	13	11	663	72.2	39.66
P0AFM6	pspA	41	8	11	8	222	25.5	39.44
P0ABH7	gltA	41	11	12	11	427	48	39.4
P16659	proS	23	9	10	9	572	63.7	38.83
P60785	lepA	23	9	11	9	599	66.5	38.16
P0A6Y5	hslO	40	7	12	7	292	32.5	37.95
P0C8J8	gatZ	42	9	12	9	420	47.1	37.93
P04036	dapB	24	4	10	4	273	28.7	37.87
P0A9Q5	accD	38	7	10	7	304	33.3	37.14
P0AC38	aspA	28	9	12	9	478	52.3	37.06
P0A7V8	rpsD	51	10	12	10	206	23.5	36.48
P08839	ptsI	29	10	11	10	575	63.5	36.3
P0A9A6	ftsZ	42	10	11	10	383	40.3	36.02
P0ABC7	hflK	34	9	10	9	419	45.5	35.2
P0A7W7	rpsH	61	8	11	8	130	14.1	34.99
P45523	fkpA	38	6	9	6	270	28.9	34.86
P0A7J3	rplJ	52	7	10	7	165	17.7	34.46
P35340	ahpF	33	11	11	11	521	56.1	34.43
P60723	rplD	32	4	10	4	201	22.1	34.39
P77395	cnoX	32	6	10	6	284	31.8	34.38
P31979	nuoF	29	9	11	9	445	49.3	33.86
P0AEK4	fabI	32	5	10	5	262	27.8	33.1
P37095	pepB	33	10	10	10	427	46.2	32.98
P0A6Z1	hscA	26	10	10	10	616	65.6	32.82
P23538	ppsA	17	11	11	11	792	87.4	32.5
P0A6H1	clpX	34	10	11	10	424	46.3	32.18
P0A9K9	slyD	67	6	8	6	196	20.8	31.86
P0ABC3	hflC	29	7	10	7	334	37.6	31.78
P69783	crr	61	7	10	7	169	18.2	31.77
P60624	rplX	54	5	9	5	104	11.3	31.6
P07118	valS	17	10	10	10	951	108.1	31.58
P37440	ucpA	34	8	10	8	263	27.8	31.52
P0A7K2	rplL	75	7	10	7	121	12.3	30.18
P02943	lamB	29	7	9	7	446	49.9	29.9
P45577	proQ	35	6	9	6	232	25.9	29.75
P04983	rbsA	24	9	10	9	501	55	29.67
P62707	gpmA	36	8	11	8	250	28.5	29.66
P0A8L1	serS	28	10	10	10	430	48.4	29.53
P68919	rplY	60	6	10	6	94	10.7	29.28
P09372	grpE	32	3	8	3	197	21.8	29.17
P23893	hemL	40	10	10	10	426	45.3	28.89
P0A9Q1	arcA	34	6	7	6	238	27.3	28.29
P0AB71	fbaA	34	6	8	6	359	39.1	28.12
P0A6F9	groES	82	6	10	6	97	10.4	27.82
P23836	phoP	55	9	9	9	223	25.5	27.48

P02358	rpsF	44	5	8	5	135	15.7	27.43
P17169	glmS	18	6	7	6	609	66.9	27.26
P0A9K3	ybeZ	35	8	8	8	346	39	26.48
P77398	arnA	13	6	9	6	660	74.2	26.27
P0AGJ9	tyrS	31	7	8	7	424	47.5	25.88
P0A7W1	rpsE	37	4	7	4	167	17.6	25.85
P0ADY3	rplN	36	3	7	3	123	13.5	25.42
P04825	pepN	17	8	8	8	870	98.9	25
P0A707	infC	37	4	6	4	180	20.6	24.81
P0A7S9	rpsM	47	4	6	4	118	13.1	24.76
P0A9C5	glnA	23	6	7	6	469	51.9	24.64
P0A805	frr	42	6	7	6	185	20.6	24.59
P0A825	glyA	28	8	8	8	417	45.3	24.3
P00959	metG	16	7	7	7	677	76.2	24.01
P0A9M8	pta	12	6	7	6	714	77.1	23.92
P0A953	fabB	16	4	6	4	406	42.6	23.57
P0A8F0	upp	49	6	7	6	208	22.5	23.41
P63224	gmhA	33	6	7	6	192	20.8	23.33
P25519	hflX	19	6	8	6	426	48.3	23.28
P33599	nuoC	16	7	8	7	596	68.2	22.88
P27298	prlC	18	8	8	8	680	77.1	22.84
P0ADZ4	rpsO	42	2	4	2	89	10.3	22.8
P33218	yebE	25	4	7	4	219	23.7	22.79
P07813	leuS	14	7	7	7	860	97.2	22.73
P21889	aspS	13	6	8	6	590	65.9	22.58
P30748	moaD	26	1	5	1	81	8.8	22.48
P08622	dnaJ	29	7	7	7	376	41.1	22.38
P00490	malP	14	7	7	7	797	90.5	22.15
P0A6R0	fabH	30	5	6	5	317	33.5	22.08
P0ABA4	atpH	35	4	6	4	177	19.3	21.98
P00562	metL	12	8	8	8	810	88.8	21.92
P0AA10	rplM	51	6	7	6	142	16	21.91
P60438	rplC	23	3	6	3	209	22.2	21.71
P76422	thiD	20	3	7	3	266	28.6	21.5
P0ABZ6	surA	22	6	7	6	428	47.3	21.48
P0A917	ompX	44	6	6	6	171	18.6	21.28
P0A7T3	rpsP	52	4	7	4	82	9.2	21.27
P0AEZ3	minD	35	7	7	7	270	29.6	21.14
P0A6G7	clpP	20	2	5	2	207	23.2	20.97
P0C058	ibpB	35	4	7	4	142	16.1	20.56
P02413	rplO	42	5	7	5	144	15	20.41
P0ADY1	ppiD	15	7	7	7	623	68.1	20.35
P0AF24	nagD	30	4	6	4	250	27.1	20.13
P0AEU0	hisJ	41	6	6	6	260	28.5	20.04
P21170	speA	10	4	5	4	658	73.9	19.72
P0A7R1	rplI	44	7	7	7	149	15.8	19.54
P0ABU2	ychF	25	6	6	6	363	39.6	19.49
P33363	bglX	14	7	7	7	765	83.4	19.43
P0AAB6	galF	31	5	6	5	297	32.8	19.26
P0AE88	cpxR	20	3	5	3	232	26.3	19.07
P15288	pepD	12	4	5	4	485	52.9	18.88
P0ABI8	cyoB	9	4	5	4	663	74.3	18.63
P77690	arnB	20	5	5	5	385	42.2	18.37
P0A817	metK	16	4	5	4	384	41.9	18.22
P69441	adk	28	6	7	6	214	23.6	18.12
P24182	accC	17	7	7	7	449	49.3	17.96
P0A749	murA	18	5	6	5	419	44.8	17.91
P0AFG0	nusG	43	5	6	5	181	20.5	17.88
P0A7E5	pyrG	14	6	6	6	545	60.3	17.85
P0A7J7	rplK	27	3	6	3	142	14.9	17.7
P0AG63	rpsQ	32	2	4	2	84	9.7	17.67
P25553	aldA	17	6	6	6	479	52.2	17.61
P0ACP5	gntR	21	5	6	5	331	36.4	17.37
P69503	apt	40	4	6	4	183	19.8	17.36
P76558	maeB	13	6	6	6	759	82.4	17.22
P0AES4	gyrA	9	6	6	6	875	96.9	17.14
P0A9J6	rbsK	24	4	6	4	309	32.3	16.98

P0A7R5	rpsJ	35	4	6	4	103	11.7	16.89
P00370	gdhA	17	5	5	5	447	48.6	16.73
P07395	pheT	13	6	6	6	795	87.3	16.51
P0A6A3	ackA	18	5	5	5	400	43.3	16.38
P0A912	pal	24	3	5	3	173	18.8	16.37
P0AG44	rplQ	27	4	6	4	127	14.4	16.35
P0A6E4	argG	25	6	6	6	447	49.9	16.34
P0A8M3	thrS	10	6	6	6	642	74	16.26
P0A9A9	fur	30	3	5	3	148	16.8	15.99
P0AGG8	tldD	13	4	5	4	481	51.3	15.92
P37665	yiaD	36	4	4	4	219	22.2	15.62
P0AEU7	skp	17	2	4	2	161	17.7	15.6
P0A7M6	rpmC	46	2	5	2	63	7.3	15.57
P0A7K6	rplS	44	4	5	4	115	13.1	15.52
P0A6T1	pgi	11	4	5	4	549	61.5	15.35
P13029	katG	7	4	5	4	726	80	15.23
P0AB91	aroG	20	5	5	5	350	38	15.1
P0A7M9	rpmE	53	3	5	3	70	7.9	14.82
P0A858	tpiA	29	4	4	4	255	27	14.8
P0A7G2	rbfA	41	4	5	4	133	15.1	14.64
P0A8B5	ybaB	45	2	4	2	109	12	14.64
P0A9W9	yrdA	37	5	6	5	184	20.2	14.52
P0A7L3	rplT	24	4	6	4	118	13.5	14.5
P0AAX8	ybiS	26	4	4	4	306	33.3	14.49
P00968	carB	7	5	5	5	1073	117.8	14.43
P61714	ribE	31	3	4	3	156	16.1	14.3
P63020	nfuA	32	3	4	3	191	21	14.3
P07014	sdhB	22	4	5	4	238	26.8	14.29
P04805	gltX	12	4	5	4	471	53.8	14.27
P06992	rsmA	20	3	4	3	273	30.4	14.26
P33195	gcvP	7	4	4	4	957	104.3	14.18
P0A8N5	lysU	14	5	5	2	505	57.8	14.18
P0A9W3	ettA	12	5	5	5	555	62.4	14.17
P0C054	ibpA	43	4	5	4	137	15.8	14.12
P30845	eptA	13	5	5	5	547	61.6	14.03
P0AAA1	yagU	26	4	5	4	204	23	13.86
P0CB39	eptC	9	4	5	4	577	66.6	13.85
P0A6T5	folE	26	5	5	5	222	24.8	13.83
P36672	treB	7	2	4	2	473	51	13.7
P0ABA0	atpF	32	4	5	4	156	17.3	13.65
P0A9S3	gatD	12	5	5	5	346	37.4	13.6
P0AC33	fumA	14	4	4	4	548	60.3	13.41
P0A7X3	rpsI	32	4	5	4	130	14.8	13.28
P27248	gcvT	13	3	4	3	364	40.1	13.23
P21599	pykA	10	4	4	4	480	51.3	13.19
P0A9U3	ybiT	14	4	4	4	530	59.8	13.15
P0A9L3	fklB	37	5	5	5	206	22.2	13.1
P0A6N4	efp	17	2	4	2	188	20.6	13.09
P03024	galR	25	4	4	4	343	37.1	13.06
P0A9Y6	cspC	78	4	4	4	69	7.4	13.04
P15042	ligA	10	4	4	4	671	73.6	13.03
P07639	aroB	15	3	4	3	362	38.9	13.03
P68679	rpsU	32	3	4	3	71	8.5	12.98
P0AFC7	nuoB	17	3	4	3	220	25	12.98
P0AG27	yibN	27	3	4	3	143	15.6	12.95
P25665	metE	9	4	5	4	753	84.6	12.9
P0A7U3	rpsS	37	3	5	3	92	10.4	12.89
P0AC69	grxD	29	2	3	2	115	12.9	12.85
P0ADY7	rplP	32	3	4	3	136	15.3	12.65
P0ACA3	sspA	27	5	5	5	212	24.3	12.56
P76472	arnD	27	3	4	3	296	33.1	12.54
P0A7U7	rpsT	36	4	5	4	87	9.7	12.52
P0AEQ3	glnH	13	2	3	2	248	27.2	12.48
P0C018	rplR	34	3	4	3	117	12.8	12.41
P0AEB2	dacA	19	5	5	5	403	44.4	12.38
P0A9P4	trxB	24	4	4	4	321	34.6	12.34
P0AB80	ilvE	18	4	4	4	309	34.1	12.22

P0A715	kdsA	17	2	3	2	284	30.8	12.01
P60906	hisS	8	3	4	3	424	47	11.98
P0A955	eda	21	3	4	3	213	22.3	11.9
P23865	prc	9	4	4	4	682	76.6	11.79
P76576	yfgM	38	4	4	4	206	22.2	11.75
P36680	zapD	21	4	4	4	247	28.3	11.74
P0AGB6	rpoE	31	4	4	4	191	21.7	11.62
P0ABD8	accB	34	3	4	3	156	16.7	11.58
P0A6K3	def	23	4	5	4	169	19.3	11.53
P0A9Q9	asd	19	4	4	4	367	40	11.47
P76034	yciT	23	4	4	4	249	27.6	11.31
P77757	arnC	19	4	4	4	322	36.3	11.3
P0AF93	ridA	58	3	3	3	128	13.6	11.22
P30850	rnb	7	4	4	4	644	72.4	11.17
P0ACG1	stpA	26	3	4	3	134	15.3	11.16
P0A7F6	speD	27	4	4	4	264	30.4	11.11
P0A6L2	dapA	11	2	3	2	292	31.3	11.08
P61517	can	24	4	4	4	220	25.1	11.05
P39177	uspG	22	2	3	2	142	15.9	11.03
P76177	ydgH	17	3	3	3	314	33.9	11
P04951	kdsB	19	4	4	4	248	27.6	10.92
P0A9X9	cspA	39	2	3	1	70	7.4	10.9
P0AE52	bcp	24	3	4	3	156	17.6	10.86
P17117	nfsA	20	3	3	3	240	26.8	10.85
P75913	ghrA	18	3	3	3	312	35.3	10.8
P00722	lacZ	5	3	3	3	1024	116.4	10.79
P0ADW3	yhcB	35	3	3	3	132	15	10.73
P00448	sodA	16	2	3	2	206	23.1	10.71
P77804	ydgA	10	4	4	4	502	54.7	10.71
P0A6Q3	fabA	24	4	4	4	172	19	10.7
P15034	pepP	8	3	4	3	441	49.8	10.68
P0AE06	acrA	11	3	4	3	397	42.2	10.66
P0ACE0	hybC	12	3	3	3	567	62.5	10.61
P62768	yaeH	34	4	4	4	128	15.1	10.57
P28904	treC	8	4	4	4	551	63.8	10.56
P77774	bamB	15	4	4	4	392	41.9	10.54
P38489	nfsB	22	3	3	3	217	23.9	10.53
P0A6L4	nanA	18	3	3	3	297	32.6	10.53
P0ADG7	guaB	17	3	3	3	488	52	10.51
P36938	pgm	12	3	3	3	546	58.3	10.5
P0AA25	trxA	48	4	4	4	109	11.8	10.49
P45565	ais	17	2	3	2	200	22.2	10.48
P0A734	minE	67	4	4	4	88	10.2	10.45
P64604	mlaD	22	2	4	2	183	19.6	10.37
P08390	usg	19	2	3	2	337	36.3	10.34
P0ABP8	deoD	24	4	4	4	239	25.9	10.3
P0A6U5	rsmG	26	3	3	3	207	23.4	10.28
P0AE78	corC	17	3	3	3	292	33.3	10.01
P0AG51	rpmD	58	3	4	3	59	6.5	9.96
P31120	glmM	12	4	4	4	445	47.5	9.92
P0A7M2	rpmB	23	2	4	2	78	9	9.82
P37902	gltI	15	3	3	3	302	33.4	9.76
P43672	uup	10	3	4	3	635	72	9.7
P0A6X7	ihfA	22	3	3	3	99	11.3	9.55
P0AGK8	iscR	14	1	2	1	162	17.3	9.48
P40874	solA	12	3	3	3	372	40.9	9.47
P0AFD1	nuoE	20	2	3	2	166	18.6	9.34
P26616	maeA	12	3	3	3	565	63.2	9.3
P0A7S3	rpsL	10	2	3	2	124	13.7	9.27
P0ABA6	atpG	14	3	3	3	287	31.6	9.26
P0A7B8	hslV	23	3	3	3	176	19.1	9.26
P05791	ilvD	7	3	3	3	616	65.5	9.23
P0A7E9	pyrH	14	2	3	2	241	26	9.13
P0ABJ1	cyoA	17	3	3	3	315	34.9	9.09
P04982	rbsD	31	3	3	3	139	15.3	9.07
P0A6D7	aroK	22	3	3	3	173	19.5	9.04
P0A9R4	fdx	38	2	2	2	111	12.3	9.03

P30843	basR	16	3	3	3	222	25	8.99
P62623	ispH	9	2	3	2	316	34.8	8.95
P31663	panC	10	2	3	2	283	31.6	8.94
P00962	glnS	6	2	3	2	554	63.4	8.91
P0AG90	secD	6	3	3	2	615	66.6	8.9
P25516	acnA	6	3	3	3	891	97.6	8.86
P0AEI1	miaB	12	3	3	3	474	53.6	8.82
P0ABJ9	cydA	8	3	3	3	522	58.2	8.76
P60651	speB	14	3	3	3	306	33.5	8.74
P0ACD4	iscU	34	3	3	3	128	13.8	8.68
P00934	thrC	13	3	3	3	428	47.1	8.64
P0A6I0	cmk	19	2	3	2	227	24.7	8.52
P0A940	bamA	7	3	3	3	810	90.5	8.41
P45578	luxS	26	3	3	3	171	19.4	8.33
P23721	serC	12	3	3	3	362	39.8	8.32
P09546	putA	3	3	3	3	1320	143.7	8.28
P05793	ilvC	10	3	3	3	491	54	8.27
P31224	acrB	4	3	3	3	1049	113.5	8.25
P00864	ppc	4	3	3	3	883	99	8.24
P0ACY1	ydjA	20	3	3	3	183	20	8.1
P0AF12	mtnN	18	2	2	2	232	24.3	7.98
P0A9M2	hpt	21	3	3	3	178	20.1	7.98
P69924	nrdB	11	3	3	3	376	43.5	7.97
P0AED0	uspA	41	2	2	2	144	16.1	7.96
P0AEP3	galU	15	3	3	3	302	32.9	7.92
P07862	ddlB	13	3	3	3	306	32.8	7.91
P0AGD7	ffh	9	3	3	3	453	49.8	7.83
P04425	gshB	15	3	3	3	316	35.5	7.73
P60716	lipA	12	2	2	2	321	36	7.71
P0AES6	gyrB	6	3	3	3	804	89.9	7.66
P69922	fucI	9	3	3	3	591	64.9	7.66
P0AFD6	nuoI	22	3	3	3	180	20.5	7.64
P0AG59	rpsN	19	2	2	2	101	11.6	7.63
P0A908	mipA	17	3	3	3	248	27.8	7.63
P61949	fldA	28	2	2	2	176	19.7	7.59
P39342	yjgR	8	3	3	3	500	54.3	7.57
P00954	trpS	7	1	2	1	334	37.4	7.57
P0AAI9	fabD	12	2	2	2	309	32.4	7.5
P0A780	nusB	19	3	3	3	139	15.7	7.46
P0ADG4	suhB	11	2	2	2	267	29.2	7.37
P0AGA2	secY	7	2	3	2	443	48.5	7.3
P0AB24	efeO	9	2	2	2	375	41.1	7.21
P0A8E7	yajQ	17	2	2	2	163	18.3	7.18
P0A877	trpA	15	2	2	2	268	28.7	7.16
P38038	cysJ	7	3	3	3	599	66.2	7.13
P0A903	bamC	9	2	2	2	344	36.8	6.96
P0AFM9	pspB	34	2	2	2	74	8.8	6.91
P0A800	rpoZ	26	2	2	2	91	10.2	6.89
P0AC53	zwf	8	3	3	3	491	55.7	6.83
P17846	cysI	8	2	2	2	570	64	6.83
P0ACF4	hupB	16	1	2	1	90	9.2	6.82
P0A7N4	rpmF	44	2	2	2	57	6.4	6.79
P22524	mukE	10	1	2	1	234	27	6.73
P0A6C8	argB	16	2	2	2	258	27.1	6.69
P00803	lepB	8	2	2	2	324	35.9	6.66
P0A8I3	yaaA	17	2	2	2	258	29.6	6.61
P45955	cpoB	16	2	2	2	263	28.2	6.61
P37188	gatB	20	1	2	1	94	10.2	6.58
P68187	malK	11	2	2	2	371	41	6.58
P0A722	lpxA	15	2	2	2	262	28.1	6.57
P25437	frmA	12	2	2	2	369	39.3	6.57
P0A6K6	deoB	6	2	2	2	407	44.3	6.55
P16456	selD	12	2	2	2	347	36.7	6.3
P0A9Z1	glnB	24	2	2	2	112	12.4	6.24
P0ACA7	gstB	9	1	2	1	208	23.7	6.16
P18843	nadE	9	2	2	2	275	30.6	6.12
P0C0S1	mscS	10	2	2	2	286	30.9	6.09

P76658	hldE	6	2	2	2	477	51	6.02
P0AFF2	nupC	9	2	2	2	400	43.4	5.99
P27434	rodZ	10	2	2	2	337	36.2	5.87
P60390	rsmH	11	2	2	2	313	34.9	5.86
P77330	borD	26	2	2	2	97	10.4	5.76
P0A7G6	recA	7	2	2	2	353	38	5.73
P0AGE0	ssb	16	2	2	2	178	19	5.68
P0ABN1	dgkA	17	2	2	2	122	13.2	5.68
P07012	prfB	9	2	2	2	365	41.2	5.67
P0A7T7	rpsR	29	2	2	2	75	9	5.66
P33136	mdoG	5	2	2	2	511	57.9	5.66
P0AA04	ptsH	35	2	2	2	85	9.1	5.64
P0AF08	mrp	5	1	2	1	369	39.9	5.63
P39199	prmB	6	1	2	1	310	35	5.63
P0A993	fbp	11	2	2	2	332	36.8	5.62
P0A6F1	carA	7	2	2	2	382	41.4	5.61
P02930	tolC	5	2	2	2	493	53.7	5.61
P0A7B5	proB	7	2	2	2	367	39	5.61
P08957	hsdM	5	2	2	2	529	59.3	5.58
P06149	dld	7	2	2	2	571	64.6	5.57
P0A763	ndk	23	2	2	2	143	15.5	5.54
P0AG48	rplU	21	2	2	2	103	11.6	5.54
P31142	sseA	9	2	2	2	281	30.8	5.52
P0C0V0	degP	3	1	2	1	474	49.3	5.5
P08312	pheS	7	2	2	2	327	36.8	5.48
P0AFK0	pmbA	6	2	2	2	450	48.3	5.43
P30860	artJ	15	2	2	2	243	26.8	5.33
P09127	hemX	7	2	2	2	393	42.9	5.29
P0A9L5	ppiC	22	2	2	2	93	10.2	5.27
P39835	gntT	7	2	2	2	438	45.9	5.22
P00894	ilvH	13	2	2	2	163	18	5.19
P37051	purU	13	2	2	2	280	31.9	5.18
P0A6R3	fis	23	1	1	1	98	11.2	5.17
P77529	tcyP	7	2	2	2	463	48.6	5.15
P0AD61	pykF	6	2	2	2	470	50.7	5.13
P0A978	cspG	31	2	2	1	70	7.8	5.08
P0ADK0	yiaF	9	2	2	2	236	25.6	5.03
P11880	murF	8	2	2	2	452	47.4	5.02
P64596	dolP	13	2	2	2	191	20	4.98
P0AB89	purB	8	2	2	2	456	51.5	4.9
P23882	fmt	10	2	2	2	315	34.1	4.89
P69797	manX	8	2	2	2	323	35	4.86
P13009	metH	2	2	2	2	1227	135.9	4.85
P07913	tdh	10	2	2	2	341	37.2	4.76
P12758	udp	9	2	2	2	253	27.1	4.75
P0ACC3	erpA	18	2	2	2	114	12.1	4.71
P60340	truB	6	2	2	2	314	35.1	4.69
P76268	kdgR	10	2	2	2	263	30	4.67
P30011	nadC	7	2	2	2	297	32.7	4.64
P0AG93	secF	10	2	2	2	323	35.4	4.61
P36771	lrhA	10	2	2	2	312	34.6	4.61
P23827	eco	17	2	2	2	162	18.2	4.59
P21165	pepQ	5	2	2	2	443	50.1	4.56
P0A9F1	mntR	16	2	2	2	155	17.6	4.49
P0ABU5	elbB	12	1	1	1	217	23	4.47
P0A9T4	tas	10	2	2	2	346	38.5	4.46
Q57261	truD	6	1	1	1	349	39.1	4.44
P60546	gmk	16	2	2	2	207	23.6	4.37
P0A7X6	rimM	14	2	2	2	182	20.6	4.34
P13445	rpoS	8	2	2	1	330	37.9	4.32
P0ACJ8	crp	9	2	2	2	210	23.6	4.24
P0A937	bamE	18	1	1	1	113	12.3	4.19
P00452	nrdA	3	2	2	2	761	85.7	4.17
P76046	ycjX	3	2	2	2	465	52.6	4.13
P0ADC1	lptE	9	1	1	1	193	21.3	4.08
P39831	ydfG	7	1	1	1	248	27.2	4
P0A7L8	rpmA	16	1	1	1	85	9.1	3.95

P0AAC0	uspE	6	1	1	1	316	35.7	3.87
P0A7R9	rpsK	12	1	1	1	129	13.8	3.84
P0AEQ1	glcG	16	1	1	1	134	13.7	3.8
P39173	yeaD	5	1	1	1	294	32.6	3.73
P08192	folC	5	1	1	1	422	45.4	3.71
P0A7D7	purC	7	1	1	1	237	27	3.68
P69411	rcsF	10	1	1	1	134	14.2	3.62
P60752	msbA	3	1	1	1	582	64.4	3.58
P0AA16	ompR	8	1	1	1	239	27.3	3.55
P76027	oppD	7	1	1	1	337	37.2	3.55
Q46845	yghU	5	1	1	1	288	32.4	3.54
P0A7C2	lexA	7	1	1	1	202	22.3	3.48
P00960	glyQ	5	1	1	1	303	34.8	3.46
P75915	ycdY	8	1	1	1	184	20.7	3.46
P0A8X0	yjgA	11	1	1	1	183	21.3	3.45
P0C0L7	proP	3	1	1	1	500	54.8	3.44
P64564	yggT	10	1	1	1	188	21.2	3.43
P76535	murQ	7	1	1	1	298	31.2	3.38
P0A8J4	ybeD	17	1	1	1	87	9.8	3.36
P37182	hybD	10	1	1	1	164	17.7	3.34
P0A7N9	rpmG	27	1	1	1	55	6.4	3.32
P23839	yicC	4	1	1	1	287	33.2	3.31
P0AAC8	iscA	13	1	1	1	107	11.5	3.25
P69054	sdhC	9	1	1	1	129	14.3	3.23
P10371	hisA	7	1	1	1	245	26	3.22
P0AE18	map	5	1	1	1	264	29.3	3.21
P27848	yigL	8	1	1	1	266	29.7	3.21
P00582	polA	2	1	1	1	928	103.1	3.2
P0AG99	secG	16	1	1	1	110	11.4	3.19
P42641	obgE	6	1	1	1	390	43.3	3.19
P24224	acpS	12	1	1	1	126	14	3.17
P16700	cysP	3	1	1	1	338	37.6	3.15
P0ADC6	lptG	6	1	1	1	360	39.6	3.15
P22939	ispA	7	1	1	1	299	32.1	3.13
P0AFL3	ppiA	8	1	1	1	190	20.4	3.09
P0AFF0	nuoN	2	1	1	1	485	52	3.09
P31802	narP	7	1	1	1	215	23.6	3.08
P0A6N8	yeiP	7	1	1	1	190	21.5	3.08
P0AF36	zapB	26	1	1	1	81	9.6	3.07
P60757	hisG	5	1	1	1	299	33.3	3.07
P0ADV7	mlaC	6	1	1	1	211	23.9	3.07
P52643	ldhA	4	1	1	1	329	36.5	3.05
P06968	dut	8	1	1	1	152	16.3	3.04
P27306	sthA	6	1	1	1	466	51.5	3.03
P37759	rfbB	4	1	1	1	361	40.5	3.03
P0A794	pdxJ	6	1	1	1	243	26.4	3.03
P23869	ppiB	7	1	1	1	164	18.1	3.03
P67087	rsmI	6	1	1	1	286	31.3	3.03
P0ACB7	hemY	3	1	1	1	398	45.2	3.01
P77488	dxs	1	1	1	1	620	67.6	2.99
P0A887	ubiE	5	1	1	1	251	28.1	2.99
P0AEH5	elaB	17	1	1	1	101	11.3	2.98
P0A6S0	flgH	7	1	1	1	232	24.6	2.97
P0A898	ybeY	10	1	1	1	155	17.5	2.97
P0AAY6	ybjN	8	1	1	1	158	17.7	2.96
P0AC19	folX	8	1	1	1	120	14.1	2.96
P0AEM0	fkpB	12	1	1	1	149	16.1	2.94
P0AFC3	nuoA	10	1	1	1	147	16.4	2.91
P06721	metC	6	1	1	1	395	43.2	2.91
P0AD12	yeeZ	8	1	1	1	274	29.7	2.89
P0ADR8	ppnN	2	1	1	1	454	50.9	2.89
P0AAS0	ylaC	10	1	1	1	156	18.3	2.87
P0A6W9	gshA	3	1	1	1	518	58.2	2.87
P0A8V6	fadR	8	1	1	1	239	27	2.87
P17993	ubiG	7	1	1	1	240	26.5	2.86
P0A6P5	der	4	1	1	1	490	55	2.86
P0AFR4	yciO	5	1	1	1	206	23.2	2.86

P00946	manA	6	1	1	1	391	42.8	2.86
P0A959	alaA	3	1	1	1	405	45.5	2.85
P0AEN8	fucU	9	1	1	1	140	15.5	2.83
P0A6J8	ddlA	4	1	1	1	364	39.3	2.82
P30958	mfd	1	1	1	1	1148	129.9	2.81
P0A9V1	lptB	5	1	1	1	241	26.8	2.8
P0AFW4	rnk	18	1	1	1	136	14.9	2.8
P23894	htpX	4	1	1	1	293	31.9	2.79
P06999	pfkB	5	1	1	1	309	32.4	2.79
P33355	yehS	12	1	1	1	156	18	2.78
P37617	zntA	2	1	1	1	732	76.8	2.77
P46837	yhgF	2	1	1	1	773	85.1	2.77
P0ADB7	ecnB	40	1	1	1	48	4.8	2.77
P0A6W5	greA	9	1	1	1	158	17.6	2.76
P0AFP6	ybgI	6	1	1	1	247	26.9	2.75
P75849	gloC	6	1	1	1	215	23.8	2.74
P0A6V8	glk	4	1	1	1	321	34.7	2.73
P37903	uspF	11	1	1	1	144	16	2.73
P12281	moeA	5	1	1	1	411	44	2.72
P64581	yqjD	16	1	1	1	101	11	2.72
P69425	tatB	8	1	1	1	171	18.4	2.69
P0AFY8	seqA	7	1	1	1	181	20.3	2.68
P0A6A8	acpP	21	1	1	1	78	8.6	2.68
P04968	ilvA	3	1	1	1	514	56.2	2.67
P77756	queC	7	1	1	1	231	25.5	2.67
P22333	add	8	1	1	1	333	36.4	2.66
P0AC02	bamD	5	1	1	1	245	27.8	2.65
P29131	ftsN	4	1	1	1	319	35.8	2.65
P45748	tsaC	9	1	1	1	190	20.8	2.64
P32131	hemN	2	1	1	1	457	52.7	2.63
P0AF70	yjeI	16	1	1	1	117	12	2.63
P03841	malM	3	1	1	1	306	31.9	2.63
P69222	infA	17	1	1	1	72	8.2	2.63
P45799	nudE	8	1	1	1	186	21.1	2.61
P0A717	prs	4	1	1	1	315	34.2	2.61
P09053	avtA	3	1	1	1	417	46.7	2.6
P33643	rluD	7	1	1	1	326	37.1	2.59
P39377	iadA	5	1	1	1	390	41.1	2.59
P0A9T0	serA	3	1	1	1	410	44.1	2.58
P0A790	panD	8	1	1	1	126	13.8	2.58
P22106	asnB	3	1	1	1	554	62.6	2.58
P37744	rfbA	4	1	1	1	293	32.7	2.57
P0AFU8	ribC	5	1	1	1	213	23.4	2.57
P0A761	nanE	5	1	1	1	229	24.1	2.56
P69776	lpp	15	1	1	1	78	8.3	2.56
P69795	chbB	17	1	1	1	106	11.4	2.55
P0ABD3	bfr	9	1	1	1	158	18.5	2.55
P0A7A9	ppa	5	1	1	1	176	19.7	2.55
P0A9Q7	adhE	2	1	1	1	891	96.1	2.54
P36879	yadG	5	1	1	1	308	34.6	2.54
P64624	yheO	11	1	1	1	240	26.8	2.53
P05637	apaH	6	1	1	1	280	31.3	2.52
P09323	nagE	3	1	1	1	648	68.3	2.52
P0ACN4	allR	4	1	1	1	271	29.3	2.51
P75949	nagZ	5	1	1	1	341	37.6	2.51
P69829	ptsN	10	1	1	1	163	17.9	2.51
P0AFX4	rsd	6	1	1	1	158	18.2	2.5
P25714	yidC	3	1	1	1	548	61.5	2.49
P11875	argS	2	1	1	1	577	64.6	2.49
P69831	gatC	3	1	1	1	451	48.3	2.48
P29217	yceH	7	1	1	1	215	24.2	2.48
P77239	cusB	3	1	1	1	407	44.3	2.47
P28248	dcd	6	1	1	1	193	21.2	2.47
P0AFX9	rseB	4	1	1	1	318	35.7	2.46
P0ACE7	hinT	11	1	1	1	119	13.2	2.45
P0A8D3	yaiI	10	1	1	1	152	17	2.44
P0AB77	kbl	4	1	1	1	398	43.1	2.43

P0A884	thyA	5	1	1	1	264	30.5	2.42
P0ADI7	yecD	5	1	1	1	188	20.4	2.42
P23847	dppA	5	1	1	1	535	60.3	2.42
P52108	rstA	4	1	1	1	239	26.7	2.41
P11557	damX	3	1	1	1	428	46.1	2.4
P04693	tyrB	2	1	1	1	397	43.5	2.38
P0ADT8	ygiM	6	1	1	1	206	23.1	2.38
P0A9U6	puuR	10	1	1	1	185	20.1	2.38
P10100	rlpA	4	1	1	1	362	37.5	2.38
P0A6L0	deoC	5	1	1	1	259	27.7	2.36
P0ADN6	yifL	34	1	1	1	67	7.2	2.35
P32099	lplA	6	1	1	1	338	37.9	2.34
P0AC13	folP	4	1	1	1	282	30.6	2.34
P0A7E3	pyrE	6	1	1	1	213	23.6	2.33
P0A7Y0	rnc	9	1	1	1	226	25.5	2.32
P06715	gor	2	1	1	1	450	48.7	2.31
P30859	artI	9	1	1	1	243	26.9	2.31
P0AE37	astA	3	1	1	1	344	38.4	2.31
P0AED7	dapE	2	1	1	1	375	41.2	2.29
P0AAG8	mglA	2	1	1	1	506	56.4	2.28
P0AC44	sdhD	9	1	1	1	115	12.9	2.27
Q46868	ubiK	9	1	1	1	96	11.3	2.26
P24251	crl	9	1	1	1	133	15.6	2.25
P16095	sdaA	3	1	1	1	454	48.9	2.25
P75914	ycdX	4	1	1	1	245	26.9	2.25
P68699	atpE	11	1	1	1	79	8.3	2.24
P76270	msrC	6	1	1	1	165	18.1	2.23
P05852	tsaD	4	1	1	1	337	36	2.21
P0A8A8	rimP	7	1	1	1	150	16.6	2.21
P0ADA5	yajG	5	1	1	1	192	20.9	2.2
P0A6L9	hscB	6	1	1	1	171	20.1	2.19
P36979	rlmN	2	1	1	1	384	43.1	2.19
P22188	murE	3	1	1	1	495	53.3	2.19
P0AEY5	mdaB	5	1	1	1	193	21.9	2.19
P07001	pntA	4	1	1	1	510	54.6	2.18
P67910	hldD	3	1	1	1	310	34.9	2.18
P32680	yjaG	6	1	1	1	196	22.6	2.17
P0AF28	narL	4	1	1	1	216	23.9	2.17
P64588	yqjI	4	1	1	1	207	23.4	2.15
P0ADZ7	yajC	8	1	1	1	110	11.9	2.12
P0A7Q1	rpmI	20	1	1	1	65	7.3	2.12
P25526	gabD	4	1	1	1	482	51.7	2.1
P0A8W8	yfbU	9	1	1	1	164	19.5	2.09
P50465	nei	5	1	1	1	263	29.8	2.09
P0A998	ftnA	6	1	1	1	165	19.4	2.07
P07604	tyrR	2	1	1	1	513	57.6	2.06
P60240	rapA	1	1	1	1	968	109.7	2.05
P0A7I0	prfA	2	1	1	1	360	40.5	2.05
P69228	baeR	7	1	1	1	240	27.6	2.04
P09158	speE	3	1	1	1	288	32.3	2.04
P0A855	tolB	4	1	1	1	430	45.9	2.02
P0ADZ0	rplW	12	1	1	1	100	11.2	2.02
P0AFM2	proX	7	1	1	1	330	36	2.02
P06983	hemC	4	1	1	1	313	33.8	2.02
P77247	hxpB	6	1	1	1	222	24.3	1.99
P0ABF8	pgsA	4	1	1	1	182	20.7	1.99
P04079	guaA	2	1	1	1	525	58.6	1.98
P75990	bluF	3	1	1	1	403	45.3	1.97
P0ABQ0	coaBC	3	1	1	1	406	43.4	1.96
P0ACL2	exuR	7	1	1	1	258	29.8	1.94
P0AB43	ycgL	15	1	1	1	108	12.4	1.93
P0A8W0	nanR	3	1	1	1	263	29.5	1.93
P52061	rdgB	4	1	1	1	197	21	1.93
P0AG07	rpe	4	1	1	1	225	24.5	1.92
P0AAQ2	yajD	7	1	1	1	115	13.4	1.92